LBL-19003
UC-94c

Lawrence Berkeley Laboratory
UNIVERSITY OF CALIFORNIA

APPLIED SCIENCE DIVISION

BIFUNCTIONAL OXYGEN ELECTRODES
Final Report

D. Tryk, W. Aldred, Z. Chen, C. Fierro,
J. Hashiguchi, M. Hossain, Z. Zhang,
F. Zhao, and E. Yeager

January 1985

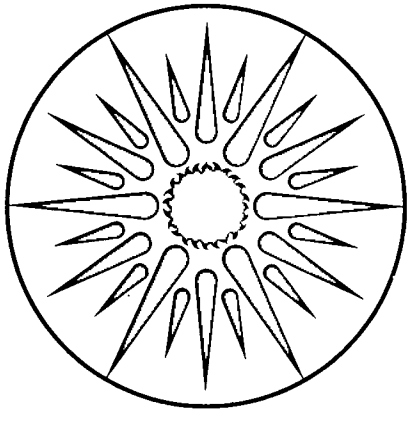

APPLIED SCIENCE
DIVISION

Prepared for the U.S. Department of Energy under Contract DE-AC03-76SF00098

DISCLAIMER

LBL-19003

BIFUNCTIONAL OXYGEN ELECTRODES

Final Report

January 1985

by

D. Tryk
W. Aldred
Z. Chen
C. Fierro
J. Hashiguchi
M. Hossain
Z. Zhang
F. Zhao
E. Yeager, Project Director

Case Center for Electrochemical Sciences
and the Department of Chemistry
Case Western Reserve University
Cleveland, Ohio 44106

for

Technology Base Research Project
Lawrence Berkeley Laboratory
University of California
Berkeley, California 94720

This work was supported by the Assistant Secretary for Conservation and Renewable Energy, Office of Energy Systems Research, Energy Storage Division of the U.S. Department of Energy under Contract No. DE-AC03-76SF00098, Subcontract No. 4521210 with Lawrence Berkeley Laboratory.

TABLE OF CONTENTS

B. Z. W. Zhang, D. Tryk and E. Yeager, in "Proceedings of the Workshop on the Electrochemistry of Carbon," August, 1983, Cleveland, Ohio, The Electrochemical Society, Pennington, N. J., 1984, pp. 158-178, "Effect of Surface Treatment of Glassy Carbon on O_2 Reduction in Alkaline Solutions"

C. J. T. Lu, D. Tryk and E. Yeager, in "Extended Abstracts," International Society of Electrochemistry, 34th Meeting, September, 1983, Erlangen, West Germany, Abstr. No. 0519, "The Formation of $O_2^{\cdot -}$: Radical Ion during O_2 Electroreduction in Alkaline Solution"

D. Z. W. Zhang, D. Tryk and E. Yeager, in "Extended Abstracts," Vol. 83-2, National Meeting of the Electrochemical Society, October, 1983, Washington, D. C., Abstr. No. 394, p.630, "Electrode Kinetics of the Oxygen/Peroxide Couple on Glassy Carbon in Alkaline Solutions"

E. Z. W. Zhang, D. Tryk and E. Yeager, in "Extended Abstracts," Vol. 83-2, National Meeting of the Electrochemical Society, October, 1983, Washington, D. C., Abstr. No. 395, p. 632, "Quinone-Like Structures and O_2 Reduction Activity on Glassy Carbon and Graphite Surfaces in Alkaline Solution"

SUMMARY

The research at Case on bifunctional oxygen electrodes during February 1983 to February 1984 has been concerned mainly with fundamental aspects of oxygen electroreduction in alkaline solution on various types of electrode surfaces, including carbons and graphites, both with and without attached catalysts, including transition metal macrocyclic complexes and quinones. A major objective has been to correlate the intrinsic electrochemical behavior of the electrode surface, as well as other physico-chemical characteristics, with the catalytic behavior. Another major concern has been the development of high activity, long-lived catalysts for bifunctional oxygen electrodes, i.e. ones that can both reduce as well as generate oxygen within a relatively narrow potential range. This development has also focused on the macrocycles, usually heat treated for greater activity and stability.

It can be very useful to examine the effect which different macrocyclic ligands have upon the transition metal ions coordinated to them. For example phthalocyanines and porphyrins have very different characteristics as ligands, especially in terms of the extent of back donation from the metal d orbitals to the antibonding orbitals of the ligand and the resulting electronic density remaining at the metal ion. In this context a new macrocycle from Ogawa's group at the University of Tokyo, a hexazatamacrocycle (HAM), has been examined electrochemically, and in addition, molecular orbital calculations were carried out. The conclusion was that for the iron compound the lack of back donation leads to high electronic density at the metal and relatively nagative redox potentials, as compared for example with iron tetrasulfonated phthalocyanine (FeTSPc). The O_2 reduction also was shifted to the negative as compared with that for FeTSPc corresponding to the shift in the Fe (III)/(II) couple, but it did not experience the same decrease in O_2 reduction current at somewhat more negative potentials observed for FeTSPc because of the highly negative Fe(II)/(I) couple for FeHAM. (The Fe(I) state is thought to be catalytically inactive.)

FeTSPc is known to catalyze the four-electron reduction of oxygen to hydroxide over a wide potential range while CoTSPc, like other monomeric cobalt complexes, only catalyzes the two electron reduction to hydrogen peroxide. Preliminary work has found that under certain conditions CoTSPc can catalyze the partial elimination of peroxide, either via direct reduction or via chemical decomposition followed by reduction of generated O_2.

As part of an ongoing effort to understand O_2 reduction on carbon and graphite surfaces, as well as to understand the electrochemistry of superoxide ($O_2^{\cdot -}$), one set of experiments was aimed at examining O_2 reduction in acetonitrile so that the proton activity could be varied over a wide range. The proton is important in the chemical follow-up reactions of superoxide. In camparision to gold, glassy carbon (GC) was more catalytically active for the one electron reduction of oxygen to superoxide in dry acetonitrile. In the presence of 0.5 - 1 $\underline{M}$ H_2O in acetonitrile, Au catalyzes the disproportionation of superoxide to oxygen and peroxide while on GC, superoxide is stable enough to be farther reduced, either to the dianion or to hydrogen peroxide. These findings shed light on the kinetics and mechanism for O_2 reduction in aqueous alkaline solution.

A large amount of our attention has been focused upon the quinonoid compounds as models for the intrinsic surface functional groups on carbons and

graphites, which may act as catalytic sites for O_2 reduction in alkaline solution. Several different quinones have been adsorbed on the basal plane surface of highly-ordered pyrolytic graphite (HOPG). The electrocatalytic activity becomes much higher, and the onset of O_2 reduction current is associated with the reduction of the quinone to its radical anion, which is often relatively stable in alkaline solution. Quinones have been successfully attached chemically to ordinary pyrolytic graphite (OPG) and the electrocatalytic behavior of OPG and chemically-modified surfaces was found to be qualitatively similar. A mechanism which fits the kinetic data has been worked out.

The research on heat-treated macrocycles has two purposes. First to try to understand the nature of the processes occurring during heat treatment and the reasons for the increased activity and stability, and second to develop "second generation" catalysts from them which are even more active for O_2 reduction. It has been found that mildly heat-treated (450°C) metal- free tetramethoxyphenylporphyrin (H_2TMPP) supported on high area carbon black without metallic impurities is able to interact with added cobalt hydroxide after the initial heat-treatment (and with only a final heat-treatment to 280°C for Teflon sintering) and give O_2 reduction performance equal to that of CoTMPP/C (450°C). The activity cannot be accounted for by the catalytic activity of $Co(OH)_2$ alone. This experiment lends support to the idea that both the macrocycle and transition metal are required for catalysis. The precise nature of the interaction has yet to be determined, but is currently the subject of intense study.

The O_2 reduction activity has been found to be very substantially increased by adding more than one transition metal hydroxide. One example of such a multicomponent catalytic system is H_2TMPP/C plus $Co(OH)_2$ and $Ni(OH)_2$. Another system with even better performance has been found, whose identity is being kept confidential pending investigation of its patentability. These systems probably provide more than one type of catalytic site, for example, one for oxygen reduction to peroxide and another for peroxide reduction to hydroxide.

A bifunctional oxygen catalytic system has also been developed based on heat-treated H_2TMPP/C, with added $Fe(OH)_3$, Co(OH) and $Ni(OH)_2$. The O_2 reduction is catalyzed by the H_2TMPP/C + $Co(OH)_2$, $Ni(OH)_2$ system while O_2 generation is catalyzed by a mixed Fe-Ni hydroxide. This system exhibits the smallest potential excursion between the cathodic and anodic modes yet seen and is quite stable in short-term cycling tests.

These multicomponent catalysts can probably be improved greatly as they become better understood. To this end a variety of electrochemical and nonelectrochemical characterization methods are being brought to bear.

GENERAL INTRODUCTION

The overall objective of the research on bifunctional oxygen electrodes for alkaline electrolytes at Case has been to improve significantly both the cathodic and anodic polarization as well as the cycle life of such electrodes. The research has focused on finding high-efficiency, long-life electrocatalysts for O_2 reduction and generation and achieving an understanding of the mechanisms of the catalysis. Such understanding is being used to guide the search for even more efficient catalysts.

During the initial two years of the project, starting in October, 1980, an understanding of the Westinghouse bifunctional oxygen electrode was achieved for both the catalytic systems and the failure modes. During the more recent phase of the research, the emphasis has been on understanding the O_2 reduction and generation reactions on various catalysts with the majority of the work on the reduction process. Catalyst systems which have been examined in alkaline electrolytes have included the following:

1. various types of carbons and graphites
2. chemically-modified carbons and graphites using adsorptive attachment (e.g., various quinones, macrocycles and chemical linkages)
3. silver and various intermetallics
4. various oxide systems including perovskites, spinels, pyrochlores and other mixed transition metal oxides
5. transition metal macrocycles including porphyrins, phthalocyanines, naphthalocyanines and tetraazaannulenes
6. thermally-treated macrocycles.

Mechanistic studies have particularly focused on the reduction of O_2 on various carbon/graphite surfaces and the role of the O_2^- radical ion.

SECTION 1

TRANSITION METAL-HEXAAZAMACROCYCLES AS OXYGEN REDUCTION ELECTROCATALYSTS

J. Hashiguchi, D. Tryk, C. Fierro and E. Yeager

1.1 INTRODUCTION

Ogawa and coworkers at the University of Tokyo have synthesized a series of transition metal macrocyclic complexes having six aza nitrogens, as shown in Fig. 1-1. Thus far, the metal-free and the Fe, Co, Ni, and Cu hexa-aza-macrocycles (HAM) have been synthesized and have been made available to our group for examination as O_2 electrocatalysts (1,2). These macrocycles are quite different from either the porphyrin or phthalocyanine types, and, as such, present the opportunity of examining the effect of varying the electronic environment around the central metal ion. The latter should have a significant effect upon the electrochemical and electrocatalytic behavior, especially for dioxygen reduction. The effect of varying the transition metal ion can also be used to probe the interactions of the metal ion and the ligand. Preliminary results for Co- and Fe-HAM as electrocatalysts for O_2 reduction in alkaline solution are presented.

1.2 EXPERIMENTAL METHODS

Experiments were done in an all-Teflon cell with a gold counter electrode in a separate compartment and a Hg/HgO (0.1 M OH^-) reference electrode separated from the cell using a solution bridge with a closed stopcock. The rotating disk electrode was fabricated from ordinary pyrolytic graphite (OPG)(Union Carbide, Carbon Products Div., Parma, Ohio). The OPG disk was mounted in Kel-F using molding powder (3M). The graphite electrode was polished using successively finer grades of Buehler emery paper and alumina pastes, the final polishing being done with 0.05 um particle size alumina. The electrode was resurfaced between experiments by polishing with alumina only, which was removed by ultrasonic agitation in distilled water. The macrocycle was pre-adsorbed by rotating the electrode in a 10^{-3} M dimethylformamide (for CoHAM) or quinoline (for FeHAM) solution followed by a gentle distilled water rinse.

The electrolyte was 0.1 M NaOH prepared from low carbonate NaOH pellets (Baker) and water prepared by reverse osmosis followed by double distillation. The nitrogen gas was purified by passing through traps containing silica gel, Alfa De-Ox catalyst and molecular sieves. Oxygen was purified using traps containing silica gel, Hopcalite (Mine Safety Appliances Co.), NaOH-asbestos and molecular sieves.

1.3 RESULTS AND DISCUSSION

Cyclic voltammetry curves for FeHAM pre-adsorbed on an OPG electrode

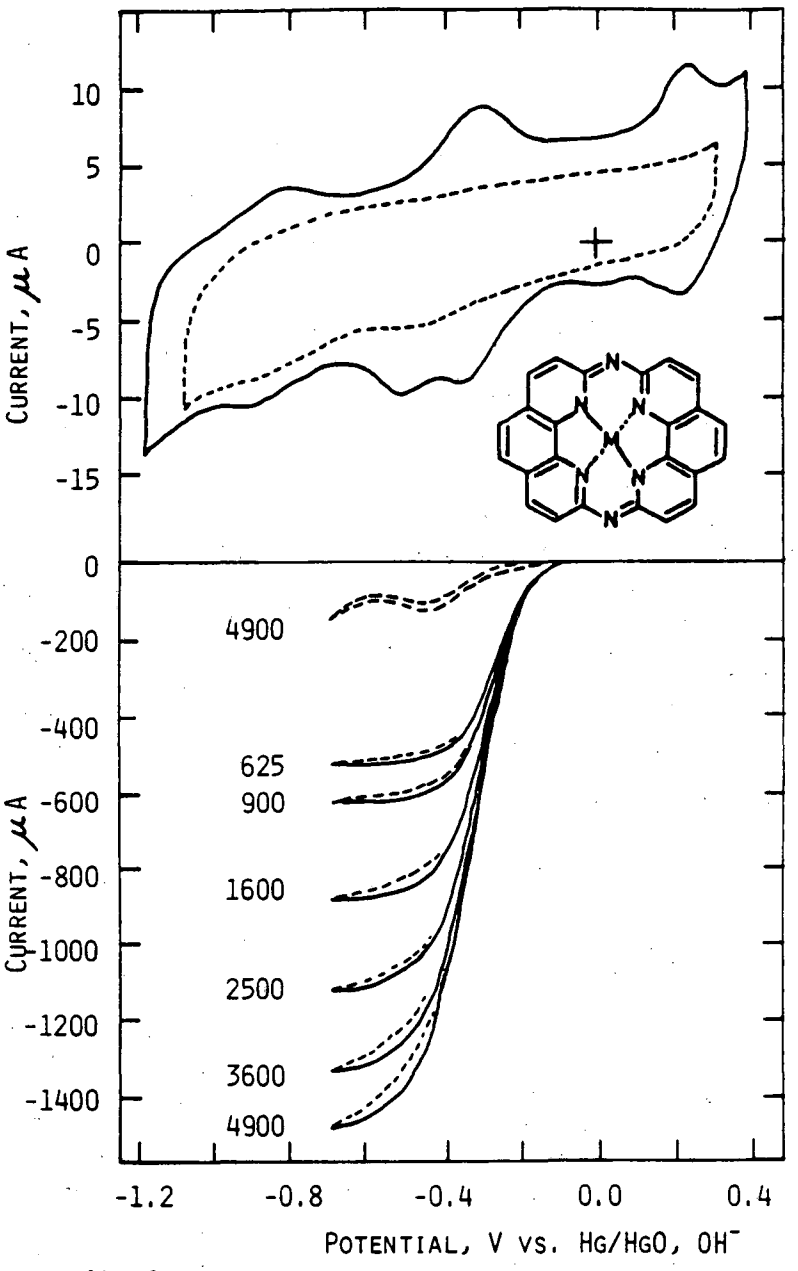

FIG. 1-1 A) CYCLIC VOLTAMMETRY FOR PRE-ADSORBED IRON HEXA-AZA-MACROCYCLE ON ORDINARY PYROLYTIC GRAPHITE (OPG) IN N_2-SATURATED 0.1 M NaOH AT 0.5 V s^{-1} (DASHED CURVE IS FOR OPG) AND B) CORRESPONDING DISK CURRENTS FOR O_2 REDUCTION AT VARIOUS ROTATION RATES (RPM) AT 20 mV s^{-1} (DASHED CURVE IS FOR OPG. DISK AREA = 0.196 cm^2.

are shown in Fig. 1-1 for the stationary electrode in N_2 saturated solution (A) and for the rotating electrode in O_2 saturated solution (B). The intrinsic voltammetry (A) exhibits three main redox transitions, with reversible potentials (obtained by averaging the cathodic and anodic peak potentials) of -0.86 V, -0.31 V and +0.20 V vs. $Hg/HgO,OH^-$. There are extra cathodic peaks at -0.60 V and 0.0 V which do not have anodic counterparts. It is not known at this time whether these are intrinsic to the macrocycle or not, but it is possible that they are due to processes involving coupled chemical reactions (see discussion below). The potentials, converted to the SCE scale, are compared with those for FeTSPc, CoHAM and CoTSPc in Table 1-1.

The charge associated with the cathodic peak at -0.30 V is 7.5 μC cm^{-2}. Assuming a one electron process and a molecular area of about 160 $Å^2$, this corresponds to a coverage of about 0.75 of a monolayer.

The rotating disk currents for O_2 reduction at -0.7 V vs. Hg/HgO, OH^- (Fig. 1-1B) yield a linear Levich plot (current vs. square root of rotation rate) with a slope corresponding to n = 3.17 electrons transferred, using the diffusion coefficient and solubility for O_2 reported in the literature for 0.1 M KOH as the values for NaOH (3). This n value indicates one of three possibilities: a) some contribution of a direct four-electron reduction of O_2 to OH^-; b) some further reduction of peroxide to OH^-; or c) chemical decomposition of peroxide followed by reduction of the O_2 produced. Further experiments can determine which pathway is being followed. This n value is to be compared with that obtained for FeTSPc by Zagal et al., 3.3 from the Levich plot or 3.1 from the $(\text{current})^{-1}$ vs. $(\text{rotation rate})^{-1/2}$ plot, at potentials positive of -0.60 V (4). It should be noted however that for O_2 reduction on FeTSPc/OPG at potentials more positive than about -0.4 V vs. SCE, there was no detectable ring current due to peroxide oxidation, a clear indication of the four electron reduction to OH^- over this potential range.

The onset of O_2 reduction as catalyzed by metal-macrocyclic complexes can often be associated with a particular redox transition of the complex, and it has been suggested that a redox mediator type mechanism is involved (5). The redox process for FeTSPc with which O_2 reduction is associated is the one at -0.09 V vs. SCE (see Table 1-1), while that for FeHAM is at -0.40 V vs. SCE. These assignments are based on the respective peak potentials for O_2 reduction, also listed in Table 1-1. The particular redox process for FeTSPc has been characterized as being predominantly Fe(III/II) in character (6). It would be reasonable to expect that the redox process at -0.40 V for FeHAM is also Fe(III/II). This can be checked using <u>in situ</u> Mossbauer spectroscopy , as was already done at Case for FeTSPc (7).

At the more negative potentials, the n value for O_2 reduction on FeTSPc becomes appreciably lower, while that for FeHAM remains nearly the same. It has been suggested (7) that the decrease in current for FeTSPc is associated with the redox process at -0.47 V vs. SCE, which has been assigned to Fe(II/I) (6). It may be that the Fe(I) complex is less active for processes leading to OH^- as a product (6). The corresponding process for FeHAM occurs at a more negative potential, -0.95 V vs. SCE.

TABLE 1-1

Comparison of redox potentials for transition metal hexa-aza-macrocycles (MeHAM) and tetrasulfonated phthalocyanines (MeTSPc)[a] in 0.1M NaOH and pH 12.8 buffer, respectively, at 25°C.

	Potentials,[b] V vs. SCE					
	Ar-saturated solution					O_2-saturated[c]
CoHAM[d]	-1.03	-0.81	0.50	-	+0.11	-0.36
CoTSPC	-1.36	-	-0.50	-	+0.53	-0.37
FeHAM[d]	-0.95	-	-0.40	-	+0.11	-0.43
FeTSPC	-1.30	-	-0.47	-0.09	+0.44	-0.20

[a] data from Ref. 4.

[b] average of cathodic and anodic voltammetric peak potentials.

[c] cathodic peak potential at 500 mV s^{-1}.

[d] potentials were measured with respect to a Hg/HgO (0.1M OH-) reference electrode and were converted to the SCE scale by subtracting 87 mV.

Thus a current decrease is not seen within the potential range examined in Fig. 1-1. Behavior similar to that for FeTSPc has also been observed for a similar compound, iron tetra-2,3-pyridinoporphyrazine, in which the outer benzo rings of phthalocyanine are replaced by pyridino rings (7).

It may be noted from Table 1-1 that the O_2 reduction peaks for CoHAM and CoTSPc occur at almost the same potential and that the associated intrinsic redox transition also occurs at the same potential, -0.50 V vs. SCE. This transition for CoTSPc has been proposed to be Co(II/I) (6).

Molecular orbital energy levels for FeHAM were calculated using a modified version of the extended Huckel method, the atom superposition - electron delocalization (ASED) molecular orbital method, developed by Anderson and Hoffman (8). Results are presented in Fig. 1-2.

The Fe $3d_{xz}$ orbital is perturbed very little after complex formation because the d_{xz} lobes lie between the aza nitrogens. The Fe $3d_{z}2$ orbital is raised slightly in energy due to an antibonding interaction of the annular shaped lobe with the aza nitrogens. The d_{yz}, $d_{x}2_{-y}2$ and d_{xy} orbitals are raised in energy to an increasing extent due to antibonding interactions with the aza nitrogens. The unpaired electron in the d_{yz} orbital and the electron pair in the $d_{z}2$ orbital of the Fe(II) complex can interact with one of the two unpaired $2p\pi_{g}^{*}$ electrons in dioxygen (9) (see Fig. 1-3).

The most important finding is that the electron density is relatively high at the Fe center and the resulting charge is +1.4, compared to +1.7 for iron porphyrin and +2.0 for iron phthalocyanine (FePc). This is because there is very little back-donation of electron density from the metal to the high-lying antibonding orbitals of the ligand. These levels are so high in energy because of the absence of conjugation across the two bridging nitrogens. In effect the two phenanthroline moieties are electronically isolated from each other.

The somewhat high electron density at the Fe center is consistent with the fact that the FeHAM III/II and II/I transitions (tentatively assigned) lie to the negative of those for FeTSPc by about 0.3 and 0.5 V respectively (Table 1-1). This is true if one assumes that the extra electron density due to the one electron reduction is localized on the Fe center. The calculated energy levels for the lowest half-occupied molecular orbitals for FePc and FeHAM are also about 0.5 eV apart: -10.4 eV (FePc, $d_{z}2$) and -9.9 eV (FeHAM, d_{yz}). (Note - the MO structures for FePc and FeTSPc are very similar.) The difference in the reversible potentials obtained from the voltammetry for the Fe(II/I) transition for the two compounds, FeHAM and FeTSPc, was also 0.5 V, but the agreement is somewhat fortuitous. It should not have been expected to be this good, due to inadequacies of the calculation method, differences in solvation, etc.

The high electron density at the iron center calculated for FeHAM means that it should have a high affinity for O_2. By analogy with the iron porphyrins, FeHAM should form a μ-oxo complex in the presence of air. It has been found by Kadish et al. (10) that the reduction of μ-oxo-tetraphenylporphyrin $(FeTPP)_2O$ in non-aqueous solution leads to two

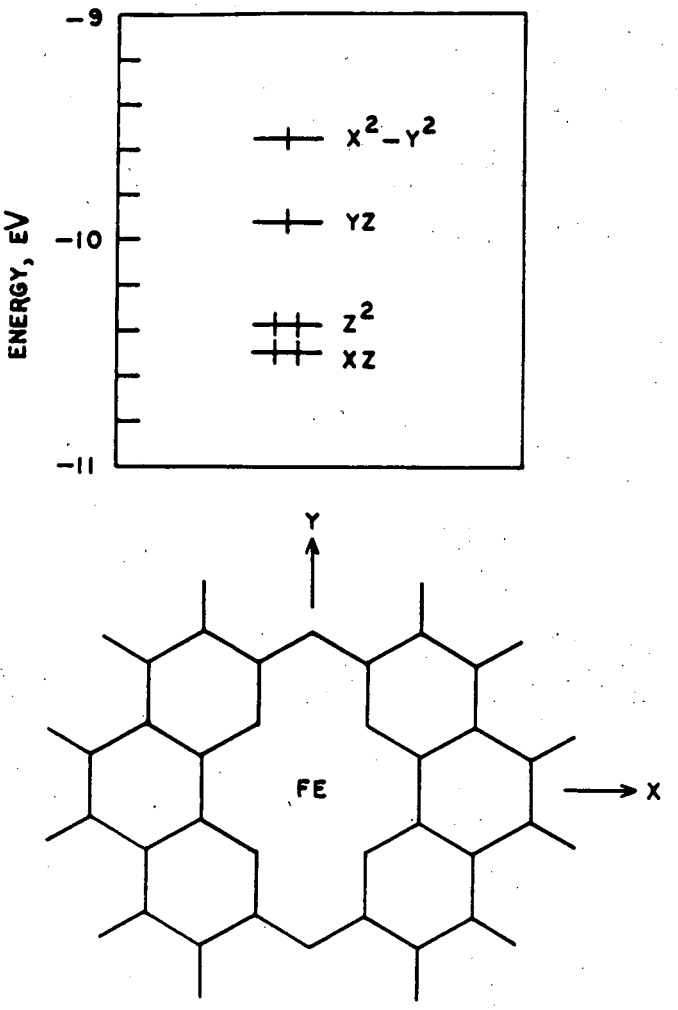

FIG. 1-2 ENERGY LEVELS FOR THE METAL-LIKE MOLECULAR ORBITALS OF IRON HEXA-AZA-MACROCYCLE AS CALCULATED BY THE ASED METHOD. THE UNPERTURBED 3D LEVELS FOR FE ARE AT -10.5 eV.

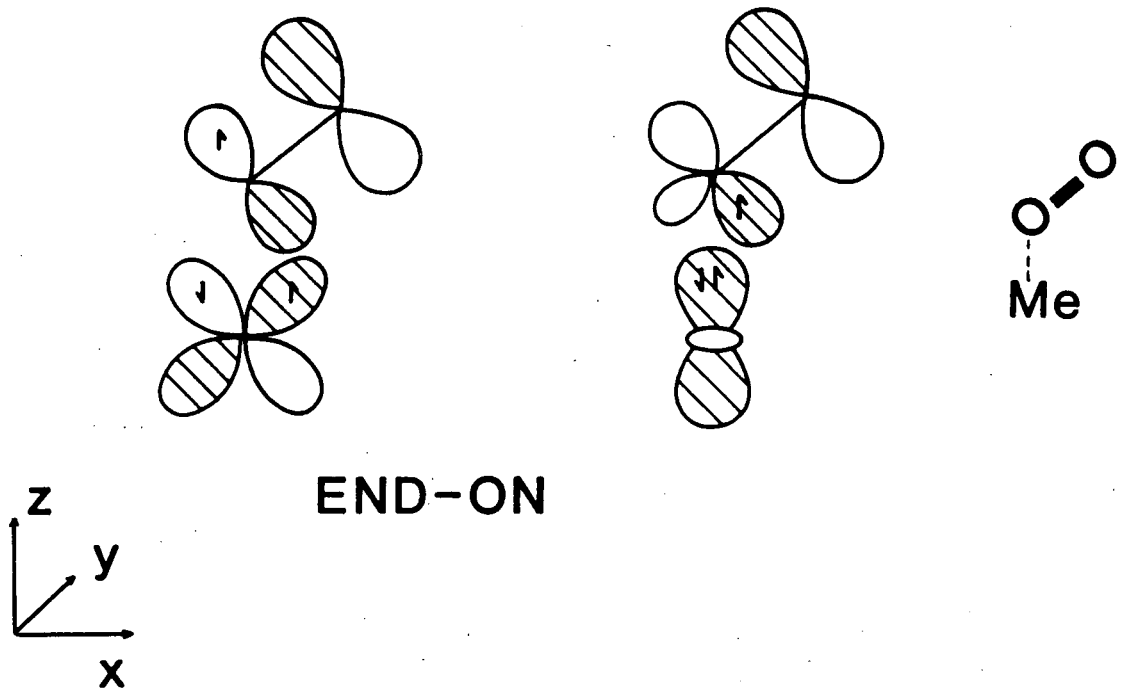

FIG. 1-3 END-ON INTERACTION OF THE $2P\pi_G^*$ ORBITAL FOR DIOXYGEN (ABOVE) WITH THE D_{XZ} (LEFT) AND D_Z^2 (RIGHT) ORBITALS AT A TRANSITION METAL ION.

cathodic peaks which do not have anodic counterparts because of coupled chemical reactions. Among others, the following reaction mechanism has been proposed:

$$[LFe(III)\text{-}O\text{-}Fe(III)L] \xrightarrow{e^-} [LFe(III)\text{-}O\text{-}Fe(II)L]^-$$

$$[LFe(III)\text{-}O\text{-}Fe(II)L]^- \xrightarrow{e^-} [LFe(II)\text{-}O\text{-}Fe(II)L]^{2-}$$

$$\xrightarrow{H^+} [Fe(II)L] + [Fe(II)LOH]^-$$

$$[Fe(II)L]^- \xrightarrow{e^-} [Fe(I)L]^{2-}$$

$$[Fe(II)OH]^- \xrightarrow{e^-} [Fe(I)LOH]^{2-}$$

$$\xrightarrow{H^+} [Fe(I)L]^- + H_2O$$

$$[Fe(I)L]^- \xrightarrow{e^-} [Fe(I)L]^{2-}$$

where L = TPP. It is possible that the extra cathodic peaks in the FeHAM voltammetry may have a similar explanation.

The stability of the cobalt and iron hexaazamacrocycles over the long term under fuel cell operating conditions has not been tested as of yet. The research thus far has been concerned more with questions of intrinsic activity. The question of stability, including the possible beneficial effects of heat treatment, will be addressed in future work.

1.4 SUMMARY

The O_2 reduction behavior in alkaline solution at room temperature and associated redox transition (probably Co II/I) are similar for CoHAM and CoTSPc. O_2 is reduced quantitatively to peroxide. For the corresponding iron compounds however the O_2 reduction peak occurred at somewhat more negative potentials for the FeHAM compared with FeTSPc. The redox transition in the complex which appears to be involved in the O_2 reduction electrocatalysis in alkaline solution has been regarded as Fe(III/II) for FeTSPc (6). The redox transition for FeHAM which occurs at a somewhat more negative potential than that for FeTSPc and is also associated with O_2 reduction has thus been assigned also to Fe(III/II). These findings are consistent with molecular orbital calculations which showed that there is very little back-donation of electron density from the metal d orbitals to the antibonding orbitals of the ligand. The resulting electron-rich center should be more difficult to reduce, as found experimentally. It should also have high affinity for O_2 and may form a μ-oxo complex. The potential region over which the O_2 reduction occurs with substantially greater than 2 electrons is wider for FeHAM however because the Fe(II/I) couple lies at a much more negative potential than that for FeTSPc.

References

1. S. Ogawa, T. Yamaguchi and N. Gotoh, J. Chem. Soc., Perkin Trans. I, 1974, 1976

2. S. Ogawa, J. Chem. Soc., Perkin Trans. I, 1977, 214

3. R. E. Davis, G. L. Horvath and C. W. Tobias, Electrochim. Acta, 12, 287 (1967)

4. J. Zagal, P. Bindra, and E. Yeager, J. Electrochem. Soc., 127, 1506 (1980)

5. F. Beck, J. Appl. Electrochem., 7, 239 (1977)

6. S. Zecevic, B. Simic-Glavaski, E. Yeager, A. B. P. Lever and P. C. Minor, submitted for publication

7. W. Aldred, C. Fierro, S. Gupta, B. Simic-Glavaski and E. Yeager, "Transition Metal Macrocycles and Related Complexes as Catalysts for Oxygen Electrodes," Final Report, Subcontract No. 4523410, Lawrence Berkeley Laboratory and the U. S. Department of Energy, July 1984

8. A. B. Anderson and R. Hoffmann, J. Chem. Phys., 60, 6271 (1974)

9. J. A. Fèe and J. S. Valentine, In "Superoxide and Superoxide Dismutases," A. M. Michelson, J. M. McCord and I. Fridovich, Editors, Academic Press, London, 1977, pp. 19-60

10. K. M. Kadish, G. Larson, D. Lexa and M. Momenteau, J. Am. Chem. Soc., 97, 282 (1975)

SECTION 2

II. OXYGEN AND HYDROGEN PEROXIDE REDUCTION ELECTROCATALYSIS BY TETRASULFONATED PHTHALOCYANINE ADSORBED ON GRAPHITE ELECTRODES

Z. B. Chen, D. Tryk and E. Yeager

2.1 SUMMARY

The iron and cobalt phthalocyanines and tetrasulfonated phthalocyanines (TSPc) have received a fair amount of attention as O_2 reduction electrocatalysts -- especially in recent years because of the demonstrated ability of FeTSPc to act as a four-electron O_2 reducer in alkaline solution (1). Some understanding of CoTSPc and FeTSPc in aqueous solutions and adsorbed on electrodes has been achieved via electrochemical measurements (1-3), relectance spectroscopy (4), Raman spectroscopy (5,6), and uv-visible absorption spectroscopy (7). A definitive understanding of the complex behavior of these compunds has yet to be achieved however.

An interesting aspect of the TSPc's is their tendency to form stacked dimers and higher aggregates. These may be important for O_2 reduction insofar as they may provide bimetallic coordination sites at which O_2 may be bridged. Such sites appear to be especially favorable for the four-electron process, as in the often-cited work of Collman et al. (8).

The present work, still in progress, focuses on oxygen and peroxide reduction catalysis by CoTSPc, and is an extension on the earlier work of Zagal et al. (1,2). Only a brief synopsis of the preliminary results will be given here.

Over the pH range 4 - 10 it was found that CoTSPc adsorbed on ordinary pyrolytic graphite (with a 10^{-5} M concentration of the complex present in the solution) catalyzed the apparent reduction of hydrogen peroxide with a voltammetric peak potential of ~-0.65 V vs. SCE. This potential was surprisingly invariant over this wide pH range. The effect was not observed at low (<1) and high pH (>13), consistent with the results of Zagal et al. (1,2).

It is probable that the mechanism for this apparent reduction process involves a potential - dependent peroxide decomposition step followed by reduction of the generated oxygen:

$$2H_2O_2 \text{ ----> } O_2 + 2H_2O \quad [1]$$

$$O_2 + 2H^+ + 2e^- \text{ ----> } H_2O_2 \quad [2]$$

$$\text{Sum: } H_2O_2 + 2H^+ + 2e^- \text{ ----> } 2H_2O \quad [3]$$

This mechanism can be somewhat difficult to distinguish from direct peroxide

reduction, but the voltammetric and rotating disk results point in this direction.

There are two possible explanations for the pH dependence of this phenomenon. The first is that step [1] actually requires the presence of the peroxide anion HO_2^- to be kinetically favored. This possibility has been discussed for the case of peroxide decomposition catalyzed in homogeneous solution by FeTSPc by Waldmeier and Sigel (9). They have shown that both FeTSPc and CoTSPc show a peak in the peroxide decomposition rates in solution at ~pH 8 (10). For the FeTSPc case they propose a pH dependent pathway involving HO_2^- (9).

The second possibility is that the pH dependence of the peroxide decomposition is due to the intrinsic pH dependence of the Co(II)TSPc / Co(I)TSPc redox potential, which is constant over the pH range 7-11 (3). This would account for a shift in the potential at which the apparent peroxide reduction is observed but not the experimentally observed decrease in current at low and high pH. The very low concentration of HO_2^- at low pH would account for the decrease in apparent peroxide reduction current. The decrease in current at high pH remains to be explained however.

References

1. J. Zagal, P. Bindra and E. Yeager, J. Electrochem. Soc., 127, 1506 (1980).
2. J. Zagal, R. Sen and E. Yeager, J. Electroanal. Chem., 83, 207 (1977).
3. S. Zecevic, B. Simic-Glavaski, E. Yeager, A. B. P. Lever and P. C. Minor, manuscript in preparation.
4. B. Z. Nikolic, R. R. Adzic and E. Yeager, J. Electroanal. Chem., 103, 281 (1979).
5. R. Kotz and E. Yeager, J. Electroanal. Chem., 113, 113 (1980).
6. B. Simic-Glavaski, S. Zecevic and E. Yeager, manuscript in preparation.
7. B. Simic-Glavaski, S. Zecevic and E. Yeager, manuscript in preparation.
8. J. P. Collman, P. Denisevich, Y. Konai, M. Marrocco, C. Koval and F. C. Anson, J. Am. Chem. Soc., 102, 6027 (1980).
9. P. Waldmeier and H. Sigel, Inorg. Chim. Acta, 5, 659 (1971).
10. P. Waldmeier and H. Sigel, Chimia, 24, 195 (1970).

SECTION 3

O_2 REDUCITON KINETICS AND MECHANISM ON GLASSY CARBON AND GOLD ELECTRODES IN ACETONITRILE

Z. W. Zhang, F. L. Zhao, D. Tryk and E. Yeager

3.1 SUMMARY

In order to examine differences between O_2 reduction mechanisms on different electrode materials in greater detail, the use of aprotic nonaqueous solvents has become extremely useful. The initial electron transfer, presumably without chemical complications, can be observed and heterogeneous electron transfer rate constants measured. Proton donors such as phenol, perchloric acid or water can then be added to examine the effect on the course of the reaction. Highly ordered pyrolytic graphite (HOPG), glassy carbon (GC) and gold electrodes have been examined thus far in acetonitrile and the heterogeneous electron transfer rates were largest for GC followed by Au with HOPG the lowest.

With the addition of 0.5 - 1.5 M H_2O, dramatic differences were found in the nature of the chemical reactions. On GC a second reduction peak at potentials negative of the O_2/O_2^- peak appeared, which is presumed to be reduction of $O_2^{\cdot -}$. In contrast, on Au the O_2/O_2^- peak doubles in height, indicating a fast ECE or disroportionation type process. This is thought to be the same mechanism which was postulated by Zurilla et al. (1) for O_2 reduction on Au in alkaline solution:

$$O_2 + e^- \longrightarrow O_2^{\cdot -}\ (ads)$$

$$2O_2^{\cdot -}(ads) + H_2O \longrightarrow HO_2^-(ads) + O_2 + OH^-$$

in which the O_2 is recycled, leading to a doubling of the current. Thus there is large difference in the reactivity of the Au and GC surfaces with superoxide in the presence of water. Some of these phenomena have also been observed by Sawyer et al. (2).

This work will be reported more fully in the next annual report since much of the work was done after February 1984.

Reference

1. R. W. Zurilla, R. K. Sen and E. Yeager, J. Electrochem. Soc., 125, 1103 (1978).

2. D. T. Sawyer, G. Cheiricato, C. T. Angelis, E. J. Nanni and T. Tsuchiya, Anal. Chem., 54, 1720 (1982).

SECTION 4

OXYGEN REDUCTION ON GRAPHITE ELECTRODES WITH ADSORPTIVELY AND CHEMICALLY ATTACHED QUINONES

M. S. Hossain, Z. W. Zhang, D. Tryk and E. Yeager

4.1 INTRODUCTION

Dioxygen reduction to hydrogen peroxide in alkaline solution is catalyzed by carbon and graphite surfaces.

$$O_2 + H_2O + 2e^- \rightleftharpoons HO_2^- + OH^- \qquad (4\text{-}1)$$

The edge plane of highly oriented pyrolytic graphite (HOPG) is catalytic whereas the basal plane is almost inert (1). It is well known that carbon surfaces can be covered by a variety of surface functional groups, the commonest ones being carboxyl, phenolic hydroxyl, quinone-type carbonyl and normal lactone (2). The question is which type of functionality is responsible for the catalysis. There are indications that surface oxidative treatments of carbons which tend to increase the coverage of quinones also make the surface more active for O_2 reduction in alkaline solution (3). The present research attempts to examine the hypothesis that quinones can operate as catalysts for O_2 reduction by using graphite electrodes with either adsorptively or chemically attached quinones.

4.2 BACKGROUND

The idea of a reduced quinonoid surface functionality on carbon surfaces as a reductant for O_2 was formulated by Garten and Weiss (4). They also hypothesized the existence of a chromene/carbonium ion couple as an alternative to the quinone/hydroquinone couple (4), but such surface groups have never been shown unequivocally to exist on carbon surfaces.

The kinetics of the solution phase reaction of hydroquinones with dioxygen was examined by LuValle and Weissberger (5), who found that for several different hydroquinones the reaction was catalyzed by the presence of the quinone species. They also found that the reaction rate was limited by the rate at which the hydroquinone and quinone could undergo the reverse of disproportionation (conproportionation) to form the semiquinone species.

$$R + T \rightleftharpoons 2S \qquad (4\text{-}2)$$

where R is the reduced species (i.e. hydroquinone), T the oxidized species (quinone) and S the semiquinone. They used weakly alkaline ethanol-water solutions, in which the semiquinone should be relatively stable.

Patel and Willson (6) used pulse radiolysis to measure the rate constants for the forward and reverse reactions of quinone radical anion $Q^{\cdot -}$ with O_2 in isopropanol - acetone - water solutions (usually 95% water).

$$Q^{\cdot -} + O_2 \rightleftharpoons Q + O_2^{\cdot -} \qquad (4\text{-}3)$$

The rate constants ranged from 0.2×10^9 to 2.8×10^9 M^{-1} s^{-1} for the forward reaction for several quinonoid compounds whose redox potentials were more negative than +0.05 V vs. SHE. For compounds with redox potentials more positive than +0.18 V, the forward reaction exhibited negligible rates whereas the reverse reaction had large rate constants. Similar methods have been used to determine the standard redox potential for dioxygen reduction to superoxide (7).

$$O_2 + e^- \rightleftharpoons O_2^{\cdot -} \qquad (4\text{-}4)$$

The use of reduced quinones to produce hydrogen peroxide from dioxygen is a well-established industrial process (8). Carbon blacks impregnated with polymeric quinones have also been used in the electrolytic production of peroxide (9).

4.3 EXPERIMENTAL METHODS

The experiments were carried out using voltammetry and the rotating disk electrode technique in an all-Teflon cell with separate compartments for the counter and reference electrodes. The reference electrodes were Hg/HgO, OH^- of the appropriate concentration. A Teflon Luggin capillary was used to minimize iR drop, with its tip approx. 3 mm below the surface of the rotating disk electrode. A gold foil counter electrode was used. The electrolytes, either 1.0 or 0.1 M NaOH were prepared from 50% solution (Fisher, low in carbonate) and diluted with distilled, reverse osmosis purified water. The highly ordered pyrolytic graphite (HOPG) and ordinary pyrolytic graphite (OPG) were obtained from the Union Carbide Corp., Carbon Products Div., Parma, Ohio. These graphites were mounted in Kel-F using molding powder (Minnesota Mining and Mfg.). The surface of the HOPG electrode was prepared prior to each experiment by peeling a layer from the graphite surface using adhesive tape. The OPG electrode was polished with 0.05 μm γ-alumina.

The 1,4-naphthoquinone was obtained from Eastman Kodak, 2-amino-9,10-anthraquinone from Aldrich and 9,10-anthraquinone-2-SO_3^- and 1-amino-9,10-anthraquinone from Fluka and were used as received. The 1,4-naphthoquinone and 9,10-anthraquinone-2-SO_3^- were adsorbed on the electrode by rotating it in the aqueous solution (10^{-3} M) for 30 min. and then gently rinsing it with distilled water. The chemical attachment procedure involved oxidation of the OPG surface with aqueous potassium peroxydisulfate solution, treatment with thionyl chloride and amidization with either 1- or 2-amino-9,10-anthraquinone.

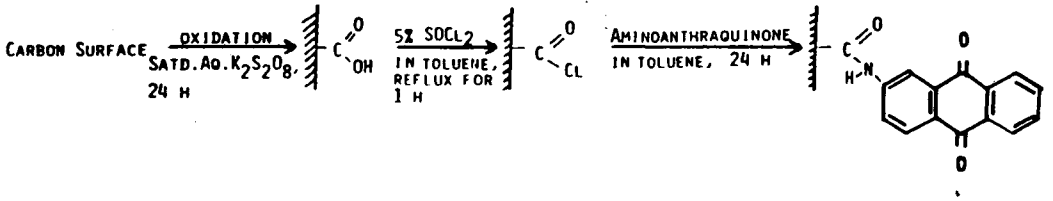

This procedure is similar to that described by Sharp (10) except that the OPG was not impregnated with wax and toluene was used as the solvent instead of benzene. In addition, the electrode with the chemically attached quinone was given a final soaking in distilled water for 48 h in order to remove adsorbed material.

4.4. RESULTS AND DISCUSSION

4.4.1 Adsorbed Quinones

The voltammetry in 1.0 M NaOH solution under inert atmosphere and the rotating disk polarization curves for O_2 reduction in O_2 saturated solution for 9,10-anthaquinone-2-SO_3^- (AQS) preadsorbed on HOPG are shown in Fig. 4-1. The voltammetry exhibits two sets of peaks, one centered at -0.50 V vs. Hg/HgO and the other at -0.64 V, both with peak separations of about 90 mV, which indicates some degree of non-reversibility (Table 4-1). These midpoint potentials are more negative than those determined by Gill and Stonehill (11) in 0.1 M NaOH solution (pH = 12.87), -0.454 V and -0.490 V vs. Hg/HgO (after conversion from SCE) for the two one-electron reductions of quinone, first to the radical anion and then to the dianion in aqueous solution (Table 4-2). The shift between the two reversible potentials was much smaller in their case (36 mV) compared to that found here (140 mV). Finally the charge under each peak (30 - 46 $\mu C\ cm^{-2}$) corresponds to approximately two equivalent monolayers according to the estimated area of the compound in the flat orientation. Using the bond length data of Soriaga and Hubbard (12) the molecular area is about 112 $Å^2$, which leads to a value of 14 $\mu C\ cm^{-2}$ for a monolayer. It is likely that the molecules are stacked with either their edge or end on the graphite surface in order to achieve these coverages.

These features of the voltammetry can be rationalized fairly simply in terms of the interaction of the quinone with the surface. The negative shift of -0.05 V for the first reversible potential for the adsorbed species vs. the solution species can be caused by a smaller adsorption energy for the radical anion vs. that of the quinone, as discussed theoretically by Wopschall and Shain (13). This could be caused by electrostatic repulsion. The 90 mV shift between cathodic and anodic peaks is probably caused by an inhibited electron transfer rate, which is difficult to rationalize.

The 140 mV difference between the two reversible potentials for the first and second reduction steps for the adsorbed species (as compared with only 36 mV for the solution phase species) may be due to a solvation effect. The degree of solvation possible for the adsorbed species is undoubtedly less than for the solution species and this effect should tend to shift the potential for the second reduction in the negative direction. This phenomenon is observed more dramatically in aprotic non-aqueous solvents, where the absence of strong solvation stabilization of the reduced species causes the reduction potentials to be quite negative.

Literature data obtained for nonaqueous solutions show differences of 0.5 V between the first and second reduction steps (see Table 4-3). When water or other proton donors are added to the nonaqueous solution,

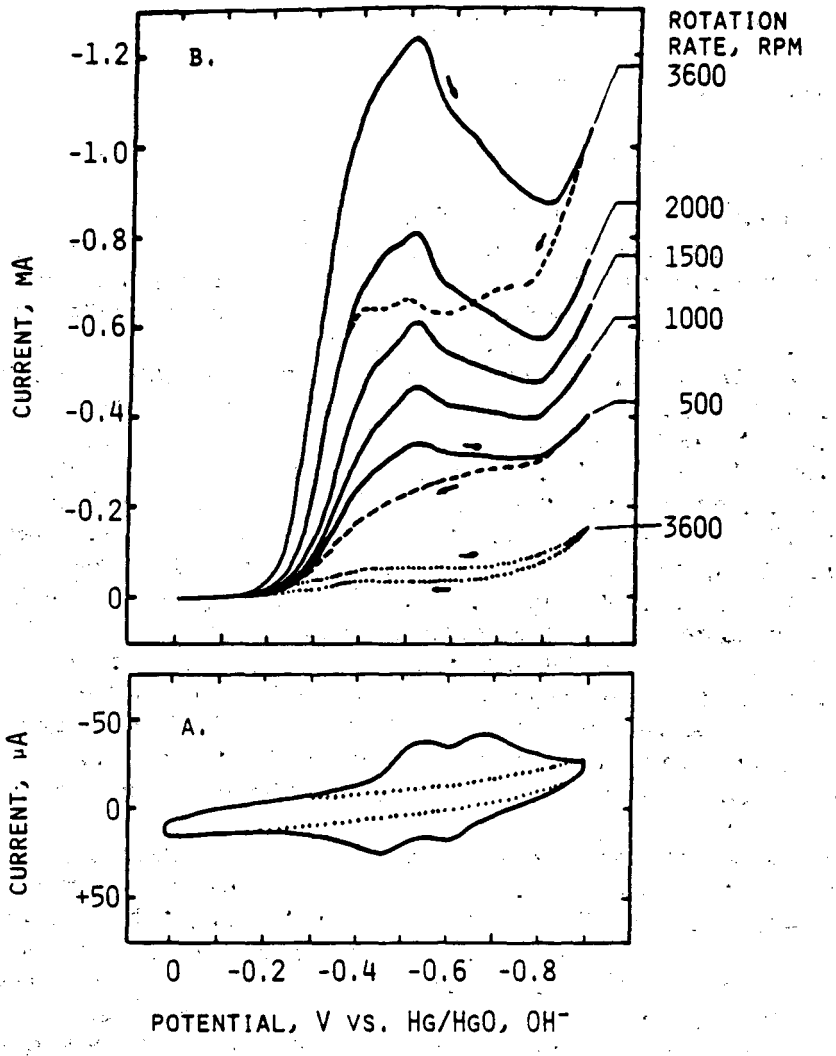

FIG. 4-1. 9,10-ANTHRAQUINONE-2-SO_3^- (AQS) PRE-ADSORBED ON THE BASAL PLANE OF HIGHLY ORIENTED PYROLYTIC GRAPHITE (HOPG) IN 1.0 M NAOH AT 22°C: A) VOLTAMMETRY AT 200 MV S^{-1} IN AR-SATURATED SOLUTION; B) DISK CURRENTS MEASURED AT 20 MV S^{-1} FOR O_2 REDUCTION IN O_2-SATURATED (1 ATM) SOLUTION. ELECTRODE AREA: 0.48 CM^2. CURVES WERE MEASURED IN ORDER OF DECREASING ROTATION RATE. FRESH BASAL PLANE (·····). THEORETICAL DISK CURRENTS FOR A 2-ELECTRON TRANSFER ARE INDICATED AT RIGHT.

TABLE 4-1

Mean Peak Potentials[a] for 1,4-Naphthoquinone and 9,10-Anthraquinone-2-SO_3^- Adsorbed on HOPG and Peak Separations (mV)[b]

compound	E,V vs. Hg/HgO,OH^-		E°, V vs. SHE	
	peak 1	peak 2	peak 1	peak 2
1,4-NQ	-0.29(80)	-0.46(60)	-0.19	-0.36
AQ-2-SO_3^-	-0.50(90)	-0.64(80)	-0.40	-0.54

[a] from the midpoint between cathodic and anodic voltammetric peak potentials.

[b] at a sweep rate of 200 mV s^{-1}.

TABLE 4-2

Thermodynamic Data for 9,10-Anthraquinone-2-SO_3^- in aqueous solution

	Reaction	E,V vs. SHE	pK	G, eV reaction	G, eV of product vs. Q
pH=14	$Q+e^- \rightleftharpoons Q^{\cdot-}$	-0.356*		+0.356	+0.356
	$Q^{\cdot-}+e^- \rightleftharpoons Q^{2-}$	-0.392*		+0.392	+0.748
	$Q+2e^- \rightleftharpoons Q^{2-}$	-0.374*			
	$QH\cdot \rightleftharpoons H^+ + Q^{\cdot-}$		9.02*	-0.295	
	$Q+H^++e^- \rightleftharpoons QH\cdot$	-0.651		+0.651	+0.651
	$QH^- \rightleftharpoons H^+ + Q^{2-}$		11.05*	-0.175	
	$Q+H^++2e^- \rightleftharpoons QH^-$	-0.462		+0.923	+0.923
pH=7	$QH\cdot \rightleftharpoons H^+ + Q^-$		9.02*	+0.120	
	$Q+H^++e^- \rightleftharpoons QH\cdot$	-0.236		+0.236	+0.236
	$Q+2H^++2e^- \rightleftharpoons QH_2$	-0.205		+0.411	+0.411
	$QH_2 \rightleftharpoons H^+ + QH^-$		8.65*	+0.098	
	$Q+H^++2e^- \rightleftharpoons QH^-$	-0.254		+0.509	+0.509
	$QH\cdot+e^- \rightleftharpoons QH^-$	-0.273			
	$QH\cdot+H^++e^- \rightleftharpoons QH_2$	-0.175			
pH=0	$QH\cdot \rightleftharpoons H^+ + Q^-$		9.02*	+0.534	
	$Q+H^++e^- \rightleftharpoons QH\cdot$	+0.178		-0.178	-0.178
	$Q+2H^++2e^- \rightleftharpoons QH_2$	+0.209		-0.418	-0.418
	$QH\cdot+H^++e^- \rightleftharpoons QH_2$	+0.240			
	$QH_2 \rightleftharpoons H^+ + QH^-$		8.65*	+0.512	
	$Q+H^++2e^- \rightleftharpoons QH^-$	-0.047		+0.094	+0.094

Disproportionation Reactions:

$Q+Q^{2-} \rightleftharpoons 2Q^{\cdot-}$ $K^{1/2} = 2.02$ at pH=12.9*

$Q+QH_2 \rightleftharpoons 2QH\cdot$ $K^{1/2} = 0.24$ at pH=7.8*

*Data from Gill and Stonehill (1952)

TABLE 4-3

Polarographic Half-Wave Potentials for Quinone Reduction in Non-Aqueous Solvents, Taken from Chambers (1974) (expressed as ranges of potentials observed by multiple investigators)

A. Acetonitrile, 25°C, with TEAP, TEAI or TBAP*

	$E_{1/2,1}$(SCE)	$E_{1/2,2}$(SCE)
1,4-benzoquinone	-0.48 ~ -0.60	-1.14 ~ -1.33
1,4-naphthoquinone	-0.68 ~ -0.85	-1.25 ~ -1.55
1,2-naphthoquinone	-0.56 ~ -0.58	-1.02 ~ -1.18
9,10-anthraquinone	-0.94 ~ -1.04	-1.45 ~ -1.69
9,10-anthraquinone-2-sulfonate	-0.91 ~ -0.98	-1.40 ~ -1.64

B. Dimethylformamide, 25°C, TEAI*

	$E_{1/2,1}$(Hg pool)	$E_{1/2,2}$(Hg pool)
1-amino-9,10-anthraquinone	-0.42 ~ -0.49	-0.80 ~ -1.04
2-amino-9,10-anthraquinone	-0.54	-1.09
9,10-anthraquinone	-0.38	-1.04

*TEAP = tetraethylammonium perchlorate; TEAI = tetraethylammonium iodide; TBAP = tetrabutylammonium perchlorate

the second reduction potential shifts in the positive direction (14,15).

Table 4-2 and Figs. 4-2 and 4-3 summarize the available thermodynamic data for AQS. Figure 4-2 is a Pourbaix-type diagram and is a diagrammatic version of the experimental data of Gill and Stonehill (11). It shows the potentials for the two possible one-electron transfers as well as that for the two-electron process. It is interesting to note that above pH 10.4 the one-electron reduction of quinone to the radical anion is the favored process, whereas below pH the two electron reduction to either QH^- or QH_2 is favored. Figure 4-3 shows two diagrams of free energy vs. number of electrons transferred, at pH 14 and 7 (after Frost, Ref. 16). These carry essentially the same information but illustrate more vividly the stabilization of the protonated species at pH 7 vs. at 14.

The data presented in Fig. 4-1b show that the onset of O_2 reduction current precedes the onset of current for quinone reduction seen in the voltammetry (Fig. 4-1a) by about 150 mV. This fact may indicate that the O_2 reduction process is extremely sensitive to the presence of the reduced quinone on the surface. The drop in reduction current at more negative potentials and the large hysteresis are consistent with the loss of area under the voltammetry peaks with cycling (not shown) and indicate that the compound is being desorbed. Desorption is probably being facilitated by electrostatic repulsion.

Even though the compound is probably desorbed at the more negative potentials, the currents at the less negative potentials can be used to make a mass transport corrected Tafel plot, i.e. $\log[i_L i/(i_L - i)]$ vs. potential. The limiting current i_L can be estimated using the diffusion coefficient and solubility data for O_2 in KOH solution (18) and assuming a two electron process. Such a Tafel plot (not shown), done for the first trace in Fig. 4-1b (3600 rpm), has two slopes, 65 mV/decade at lower current densities and 89 mV/decade at higher current densities.

Desorption of the compound obviously prevents stable behavior from being obtained. This situation can be alleviated by having the quinone present in the solution, as seen in Fig. 4-4, but the kinetic analysis becomes somewhat more complicated. The reduction of solution phase quinone leads to plateau currents which are in excess of those predicted for the two electron reduction of O_2 to HO_2^-. According to literature data for KOH solutions, which should be reasonably similar to NaOH ones for concentrations of 1 M or less (17,18), the coefficient B in the Levich equation

$$I = Bf^{-1/2} \qquad (4\text{-}5)$$

where I is current in amperes and f is the rotation rate in rpm, should be 1.96×10^{-5} A $rpm^{-1/2}$. This value is based on a two electron reduction and an electrode area of 0.48 cm^2. The calculated currents are shown at the right of the figure.

At the lower rotation rates, the excess disk current can be accounted for by the reduction of the solution phase quinone. This process also involves two electrons according to the published diffusion

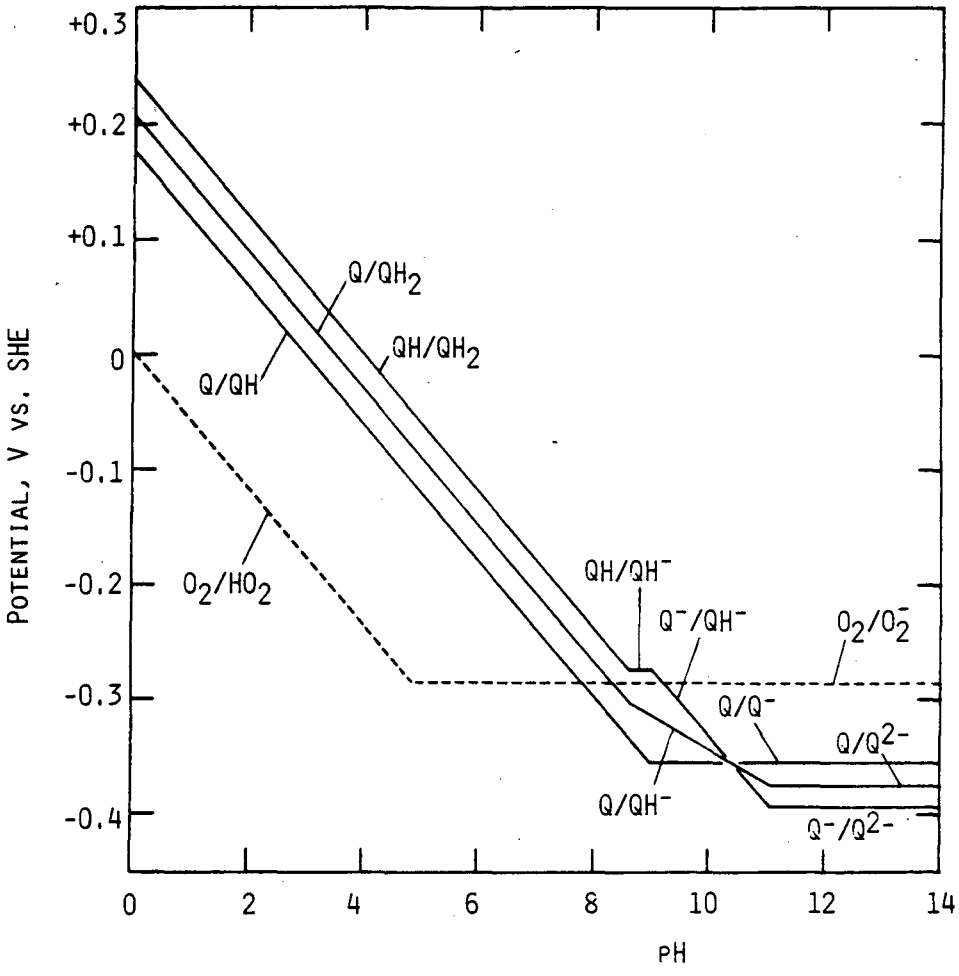

FIG. 4-2. POTENTIAL VS. PH DIAGRAM FOR 9,10-ANTHRAQUINONE-2-SO_3^- IN AQUEOUS SOLUTION AT 25°C. THE POTENTIALS ARE BASED ON 1 M CONCENTRATIONS EXCEPT FOR O_2, WHICH IS BASED ON 1 ATM. VALUES ARE CALCULATED BASED ON DATA OF GILL AND STONEHILL (1952). THE O_2/O_2^- POTENTIAL IS FROM LU ET AL. (1982) AND THE PK FOR O_2^-/HO_2 IS FROM FEE AND VALENTINE (1977).

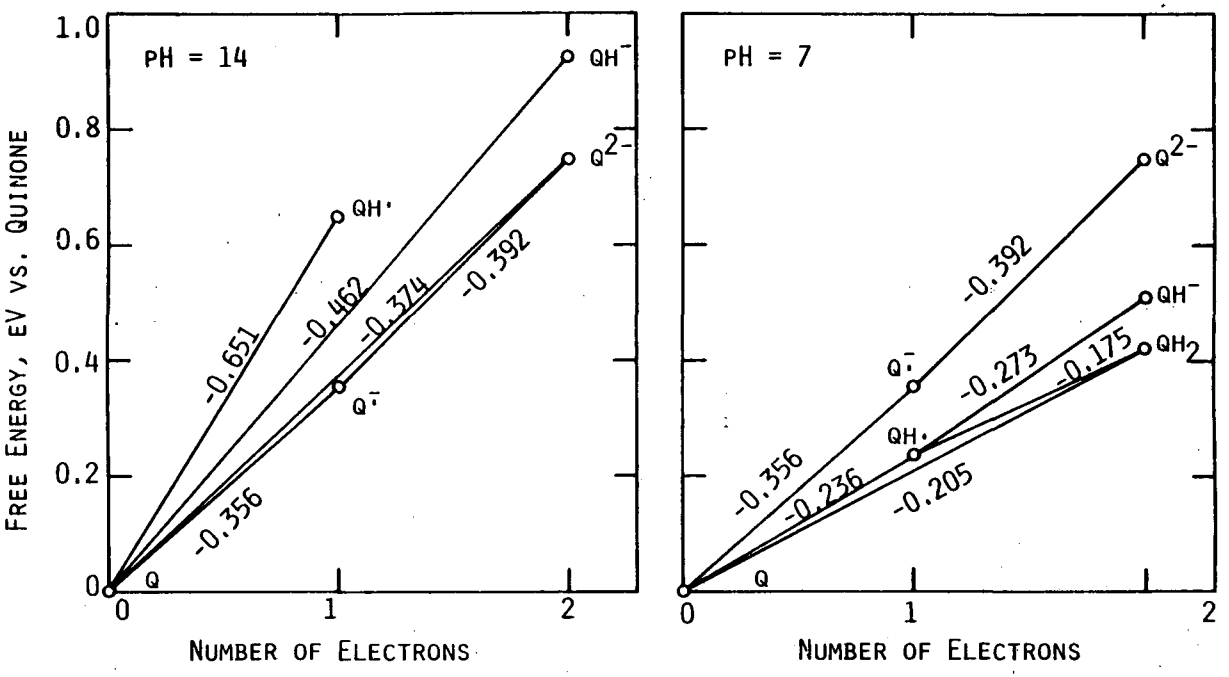

FIG. 4-3. FROST DIAGRAMS (FREE ENERGY VS. NUMBER OF ELECTRONS TRANSFERRED) FOR 9,10-ANTHRAQUINONE-2-SO_3^- IN AQUEOUS SOLUTION AT 25°C AT PH 14 AND 7. Q REFERS TO THE QUINONE WITH A SINGLE NEGATIVE CHARGE DUE TO THE SULFONATE. THE STANDARD ELECTRODE POTENTIALS (V VS. SHE) ARE DESIGNATED. VALUES ARE CALCULATED BASED ON DATA OF GILL AND STONEHILL (1952).

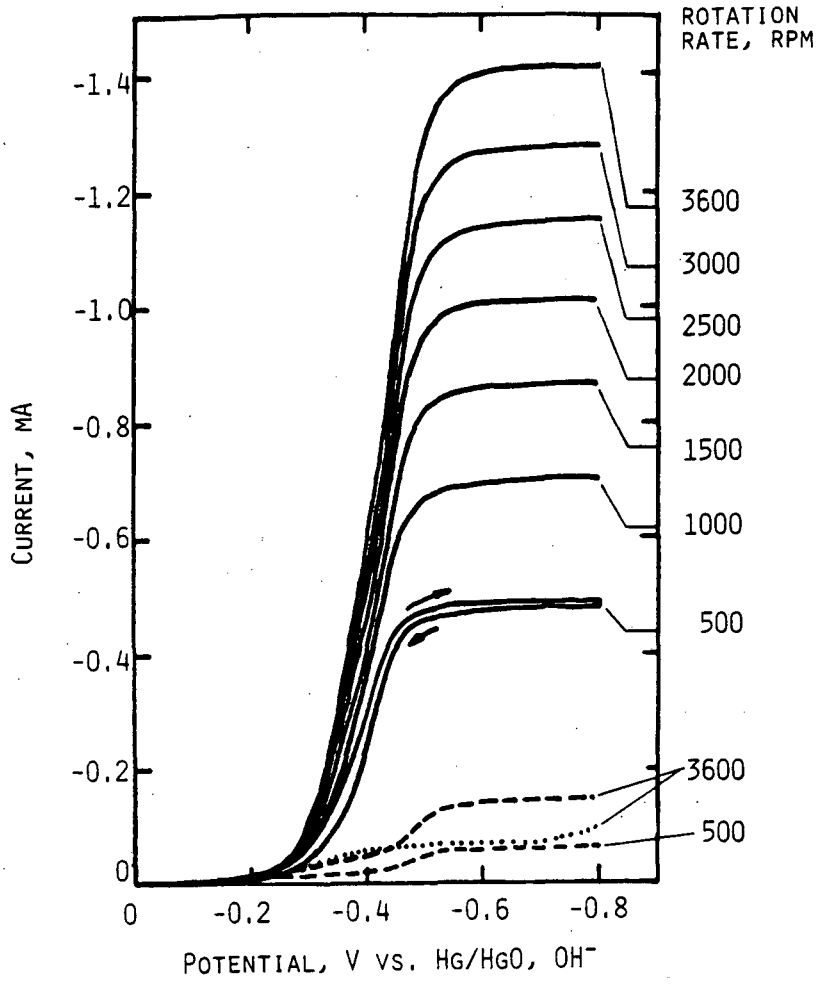

FIG. 4-4. DISK CURRENTS FOR O_2 REDUCTION ON BASAL PLANE HOPG WITH ADSORBED AQS WITH 2 x 10^{-4} M AQS IN SOLUTION IN 1.0 M NAOH AT 22°C. ELECTRODE AREA: 0.48 CM^2. CURVES WERE MEASURED AT 20 MV S^{-1}. AR-SATURATED SOLUTION (---). FRESH BASAL PLANE (···).

coefficient for AQS of 6.15 X 10^{-6} cm^2 s^{-1} (11). For a concentration of 2 X 10^{-4} M, the B value should be 2.76 X 10^{-6} A $rpm^{-1/2}$ and the current should be 0.159 mA at 3600 rpm. At the higher rotation rates, the excess current cannot be completely accounted for in this way, and this fact remains to be explained.

The disk currents for O_2 reduction for the case where the quinone is in solution lie about 100 mV to the negative of the corresponding curves for the preadsorbed quinone case. This is somewhat surprising and may indicate some inhibition for the O_2 reduction when there is a large surface concentration of the quinone.

Rotating disk polarization curves are shown for O_2 reduction on HOPG with pre-adsorbed 1,4-naphthoquinone (NQ) (Fig. 4-5) and for NQ in solution (Fig. 4-6). The voltammetry under inert atmosphere is not shown because of difficulty in obtaining reproducible adsorption. The disk currents for the pre-adsorbed case (Fig. 4-5) are slightly low, again possibly due to decreased coverage after desorption of the compound. As for AQS the first trace, obtained at 3600 rpm, can be used to obtain reliable kinetic data, since the compound is probably not appreciably desorbed until relatively negative potentials. Again the mass transport corrected Tafel plot yielded two slopes, 58 mV/decade and 107 mV/decade at lower and higher current densities respectively. These values are quite similar to those obtained for AQS. In fact the trace for NQ is remarkably similar to that for AQS, and is shifted by only about 10 mV in the positive direction.

The first trace for the preadsorbed NQ lies slightly positive as compared with the corresponding trace with the quinone in solution, but the effect is not as pronounced as for AQS. With NQ in solution the O_2 reduction plateau currents are larger than the predicted ones at the lower rotation rates but the effect disappears at the higher rotation rates. Perhaps the reason may be that the reduction of solution phase NQ is kinetically hindered.

The comparison of NQ and AQS, both pre-adsorbed and in solution is summarized in Fig. 4-7. The predicted current at 500 rpm is shown at the right of the figure. From the lack of a pronounced drop-off in the O_2 reduction currents, it appears that NQ is not as readily desorbed from the electrode as is AQS, perhaps because of the fact that NQ is neutral while AQS is negatively charged.

This figure is slightly misleading in that, for the preadsorbed case, much of the quinone layer has already desorbed by the time the 500 rpm rotation rate trace is recorded. Also the apparent inhibition of O_2 reduction when the quinone is present in solution is a complicating factor. It should be reemphasized that the first traces for O_2 reduction for the two preadsorbed quinones are remarkably similar and are displaced from each other by only about 10 mV.

It would be very interesting to examine the kinetics of the O_2 reduction in more detail with these two compounds, because the electron transfer rate should be different on theoretical as well as experimental grounds. Hale and Parsons (19) showed that the electron transfer rate

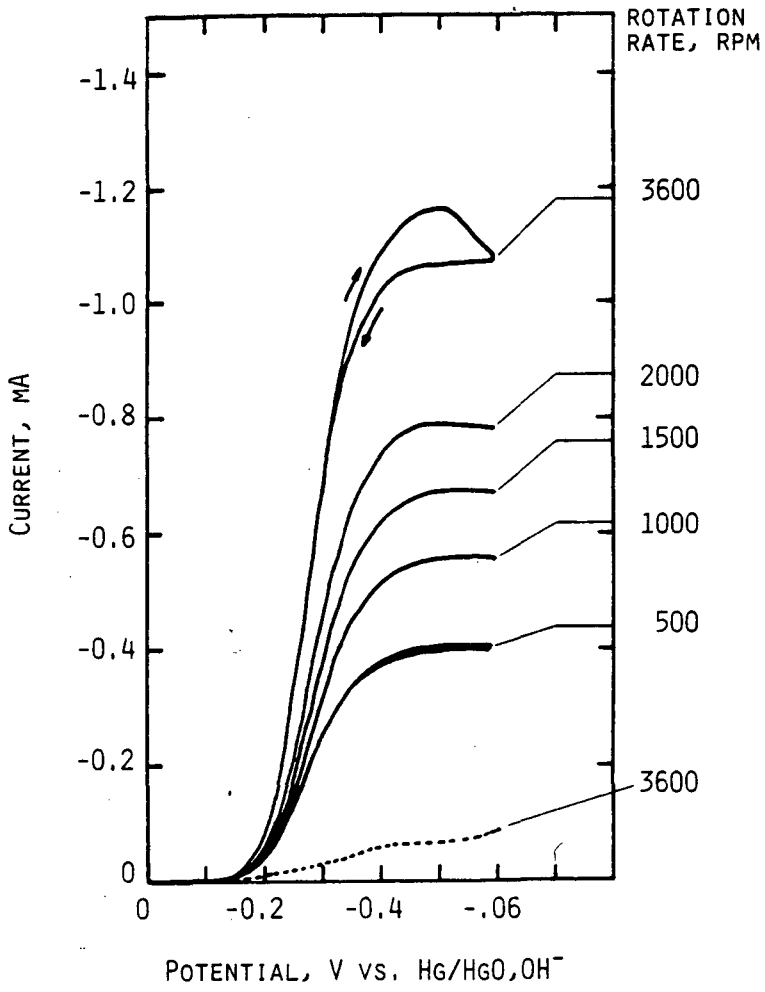

FIG. 4-5. DISK CURRENTS FOR O_2 REDUCTION ON BASAL PLANE HOPG WITH PRE-ADSORBED 1,4-NAPHTHOQUINONE IN O_2-SATURATED (1 ATM) 1.0 M NAOH AT 22°C. ELECTRODE AREA: 0.48 CM^2. CURVES WERE MEASURED AT 20 MV S^{-1} IN ORDER OF DECREASING ROTATION RATE. FRESH BASAL PLANE (···).

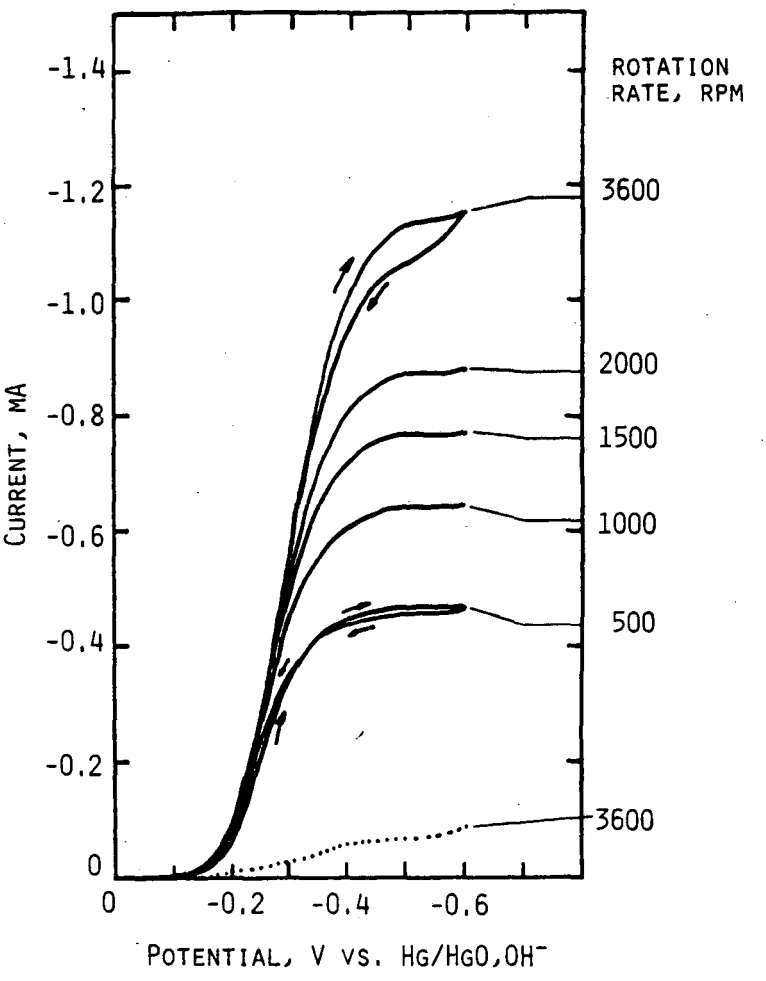

FIG. 4-6. DISK CURRENTS FOR O_2 REDUCTION ON BASAL PLANE HOPG WITH 10^{-4} M 1,4-NAPHTHO-QUINONE IN SOLUTION IN O_2-SATURATED (1 ATM) 1.0 M NAOH AT 22°C. ELECTRODE AREA: 0.48 CM^2. CURVES WERE MEASURED AT 20 MV S^{-1} IN ORDER OF DECREASING ROTATION RATE. FRESH BASAL PLANE (···).

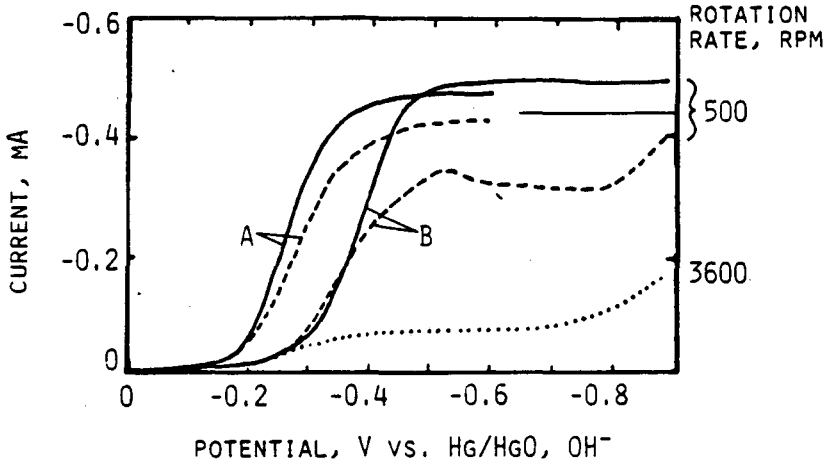

FIG. 4-7. DISK CURRENTS FOR O_2 REDUCTION ON BASAL PLANE HOPG WITH ADSORBED QUINONES IN O_2-SATURATED (1 ATM) 1.0 M NAOH AT 22°C: A) 1,4-NAPHTHOQUINONE; B) 9,10-ANTHRAQUINONE-2-SO_3^-. PREADSORBED QUINONE (---); QUINONE IN SOLUTION (——); (10^{-4} M FOR NQ; 2 x 10^{-4} M FOR AQS).

for quinone reduction should increase with increasingly negative free energy for the conproportionation reaction (Eq. 4-2). This free energy should become more negative as the standard electrode potential for the quinone/radical anion couple is made more negative. Patel and Willson (6) also found that there is a rough correlation between the rate constant for the electron transfer (Eq. 4-3) and the standard electrode potential, with the rate constant increasing as the potential becomes more negative.

From the Tafel slopes of near 60 mV/decade and approaching 120 mV/decade at low and high current densities, respectively, the first few steps of a mechanism could be proposed:

$$Q(ads) + e^- \rightleftharpoons Q^{\cdot -}(ads) \qquad (4\text{-}6)$$

$$Q^{\cdot -}(ads) + O_2 \rightleftharpoons Q(ads) + O_2^{\cdot -} \qquad (4\text{-}7)$$

$$O_2^{\cdot -} + H_2O \rightleftharpoons HO_2^{\cdot} + OH^- \qquad (4\text{-}8)$$

If the second step is rate determining, the current will depend on the surface activity of the reduced quinone, which ideally would respond in a Nernstian fashion:

$$i = Fk(Q^{\cdot -})_s(O_2) \qquad (4\text{-}9)$$

$$(Q^{\cdot -})_s = (Q)_s \exp[(nF/RT)(E - E^{0\prime})] \qquad (4\text{-}10)$$

where the subscript s refers to surface concentration. Assuming the number of electrons n is unity, these equations lead to a Tafel slope of RT/F = 60 mV/decade at 25°C. This is similar to the analysis of Martigny and Anson (24) and of Oyama et al. (25) for O_2 reduction with poly(xylylviologen) coated electrodes. On the other hand, the third step (4-8) could be the rate determining one and this would also lead to a 60 mV/decade slope.

At the higher current densities the electron transfer step (4-6) could become rate determining and the Tafel slope would then become RT/αnF = 120 mV/decade for α = 0.5. Taken together, reactions 4-6 and 4-7 are in effect the same as reaction 4-4, the simple reduction of dioxygen. If this step is rate determining, it would also yield a 120 mV/decade slope. Implicit in the above discussion is the assumption of low surface coverage of the quinone radical anion, so that the coverage is proportional to the surface concentration. A more detailed analysis would take into account the possibility of high coverage.

The fact that the Tafel plots for O_2 reduction with NQ and AQS are so similar could indicate one of two possibilities: 1) that there is a compensation effect, i.e. that although the surface concentration of AQS radical anion is less at any given potential than that for NQ radical anion due to the difference in $E^{0\prime}$ values, the rate constant k in Eq. 4-9 for AQS is greater than that for NQ or 2) that the rate of Eq. 4-8 is rate determining and the individual characteristics of the quinones are relatively unimportant. Further results with a wider range of quinones would be necessary to check this latter possibility.

4.4.2 Chemically Attached Quinones

O_2 reduction activity for the chemically-attached quinones on graphite is stable, which is a distinct advantage over the adsorptively--attached quinones, but the analysis of the data is also slightly more complicated because of the intrinsic activity of the substrate graphite itself in alkaline solution (see Fig. 4- 8). The disk currents for O_2 reduction on the ordinary pyrolytic graphite (OPG) surface have the distinctive profile reported by Morcos and Yeager (1), but they are only about half the predicted value for a two electron transfer. The Levich coefficient for this electrode area (0.196 cm^2) would be 8.0 X 10^{-6} A $rpm^{-1/2}$. At 3600 rpm the predicted current would then be 0.48 mA compared with 0.36 mA in Fig. 4-8. There are several possible reasons for this discrepancy, including 1) that the polishing process causes the surface to begin to resemble somewhat that of the basal plane of HOPG and 2) that the polishing process leaves traces of Teflon or Kel-F as blocking layers on the surface. Experiments are being planned to resolve this question.

The O_2 reduction activity is significantly greater with the chemically-modified surface (Fig. 4-9). The plateau currents approach the predicted values much more closely. The voltammetry in Ar-saturated solution is also shown both for the OPG substrate and for the modified surface (Fig. 4-9b). The latter exhibits a small pair of peaks and a background current which begins increasing at about -0.7 V. The charge under the cathodic and anodic peaks are approximately 7 and 9 $\mu C\ cm^{-2}$ respectively. For the purposes of comparison, an adsorbed monolayer of an anthraquinone of 100 $Å^2$ accepting two electrons would yield a charge of 32 $\mu C\ cm^{-2}$. Sharp (10) obtained approximately 34 $\mu C\ cm^{-2}$ for the voltammetry done in acid solution for graphite with attached 1-amino-9,10-anthraquinone (1-AAQ).

Results were also obtained in 0.1 M NaOH solution, in which the O_2 solubility is higher (Fig. 4-10). The Levich coefficient for this solution with two electrons transferred and an electrode area of 0.196 cm^2 is 1.43 X 10^{-5} A $rpm^{-1/2}$. The plateau currents do not match the predicted ones as closely as in the previous figure. The surface coverage of the quinone is also somewhat less. The charge for the small cathodic peak is approximately 2 $\mu C\ cm^{-2}$. The potential was swept to more negative values and it can be seen that the background current observed in the previous figure was actually part of a larger peak. In Fig. 4-10 the large cathodic peak contains 11 $\mu C\ cm^{-2}$.

There are two steps in the O_2 reduction current which match with the two cathodic peaks in the voltammetry (Fig. 4-10). It is interesting to note that the height of the first step is roughly three times that of the second. This may indicate that the redox process associated with the first small cathodic peak is more important for the electrocatalysis than that for the second peak. The reversible potentials and peak separations for 1- and 2-AAQ in acid and alkaline solution are given in Table 4-4. The value reported for 1-AAQ in acid by Sharp (10) was slightly more positive due to the higher acid concentration (1 vs 0.1 M). Sharp did not observe a peak for 2-AAQ but it may have been obscured by background

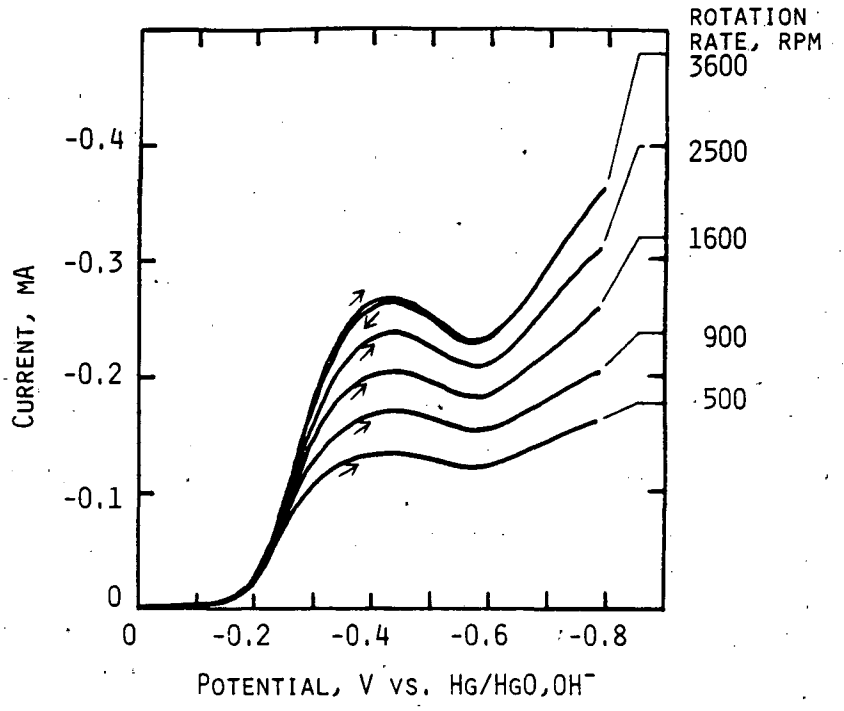

FIG. 4-8. DISK CURRENTS FOR O_2 REDUCTION ON ORDINARY PYROLYTIC GRAPHITE (OPG) IN O_2-SATURATED (1 ATM) 1.0 M NAOH AT 22°C. SWEEP RATE: 20 MV S^{-1}. ELECTRODE AREA: 0.196 CM^2.

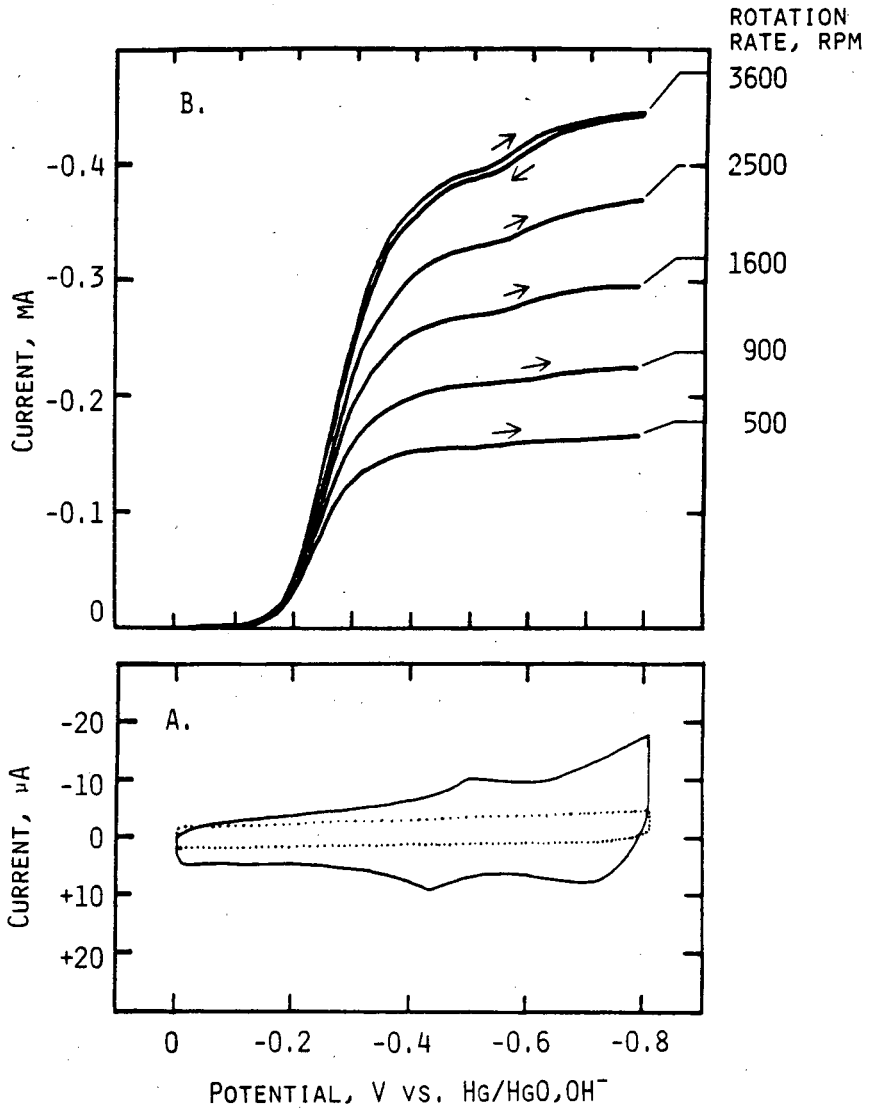

FIG. 4-9. OPG WITH CHEMICALLY ATTACHED 2-AMINOANTHRAQUINONE (AAQ) IN 1.0 M NaOH AT 22°C: A) VOLTAMMETRY AT 200 mV s^{-1} IN Ar-SATURATED SOLUTION; B) DISK CURRENTS MEASURED AT 20 mV s^{-1} FOR O_2 REDUCTION (1 ATM) SOLUTION. ELECTRODE AREA: 0.196 cm^2. UNTREATED OPG (···).

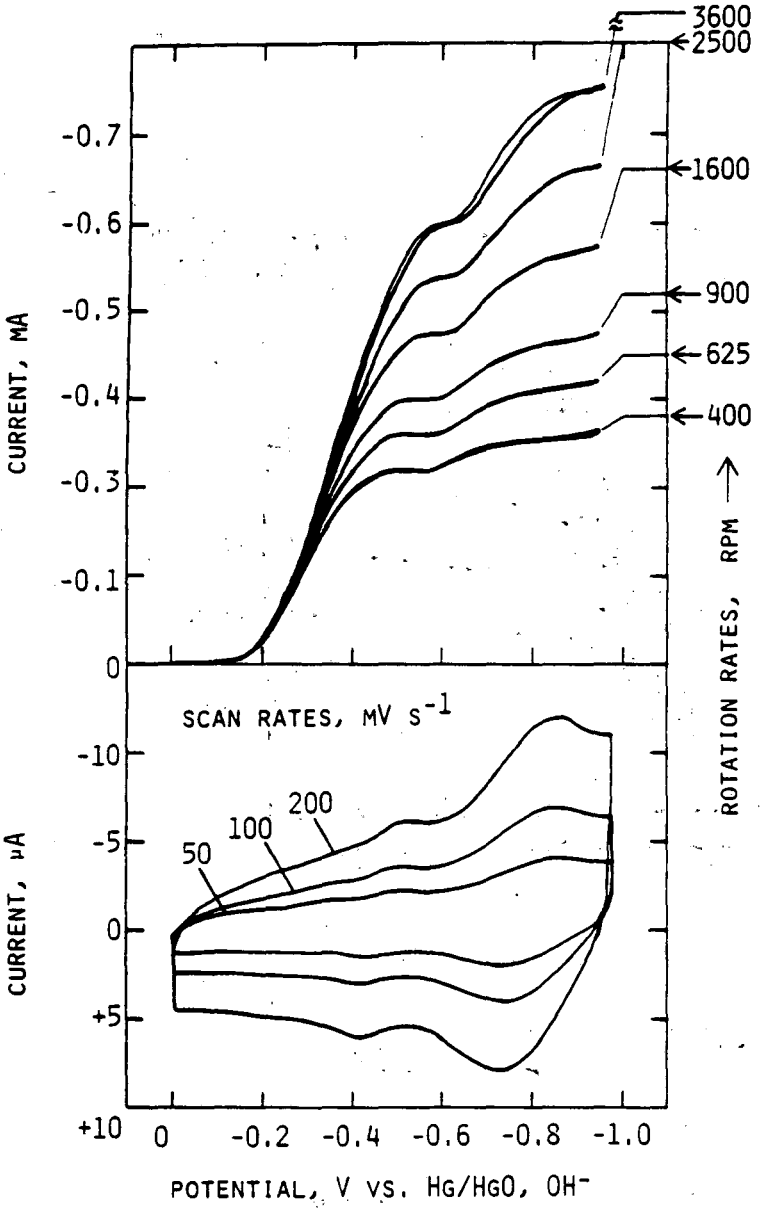

FIG. 4-10. OPG WITH CHEMICALLY ATTACHED 2-AMINOANTHRAQUINONE IN 0.1 M NAOH AT 22°C: A) VOLTAMMETRY AT VARIOUS SCAN RATES IN AR-SATURATED SOLUTION; B) DISK CURRENTS MEASURED AT 20 MV S^{-1} FOR O_2 REDUCTION IN O_2-SATURATED (1 ATM) SOLUTION.

TABLE 4-4

Mean Peak Potentials[a] for Chemically Attached Aminoanthraquinones, V vs. SCE, and Peak Separations (mV)[b]

	0.05 M H_2SO_4	0.1 M NaOH	ΔE^d
1-amino-9,10-AQ			
small peak[e]	-0.082 (10)	-0.574 (18)	0.492
large peak	-0.210 (37)	-0.875 (20)	0.665
	ΔE = 0.128	ΔE = 0.301	
2-amino-9,10-AQ			
small peak	+0.148 (22)[c]	-0.610 (22)	0.758
large peak	-0.180 (37)	-0.928 (20)	0.748
	ΔE = 0.328	ΔE = 0.318	

[a] from differential pulse voltammetry, calculated by taking the average of the cathodic and anodic peaks.

[b] the 25 mV pulse height was substracted from the peak potential value in the negative sweep direction and added to the peak potential value in the positive sweep direction. The sweep rate was 5 mV s^{-1}.

[c] value for compound adsorbed on HOPG, since OPG had an intrinsic interfering peak.

[d] shifts in mean peak potentials from acidic to basic solutions.

[e] see Fig. 4-10.

current.

It has been assumed for the moment that the redox processes involve two electrons because there is no evidence for the kind of twin peaks observed for the adsorbed NQ and AQS and because the peak areas are roughly the same in alkaline solution as in acid, in which the process should definitely involve two electrons. It is not known why AAQ should exhibit a two electron peak, since its behavior should be reasonably similar to that for AQS. Another important question is why there are two peaks of such disparate size. It may be that there are two different states of interaction with the electrode surface or two different states of aggregation which have different populations and which lead to relatively widely separated potentials (approx. 0.3 V). Spectroscopic measurements are planned to try to shed more light on this problem.

Based on the data in Fig. 4-10, a detailed kinetic analysis was done. The Koutecky-Levich plots for the OPG and modified OPG surfaces are shown in Fig. 4-11. Both show parallel, linear plots, with a slope expected for a two electron process. This is consistent with a kinetically controlled process which is first order in O_2 concentration.

The reaction order for O_2 can be determined more reliably using the type of plot shown in Fig. 4-12 (see Zurilla, Sen and Yeager, Ref. 20). These plots show unequivocally that the reaction order is unity on both surfaces over a range of potentials.

The Tafel plots for O_2 reduction on the two surfaces are shown in Fig. 4-13. The term $(i_L/(i_L - i))$ corrects for mass transport if one takes i_L as being the mass transport limited current based on the Levich equation (Eq. 4-5). One can also correct for other limiting factors such as the presence of a blocking layer simply by taking i_L as the observed limiting current. The intercepts of the Koutecky-Levich plots in Fig. 4-11 give values of the so-called kinetic limiting current, without the effect of mass transport, but they must be further corrected if the experimental limiting current is less than that predicted on the basis of mass transport control. This was done using the equation

$$\frac{1}{i} = \frac{1}{i_{diff}} + \frac{1}{i_{kin}} + \frac{1}{i_{chem}} \qquad (4\text{-}11)$$

where i_{diff} is the mass transport limited current, i_{kin} is the kinetically (electron transfer) limited current and i_{chem} is the potential independent or chemically limited current (1). As mentioned above, two possible sources for i_{chem} are the presence of a basal plane-like surface or the presence of a blocking layer. The assumption here is that the reason for the inactivity of the basal plane is the very low concentration of active sites. The behavior of an inert blocking layer on a rotating disk electrode has recently been reviewed by Leddy and Bard (21). Various workers have treated this problem and shown that there can be a mass transport limited current which is independent of rotation speed either because of transport to isolated sites or through a membrane-like layer.

The i_{chem} term is much lower for the OPG surface than for the

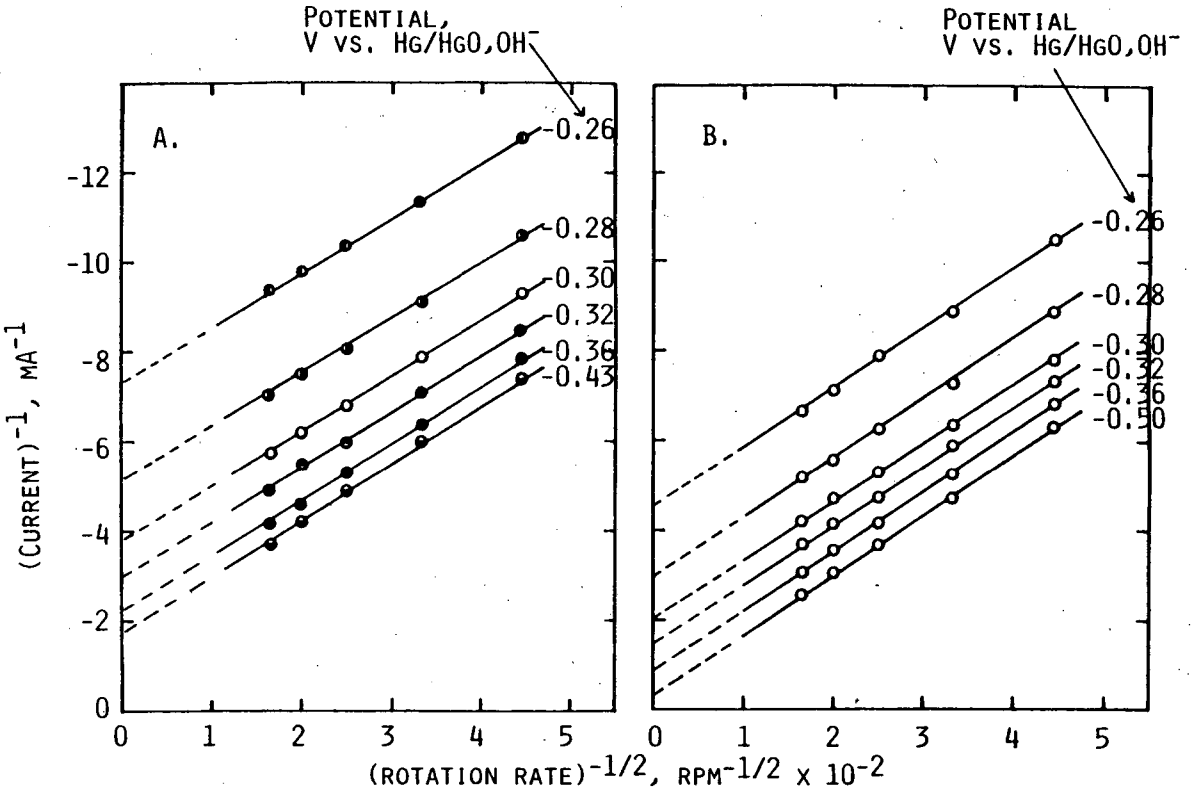

FIG. 4-11. KOUTECKY-LEVICH PLOTS FOR O_2 REDUCTION IN O_2-SATURATED (1 ATM) 1.0 M NAOH AT 22°C (SLOPE = 8.0×10^{-3} MA $RPM^{-1/2}$): A) UNTREATED OPG; B) CHEMICALLY ATTACHED 2-AMINOANTHRAQUINONE ON OPG.

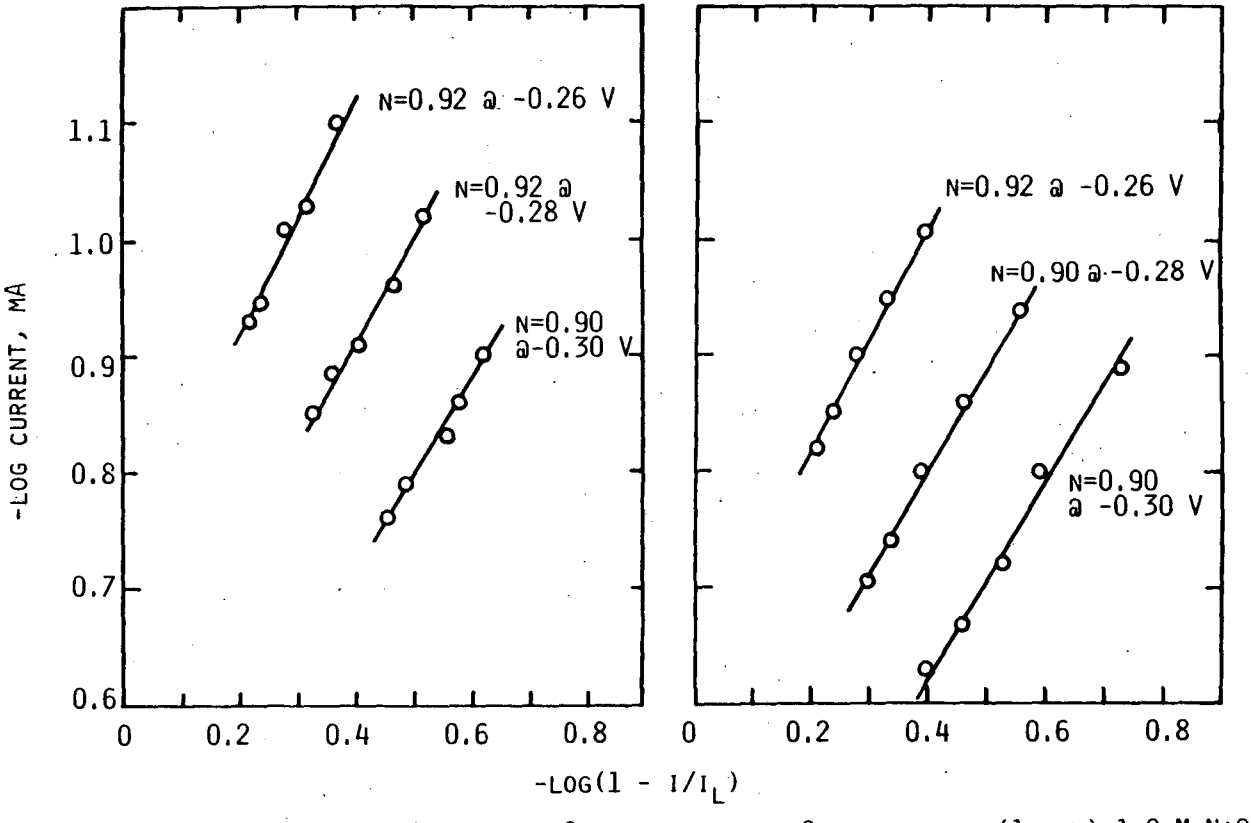

FIG. 4-12. REACTION ORDER PLOTS FOR O_2 REDUCTION IN O_2-SATURATED (1 ATM) 1.0 M NAOH AT 22°C: A) UNTREATED OPG; B) OPG WITH CHEMICALLY ATTACHED 2-AMINOANTHRAQUINONE.

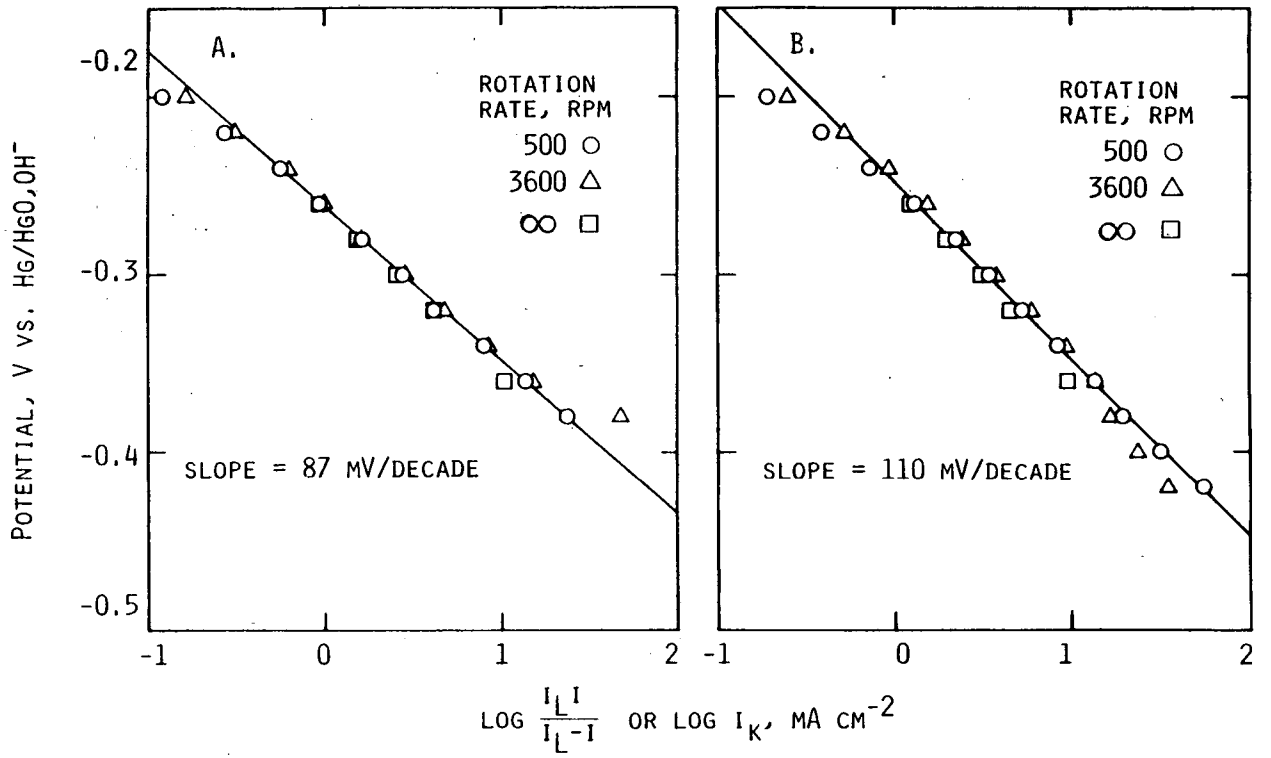

FIG. 4-13. TAFEL PLOTS FOR O_2 REDUCTION IN O_2-SATURATED (1 ATM) 1.0 M NAOH AT 22°C: A) UNTREATED OPG; B) OPG WITH CHEMICALLY ATTACHED 2-AMINOANTHRAQUINONE. KINETIC CURRENTS I_K WERE OBTAINED FROM THE INTERCEPTS AT INFINITE ROTATION RATE OF THE KOUTECKY-LEVICH PLOTS AND WERE CORRECTED FOR THE POTENTIAL-INDEPENDENT LIMITING CURRENT $I_{K,MAX}$ OPG: $I_{K,MAX}$ = 2.95 MA CM^{-2} 2-AAQ/OPG: $I_{K,MAX}$ = 15.8 MA CM^{-2}

chemically modified surface, 3 vs. 16 mA cm^{-2} respectively. It may be that this difference is due to a difference in the concentration of active sites on the electrode surface.

After correction for this term, most of the data points for 500 rpm, 3600 rpm and infinite rotation rate lie close to a single line (Fig. 4-13). The Tafel slopes are slightly different, approximately 90 mV/decade for OPG and 110 mV/decade for OPG with attached 2-AAQ. Slopes of around 90 mV/decade have been observed for graphite previously (22) but the exact mechanistic reason is unclear. The 110 mV slope can be ascribed to a rate determining first electron transfer step.

The mechanism for O_2 reduction should be similar for both the adsorptively and chemically attached surfaces, but the rate constants for individual steps can be quite different. For example the rate of the first electron transfer might be expected to be greater for the adsorbed quinone possibly because of better coupling of orbitals with the electrode surface.

The fact that the Tafel slopes for O_2 reduction on the adsorbed quinone surfaces are close to 60 mV/dedade while that for the chemically modified surface is close to 120 mV/decade suggests that a chemical step following the initial electron transfer is rate determining in the first case, while the initial electron transfer itself is rate determining in the second case. Even so, the Tafel plots for all four cases, adsorbed AQS, adsorbed NQ, OPG and OPG with chemically attached AQS, are remarkably similar. This seems to suggest that the individual differences in the surface properties are not as important as had been anticipated.

It is interesting to speculate on the exact mode of interaction between the quinone radical anion and dioxygen on the molecular orbital level. Preliminary MO calculations have not shown up any bonding interactions between the two species. For example it is known that singlet dioxygen can interact with two double-bonded carbons to give a 2 + 2 cycloaddition product, a dioxetane (23), but such an interaction with the ground state dioxygen was not found in the MO calculations results. From the high rate of electron transfer for the solution species (6), it is believed that the process is a barrierless one. It would be useful to measure a similar rate constant for the reaction of the surface bound radical anion with O_2. This was done by Martigny and Anson (24) for the polymer bound xylylviologen. They found the rate constant to be much decreased for the polymer bound species as compared with the solution phase species.

4.5 SUMMARY AND CONCLUSIONS

The adsorbed quinones 1,4-naphthoquinone (NQ) and 9,10-anthraquinone-2-SO_3^- (AQS) on the surface of highly oriented pyrolytic graphite catalyze dioxygen reduction to hydrogen peroxide in alkaline solution. The onset of O_2 reduction current occurs more than 100 mV positive of the peak potential for the AQS reduction to the radical anion. The desorption of the quinones from the electrode surface at the more negative potentials made a detailed kinetic analysis impossible, but the

first current-potential curve for the rotating disk electrode with a freshly adsorbed layer could be used to make a mass transport corrected Tafel plot. The plots exhibited slopes of 65 and 58 mV/decade at the lower current densities for AQS and NQ respectively and 89 and 107 mV/decade respectively at the higher current densities. In every respect the first current-potential traces for the two quinones were remarkably similar, with only a 10 mV displacement, indicating that the differences in the behavior were not as dependent upon the individual quinone/quinone radical anion redox potentials as had been anticipated. A mechanism was proposed involving reduction of quinone to its radical anion, reaction of the radical anion with dioxygen to produce superoxide, followed by protonation of superoxide.

Chemically linked 2-amino-9,10-anthraquinone on ordinary pyrolytic graphite also catalyzes dioxygen reduction to hydrogen peroxide in alkaline solution. The onset of reduction current again correlates with the voltammetric peak potential for the quinone reduction, which however appears to be a two electron peak. There are two sets of peaks, possibly corresponding to reductions of quinone species which are in different states of adsorption or aggregation. The process corresponding to the smaller, more positive peak appears to be more important for the electrocatalysis. The O_2 reaction order is unity, and the Tafel slope is 110 mV/decade, both of which indicate that the first electron transfer step, either of quinone to quinone radical anion or of dioxygen to superoxide, is the rate determining step.

The overall mechanism is postulated to involve first the reduction of dioxygen to superoxide by a surface quinone radical anion and then a following chemical reaction, which could be either 1) protonation of superoxide by water or 2) disproportionation of two superoxides. Disproportionation between superoxide and protonated superoxide is also a possibility, since that between two superoxides is relatively slow.

References

1. L. Morcos and E. Yeager, Electrochim Acta, 15, 953 (1970)

2. J. S. Mattson and H. B. Mark, "Activated Carbon", Marcel Dekker, New York, 1971

3. Z. W. Zhang, D. A. Tryk and E. B. Yeager, in "The Electrochemistry of Carbon", S. Sarangapani, J. R. Akridge and B. Schumm, Editors, The Electrochemical Society Proceedings Volume 84-5, Pennington, N. J., 1984, pp. 158-178

4. V. A. Garten and D. E. Weiss, Austral. J. Chem., 8, 68 (1955), 10, 309 (1957)

5. J. E. LuValle and A. Weissberger, J. Am. Chem. Soc., 69, 1567 (1947)

6. K. B. Patel and R. L. Willson, J. Chem. Soc., Farad. Trans. I, 69, 814 (1973)

7. Y. A. Ilan, D. Meisel and G. Czapski, Israel J. Chem., 12, 891 (1974)

8. R. Powell, "Hydrogen Peroxide Manufacture, 1968", Noyes Development Corp., Park Ridge, N.J., 1968

9. D. H. Grangaard, U. S. Patents 3, 454, 477, July 1969 and 3, 529, 997, September 1970

10. M. Sharp, Electrochim Acta, 23, 287 (1978)

11. R. Gill and H. I. Stonehill, J. Chem. Soc., 1952, 1845

12. M. P. Soriaga, P. H. Wilson, A. T. Hubbard and C. S. Benton, J. Electroanal. Chem., 142, 317 (1982)

13. R. H. Wopschall and I. Shain, Anal. Chem., 39, 1514 (1967)

14. S. Wawzonek, R. Berkey, E. W. Blaha and M. E. Runner, J. Electrochem. Soc., 103, 456 (1956)

15. L. Jeftic and G. Manning, J. Electroanal. Chem., 26, 195 (1970)

16. A. A. Frost, J. Am. Chem. Soc., 73, 2680 (1951)

17. S. U. Falk and A. J. Salkind, "Alkaline Storage Batteries", John Wiley, New York, 1969, Chap. 8

18. R. E. Davis, G. L. Horvath and C. W. Tobias, Electrochim. Acta, 12, 287 (1967)

19. J. M. Hale and R. Parsons, Trans. Farad. Soc., 59, 1429 (1963)

20. R. W. Zurilla, R. K. Sen and E. Yeager, J. Electrochem. Soc., 125, 1103 (1978)

21. J. Leddy and A. J. Bard, J. Electroanal. Chem., 153, 223 (1983)

22. J. Molla, Ph. D. Dissertation, Case Western Reserve University, 1983

23. P. D. Bartlett, Chem. Soc. Rev., 5, 149 (1976)

24. P. Martigny and F. C. Anson, J. Electroanal. Chem., 139, 383 (1982)

25. N. Oyama, N. Oki, H. Ohno, Y. Ohnuki, H. Matsuda and E. Tsuchida, J. Phys. Chem., 87, 3642 (1983).

SECTION 5

OXYGEN REDUCTION AND GENERATION CATALYSIS ON HEAT TREATED MACROCYCLES SUPPORTED ON CARBON WITH ADDED TRANSITION METAL HYDROXIDES- POLARIZATION MEASUREMENTS USING GAS FED ELECTRODES

W. Aldred, D. Tryk and E. Yeager

5:1 INTRODUCTION

Heat treated transition metal macrocyclic complexes supported on carbon have received much attention during the past decade due to their excellent activity and stability as dioxygen reduction electrocatalysts in both acidic and basic electrolytes. These are several major research groups worldwide which have been studying these materials in an effort to characterize them and to explain their enhanced activity and stability: the Soviet group (1,2), the East German group (3-5), the Bulgarian group (4-11), the Dutch group (12-16) as well as the authors' group (17-19).

There is a wide spectrum of viewpoints concerning the exact roles of the transition metal ion and the ligand and the extent to which the ligand structure is retained after heat treatment at temperatures up to 800-1000°C.

Concerning the role of the metal ion, the Bulgarian group takes the view that the major function of the cobalt in heat treated cobalt tetramethoxyphenylporphyrin (CoTMPP) is to enhance the hydrophobic properties and O_2 mass transport of the porous electrode (9-11). Most of the other workers in the field consider the possibility that the metal takes part in the actual electrocatalysis.

Concerning the extent of modification of the ligand structure during heat treatment, the Dutch group concluded that the porphyrins lose the meso carbon atoms, leaving the pyrrole groups to rotate freely about the Co-N bond, so that an N_4 center is retained (14-16). This conclusion was based on a wide range of experimental data, including EXAFS (extended X-ray absorption fine structure).

On the basis of voltammetry, electron microscopy, Mossbauer spectroscopy as well as other evidence, the Case group concluded that the ligand structure is modified greatly and that much of the transition metal becomes incorporated into metal oxide particles (18,19).

At least some of these discrepancies may be due to differences among the various carbon black supports used. For example, almost all of the Bulgarian work made use of an activated charcoal (P-33) with significant iron content (~0.5%). Thus, their contention that a metal-free porphyrin does not require added transition metal ion for electrocatalytic activity must be discussed in the light of this fact (see Ref. 20).

In order to avoid difficulties such as this, workers at Case have

relied on carbons which are relatively free of inorganic impurities, such as Vulcan XC72 (Cabot, 250 m^2g^{-1}). In general, O_2 activity is not as high on these carbons as on higher area activated carbons such as RB carbon (Calgon, ~1200 m^2g^{-1}). One practical advantage however is that these carbons, especially Shawinigan black, are not as oxidizable as the activated carbons. This is extremely important in electrodes which experience very positive potentials such as bifunctional O_2 electrodes.

Using a relatively pure carbon such as SB loaded with a heat treated metal-free macrocycle such as H_2TMPP, one can conveniently examine the effect on O_2 reduction activity of any transition metal one chooses, without the need for separate syntheses. In the present work these metals were precipitated as hydroxides in the presence of an aqueous suspension of the macrocycle loaded carbon. Interaction of the metal with the substrate could then take place during subsequent heat treatment or even during operation of the electrode in the electrolyte. The examination of the substrate itself was not undertaken in this work but is being actively pursued in parallel research at Case.

Since the metal hydroxides were present in excess with respect to the number of moles of macrocycle or even of smaller fragments which could act as ligands, there would be an excess amount of metal hydroxide or oxide present after any interaction might have taken place. Thus, the results are ambiguous in that these compounds can act as catalysts for O_2 reduction or, more likely, as peroxide decomposition catalysts. The main results which will be presented, however, are due principally to species formed by interaction of the transition metals (probably in ionic form) with the heat treated macrocycle/carbon substrate.

It is also possible to examine the effects of combinations of transition metals. It was hoped that synergistic interactions between metals would lead to enhanced activity for O_2 reduction, and this hope has been borne out. The rationale for this approach is that different types of catalytic sites could be formed at a molecular level of dispersion so that for example one type could catalyze the two-electron reduction of dioxygen to hydrogen peroxide while an adjacent site would catalyze either the reduction or chemical decomposition of the hydrogen peroxide. These concepts are based in part on the work of Collman and Anson and coworkers, who have synthesized and examined the electrochemical behavior of a series of heterobimetallic face-to-face porphyrins (21,22) and have also devised a pair of catalysts which work in series to reduce oxygen to water (23).

It should be emphasized that this research is preliminary and is meant to uncover the broad outlines of the area. Now that several very promising new electrocatalysts have been discovered, two for O_2 reduction and one for O_2 reduction/generation, they will be thoroughly characterized physically, chemically and electrochemically.

5.2 EXPERIMENTAL METHODS

5.2.1 Preparation of Catalysts

H_2TMPP was synthesized according to the method of Adler et al. (24). An acetone solution was made up and the Shawinigan black was slowly added while the solution was ultrasonically agitated. The agitation was continued for 2 h. The amount of H_2TMPP used was 3% of the weight of the carbon, which would be

approximately 1.2 monolayers based simply on the calculated molecular area of 3.12 nm^2, the nominal surface area of the carbon (65 m^2g^{-1}) and the assumption of flat orientation. The actual equilibrium adsorptive coverage is expected to be somewhat less than the theoretical value however because of less than ideal abutting of the molecules on the surface.

The acetone was removed by bubbling He through the suspension, which was warmed on a water bath. The material was heat treated at either 450°C or 800°C in a horizontal quartz tube furnace while dried, deoxygenated He was passed over it for 2 h. A reddish-brown film was deposited on the walls of the tube during the HT.

The heat-treated macrocycle/carbon was suspended in water and boiled for a few minutes to ensure wetting. Appropriate amounts of the transition metal salts in the form of nitrates or chlorides were added, typically so that the loading would be 10 weight % in terms of the metal itself with respect to the macrocycle/carbon. While the suspension was ultrasonically agitated, a 0.1 M KOH solution was slowly added until the pH was at least 12 to precipitate the metal hydroxides.

The suspension was filtered using a nucleopore 1 m polycarbonate filter membrane. The material was then dried in the tube furnace under flowing He at either 100°C or 280°C for 2 h.

5.2.2. Gas-Fed Electrode Fabrication

The dried H_2TMPP/SB with metal hydroxides was resuspended in water and a highly diluted Teflon T30B (Dupont) suspension was added slowly while the suspension was ultrasonically agitated. The Teflon content was 25% based on the weight of H_2TMPP/SB plus Telon (excluding hydroxides). The suspension was filtered, worked slightly with a spatula and heated treated at 280°C in flowing He for 2 h in order to deactivate the Titon X-100 surfactant and to "pre-sinter" the Teflon.

About 70 mg of the material was shaped in a stainless steel die of 1.75 cm^2 diameter using hand pressure and then pressed at aout 6000 psi together with a 20 mesh Ni screen to form a disk of 2.4 cm^2 area. A 0.5 mm thick disk of hydrophobic backing material made from acetylene black and Teflon (obtained from Electromedia Corp., Englewood, NJ) was pressed onto the electrode active layer at 3000 psi. A diagram of the electrode is shown in Fig. 5-1.

5.2.3. Electrochemical Measurements

The electrode was put into a holder constructed from Teflon and nickel. The exposed electrode area was 0.97 cm^2. The electrode was held in a vertical position and gas was flowed across the back of the electrode at slightly more than one atmosphere. Two initial cathodic polarization curves were measured galvanostatically point-by-point, waiting for equilibrium at each point, using a Stonehart BC 1200 potentiostat. During the measurement of the first polarization curve the electrode becomes partially wetted, but during the measurement of the second curve there is little further change in the degree of wetting, as evidenced by the similarity of the ascending and descending points. Polarization curves were also measured with air and with O_2 - He (21:79, v/v). Potential values were corrected for IR drop using the interruptor method.

FIG. 5-1

CWRU GAS-FED ELECTRODE FOR CATALYST EVALUATION IN ALKALINE ELECTROLYTES (BIFUNCTIONAL)

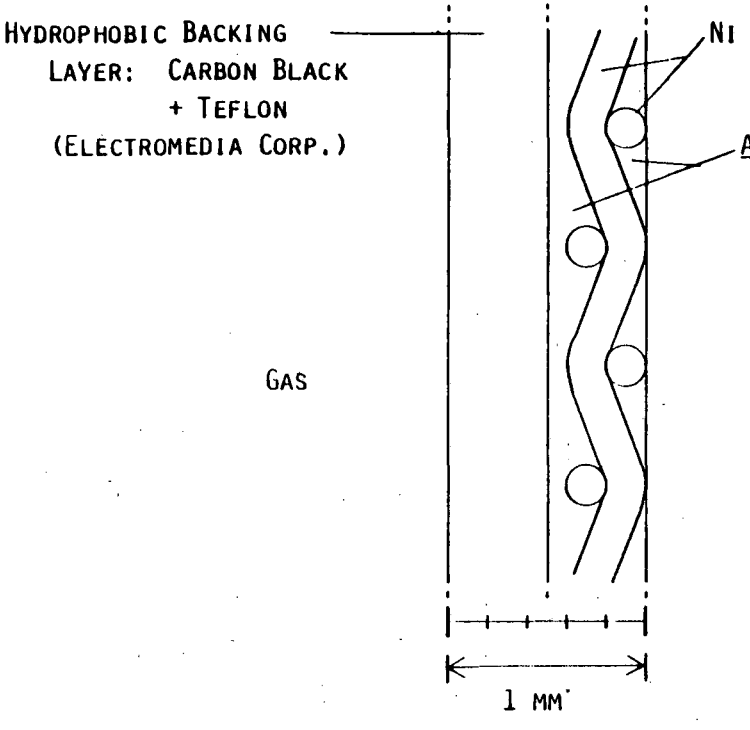

ACTIVE LAYER	LOADING, MG CM^{-2} ELECTRODE AREA	RATIO TO CARBON WT.
CARBON BLACK (SHAWINIGAN)	27.1	100 %
METAL-MACROCYCLIC COMPLEX	0.81	3.0
TEFLON	9.0	33
$Ni(OH)_2$ (AS NI)	1.75	6.5
$Fe(OH)_2$ (AS FE)	1.75	6.4
$Co(OH)_2$ (AS CO)	2.7	10

An initial anodic polarization curve was measured potentiostatically point-by-point. Then the electrode was cycled galvanostatically cathodically and anodically (one cycle consisted of -26 mA cm^{-2} for 15 min followed by +13 mA cm^{-2} for 15 min). The potentials reached at the end of each half-cycle were recorded. After approximately 35 cycles, both cathodic and anodic polarization curves were again measured.

5.3 RESULTS AND DISCUSSION

5.3.1. O_2 Reduction/Generation Catalytic Systems

A number of workers have found that H_2TMPP (or also metal-free debenzotetraazaannulene, H_2DBTAA) could be adsorbed on carbon black and heat treated at 650°C - 850°C and cobalt acetate, $Co(Ac)_2$, added in a second step with heat treatment again at 650-850°C such that the activity was very similar to that of CoTMPP or CoDBTAA (4,5,8,10,11). Research on the bifunctional oxygen electrode at Case has found that the conditions under which Co compounds can be added to H_2TMPP/C after the initial heat treatment (such that the activity of CoTMPP is matched) are relatively mild, especially if the original heat treatment is at a relatively low temperature, like 450°C (17). At this temperature the macrocycle is considered to survive without excessive damage (14,19). As described in the experimental section, the deposited metal hydroxide together with H_2TMPP/C were dried, usually at 100°C, Teflon was deposited and the material heat treated at 280°C for 2 h.

As shown in Fig. 5-2, the activity for the H_2TMPP/C + $Co(OH)_2$ was almost identical to that of a comparable loading of CoTMPP, irrespective of whether there was a very slight excess of $Co(OH)_2$ with respect to moles of H_2TMPP or a large excess (0.4% Co is a 1.6 fold excess while 10% is a 42 fold excess). The activities were much greater than for H_2TMPP/C without Co. Scherson et at. (18) have pointed out the fact that the activity is only high if the carbon support contains iron compounds as impurities.

It is also interesting to note that the carbon with no macrocycle but with 10% Co is quite active for O_2 reduction (Fig. 5-2). Cobalt oxides or hydroxides are well-known to catalyze the decomposition of hydrogen peroxide (25). The $Co(OH)_2$ was found to be more active if the catalyst mixture was dried at 100°C rather than 280°C probably because the higher temperature tends to dehydrate the hydroxide to a greater extent and to decrease the effective surface area.

Similar experiments were conducted with H_2TMPP/C with iron and manganese hydroxides. Both showed gains in activity as compared with H_2TMPP/C but neither was as active as the material containing $Co(OH)_2$ (Fig 5-3). The anodic polarization curves also showed no special activity (Fig 5-4). This was somewhat surprising since Co and Fe oxides are considered to be somewhat active O_2 generation catalysts. It should be noted in these anodic polarization curves that a slight leveling effect is operative: for poor O_2 generation catalysts in our electrode holder, the 1-2 cm^2 of exposed Ni metal of the holder and the Ni screen on the electrolyte side of the electrode are probably responsible in good part for the small O_2 generation activity seen in these polarization curves (Fig 5-4).

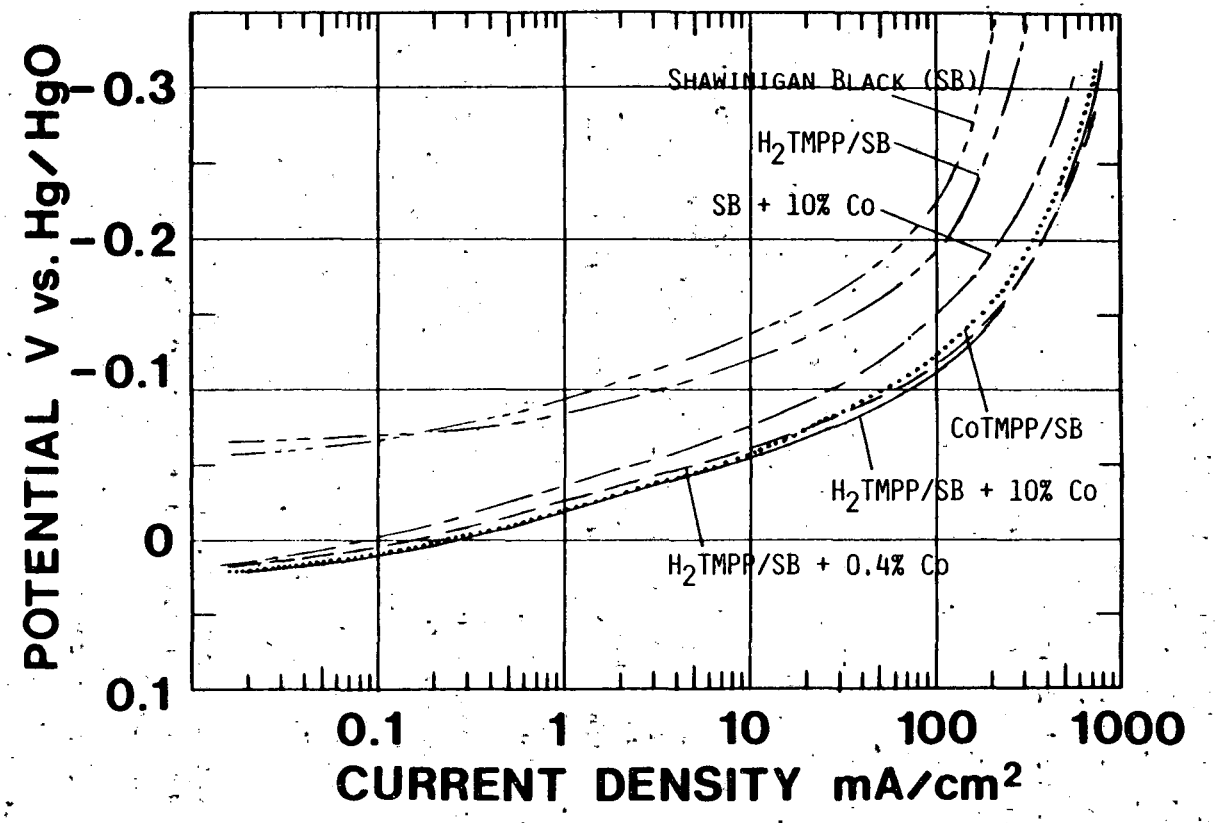

FIG. 5-2. POLARIZATION CURVES FOR O_2 REDUCTION WITH POROUS O_2-FED (1 ATM) ELECTRODES IN 5.5 M KOH AT 25°C; 3% MACROCYCLE/CARBON WAS HEAT TREATED AT 450°C BEFORE DEPOSITION OF METAL HYDROXIDES (LOADINGS EXPRESSED AS % METAL). MATERIAL WAS DRIED AT 100°C, TEFLONATED AND HEAT TREATED AT 280°C.

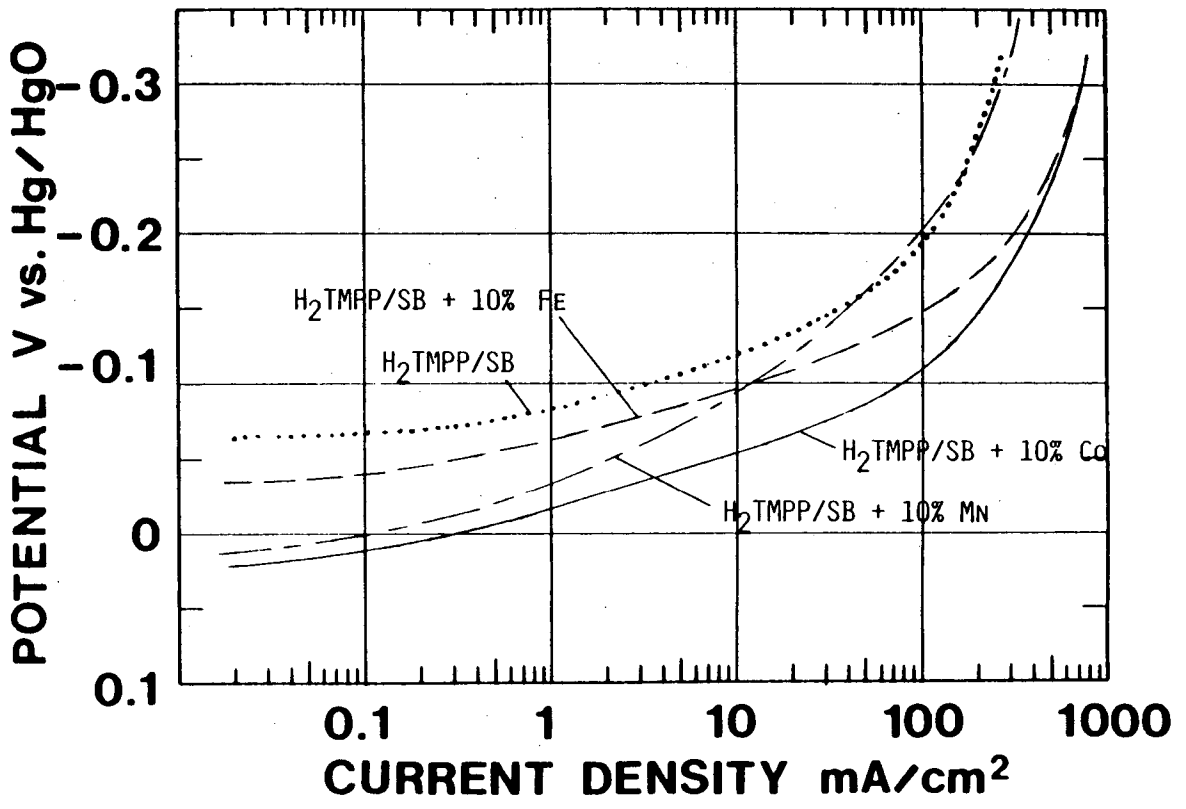

FIG. 5-3. POLARIZATION CURVES FOR O_2 REDUCTION WITH POROUS O_2-FED (1 ATM) ELECTRODES IN 5.5 M KOH AT 25°C; 3% MACROCYCLE/CARBON WAS HEAT TREATED AT 450°C BEFORE DEPOSITION OF METAL HYDROXIDES (LOADINGS EXPRESSED AS % METAL). MATERIAL WAS DRIED AT 100°C, TEFLONATED AND HEAT TREATED AT 280°C.

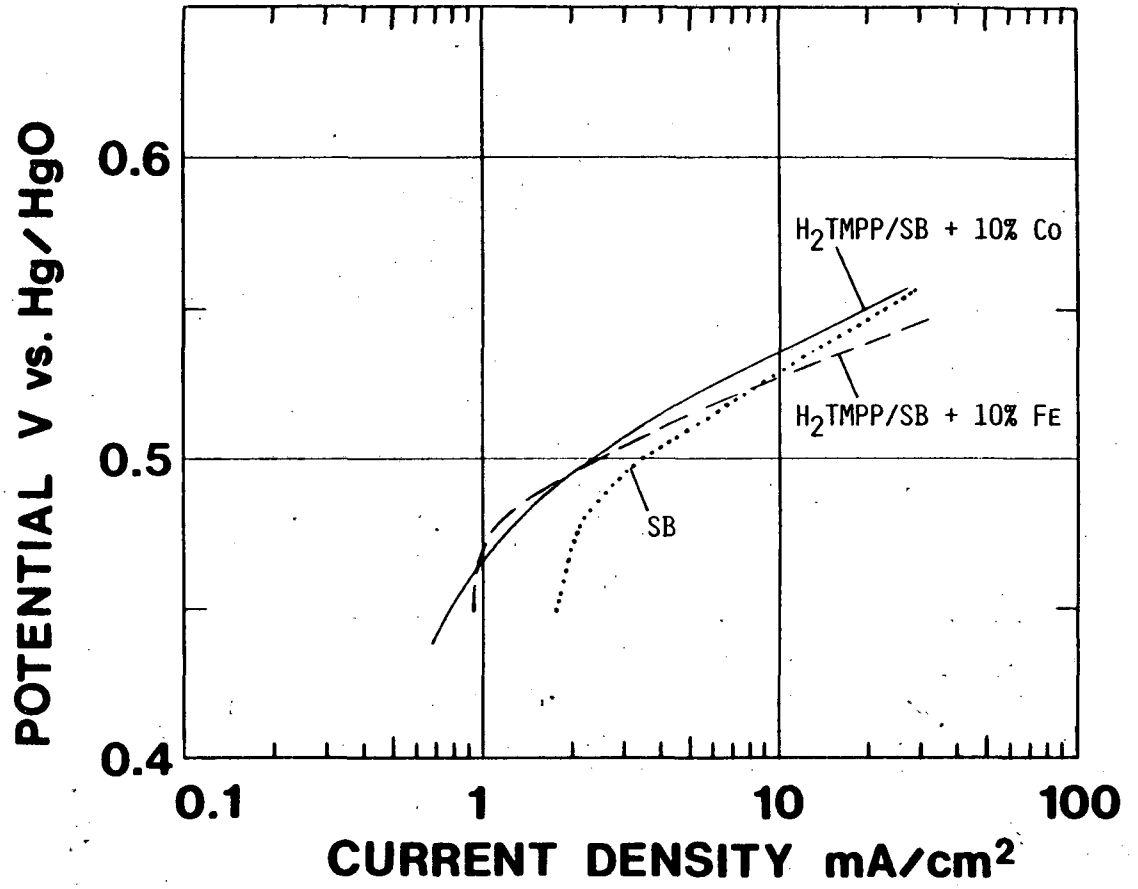

FIG. 5-4. POLARIZATION CURVES FOR O_2 GENERATION WITH POROUS O_2-FED (1 ATM) ELECTRODES IN 5.5 M KOH AT 25°C; 3% MACROCYCLE/CARBON WAS HEAT TREATED AT 450°C BEFORE DEPOSITION OF METAL HYDROXIDES (LOADINGS EXPRESSED AS % METAL). MATERIAL WAS DRIED AT 100°C, TEFLONATED AND HEAT TREATED AT 280°C.

As mentioned in the introduction, enhancements in O_2 reduction activity were found with catalyst preparations containing a second metal hydroxide in addition to cobalt. As seen in Fig. 5-5, all of these preparations had enhanced activity. Nickel had the largest effect followed by silver and iron, with roughly equal activity. Durand et al. found significantly higher activity for Co-Ag than for Co-Fe and the highest acitivity for Co-Co in their face-to-face porphyrins (22).

The highest activity in our experiments was found for still another combination of metal hydroxides, X and Z, whose identity is being temporarily kept confidential pending further investigation of patentability. This combination exhibited polarization very similar to that of the most active catalyst tested so far at Case, $(FeTMPP)_2O$/RB. This is especially surprising since the RB carbon has a surface area approximately 50 times as great as that of SB. The high activity for this catalyst is partially due to the presence of the metal hydroxides, but only at the lowest current densities, as seen in Fig. 5-6.

The anodic polarization behavior of these bimetallic systems is shown in Fig. 5-7. There is some enhancement of O_2 generation activity, for the catalysts with added $Ni(OH)_2$ and $Fe(OH)_3$ as compared with $Co(OH)_2$ alone. It is thought that the activity is due to mixed hydroxides with cobalt. In contrast to claims of the Savy group (26,27), it is thought that the O_2 generation activity for most macrocycle based catalysts is relatively minor based on previous research on bifunctional oxygen electrodes at Case (28).

The catalyst with X and Z hydroxides shows very low polarization (Fig 5-7) but this is misleading because, during anodic polarization, the metal hydroxides undergo active dissolution. The effect of this dissolution can be seen in the cycling curves for the cathodic and anodic half-cycles (Figs 5-8 and 5-9, respectively). The cathodic polarization increases gradually, demonstrating again that the activity is not due principally to the hydroxides. The anodic polarization however climbs much more steeply because in this case the catalysis is based upon the presence of the hydroxides. Preliminary results show that this catalyst is stable for at least 1-2 days under steady cathodic polarization. Thus, it is unsuitable for the bifunctional mode but appears extremely promising for the monofunctional (cathodic) mode.

All of the other catalysts based on H_2TMPP/C plus two metal hydroxides show very stable polarization during the cycling tests, although no single system shows promise as a bifunctional catalyst (Fig 5-8, 5-9).

During previous work in this project it was found that the best O_2 generation catalysis could be obtained with a mixture of iron and nickel hydroxides (28). These probably form an identifiable mixed hydroxide but this has not been characterized as yet. It was thought that the best bifunctional catalyst should contain these hydroxides in combination with a third metal hydroxide which would assist in the O_2 reduction activity since it had been found that the activity for the $H_2TMPP/C + Ni(OH)_2$, $Fe(OH)_3$ system was only moderate (not shown).

Three candidates were the manganese, cobalt and silver hydroxides. The O_2 reduction polarization behavior for these three hydroxides in combination with $H_2TMPP/C + Ni(OH)_2$, $Fe(OH)_3$ is shown in Fig. 5-10. The combination with

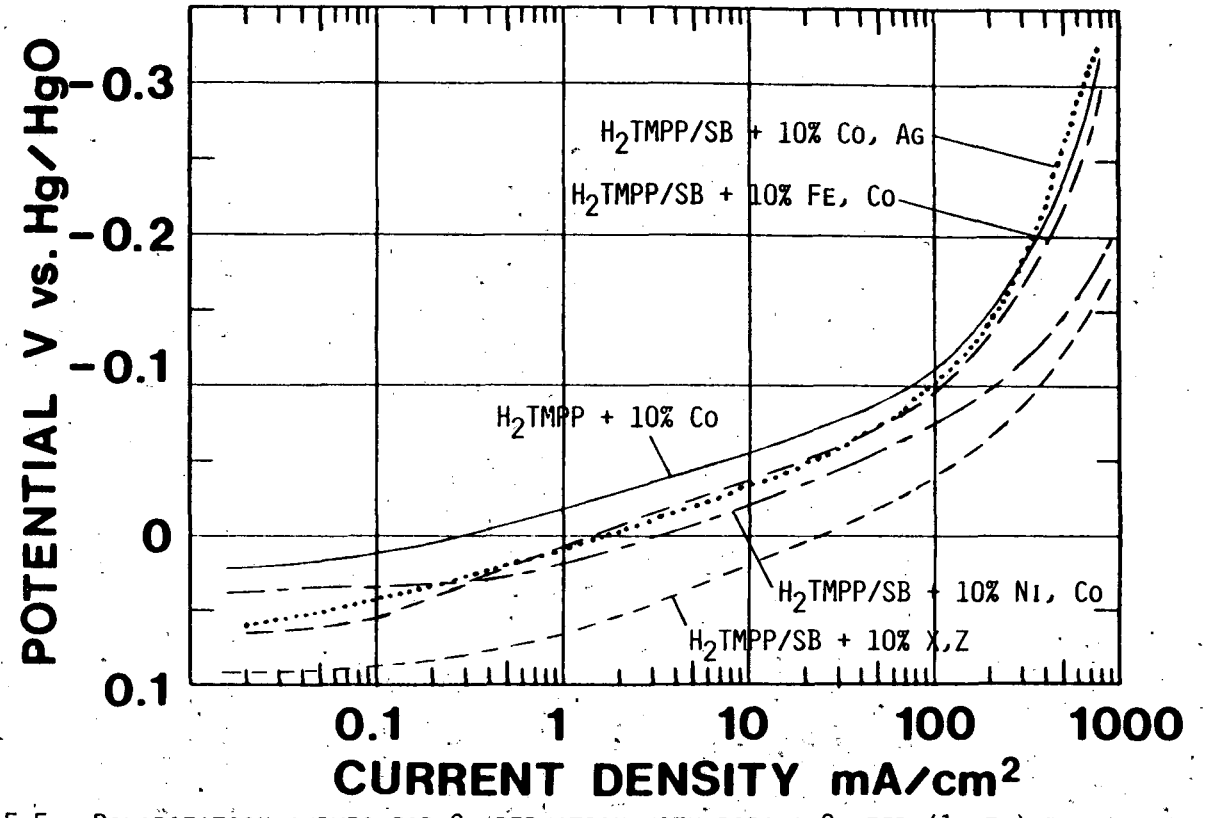

FIG. 5-5. POLARIZATION CURVES FOR O_2 REDUCTION WITH POROUS O_2-FED (1 ATM) ELECTRODES IN 5.5 M KOH AT 25°C; 3% MACROCYCLE/CARBON WAS HEAT TREATED AT 450°C BEFORE DEPOSITION OF METAL HYDROXIDES (LOADINGS EXPRESSED AS % METAL). MATERIAL WAS DRIED AT 100°C, TEFLONATED AND HEAT TREATED AT 280°C.

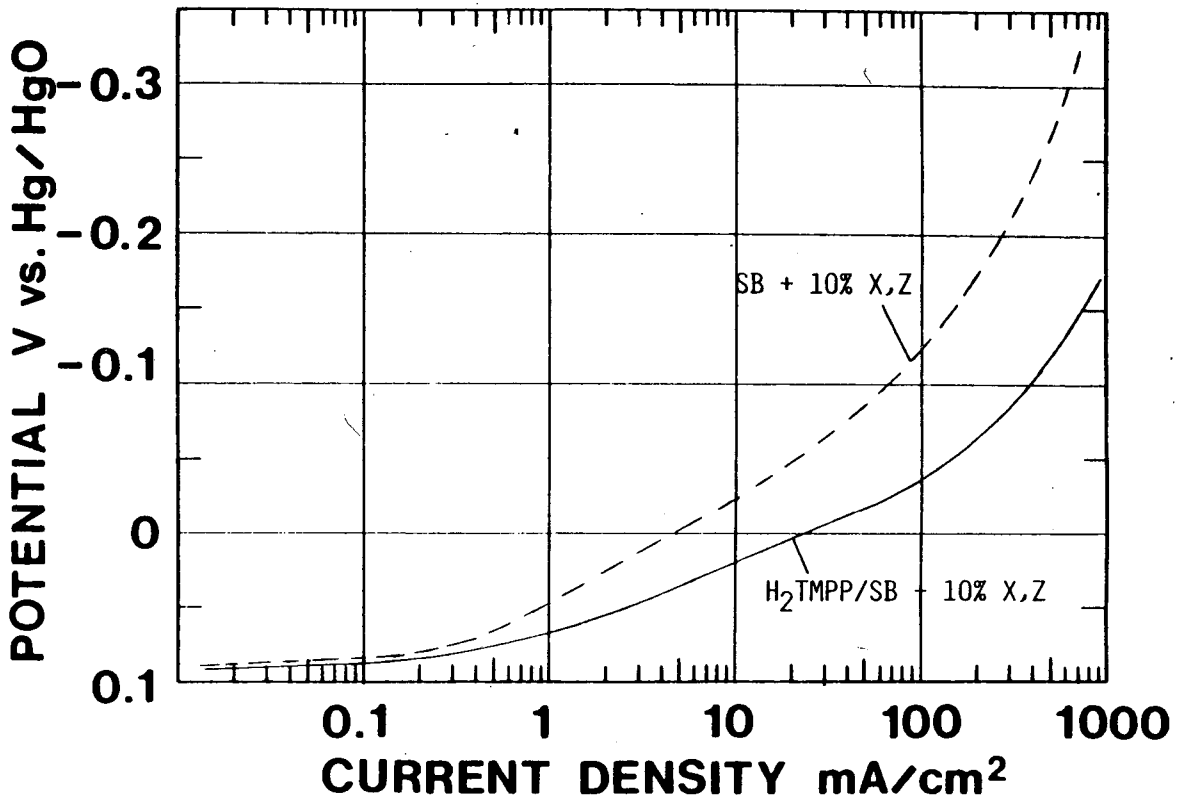

FIG. 5-6. POLARIZATION CURVES FOR O_2 REDUCTION WITH POROUS O_2-FED (1 ATM) ELECTRODES IN 5.5 M KOH AT 25°C; 3% MACROCYCLE/CARBON WAS HEAT TREATED AT 450°C BEFORE DEPOSITION OF METAL HYDROXIDES (LOADINGS EXPRESSED AS % METAL). MATERIAL WAS DRIED AT 100°C, TEFLONATED AND HEAT TREATED AT 280°C.

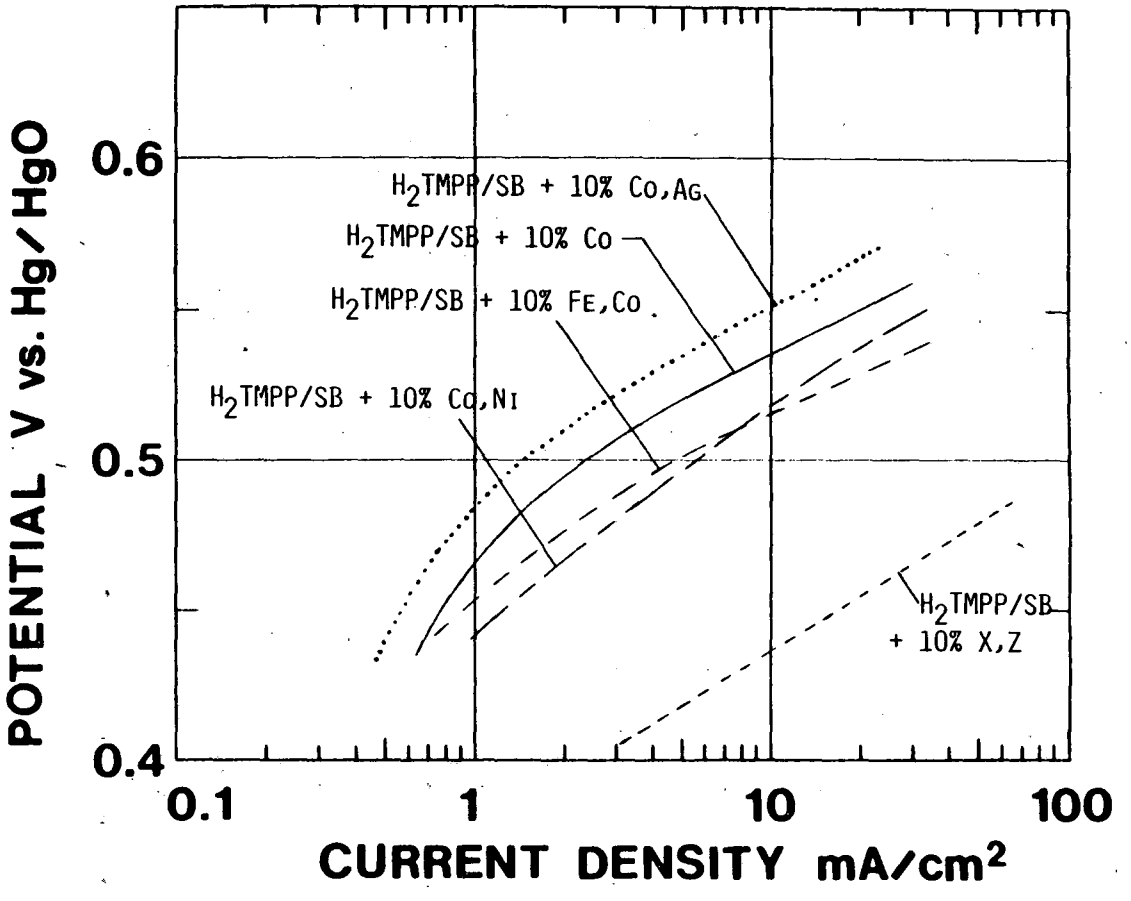

FIG. 5-7. POLARIZATION CURVES FOR O_2 GENERATION WITH POROUS O_2-FED (1 ATM) ELECTRODES IN 5.5 M KOH AT 25°C; 3% MACROCYCLE/CARBON WAS HEAT TREATED AT 450°C BEFORE DEPOSITION OF METAL HYDROXIDES (LOADINGS EXPRESSED AS % METAL). MATERIAL WAS DRIED AT 100°C, TEFLONATED AND HEAT TREATED AT 280°C.

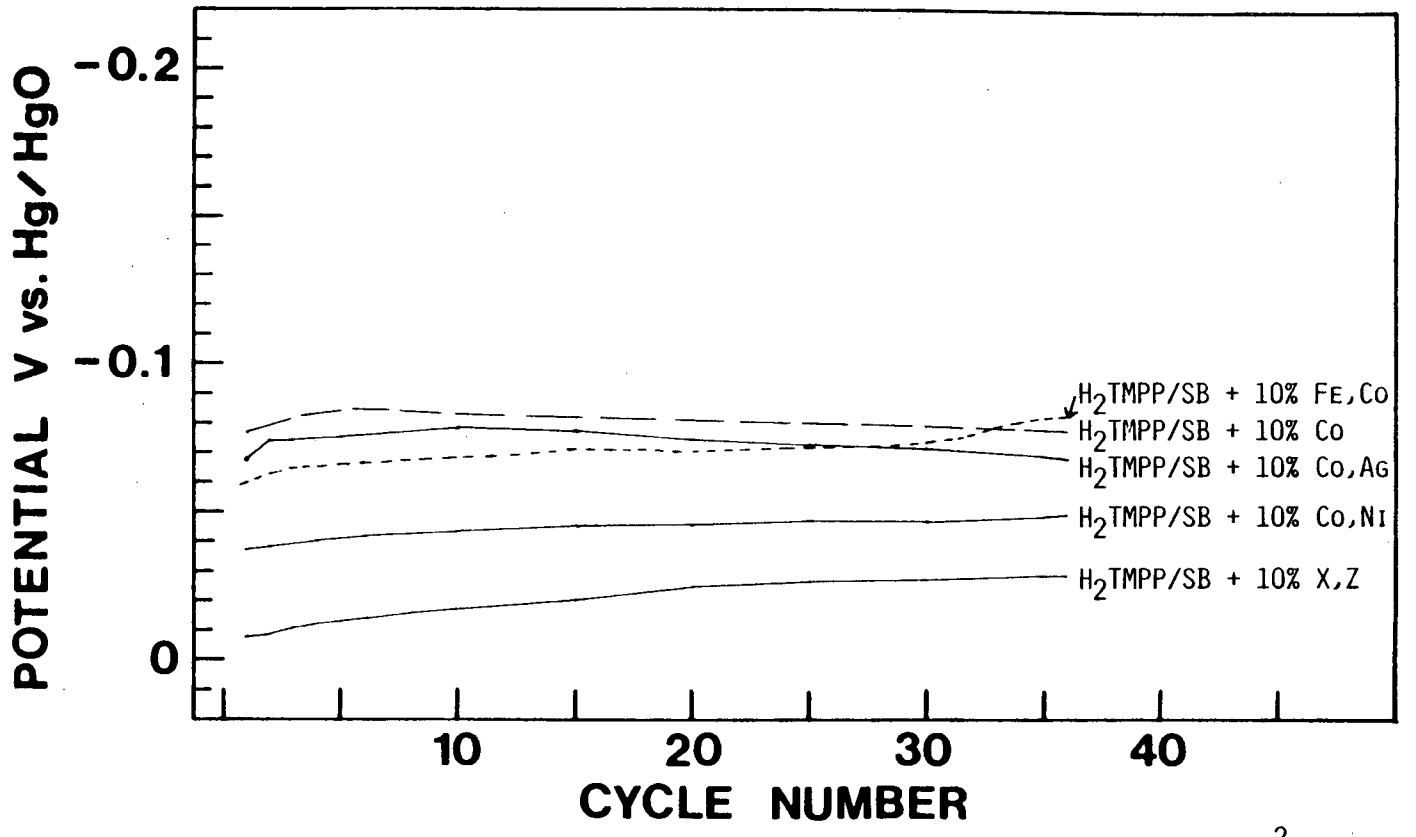

FIG. 5-8. POTENTIALS FOR THE CATHODIC HALF CYCLES IN BIFUNCTIONAL CYCLING (-26 mA cm^{-2} FOR 15 MIN; +13 mA cm^{-2} FOR 15 MIN) FOR POROUS O_2-FED (1 ATM) ELECTRODES IN 5.5 M KOH AT 25°C; 3% MACROCYCLE/CARBON WAS HEAT TREATED AT 450°C BEFORE DEPOSITION OF METAL HYDROXIDES (LOADINGS EXPRESSED AS % METAL). MATERIAL WAS DRIED AT 100°C, TEFLONATED AND HEAT TREATED AT 280°C.

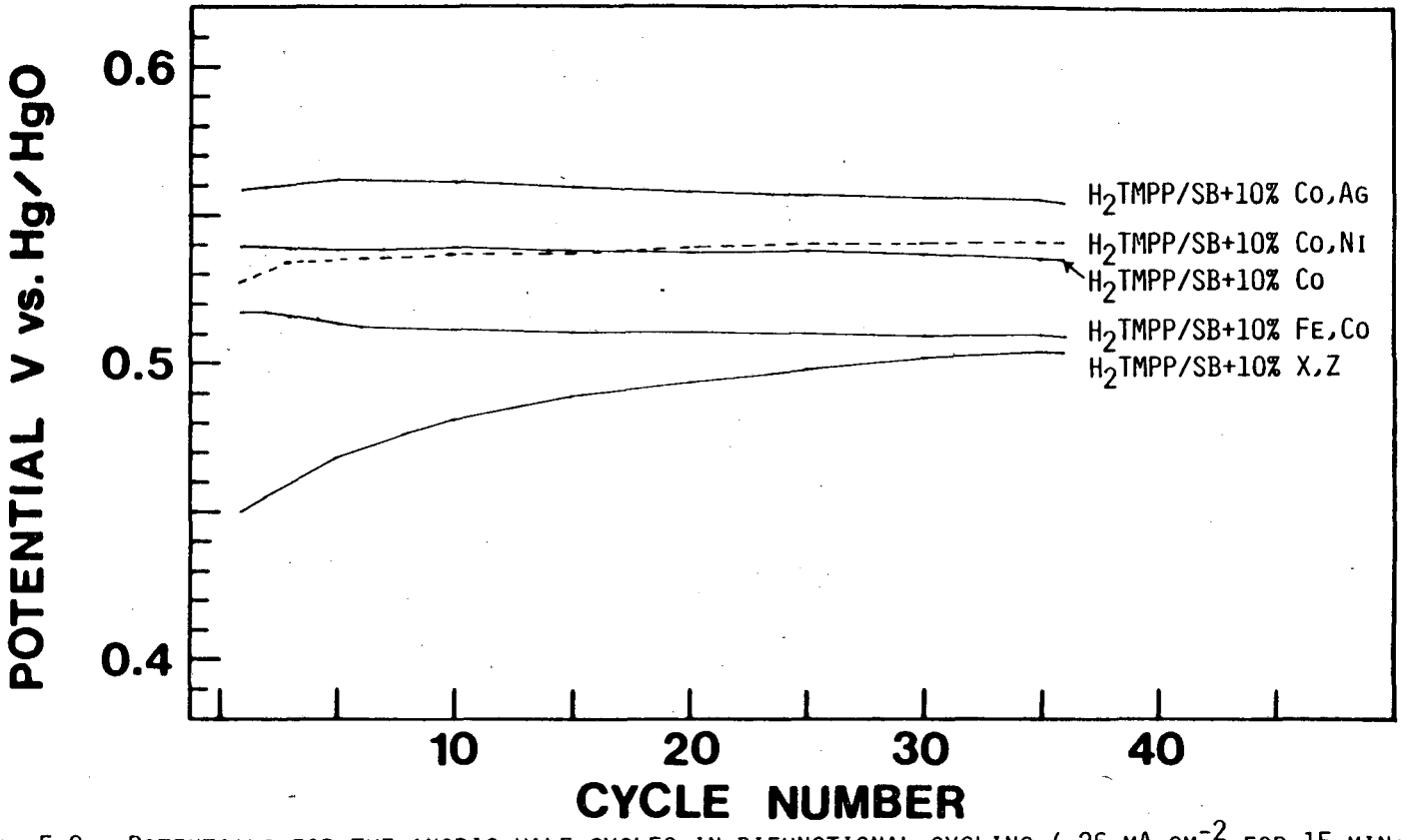

FIG. 5-9. POTENTIALS FOR THE ANODIC HALF CYCLES IN BIFUNCTIONAL CYCLING (-26 MA CM^{-2} FOR 15 MIN; +13 MA CM^{-2} FOR 15 MIN) FOR POROUS O_2-FED (1 ATM) ELECTRODES IN 5.5 M KOH AT 25°C; 3% MACROCYCLE/CARBON WAS HEAT TREATED AT 450°C BEFORE DEPOSITION OF METAL HYDROXIDES (LOADINGS EXPRESSED AS % METAL). MATERIAL WAS DRIED AT 100°C, TEFLONATED AND HEAT TREATED AT 280°C.

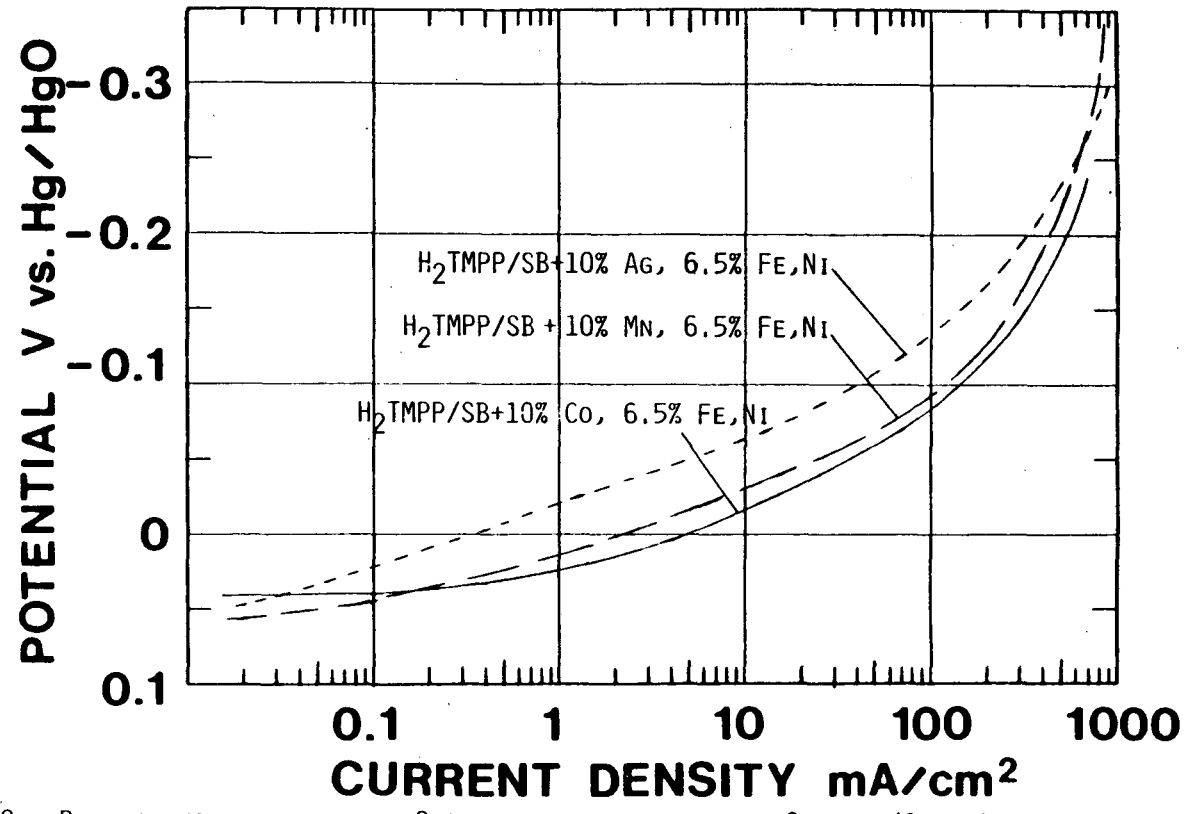

FIG. 5-10. POLARIZATION CURVES FOR O_2 REDUCTION WITH POROUS O_2-FED (1 ATM) ELECTRODES IN 5.5 M KOH AT 25°C; 3% MACROCYCLE/CARBON WAS HEAT TREATED AT 450°C BEFORE DEPOSITION OF METAL HYDROXIDES (LOADINGS EXPRESSED AS % METAL). MATERIAL WAS DRIED AT 100°C, TEFLONATED AND HEAT TREATED AT 280°C.

$Co(OH)_2$ exhibited the lowest polarization. In addition, the anodic polarization was also the lowest (Fig 5-11). This system, therefore, is the most favorable one tested thus far for the bifunctional mode. It shows a smaller potential swing between cathodic and anodic modes (ΔE = 528 mV between -25 and +12.5 mA cm^{-2}) than the best catalysts reported last year, systems based upon Fe,Co,Ni and Ag hydroxides (ΔE = 566 mV) or upon iron naphthalocyanine with Fe,Co and Ni hydroxides (ΔE = 552 mV). The stability of this system during cycling is also superior (Figs. 5-12, 5-13). The reproducibility is also excellent. Figs. 5-14 and 5-15 present actual data points for three separate electrodes made over a period of several months and using different batches of H_2TMPP/C (450°C HT).

The O_2 reduction catalytic activity is again, as for the X - Z hydroxide containing system, highly dependent upon the presence of the macrocycle (Fig 5-16). The O_2 generation activity however is almost totally dependent upon the presence of the metal hydroxides (Fig 5-17).

5.3.2 Optimization of a Bifunctional Catalyst

In order to gain some understanding of this complex multicomponent catalytic system, various fabrication parameters were varied, such as the heat treatment temperature of the macrocycle, the metal hydroxide loadings, the metal hydroxide drying temperature, the type of Teflon and the method used to deactivate the Triton X-100 surfactant. As a result of these experiments a general if not detailed understanding of this system has been achieved.

On the basis of results of Iliev (7) and of Wiesener (3-5), the maximum O_2 reduction activity should have been found for a relatively high-temperature heat-treatment of the macrocycle/carbon. In fact Wiesener found that for H_2DBTAA on P-33 carbon, the maximum activity was obtained at a heat treatment temperature of 950°C (4). The H_2TMPP/C + Fe, Co, Ni hydroxides, however, greater activity was found for a 450°C rather than an 800°C treatment (Fig 5-18). As suggested in the introduction, the discrepancy probably arises due to differences in the carbons being used and especially due to the metallic content of the carbon. For example the Wiesener result is for a metal-free macrocycle on an impure carbon with no other source of transition metal other than the carbon (4). It may be that the high temperature (950°C) is needed for an interaction between macrocycle and iron impurites to occur. The material which had not been heat treated at all was somewhat inferior as compared with the 450°C treated material (Fig 5-18). Inexplicably the 450°C treated material was significantly better for the O_2 generation mode than were the other materials (Fig 5-19). One possible explanation is that the 450°C treated material may be less hydrophobic, and the increased wetting of the electrode allows more of the Fe-Ni hydroxide to contact the electrolyte. This effect could be assessed using voltammetry.

The H_2TMPP/C which had received no heat treatment increased in cathodic polarization rather dramatically during cycling (Fig 5-20) whereas the 450°C treated material increased only very slightly in polarization. The 800°C treated material decreased significantly in polarization. There were no significant changes in the anodic polarization during cycling (Fig 5-21).

Although the macrocycle is necessary for the high O_2 reduction activity, there is an unexplained effect due to the presence of the large excesses of Fe, Co and Ni hydroxides compared with near stoichiometric amounts (Fig 5-22).

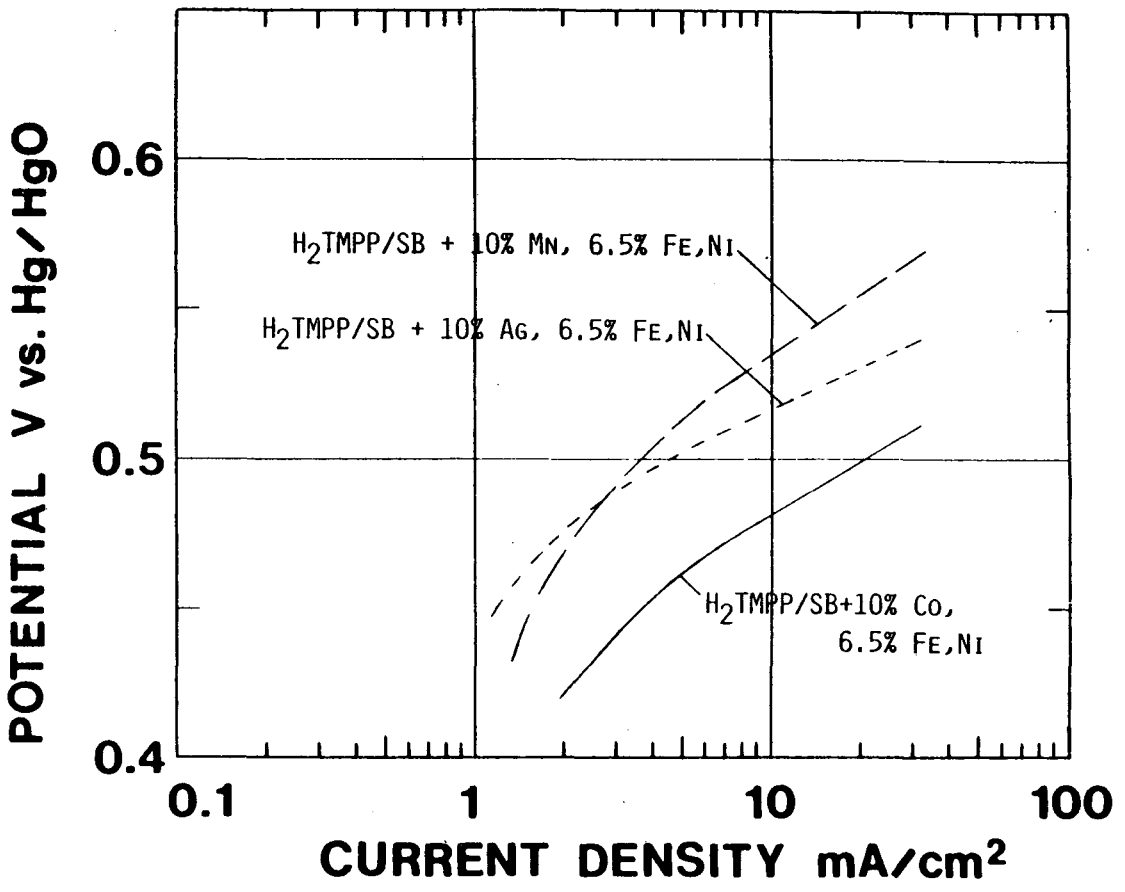

FIG. 5-11. POLARIZATION CURVES FOR O_2 GENERATION WITH POROUS O_2-FED (1 ATM) ELECTRODES IN 5.5 M KOH AT 25°C; 3% MACROCYCLE/CARBON WAS HEAT TREATED AT 450°C BEFORE DEPOSITION OF METAL HYDROXIDES (LOADINGS EXPRESSED AS % METAL). MATERIAL WAS DRIED AT 100°C, TEFLONATED AND HEAT TREATED AT 280°C.

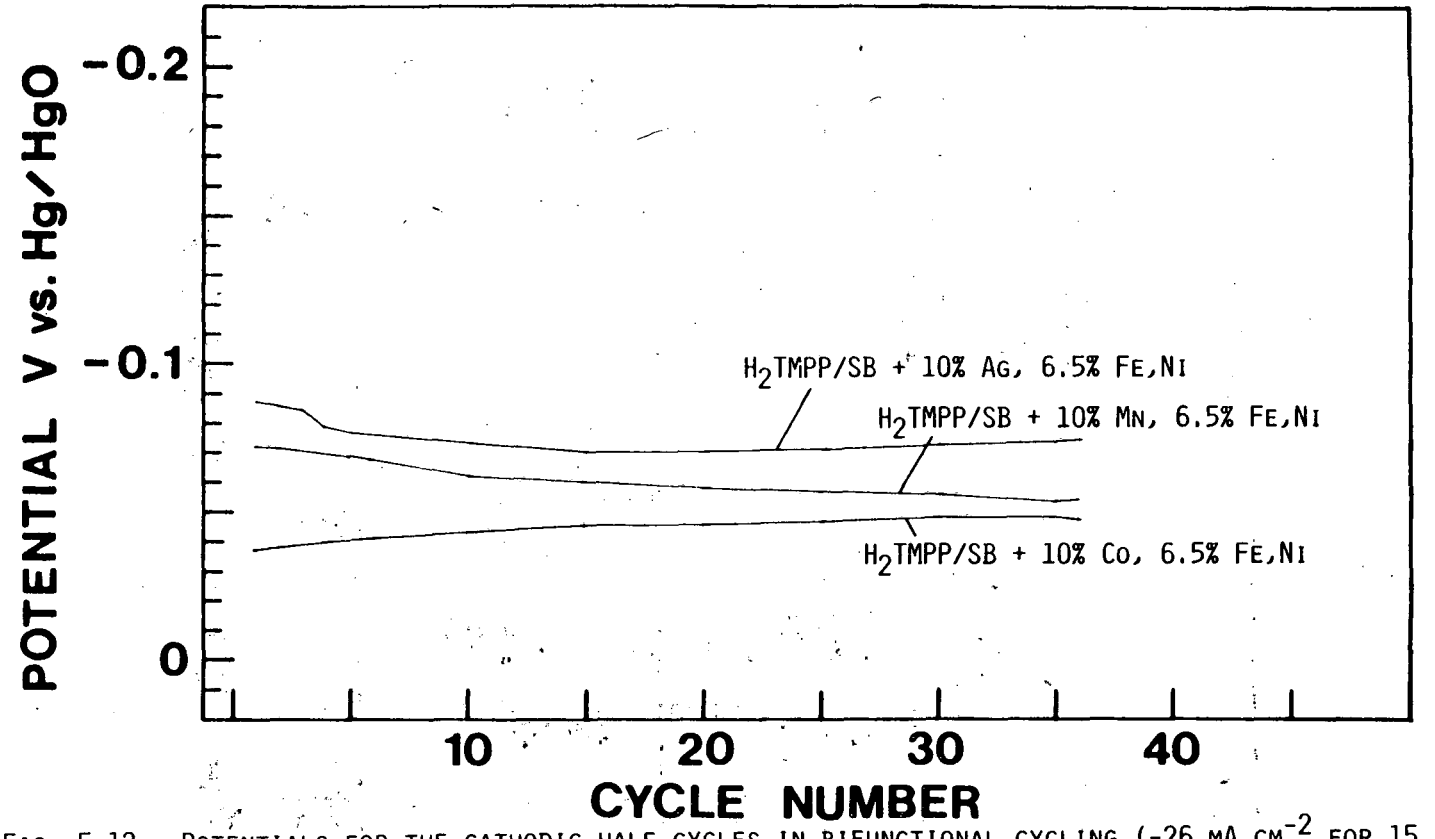

FIG. 5-12. POTENTIALS FOR THE CATHODIC HALF CYCLES IN BIFUNCTIONAL CYCLING (-26 MA CM^{-2} FOR 15 MIN; +13 MA CM^{-2} FOR 15 MIN) FOR POROUS O_2-FED (1 ATM) ELECTRODES IN 5.5 M KOH AT 25°C; 3% MACROCYCLE/CARBON WAS HEAT TREATED AT 450°C BEFORE DEPOSITION OF METAL HYDROXIDES (LOADINGS EXPRESSED AS %.METAL). MATERIAL WAS DRIED AT 100°C, TEFLONATED AND HEAT TREATED AT 280°C.

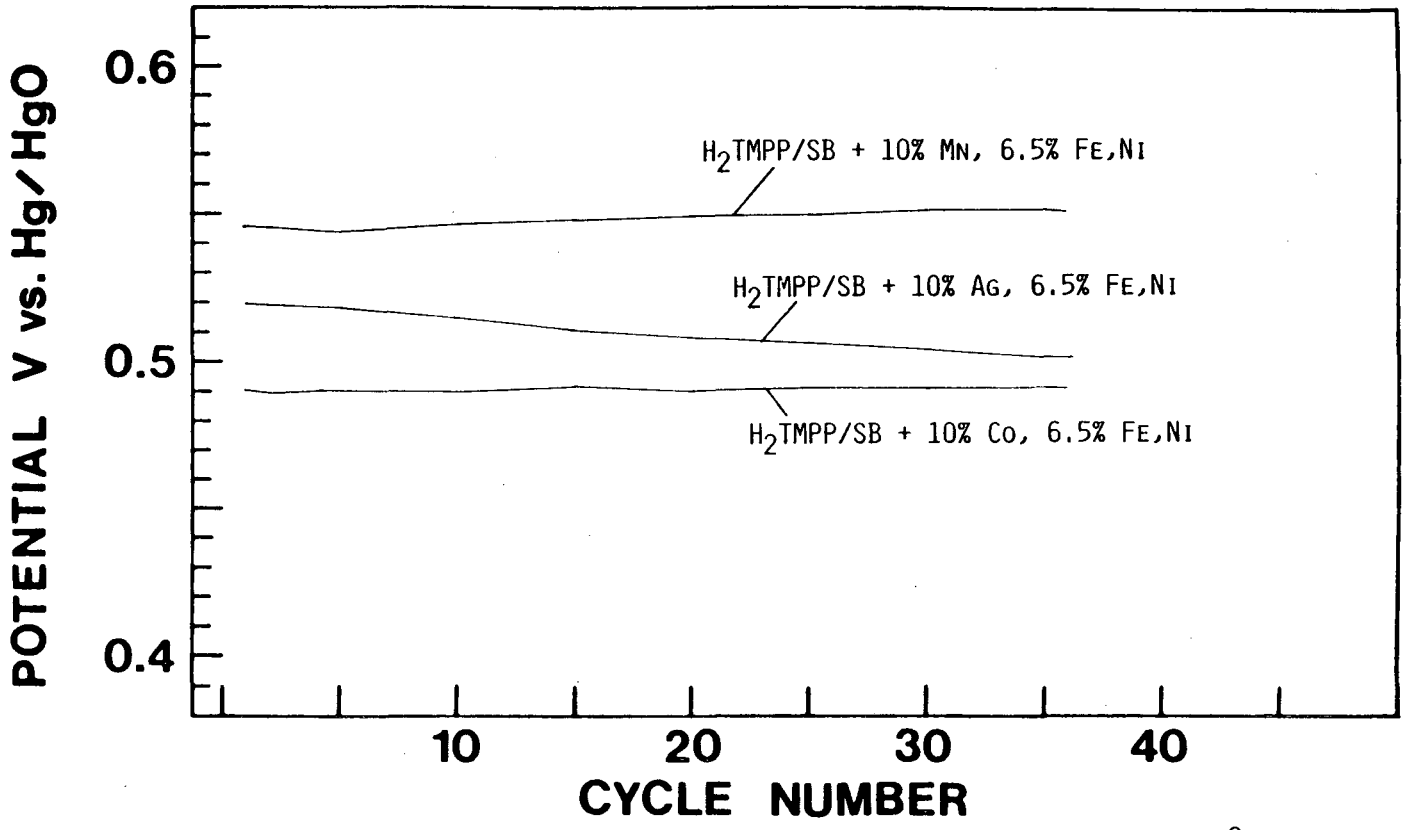

FIG. 5-13. POTENTIALS FOR THE ANODIC HALF CYCLES IN BIFUNCTIONAL CYCLING (-26 MA CM^{-2} FOR 15 MIN; +13 MA CM^{-2} FOR 15 MIN) FOR POROUS O_2-FED (1 ATM) ELECTRODES IN 5.5 M KOH AT 25°C; 3% MACROCYCLE/CARBON WAS HEAT TREATED AT 450°C BEFORE DEPOSITION OF METAL HYDROXIDES (LOADINGS EXPRESSED AS % METAL). MATERIAL WAS DRIED AT 100°C, TEFLONATED AND HEAT TREATED AT 280°C.

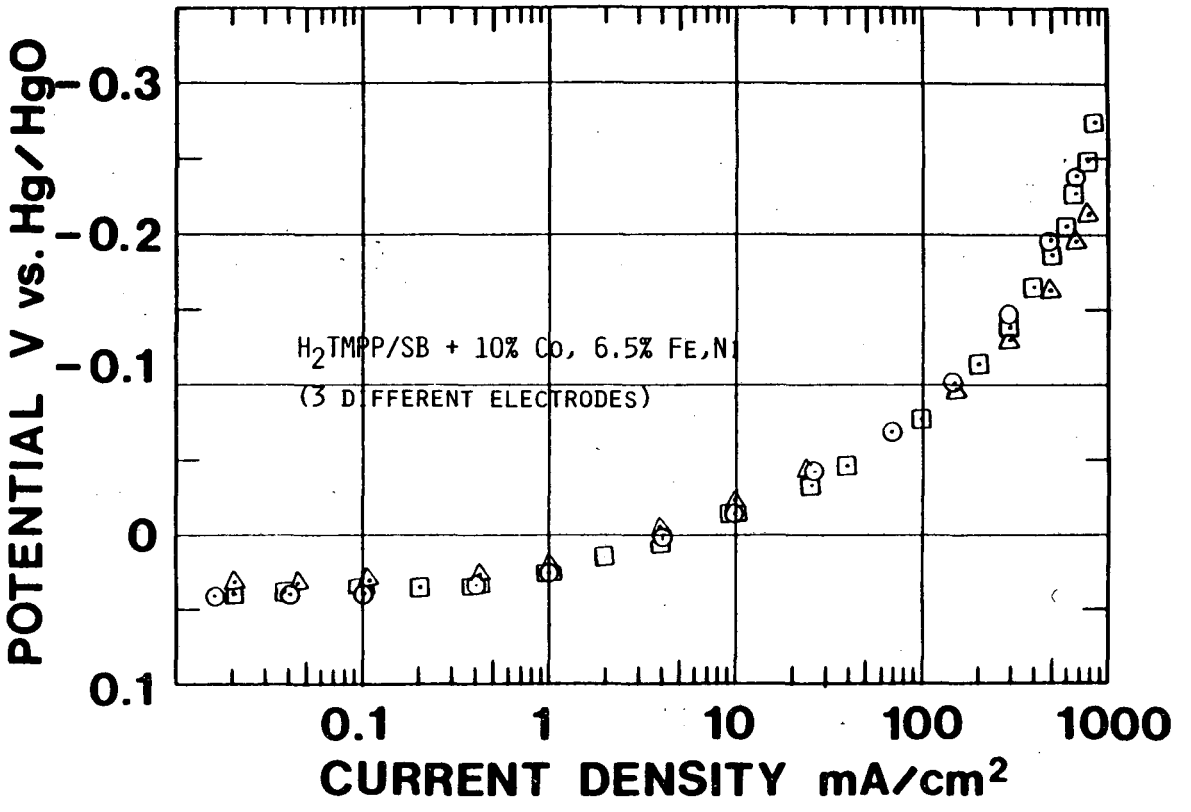

FIG. 5-14. POLARIZATION CURVES FOR O_2 REDUCTION WITH POROUS O_2-FED (1 ATM) ELECTRODES) IN 5.5 M KOH AT 25°C; 3% MACROCYCLE/CARBON WAS HEAT TREATED AT 450°C BEFORE DEPOSITION OF METAL HYDROXIDES (LOADINGS EXPRESSED AS % METAL). MATERIAL WAS DRIED AT 100°C, TEFLONATED AND HEAT TREATED AT 280°C.

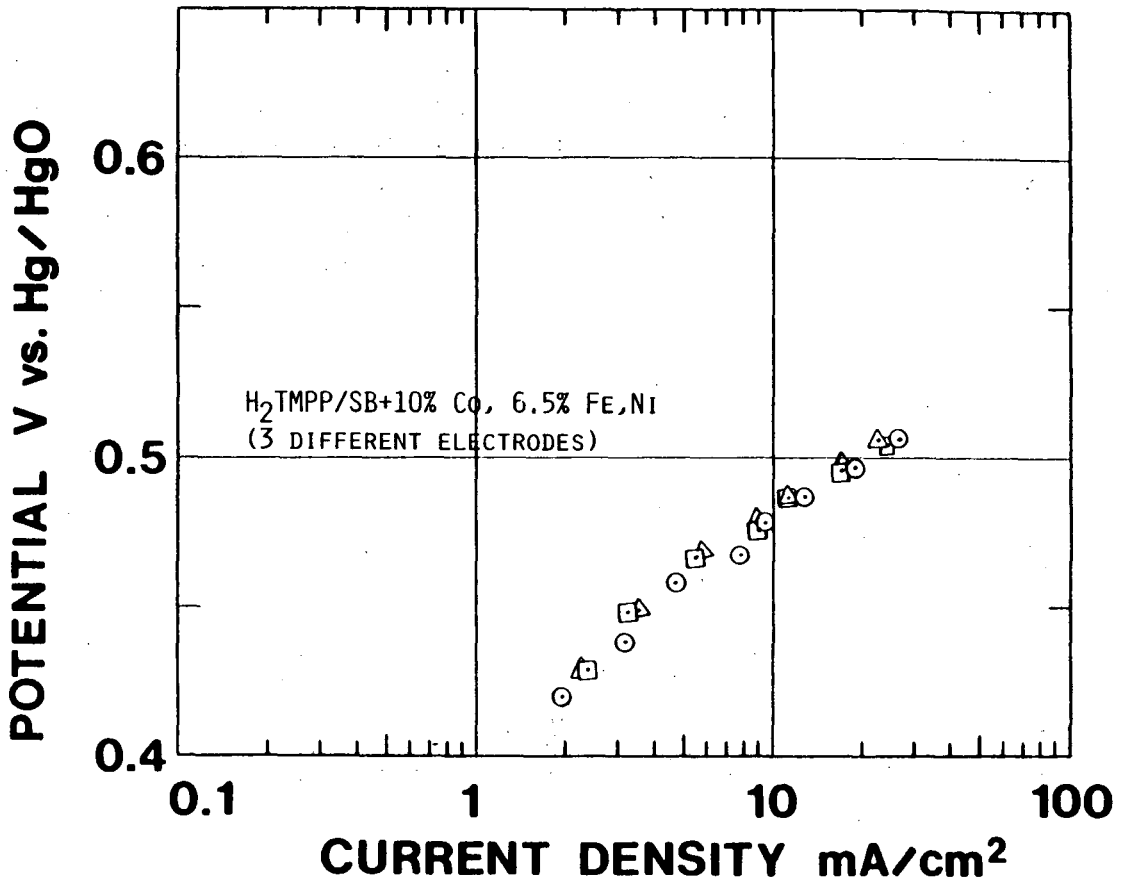

FIG. 5-15. POLARIZATION CURVES FOR O_2 GENERATION WITH POROUS O_2-FED (1 ATM) ELECTRODES IN 5.5 M KOH AT 25°C; 3% MACROCYCLE/CARBON WAS HEAT TREATED AT 450°C BEFORE DEPOSITION OF METAL HYDROXIDES (LOADINGS EXPRESSED AS % METAL). MATERIAL WAS DRIED AT 100°C, TEFLONATED AND HEAT TREATED AT 280°C.

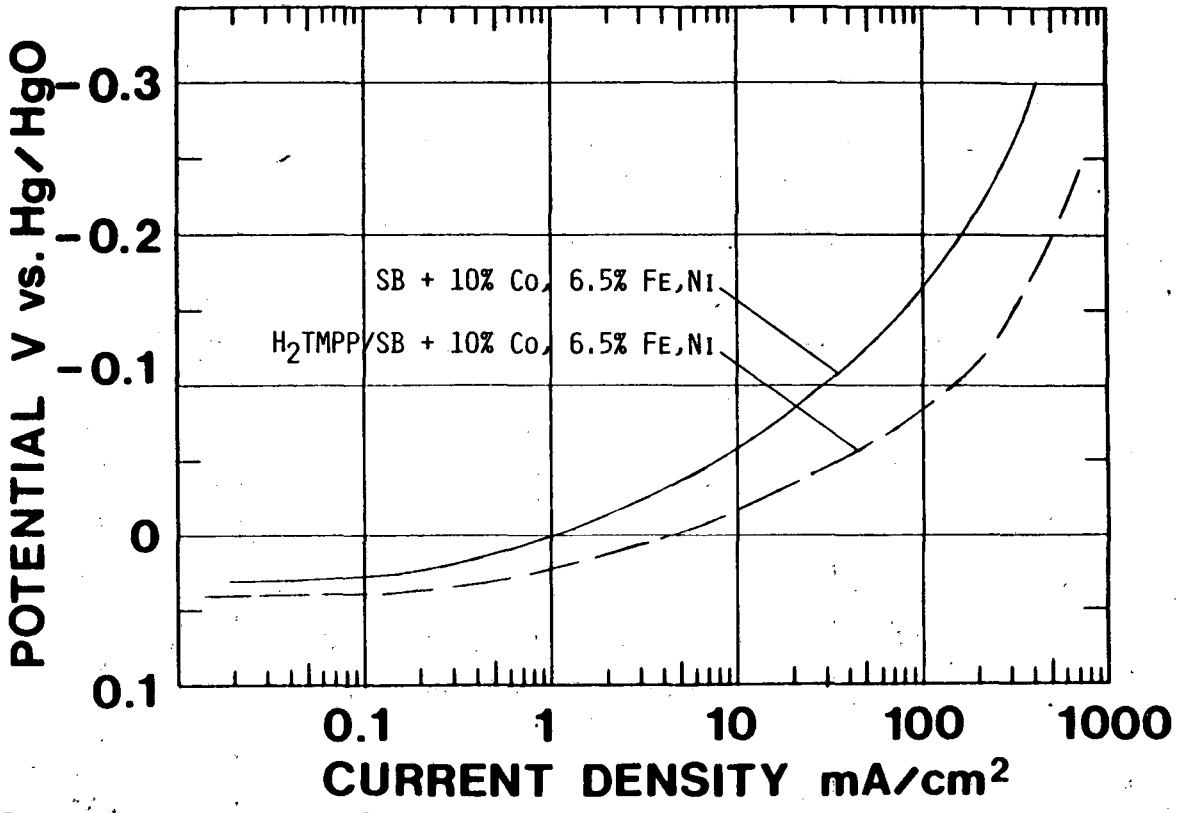

FIG. 5-16. POLARIZATION CURVES FOR O_2 REDUCTION WITH POROUS O_2-FED (1 ATM) ELECTRODES IN 5.5 M KOH AT 25°C; 3% MACROCYCLE/CARBON WAS HEAT TREATED AT 450°C BEFORE DEPOSITION OF METAL HYDROXIDES (LOADINGS EXPRESSED AS % METAL). MATERIAL WAS DRIED AT 100°C, TEFLONATED AND HEAT TREATED AT 280°C.

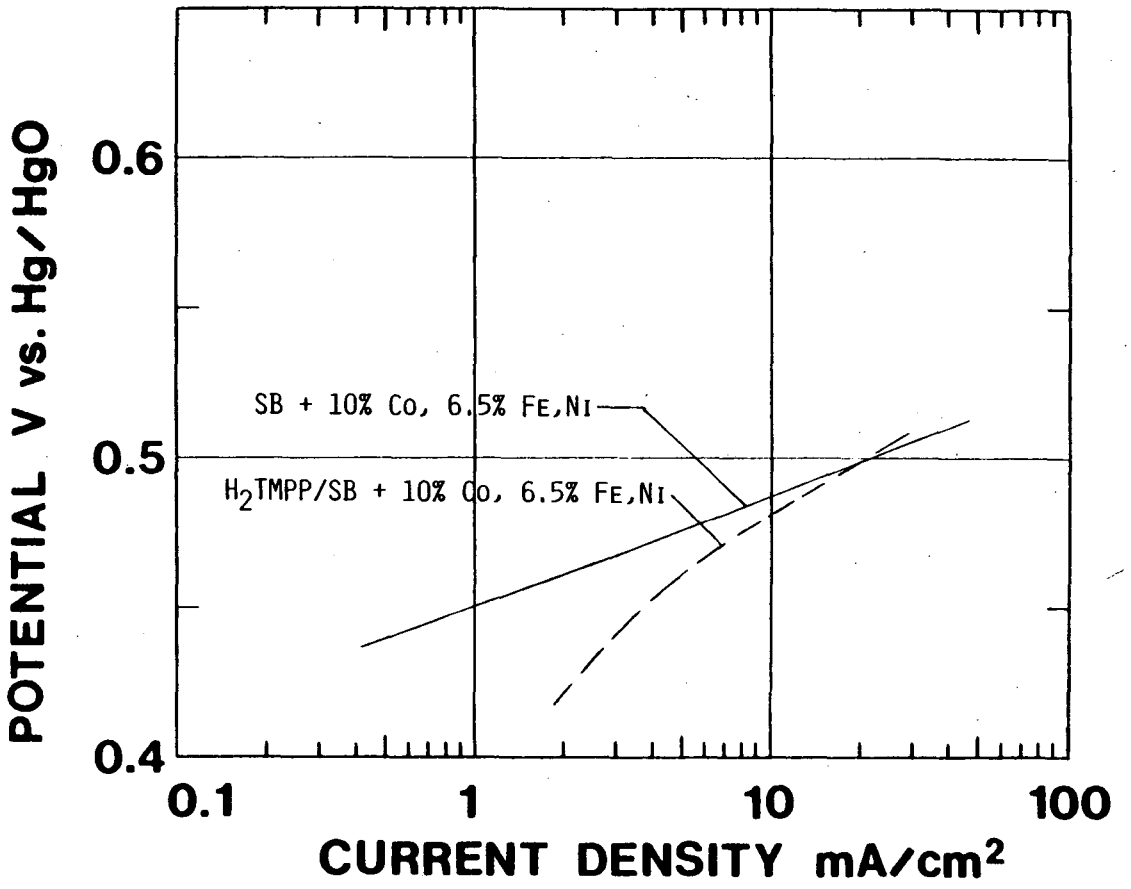

FIG. 5-17. POLARIZATION CURVES FOR O_2 GENERATION WITH POROUS O_2-FED (1 ATM) ELECTRODES IN 5.5 M KOH AT 25°C; 3% MACROCYCLE/CARBON WAS HEAT TREATED AT 450°C BEFORE DEPOSITION OF METAL HYDROXIDES (LOADINGS EXPRESSED AS % METAL). MATERIAL WAS DRIED AT 100°C, TEFLONATED AND HEAT TREATED AT 280°C.

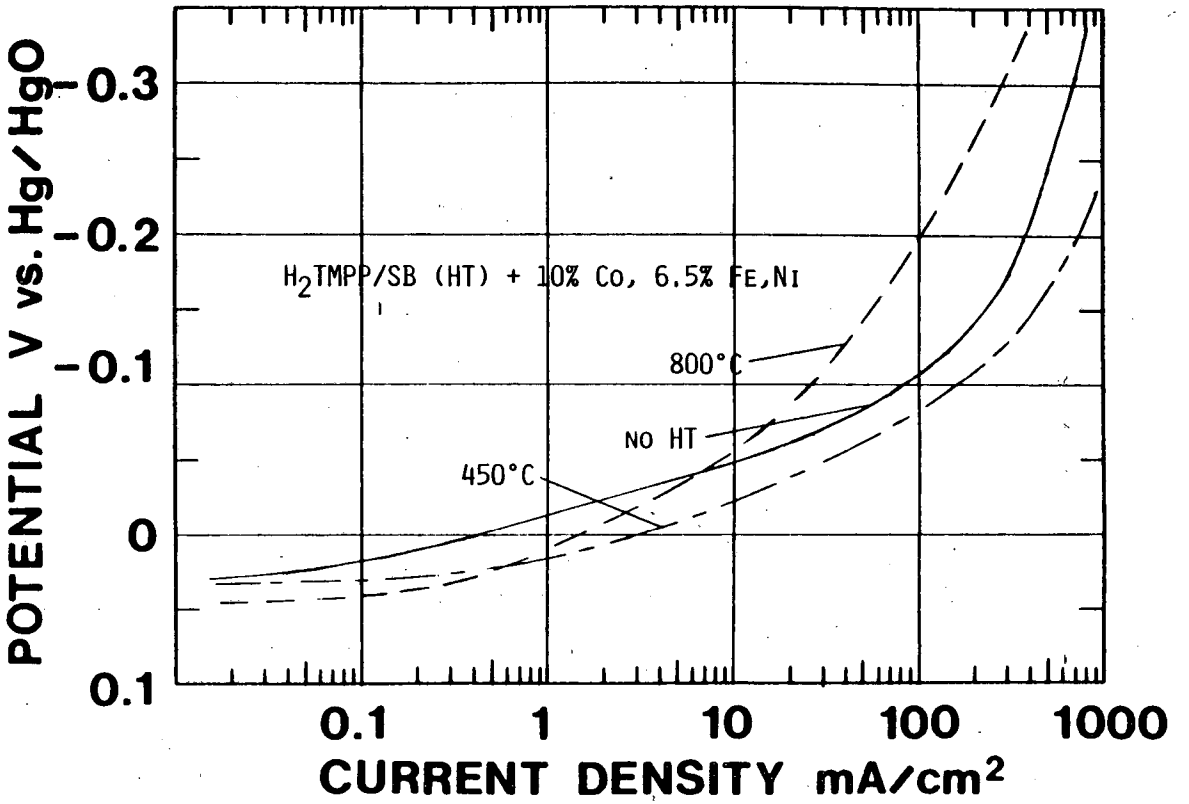

FIG. 5-18. POLARIZATION CURVES FOR O_2 REDUCTION WITH POROUS O_2-FED (1 ATM) ELECTRODES IN 5.5 M KOH AT 25°C; 3% H_2TMPP/SB WAS HEAT TREATED AT VARIOUS TEMPERATURES BEFORE DEPOSITION OF METAL HYDROXIDES (LOADINGS EXPRESSED AS % METAL). MATERIAL WAS DRIED AT 100°C, TEFLONATED AND HEAT TREATED AT 280°C.

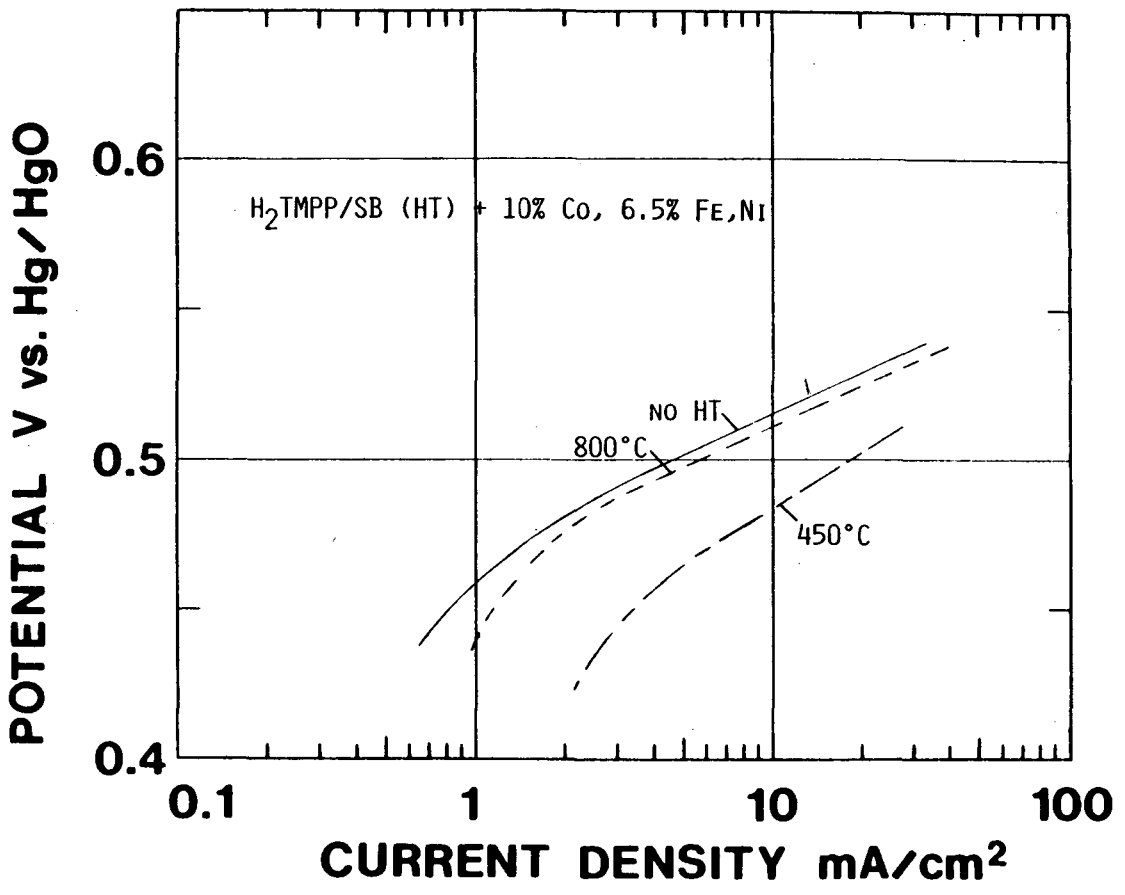

FIG. 5-19. POLARIZATION CURVES FOR O_2 GENERATION WITH POROUS O_2-FED (1 ATM) ELECTRODES IN 5.5 M KOH AT 25°C; 3% H_2TMPP/SB WAS HEAT TREATED AT VARIOUS TEMPERATURES BEFORE DEPOSITION OF METAL HYDROXIDES (LOADINGS EXPRESSED AS % METAL).

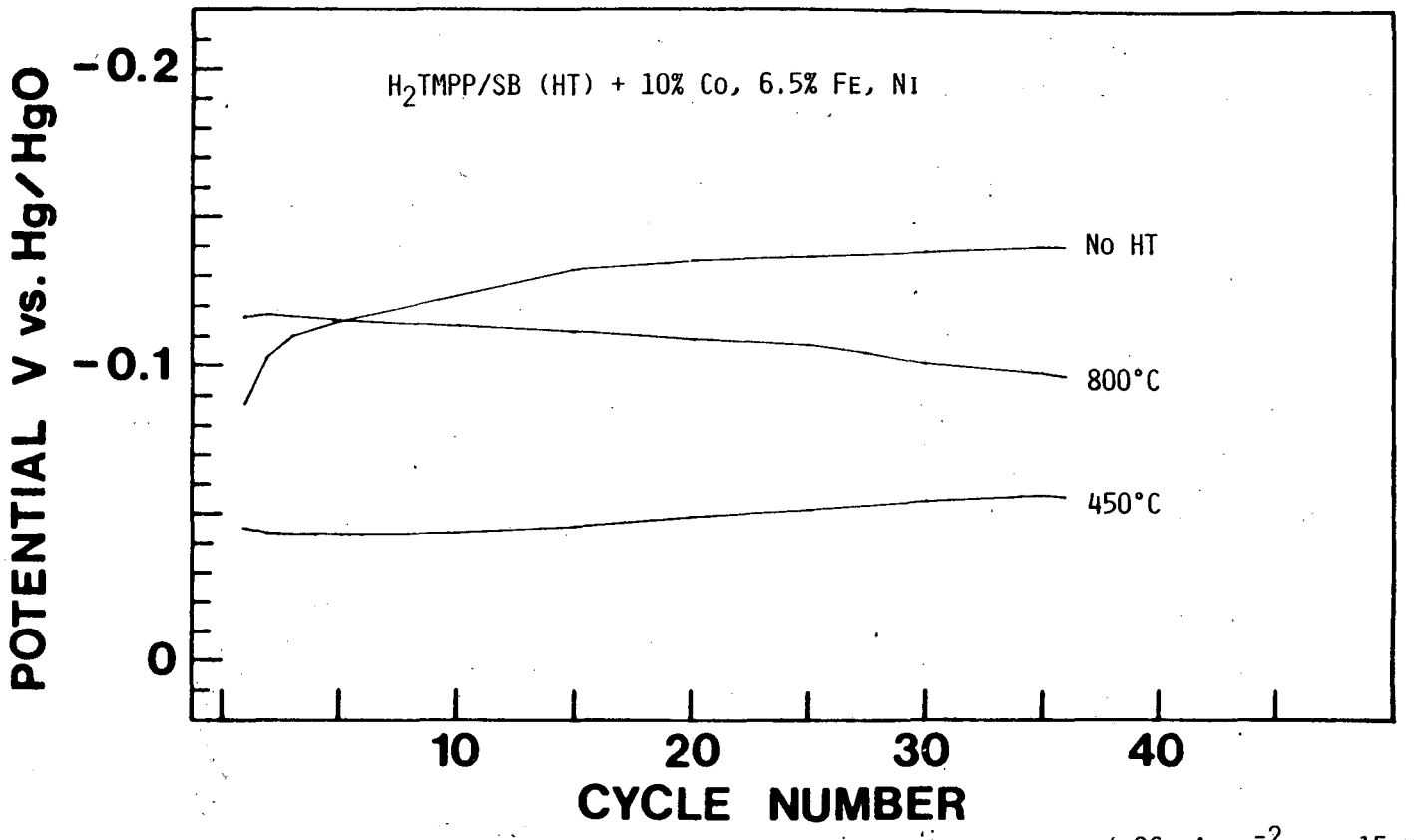

FIG. 5-20. POTENTIALS FOR THE CATHODIC HALF CYCLES IN BIFUNCTIONAL CYCLING (-26 MA CM^{-2} FOR 15 MIN; +13 MA CM^{-2} FOR 15 MIN) FOR POROUS O_2-FED (1 ATM) ELECTRODES; 3% H_2TMPP/SB WAS HEAT TREATED AT VARIOUS TEMPERATURES BEFORE DEPOSITION OF METAL HYDROXIDES (LOADINGS EXPRESSED AS % METAL). MATERIAL WAS DRIED AT 100°C, TEFLONATED AND HEAT TREATED AT 280°C.

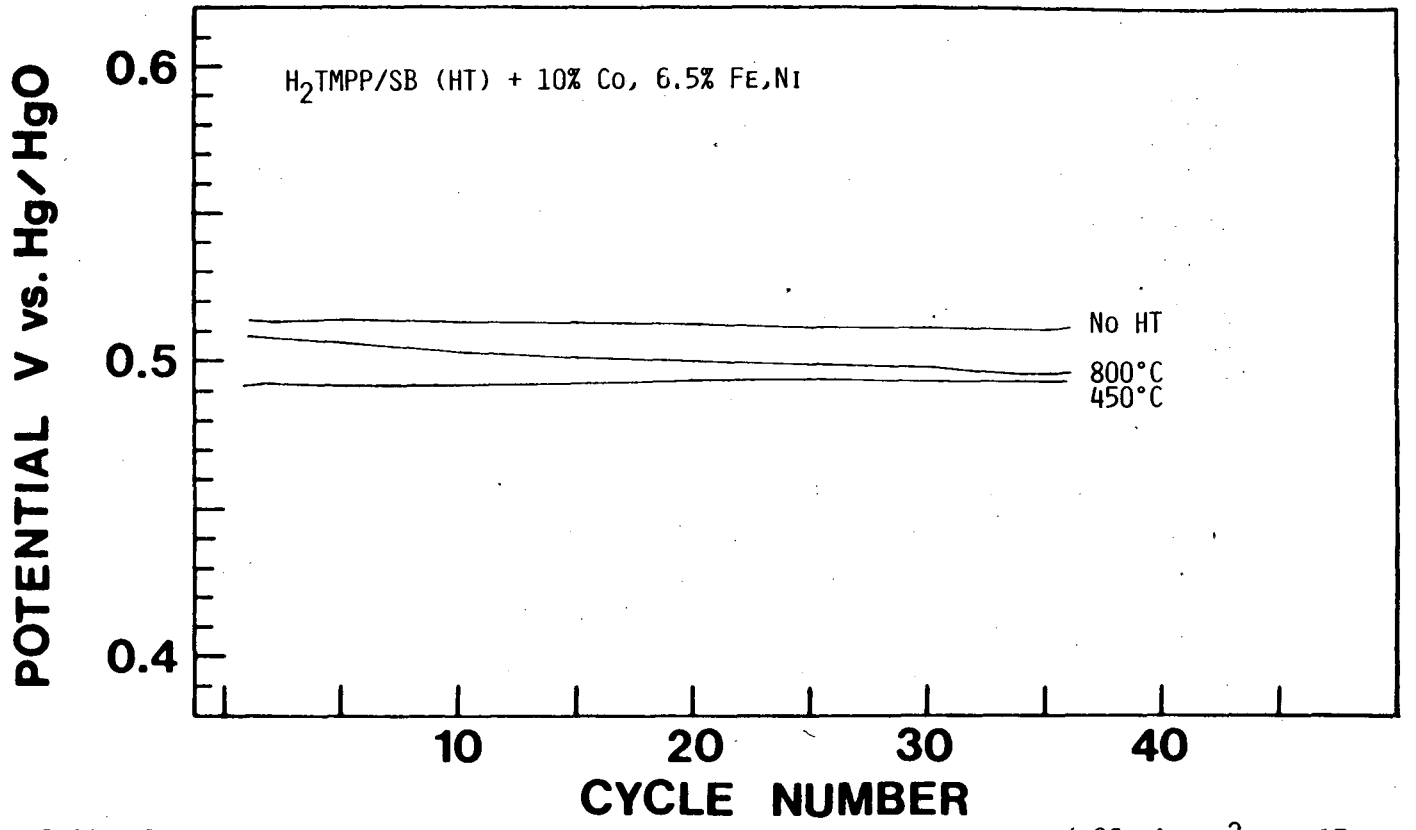

FIG. 5-21. POTENTIALS FOR THE ANODIC HALF CYCLES IN BIFUNCTIONAL CYCLING (-26 mA cm^{-2} FOR 15 MIN; +13 mA cm^{-2} FOR 15 MIN) FOR POROUS O_2-FED (1 ATM) ELECTRODES; 3% H_2TMPP/SB WAS HEAT TREATED AT VARIOUS TEMPERATURES BEFORE DEPOSITION OF METAL HYDROXIDES (LOADINGS EXPRESSED AS % METAL). MATERIAL WAS DRIED AT 100°C, TEFLONATED AND HEAT TREATED AT 280°C.

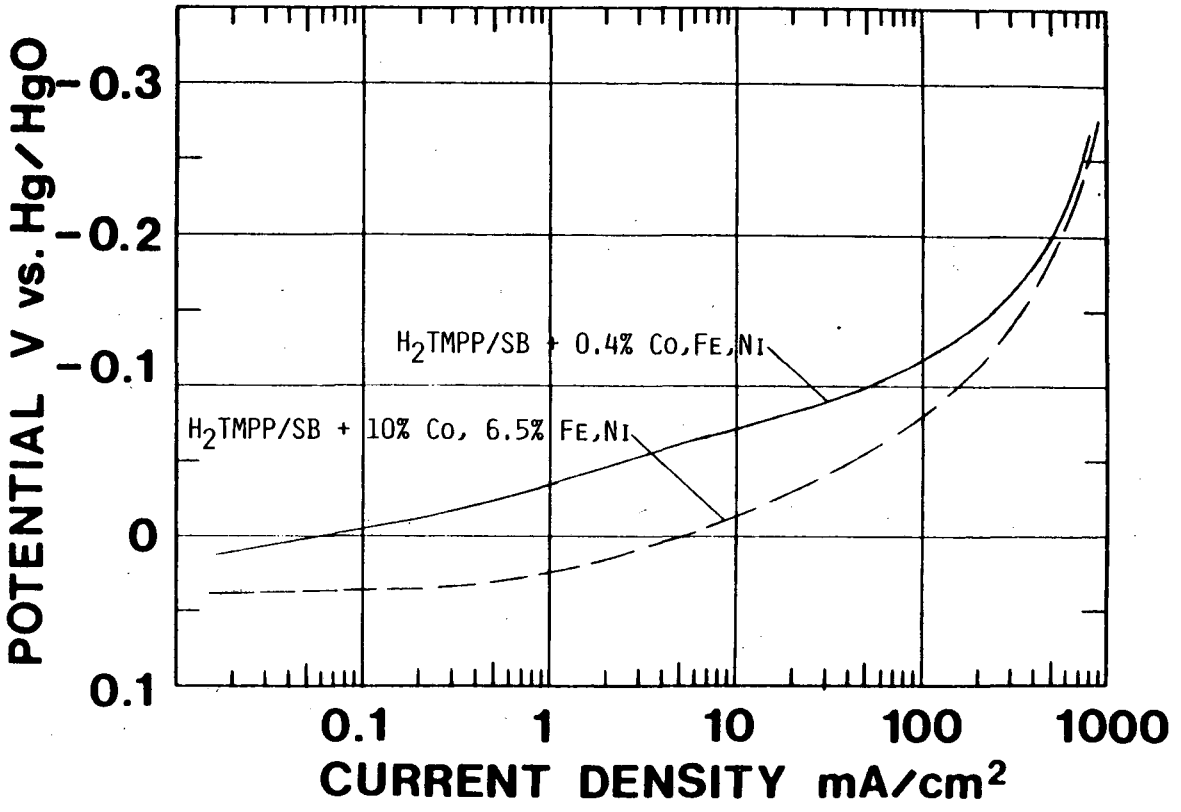

FIG. 5-22. POLARIZATION CURVES FOR O_2 REDUCTION WITH POROUS O_2-FED (1 ATM) ELECTRODES IN 5.5 M KOH AT 25°C; 3% MACROCYCLE/CARBON WAS HEAT TREATED AT 450°C BEFORE DEPOSITION OF METAL HYDROXIDES (LOADINGS EXPRESSED AS % METAL). MATERIAL WAS DRIED AT 100°C, TEFLONATED AND HEAT TREATED AT 280°C.

For the lower curve, the Fe,Co and Ni were present at nominal 28-fold, 42-fold and 27-fold excesses with respect to the H_2TMPP, whereas the 0.4% loadings were approximately 1.6 fold excesses (considered separately, i.e. moles of each individual metal vs. total moles of H_2TMPP). There is certainly some electrocatalysis as well as peroxide decomposition due to the excess metal hydroxides, but not enough to account for this large difference in Fig. 5-22. In fact the upper polarization curve for the 0.4% loadings is almost coincident with those in Fig. 5-2 for systems containing cobalt only. This fact points to the possibility that there may be a competition for adsorption sites on the substrate and that Co is favored either thermodynamically or kinetically. At the higher loadings, the other metals may have a better chance to adsorb. In order to shed light on problems such as this, ion-exchange equilibrium measurements are planned for the future.

It is not surprising to see that the 0.4% loading for the Fe, Co and Ni hydroxides was much less active for O_2 generation than was the high loading (Fig 5-23). It is expected that the O_2 generation current should be an almost linear function of the amount of these hydroxides in contact with the electrolyte. Experiments along these lines are planned for the future.

The temperature at which the metal hydroxides were dried during the catalyst preparation should affect their dehydration, and consequently the amount of material which is electrochemically active and which should be available for O_2 generation polarization behavior (Fig 5-25). During galvanostatic cycling, the initial part of the potential-time trace after each change in polarity provides an approximate measure of the amount of electroactice material, and these amounts were found to depend upon the drying temperature. After drying at 100°C, there remained more electroactive material than after the drying at 280°C.

The electrode potential during the anodic half-cycle is expected to adversely affect the macrocycle/carbon substrate due to electrooxidation (28,29). A lower potential should produce less oxidation current. In fact a 185 mV/decade tafel-like slope was found for Shawinigan black electrooxidation in previous research for the bifunctional O_2 electrode project (29). Thus, the fact that the electrode, which had experienced lower anodic potentials during cycling, seemed to experience relatively little degradation in O_2 reduction performance after cycling comes as no surprise (100°C drying, after cycling, Fig 5-24). Another important parameter besides the final potential however is the actual amount of charge passed for carbon oxidation. For the electrode material which had been dried at 100°C, there was more electractive material than for the 280°C dried material, and consequently a larger portion of the 15 minute anodic cycle was consumed for "charging" of the metal hydroxides.

In order to assess the gas-mass transport properties of the electrodes, air and O_2-He (21:79, v/v) were used as feed gases. The potential separation between the O_2 and air curves remains remarkably constant over a wide range of current densities in Fig. 5-26, which indicates a Nernstian response rather than a kinetically limited response, which would normally be first order in O_2 partial pressure. This type of behavior may indicate that the current is limited by the rate of peroxide decomposition over this range and that the O_2 reduction to peroxide is relatively rapid (28). Other explanations are certainly possible and work in progress may answer this question. The O_2 mass transport is relatively good, as seen by the fact that

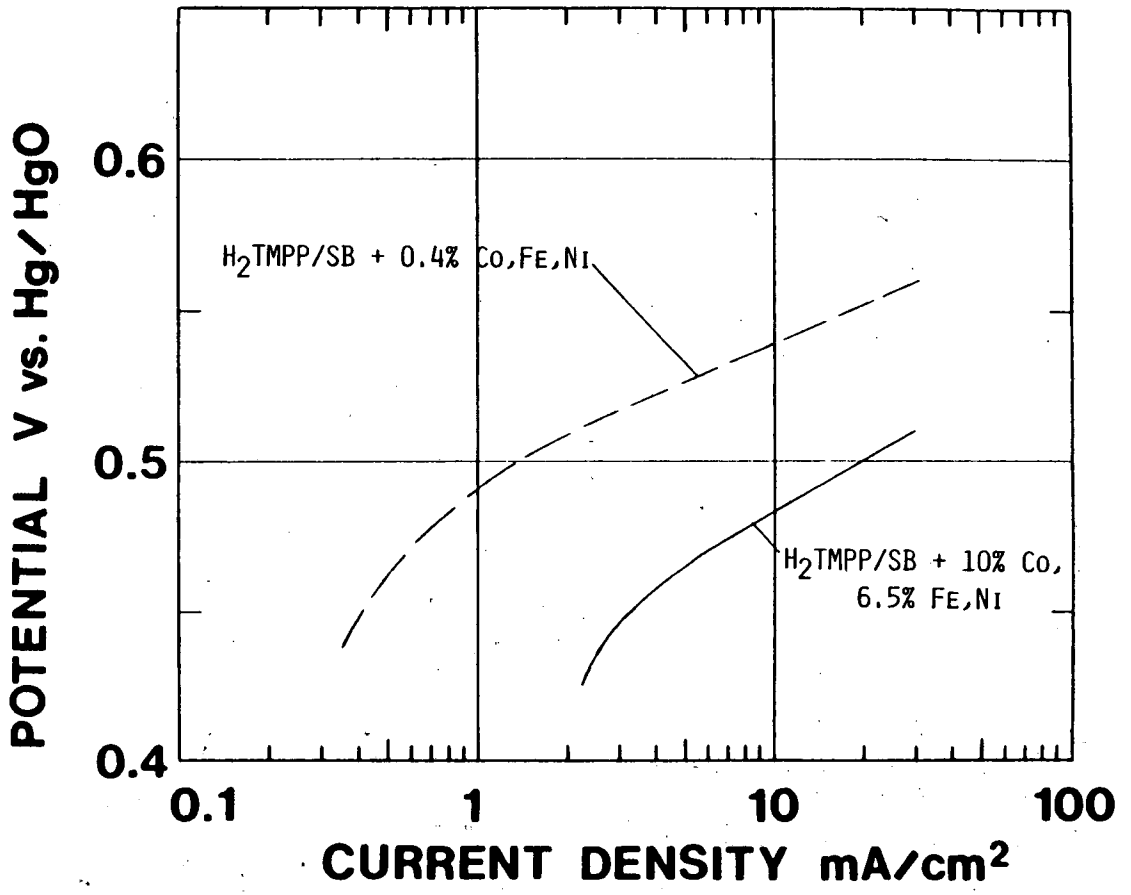

FIG. 5-23. POLARIZATION CURVES FOR O_2 GENERATION WITH POROUS O_2-FED (1 ATM) ELECTRODES IN 5.5 M KOH AT 25°C; 3% MACROCYCLE/CARBON WAS HEAT TREATED AT 450°C BEFORE DEPOSITION OF METAL HYDROXIDES (LOADINGS EXPRESSED AS % METAL). MATERIAL WAS DRIED AT 100°C, TEFLONATED AND HEAT TREATED AT 280°C.

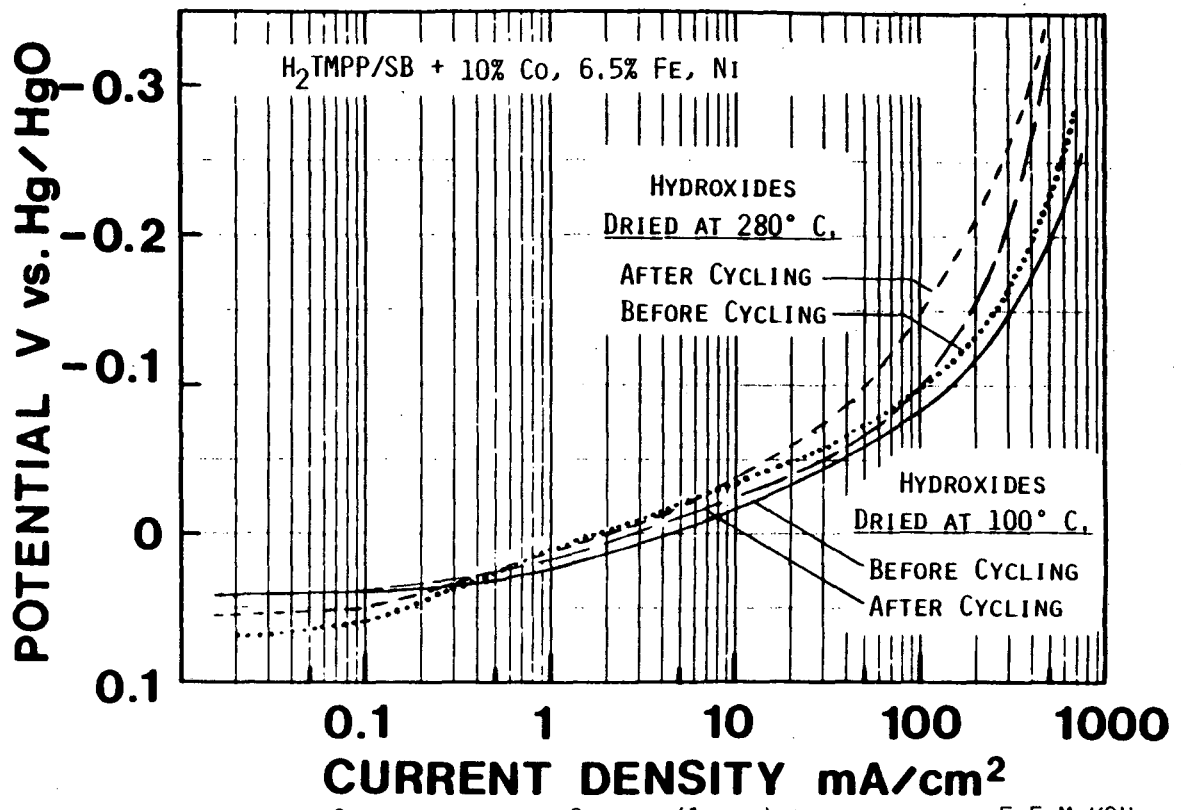

FIG. 5-24. POLARIZATION CURVES FOR O_2 REDUCTION ON O_2-FED (1 ATM) ELECTRODES IN 5.5 M KOH AT 25°C BEFORE AND AFTER CYCLING (35 CYCLES: -26 MA CM^{-2} FOR 15 MIN; +13 MA CM^{-2} FOR 15 MIN); 3% MACROCYCLE/CARBON WAS HEAT TREATED AT 450°C BEFORE DEPOSITION OF METAL HYDROXIDES. MATERIAL WAS DRIED AT EITHER 100°C OR 280°C, TEFLONATED AND HEAT TREATED AT 280°C.

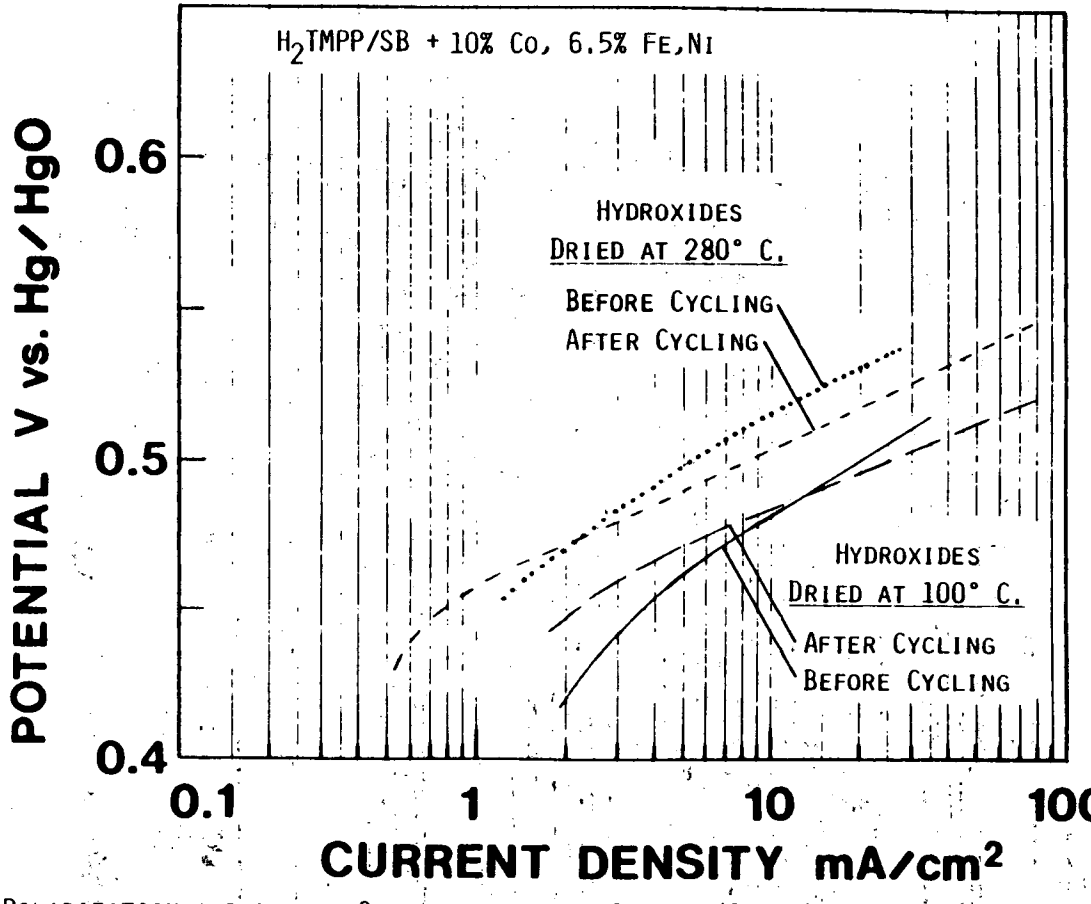

FIG. 5-25. POLARIZATION CURVES FOR O_2 GENERATION ON O_2-FED (1 ATM) ELECTRODES IN 5.5 M KOH AT 25°C BEFORE AND AFTER CYCLING (35 CYCLES: -26 MA CM^{-2} FOR 15 MIN; +13 MA CM^{-2} FOR 15 MIN); 3% MACROCYCLE/CARBON WAS HEAT TREATED AT 450°C BEFORE DEPOSITION OF METAL HYDROXIDES. MATERIAL WAS DRIED AT EITHER 100°C OR 280°C, TEFLONATED AND HEAT TREATED AT 280°C.

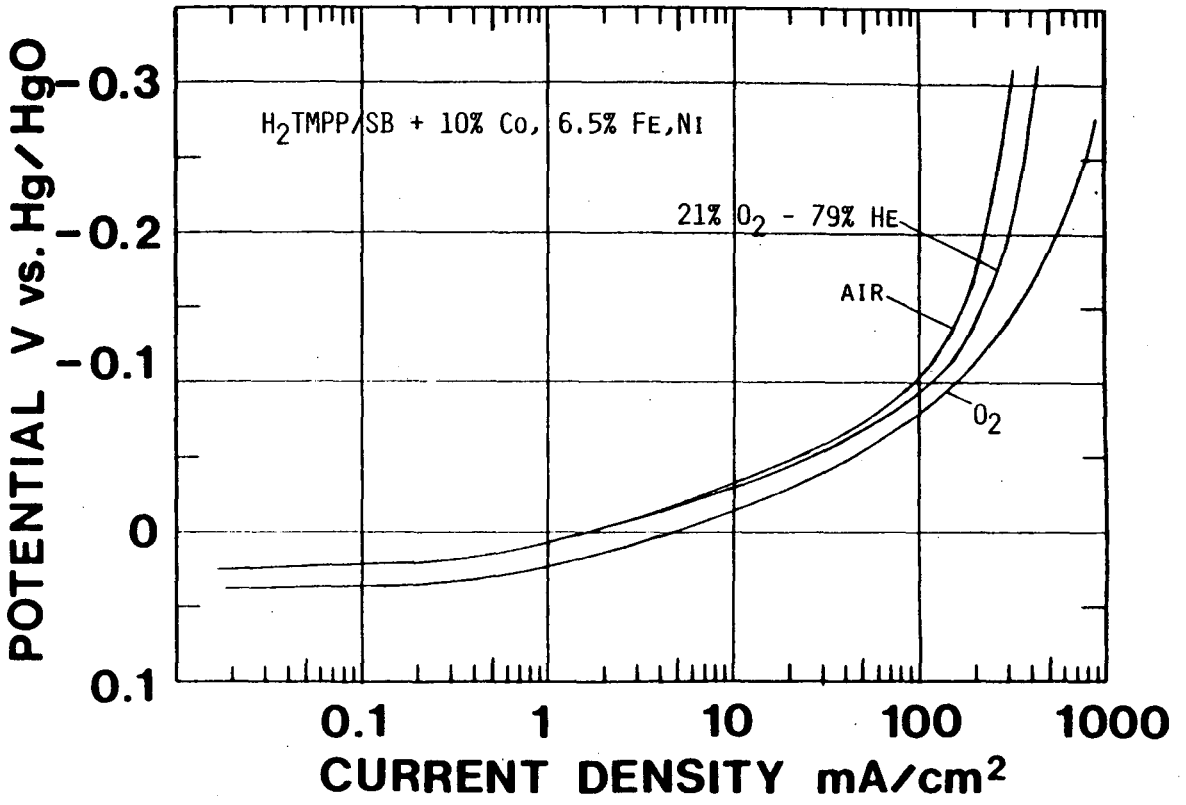

FIG. 5-26. POLARIZATION CURVES FOR O_2 REDUCTION WITH GAS-FED ELECTRODES IN 5.5 M KOH AT 25°C WITH VARIOUS FEED GASES (1 ATM); 3% MACROCYCLE/CARBON WAS HEAT TREATED AT 450°C BEFORE DEPOSITION OF METAL HYDROXIDES (LOADINGS EXPRESSED AS % METAL). MATERIAL WAS DRIED AT 100°C, TEFLONATED AND HEAT TREATED AT 280°C.

the O_2-He and air curves only deviate significantly starting at around 50 mA cm^{-2}.

It was expected that different types of Teflon would have effects mainly on the polarization at the higher current densities due to differences in O_2 mass transport, but other differences were also observed. For all of the measurements described in this report, an aged-batch of Teflon T30B supension was used. Several electrodes were also fabricated using fresh-batches of Teflon suspension and marked differences were found in the O_2 reduction and generation behavior (Figs. 5-27 and 5-28, respectively). The O_2 reduction behavior is difficult to explain, but the somewhat higher O_2 generation activity for the sample prepared with the aged Teflon (Fig 5-28) indicates either that the fresh Teflon makes the electrode more hydrophobic, or that it allows the metal hydroxides to become more dehydrated during the final heat treatment at 280°C. One reason for preferring the latter explanation is that scanning electron microscopy of deposits of the two types of Teflon show that the fresh Teflon forms a porous deposit, whereas the aged Teflon forms a nonporous, continuous one. The latter would tend to form a protective coating over the metal hydroxides, which might prevent them from losing as much water during the heat treatment.

On the basis of the previous experiment it was thought that even better behavior (at least for O_2 generation) could be expected if the 280°C heat treatment was circumvented by extracting the Triton X-100 surfactant with chloroform, which would be done by refluxing at the boiling point (~ 80°C). The upper curve in Fig. 5-29 shows that this was not a beneficial procedure for the O_2 reduction activity. As expected, the O_2 generation behavior was significantly better after extraction of the surfactant at low temperature (Fig. 5-30). The galvanostatic potential vs. time traces also showed that almost the entire amount of added metal hydroxide was electroactive.

In terms of O_2 reduction, the 280°C heat treatment may do several things. First it almost certainly has a beneficial effect on the O_2 mass transport properties of Teflon. Second, it may serve to contract the Teflon fibers, pulling together the material and making its electronic conductivity larger. If this were true, however, the anodic polarization curve for the sample which had only been extracted with chloroform should have shown a bending up at the high current density end due to internal iR drop. Lastly, heat treatment may be necessary for the interaction between the $Co(OH)_2$ and other hydroxides with the macrocycle/carbon substrate. The middle curve in Fig. 5-29 was meant to test this hypothesis. The catalyst preparation was heat treated at 280°C prior to Teflon deposition but not afterwards in order to separate the two effects. There was an increase in activity at the low current density end compared to the electrode which had received no heat treatment but only chloroform extraction. This result may be consistent with the expectation of higher catalytic activity due to Co-substrate interaction but inferior O_2 mass transport due to lack of Teflon "pre-sintering". Less ambiguous experiments are now in progress which show that Co(II) can interact with the heat treated (450°C) macrocycle/carbon substrate in a boiling (120°C) glacial acetic acid suspension.

5.4 SUMMARY AND CONCLUSIONS

A finding which is significant for the understanding of the nature of heat-treated transition-metal macrocyclic complexes supported on high area

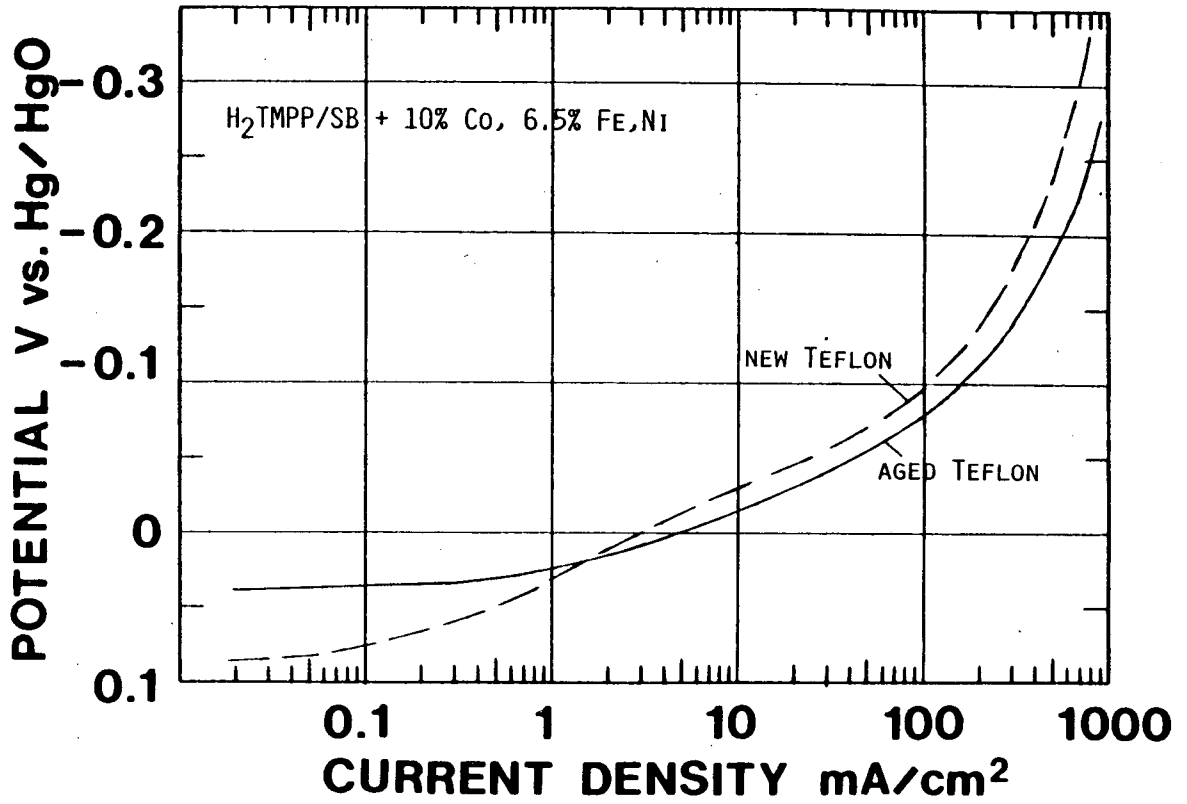

FIG. 5-27. POLARIZATION CURVES FOR O_2 REDUCTION WITH POROUS O_2-FED (1 ATM) ELECTRODES IN 5.5 M KOH AT 25°C; 3% MACROCYCLE/CARBON WAS HEAT TREATED AT 450°C BEFORE DEPOSITION OF METAL HYDROXIDES (LOADINGS EXPRESSED AS % METAL). MATERIAL WAS DRIED AT 100°C, TEFLONATED AND HEAT TREATED AT 280°C.

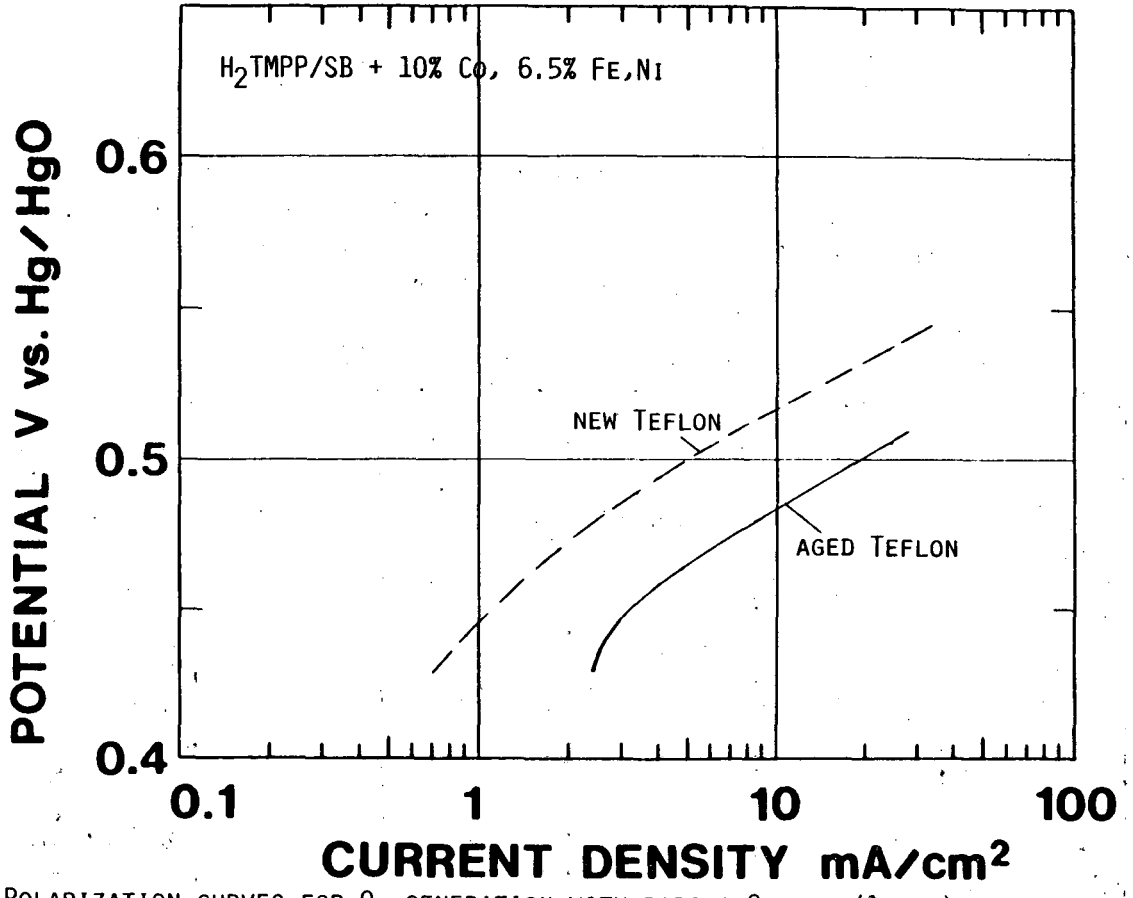

FIG. 5-28. POLARIZATION CURVES FOR O_2 GENERATION WITH POROUS O_2-FED (1 ATM) ELECTRODES IN 5.5 M KOH AT 25°C; 3% MACROCYCLE/CARBON WAS HEAT TREATED AT 450°C BEFORE DEPOSITION OF METAL HYDROXIDES (LOADINGS EXPRESSED AS % METAL). MATERIAL WAS DRIED AT 100°C, TEFLONATED AND HEAT TREATED AT 280°C.

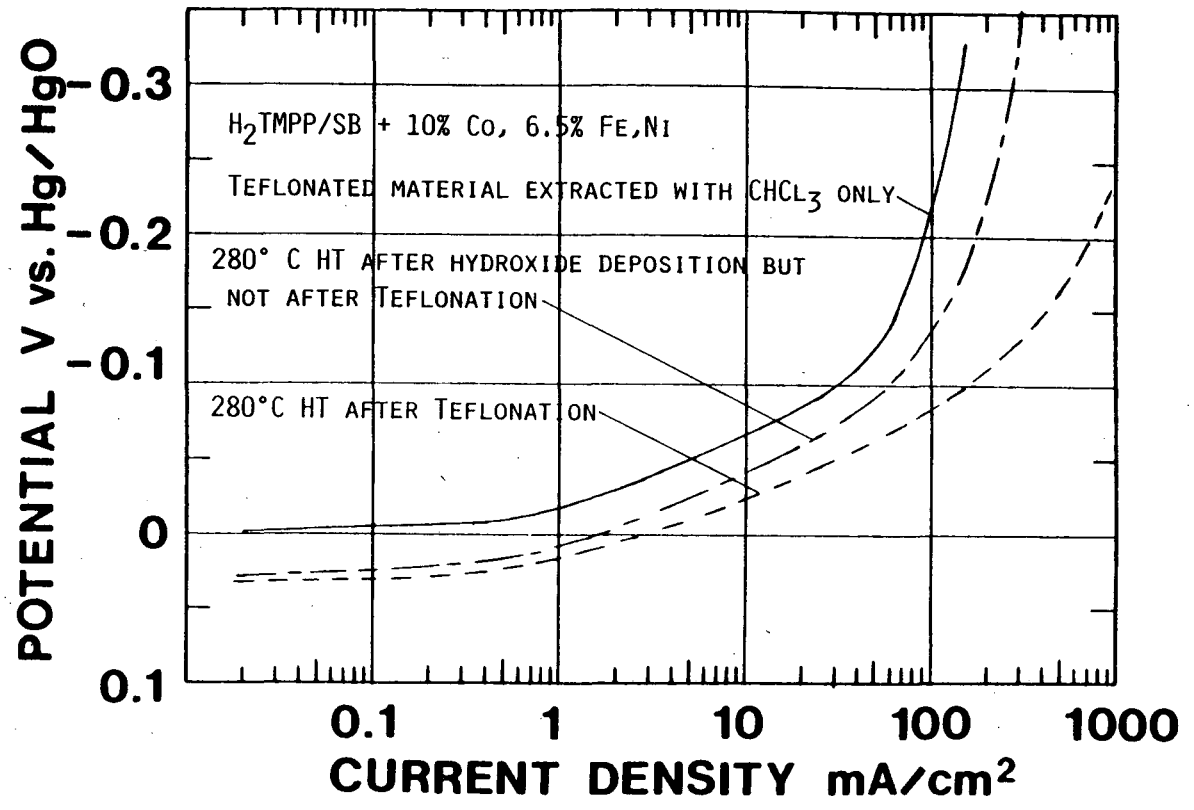

FIG. 5-29. POLARIZATION CURVES FOR O_2 REDUCTION WITH POROUS O_2-FED (1 ATM) ELECTRODES IN 5.5 M KOH AT 25°C; 3% MACROCYCLE/CARBON WAS HEAT TREATED AT 450°C BEFORE DEPOSITION OF METAL HYDROXIDES (LOADINGS EXPRESSED AS % METAL).

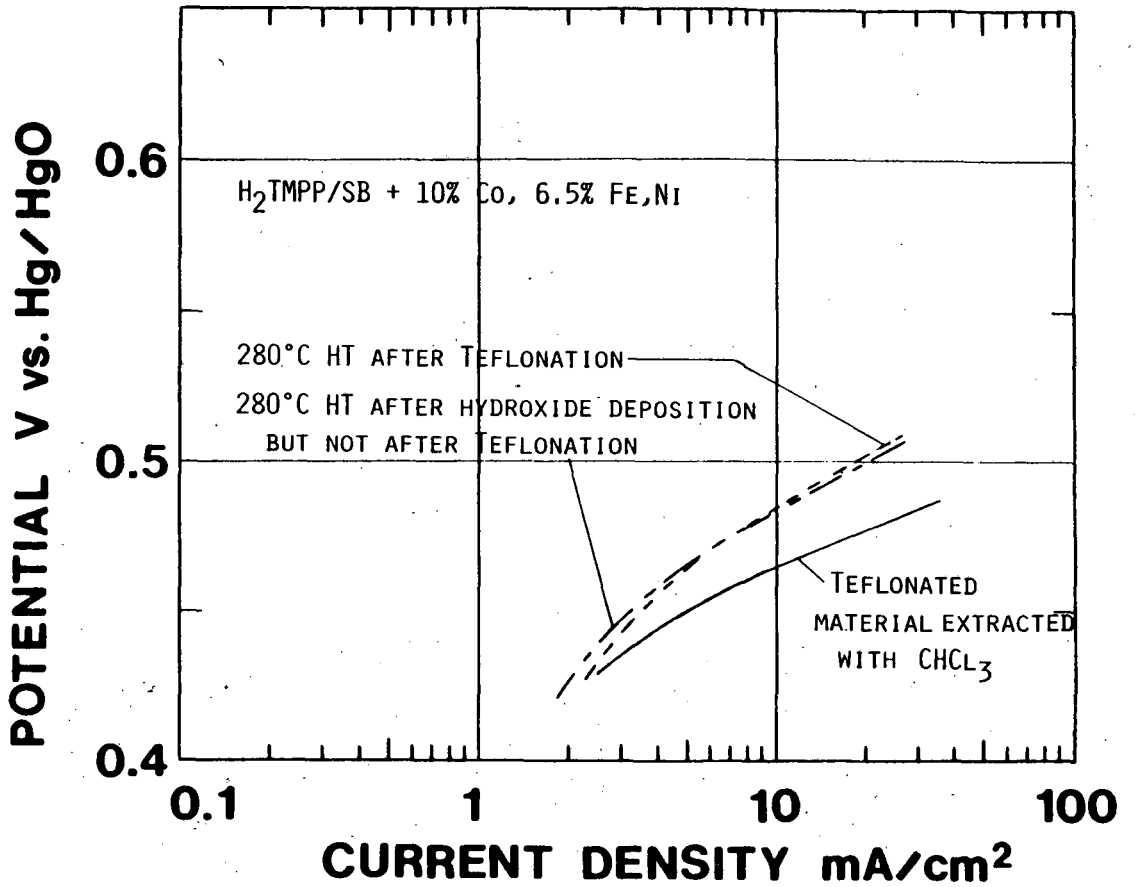

FIG. 5-30. POLARIZATION CURVES FOR O_2 GENERATION WITH POROUS O_2-FED (1 ATM) ELECTRODES IN 5.5 M KOH AT 25°C; 3% MACROCYCLE/CARBON WAS HEAT TREATED AT 450°C BEFORE DEPOSITION OF METAL HYDROXIDES (LOADINGS EXPRESSED AS % METAL).

carbon blacks is that cobalt can be added to the metal-free macrocycle on a carbon free of metallic impurities after the primary heat treatment at 450°C to 800°C. Interaction of the transition metal with the macrocycle/carbon substrate can then occur during subsequent heat treatment at 280°C or possibly during operation in alkaline solution in a gas diffusion electrode. The O_2 reduction activity is much better for the 450°C heat treatment than for either no heat treatment or the 800°C heat treatment and is quite comparable to that for CoTMPP/C treated at 450°C.

Even more significant for practical application is the finding that the O_2 reduction activity of H_2 TMPP/C plus added $Co(OH)_2$ can be improved very significantly with the addition of a second metal hydroxide, with $Ni(OH)_2$ being the best thus far. The best performance was found for another combination of metal hydroxides, X and Z whose identity is being kept confidential pending patent application. Its O_2 generation activity was unstable, however, due to anodic dissolution. Its stability still may be adequate for cathodic-only operation. It is proposed that at least two types of catalytic sites are formed, one for the two-electron reduction of oxygen to hydrogen peroxide and one for either the further reduction or chemical decomposition of hydrogen peroxide. Further research is in progress to determine the kinetics and mechanisms for these processes using the rotating ring-disk electrode as well as other techniques.

For bifunctional operation, the most promising system is H_2TMPP/C plus $Fe(OH)_3$, $Co(OH)_2$ and $Ni(OH)_2$. The activity is quite good for both O_2 reduction and generation and the stability in accelerated short-term cycling tests is also quite good. As with previously mentioned systems, O_2 reduction may involve multiple catalytic sites. The O_2 generation catalysis is catalyzed mainly by a mixed hydroxide or oxide of iron and nickel, with little contribution by the macrocycle.

The optimum processing conditions for this catalyst were found to be: 450°C heat treatment of the macrocycle on high area carbon, high-transition metal hydroxide loadings, 100°C hydroxide drying temperature, the use of aged Teflon suspension and a 280°C final heat treatment. There is much more optimization which could be done however. For example, higher macrocylce loadings might be used if a higher-area oxidation resistant carbon could be found. It may also be advantageous to use a metal-containing macrocycle for the initial heat treatment if it is found that the metal performs a useful function such as catalyzing a beneficial transformation of the substrate.

Further improvements in these catalytic systems depend heavily upon a fundamental understanding of the processes occurring during heat treatment of the macrocycle and during further processing and actual operation. Experimental efforts which are in progress include a wide range of electrochemical and nonelectrochemical methods: electron microscopy, X-ray diffraction, the spectroscopic methods: X-ray photoelectron, Mossbauer and Fourier transform infrared and the thermal methods: thermogravimetry, differential thermal analysis and pyrolysis-mass spectroscopy.

References

1. V. S. Bagotski, M. R. Tarasevich, O. A. Levina, K. A. Radyushkina and S. I. Andruseva, Dokl. Akad. Nauk SSR, 233, 889 (1977).

2. K. A. Radyushkina, J. Res. Inst. Catalysis, Hokkaido, Japan, 30, 155 (1982).

3. K. Wiesener, Sov. Electrochem., 18, 672 (1982).

4. G. Gruenig, K. Wiesener, S. Gamburtsev, I. Iliev and A. Kaisheva, J. Electroanal. Chem., 159, 155 (1983).

5. G. Gruenig, K. Wiesener, A. Kaisheva, S. Gamburtsev and I. Iliev, Sov. Electrochem., 19, 1408 (1983).

6. I. Iliev, In "Extended Abstracts," National Meeting of the Electrochemical Society, Denver, Colorado, October, 1981, Abstr. No. 106, p. 268.

7. I. Iliev, S. Gamburtsev and S. Kaisheva, in "Extended Abstracts," 32nd Meeting of the International Electrochemical Society, Dubrovnik/Cavtat, Yugoslavia, September, 1981, Abstract No. A43, p. 134.

8. S. Gamburtsev, Sov. Electrochem., 18, 123 (1982).

9. S. Gamburtsev, I. Iliev and A. Kaisheva, Sov. Electrochem., 18, 1430 (1982).

10. A. Kaisheva, S. Gamburtsev and I. Iliev, Sov. Electrochem., 18, 127 (1982).

11. S. Gamburtsev, I. Iliev and A. Kaisheva, Sov. Electrochem., 18, 1430 (1982).

12. J. A. R. van Veen and C. Visser, Electrochim. Acta, 24, 921 (1979).

13. J. A. R. van Veen and H. A. Colijn, Ber. Bunsenges. Phys. Chem., 85, 700 (1981).

14. J. A. R. van Veen, J. F. van Baar and K. J. Kroese, J. Chem. Soc., Faraday Trans. I, 77, 2827 (1981).

15. J. A. R. van Veen, J. F. van Baar, C. J. Kroese, J. G. F. Coelgem, N. DeWit and H. A. Colijn, Bev. Bunsenges. Phys. Chem., 85, 693 (1981).

16. R. W. Joyner, J. A. R. van Veen and W. M. H. Sachtler, J. Chem. Soc. Faraday Trans. I, 78, 1021 (1982).

17. S. L. Gupta W. A. Aldred and E. Yeager, in "Extended Abstracts," Vol. 83-2, National Meeting of the Electrochemical Society, Washington, D. C., October, 1983, Abstr. No. 391, p. 624.

18. D. Scherson, S. L. Gupta, E. Yeager, M. E. Kordesch, J. Eldridge and R. W. Hoffman, in "Extended Abstracts," Vol. 82-2, National Meeting of the Electrochemical Society, Detroit, Michigan, October, 1982, Abstr. No. 35, p. 57.

19. S. A. Scherson, S. L. Gupta, C. Fierro, E. Yeager, M. E. Kordesch, J. Eldridge, R. W. Hoffman and J. Blue, Electrochim. Acta, 28, 1205 (1983).

20. D. A. Scherson, S. B. Yao, E. B. Yeager, J. Eldridge, M. E. Kordesch and R. W. Hoffman, J. Phys. Chem., 87, 932 (1983).

21. J. P. Collman, C. S. Bencosme, R. R. Durand Jr., R. P. Kreh and F. C. Anson, J. Am. Chem. Soc., 105, 2699 (1983).

22. R. R. Durand, Jr., C. S. Bencosme, J. P. Collman and F. C. Anson, J. Am. Chem. Soc., 105, 2710 (1983).

23. K. Shigehara and F. C. Anson, J. Electroanal. Chem., 132, 107 (1982).

24. A. D. Adler, F. R. Longo, J. D. Finarelli, J. Goldmacher, J. Assour and L. Korsakoff, J. Org. Chem., 32, 976 (1967).

25. W. C. Schumb, C. N. Satterfield and R. L. Wentworth, "Hydrogen Peroxide," American Chemical Society Monograph Series, Reinhold, New York, 1955.

26. G Magner, M. Savy and G. Scarbeck, J. Electrochem. Soc., 127, 1076 (1980).

27. G. Magner, M. Savy, G. Riga and J .Verbist, J. Electrochem. Soc., 128, 1674 (1981).

28. D. Tryk, W. Aldred, T. Ohzuku and E Yeager, "Bifunctional Oxygen Electrodes," Final Report, October 1980 - April 1983, Lawrence Livermore Laboratory - U.S. Department of Energy, Subcontract No. 1377901.

APPENDIX A

D. Tryk, W. Aldred and E. Yeager, In "Proceedings of the Workshop on the Electrochemistry of Carbon," August, 1983, Cleveland, Ohio, The Electrochemical Society, Pennington, N.J., 1984, pp. 192-220.

CARBON IN BIFUNCTIONAL AIR ELECTRODES IN ALKALINE SOLUTION

D. Tryk, W. Aldred and E. Yeager
Case Center for Electrochemical Sciences
and the Department of Chemistry
Case Western Reserve University
Cleveland, Ohio 44106

ABSTRACT

Bifunctional O_2 electrodes can be used both to reduce and to generate O_2 in rechargeable metal-air batteries and fuel cells. The factors controlling the O_2 reduction and generation reactions in gas-diffusional bifunctional O_2 electrodes are discussed. For a carbon black-based electrode in alkaline solution, the major problem is oxidation of the carbon during the O_2-generation mode. This leads to decreased capability for gas-phase mass transport, decreased electronic conductivity, generally degraded structural integrity and, in some instances, a decrease in electrocatalytic activity for O_2 reduction. Shawinigan acetylene black has been used in some bifunctional O_2 electrodes because of its relatively low surface area and resistance to oxidative attack. Even with such electrodes, however, SEM, XPS, weight loss and visual examination indicate a substantial loss of carbon and increase of bound oxygen in electrodes that have been extensively cycled between O_2-reduction and -generation modes. The resistance of such electrodes, as established from voltammetry curves, has been found to increase markedly during anodic polarization and to be dependent upon the electrode fabrication technique. Carbon blacks with more graphitic structure than Shawinigan black have been found to be more resistant to electro-oxidation.

The further extension of cycle life of bifunctional electrodes using carbon is critically dependent on finding more oxidation-resistant carbons that at the same time have other surface properties meeting the requirements for catalyzed gas-diffusion electrodes.

I. INTRODUCTION

Carbon is the most commonly used support material for oxygen and air positive electrodes in alkaline and acid electrolytes. The technology developed for these electrodes can also be used in alkaline electrolytes for bifunctional oxygen electrodes which can both reduce and generate O_2 within a single structure. Such electrodes, if sufficiently efficient, may find application in rechargeable metal-air batteries employing, for example, iron or zinc negative electrodes, or

even in regenerative H_2-O_2 fuel cells. The major problem with such O_2 electrodes is that the wide potential range experienced by the electrode severely limits the choice of support as well as catalyst materials. Certain materials that have been found to be the most effective for unifunctional operation cannot be used for the bifunctional mode. For example, activated carbons and highly dispersed Pt are often used for O_2-consuming positive electrodes in alkaline electrolytes, but they are not stable at typical O_2-generation potentials.

The O_2 electrode reactions of interest are as follows:[1,2]

	E^o V vs. SHE*	E V vs. RHE* (1 atm)
$O_2+2H_2O+4e^- \rightleftharpoons 4OH^-$	+0.40	+1.23
$O_2+H_2O+2e^- \rightleftharpoons HO_2^-+OH^-$	-0.06	+0.77
$HO_2^-+H_2O+2e^- \rightleftharpoons 3OH^-$	+0.87	+1.70
$2HO_2^- \longrightarrow O_2+2OH^-$	ΔG=-179.5 kJ mol^{-1}	

The Westinghouse Corporation has developed an advanced alkaline iron-air cell with an air positive electrode capable of extensive cycling. In half-cell tests, this electrode exhibits approximately -0.4 V overpotential for O_2 reduction on pure O_2 (1 atm) at $\sim$ 25°C at a current density of -25 mA cm^{-2} and 0.2 V overpotential for O_2 generation at +12.5 mA cm^{-2}. With new, improved electrocatalysts, the overpotentials (particularly for reduction) can be reduced, increasing the efficiency and indirectly also the cycle life.

Even aside from questions of stability of materials, the design of a bifunctional O_2 electrode for maximum efficiency is a multi-faceted engineering problem. Mass transport of reactants and products, electrochemical (and chemical) kinetics for the various reactions, and the electronic conductivities of the various phases must all be considered. The characteristics of the particular carbon being used enter into all of these considerations in extremely important ways, some of which are listed in Table I, along with an indication of some of the types of basic data needed to make rational choices between different types of available carbons for use in bifunctional electrodes. With increasing understanding of the interplay between carbon functions and properties, one should be able to develop a list of specific properties for a carbon or similar material which could then serve as the basis for the design and preparation of such a material.

The aspects of the overall problem that will be discussed in more detail are: O_2-reduction and -generation catalysis and polarization, peroxide decomposition and carbon electro-oxidation. Evidence of elec-

*SHE = Standard Hydrogen Electrode. RHE = Reversible Hydrogen Electrode in the same medium, with H_2 at 1 atm.

trode degradation as a function of cycle life in bifunctional O_2 electrodes will be presented. Results of studies using simple Teflon-bonded electrodes will be used to help explain the degradation process and to suggest ways of fabricating improved electrodes.

II. O_2-REDUCTION AND -GENERATION POLARIZATION

Two types of electrode structures used by Westinghouse are shown in Figure 1, one with two active layers and the other with four. The active layers consist of Shawinigan acetylene black (Shawinigan Products Corp., Englewood Cliffs, NJ), Teflon T30B (DuPont) and NiS, $FeWO_4$ and WC (including 12% Co) powders.[3] The carbon black is loaded with 3.7% silver metal in high-area form. The current collectors consist of Ni fibers, and the hydrophobic layers consist of Shawinigan black plus Teflon T30B. The gas-fed electrode structure used for test purposes in the authors' laboratory at CWRU employs only a single active layer, an Ni mesh current collector and a hydrophobic layer (Fig. 2).

Polarization curves for O_2 reduction using several simple catalyst systems are shown in Figure 3. These curves, together with those for O_2 generation (Fig. 4), demonstrate the properties of some of the individual constituents of the Westinghouse catalytic system. They show that the O_2-reduction catalysts (particularly Ag) are most effective in lowering the overpotential in the lower current density region (reversible potential is +0.30 V vs. Hg/HgO, OH^-). At the upper end, all of the curves tend to converge, showing that in electrodes with these catalysts, which are peroxide decomposers, the carbon itself (plus fabrication) is most important. The working hypothesis is that the lower currents are limited by the rate of the heterogeneous chemical decomposition of peroxide with the potentials within the electrode corresponding to the O_2-HO_2^- couple and hence controlled principally by the ratio of O_2 partial pressure and peroxide concentration, with the activities of H_2O and OH^- essentially constant. The higher currents are limited by a combination of three factors: 1) the rate of electro-reduction of O_2 to peroxide, 2) gas- and solution-species mass transport and 3) electronic conductivity.

Of these catalysts, NiS plus FeS is the only system showing significant activity for O_2 generation. These initial constituents, however, undergo chemical changes during the operation of the electrode, which convert them to the oxides of nickel and iron. It is these oxides that catalyze the O_2-generation process in the charging mode. In the discharge mode, the O_2 reduction proceeds principally through the peroxide pathway with Ag catalyzing the peroxide decomposition. The presence of the sulfide appears to retard the loss of Ag from the electrode during the cycling, probably because of the very low solubility of Ag_2S even in alkaline electrolytes.

Certain types of carbons, such as the mineral-containing activated carbons, have intrinsic acitivity for peroxide decomposition, while tne purer carbons, such as acetylene black, have very little activity for such. With the latter type, the peroxide concentration can reach quite high levels (e.g. $\geq$ 0.1 M), resulting in relatively high polarization even at lower current densities, as well as decreased life expectancy due to peroxide attack on the carbon and Teflon surfaces.

If a very high-area carbon black is used, such as Ketjen black (Armak Co., McCook, IL) with 1000 m^2g^{-1}, significantly lower cathodic polarization can be obtained than for a low-area carbon, but the higher area also leads to increased susceptibility to electro-oxidation (Figure 5). This in turn leads to an increasing polarization during cathodic-anodic cycling. (Note - the discrepancy in polarization at 25 mA cm^{-2} for SB between Figs. 3 and 5 is partly due to the fact that the electrodes in Figure 3 were fabricated using more advanced techniques.)

III. ELECTRODE DEGRADATION

A. Electrochemical Performance

If bifunctional O_2 electrodes experience highly positive potentials during O_2 generation, their performance in the O_2-reduction mode degrades relatively quickly. For example, a Shawinigan black floating gas-fed electrode was subjected to potential scanning at 5 mV s^{-1} up to 0.67 V vs. Hg/HgO, OH^- in 4 M KOH at 25°C for a total of 17 h (Fig. 6). During this treatment, the O_2 reduction performance degraded considerably. The lower apparent limiting current density for the cycled electrode in Figure 6 indicates that the mass transport of O_2 has become a more severe limitation, probably because of redistribution of the electrolyte within the electrode. Another major factor may be ohmic loss, which becomes very high after extended exposure of the electrode to positive potentials; i.e., > +0.5 V vs. Hg/HgO, OH^-.

In Westinghouse bifunctional electrodes, the O_2 reduction potential degrades, although over a much longer time scale, due to the moderate potentials for the anodic mode (+0.55 to +0.60 V) and the larger amount of carbon used in the electrode (88 mg cm^{-2}) (Fig. 7).

B. Surface Analysis - XPS

X-ray photoelectron spectroscopy (XPS) was used to compare the surface characteristics of active layer material from Westinghouse electrode cycled for various lengths of time. A Varian IEE-15 XPS spectrometer was used for these measurements. The electrode was broken up mechanically, chopped with a razor blade, and then attached to the sample mount of the spectrometer using the double-sided adhesive tape technique. The carbon 1 s and oxygen 1 s spectra were corrected for instrumental background signals. It is possible to follow chemical effects on the C(1 s) and O(1 s) spectral profiles due to varying

intensities of several sub-peaks of higher binding energy than the main peak (4). The combined resolution and signal-to-noise, however, were not sufficient for such an analysis to be done with the spectra reported herein. In addition, charging effects with the double-sided adhesive tape technique might produce small shifts in the apparent binding energy. Instead, the ESCA spectra were used mainly to determine the O(1 s)/C(1 s) and F(1 s)/C(1 s) peak height ratios as a function of the number of cycles (Table II). The spectra are shown in Figures 8-10. There was a steady increase in these ratios with increasing cycle number. The consistency in the data for duplicate electrodes cycled the same number of cycles but removed from testing after discharge vs. after-charge was reasonably good. The increasing O(1 s)/C(1 s) ratio suggests that the carbon was undergoing surface oxidation, and the increasing F(1 s)/C(1 s) ratio suggests that carbon was being depleted with respect to the Teflon. Taken together, these results indicate that the acetylene black was slowly being oxidized away.

C. Morphology Changes - SEM

A fair number of unused and cycled Westinghouse electrodes were examined with a Cambridge Model S4 10 scanning electron microscope (SEM) using a 20-kV acceleration potential and a tilt angle of 30° from normal. Definite changes in morphology were seen with increasing cycle number. Typical examples are seen in Figures 11-13, which show a comparison of an unused vs. a cycled electrode at low, medium and high magnification. At low magnification, widespread cracking in the cycled electrode can be seen (Fig. 11). At medium magnification, there is increased porosity evident as compared with the unused electrode (Fig. 12). The unused electrode shows small white areas (in the positive prints used in this report) and particles that are probably due to Teflon, which often appears white because of a slight charging effect, even though the samples were vapor-deposited with a thin coating of carbon ($\sim$ 10-100 Å) to prevent charging. The cycled sample both at low and medium magnification exhibits more extensive lightening. This is thought to be due either to exposed Teflon or to carbon surface oxides with low conductivity. At low magnification, the lightening can be seen, especially at the edges of the cracks. Another possible source of the white color could be residual potassium hydroxide, which would show up lighter than carbon due to atomic number contrast, but this possibility has been ruled out for similar samples based on elemental mapping for K.

At high magnification, the increased porosity of the cycled electrode is even more evident (Fig. 13). The unused electrode shows a uniform mass of particles from 50 to about 300 nm, which is typical of Shawinigan black. Some of the white particles may be Teflon. In the cycled electrode, the small particles have disappeared, and what is left appears to have a significantly lower surface area. In Figure 13b, the lighter area on the left probably has less conductivity (and thus more charging) due to a higher content of either Teflon or non-

conducting carbon oxides.

These results are consistent with those for the XPS. Both suggest that carbon is being oxidized and removed from the surface during bifunctional operation in alkaline solution.

D. Discussion of Results

As mentioned previously, the O_2-reduction behavior at the higher current densities should be affected by 1) electrocatalytic activity for O_2 reduction to peroxide and peroxide elimination, 2) gas mass transport and 3) electronic conductivity. All of these should be adversely affected by electro-oxidation. Soviet workers have reported on the effects of various types of chemical and electrochemical oxidation on the O_2 reduction acitivity of activated carbons[6,7] and have demonstrated that most of the different oxidative treatments lowered the activity for O_2 reduction to peroxide. Their results are complicated somewhat by the intrinsic peroxide decomposition activity of the carbons, however. They concluded that lower valent surface oxides are important for electrocatalysis while stringent oxidation tends to favor the higher-valent surface oxides such as carboxylic acid groups, which are not active for O_2 reduction.

Results from the authors' laboratory concerning O_2 reduction on smooth glassy carbon rotating disk electrodes may shed some light on the above discussion.[8] Chemical oxidation of the surface with HNO_3 caused an increase in the activity of the glassy carbon for O_2 reduction, perhaps because of the formation of quinonoid groups. Electrochemical oxidation in alkaline solution resulted in a decrease in O_2-reduction activity perhaps because this treatment produces different surface groups that are not as effective or are ineffective for O_2 reduction.

Puri, in his comprehensive review of the surface chemistry of carbon,[9] mentions work pertinent to gas transport and electronic conductivity: oxidation of carbon tends to both decrease the hydrophobicity and increase the resistivity of carbons. Some work done in our laboratory concerning the latter effect will be presented in the next section.

IV. CARBON ELECTRO-OXIDATION

Even with effective catalysts for O_2 generation in carbon-based bifunctional O_2 electrodes, the potential in the charging mode (and even in the discharge mode) is far positive of the thermodynamic potential for the complete oxidation of carbon:[10]

$$C + 3H_2O \rightleftharpoons CO_3^{2-} + 6H^+ + 4e^- \qquad (1)$$

$$E^{o} = +0.475 - 0.0886\ pH + 0.0148 \log (CO_3^{2-}) \qquad (2)$$

which equals -0.780 V vs. SHE (or -0.682 V vs. Hg/HgO, OH^-) at pH 14 and 0.1 M CO_3^{2-}. This process has a high overpotential, with an onset potential close to 0.0 V vs. Hg/HgO, OH^- on carbons such as Shawinigan black.

In order to compare the resistances of carbons to anodic oxidation, Teflon-bonded electrodes were fabricated and potentiostatted at +0.50 V vs. Hg/HgO, OH^- in N_2-saturated 4M KOH at 25°C. The anodic current was monitored as a function of time. In some cases, cyclic voltammetry was run at selected intervals to estimate the double-layer capacitance and resistivity of the electrodes. After approximately 20 h of electrolysis, the steady-state anodic polarization characteristics were measured. At that point, the behavior was relatively stable. For shorter times, the polarization changes significantly during the long equilibrium times necessary to collect the data, as discussed by Stonehart concerning similar work in phosphoric acid.[11]

A. Voltammetric Characteristics

The initial positive sweep produces a significant anodic current with an onset potential of about +0.05 V vs. Hg/HgO, OH^- (Fig. 14, Section A) for a flooded Shawinigan black in 4 M KOH at 25°C. Successive sweeps yielded decreasing amounts of anodic current. The large double-layer capacity of the electrode is evident, being 0.23 F in this case for an electrode with 2.4 cm^2 apparent area. [The capacitance is obtained from the value of the plateau current in the potential sweeps (Curves 1 and 2 of Section A in Fig. 14).] Since the electrode contained 100 mg of Shawinigan black, with a nominal surface area of 65 m^2g^{-1}, this capacitance corresponds to a value of approximately 3.5 $\mu F/cm^2$ of real surface area. Similar values have also been obtained by Oren and Soffer for a graphitized carbon black with an area of about 100 m^2g^{-1},[12] but Gagnon obtained values of $\sim$ 10 μf cm^{-2} for several types of carbon blacks.[13] This discrepancy may be due to differences in the properties of these carbons. The presence of Teflon in the electrodes used in the present work may also have slightly decreased the electrochemically available surface area of the carbon.

As the electrode is polarized for 19 h and finally for 48 h, the voltammetry shows an increasing resistance to charging of the double layer (Fig. 14, Sections B and C). At this sweep rate (5 mV s^{-1}) and wide potential range, the current failed to reach a plateau value, partly because of an interfering Faradaic current; but when the sweep rate was lowered to 1 mV s^{-1} and the potential range narrowed, the current approached a plateau so that a rough value for the capacitance (0.32 F) could be estimated (Fig. 14, Section D).

The voltammetry in the absence of a Faradaic current can be analyzed in terms of a distributed resistance-capacitance network model according to the methods of Austin and Gagnon.[14] Values calculated according to their equations are plotted in Fig. 14, Section D, showing fair agreement with experiment. It was assumed that the solution resistance was negligible with respect to that of the electrode. Values of specific capacitance and electrode resistance were calculated for two Shawinigan black electrodes that both contained 20% Teflon (based on the weight of carbon) but which were fabricated somewhat differently from each other (Table III). The first was fabricated for maximum mechanical strength and was rather dense while the second had a density more typical of porous O_2-fed electrodes, in which a more open structure is desired for mass transport. The carbon-Teflon material used in the first electrode was worked in isopropanol until it was rubbery and then pressed, while the second electrode was pressed from dry powdered material. In both cases, the material had initially been heat treated at 280° in flowing inert gas to eliminate the surfactant (Triton X-100) used as an emulsifying agent in the Teflon emulsion. The elimination is believed to be principally by sublimation but some decomposition may also occur. There is a dramatic difference in the resistivities of the two electrodes as a function of anodic polarization time.

These data do not provide any fundamental knowledge concerning resistivity changes for the pure carbon as a function of electrolysis time, but the practical implications are very important. It would be useful to use this technique on gas-fed electrodes both to assess the degree of wetting and the resistivity as a function of time. Gagnon has used the technique effectively for porous carbon,[14], silver[15] and nickel electrodes.[16] The difficulty for O_2 cathodes and bifunctional electrodes is that the cell and electrode must be completely free of O_2, but this is experimentally possible, especially for thinner electrodes.

The effect of having O_2 in the electrode can be seen dramatically in Figure 15. Two Shawinigan black electrodes were potentiostatted for 4.0 h and 3.5 h, respectively, at +0.50 V vs. Hg/HgO, OH^-, but the second electrode was then subjected to steady-state anodic polarization measurements up to a maximum of +0.65 V for several minutes, so that O_2 was generated within the porous carbon electrode. The voltammetric sweep corresponding to Curve B in Figure 15 clearly shows reduction of the O_2 at potentials negative of -0.05 V and subsequent re-oxidation of the product peroxide with an anodic peak at +0.05 V.

It is important to note that there is little evidence of O_2 reduction current in the cathodic sweep for the electrode that only experienced +0.50 V in the anodic sweep (Fig. 15, Section A). This result is consistent with those of Ross and Sokol,[17] who showed that for Shawinigan black electrodes in KOH at 45°C at +0.5 V the O_2-generation current is about 20% of the total (O_2 reduction plus carbon electro-oxidation), while at +0.64 V the O_2 generation approaches 100%

of the total current.

B. Anodic Current as a Function of Time and Potential

If the anodic current is monitored as a function of time for SB and ExCO carbon, one finds an approximately linear relation between the current and the logarithm of time for a period of up to 50 min, followed by a decay that is more gradual (Fig. 16). Part of this current corresponds to the Faradaic current seen in the cyclic voltammetry (Figs. 14 and 15). Stonehart[11] has suggested that this current corresponds to oxidation of more disordered carbon material. Another part of the initial current is double-layer charging current. The double-layer charge is on the order of 1 C g^{-1} for a change in potential of 0.5 V for these carbons [based on $\frac{Q}{w} = \frac{C}{w}\Delta E$, where Q=charge (C), C=capacitance (F), ΔE=change in potential (V) and w=weight (g), in which $\frac{C}{w}$ = 2.3 F g^{-1} for Shawinigan black, experimentally]. This charging current should decrease exponentially with time, with an RC time constant of about 10 s (R=45 Ω, C=0.23 F for a 100 mg SB electrode). Thus, the double-layer charge expected for these electrodes is about 0.1 C for ΔE=0.5 V and the current should have decayed to about 5% of the initial current in roughly 30 s.

In principle, the observed current does not correspond to just carbon oxidation to CO_3^{2-}, but includes also partial oxidation as well as O_2 generation. In practice, at 0.5 V vs. Hg/HgO, OH^- the principal component is the carbon oxidation to CO_3^{2-} as has been shown by Ross and Sokol.[17]

These experiments were done with Shawinigan black and two other carbons (ExCO and V_3G) which have similar surface area but which have higher structural order. Their respective properties are listed in Table IV. Both ExCO and V_3G carbons showed lower initial currents than did Shawinigan black (Fig. 16), and the currents at 1000 min remained lower, with ExCO showing approximately 65% and V_3G 35%, respectively, of the residual current shown by Shawinigan black (1.9 mA g^{-1}).

It is well known that certain metals and metal oxides can catalyze the gas-phase oxidation of carbon.[18] Thus, it was of interest to determine whether Ag as loaded on Shawinigan black in highly dispersed form would influence the anodic current. Initially, there was a large amount of charge passed due to Ag oxidation to Ag_2O, the charge corresponding approximately to the amount expected based on the weight of the Ag in the electrode. After 100 min, however, the anodic currents were virtually identical with those observed for Shawinigan black itself, indicating that the Ag_2O produced had no effect on the anodic current.

After approximately 20 h at 0.5 V vs. Hg/HgO, OH^-, measurements were taken for the electrodes made from the three carbons. These are shown in Figure 17. After initially being at +0.50 V, the potential was decreased in small increments and the current was monitored until

it had reached a steady value. As the potential entered the +0.1 to +0.3 V range, the current took increasing amounts of time to stabilize. This was due to the time needed to charge the double-layer capacitance through the large distributed resistance (see Table III). After the lowest potential was reached, the potential was increased again in small increments up to about +0.65 V, at which point the potential was again decreased to +0.50 V. Only the data obtained decreasing from +0.50 V and that obtained increasing from +0.50 V are shown for SB in Figure 17, while the entire curve for V_3G is shown to illustrate the hysteresis effect due to the charging of the double-layer capacitance. The curve for ExCO fell between the others and was omitted for clarity.

The slope of the E-log i plot was fairly linear for Shawinigan black, about 185 mV decade^{-1}. The plot for V_3G showed some curvature, with the upper part of the curve (presumably O_2 generation) showing a lower slope. If allowance is made for the hysteresis, the plot for ExCO (not shown) was also fairly linear, with a slope similar to that for Shawinigan black. The polarization curves do not show marked differences in anodic current partially due to the logarithmic scale, but the data are consistent with the currents measured at +0.50 V at 1000 min in Figure 16.

It should be noted that the steady-state current at +0.50 V for SB, $\sim$ 2 mA g^{-1}, corresponds approximately to a 40% weight loss over a period of 2000 h, which is the amount of time that the electrode would be on charge in 500 cycles of the Westinghouse type. Thus, an electrode made using a graphitized carbon black such as V_3G could be expected to take roughly three times as long to experience a similar weight loss.

These results fit the general conception that more highly ordered carbons are more resistant to electro-oxidation.[11,19,20] It is assumed that Shawinigan black, while possessing more structural order than other carbon blacks,[17] is still relatively disordered. The x-ray diffraction showed two broad peaks typical of other carbon blacks. The V_3G carbon, graphitized at 2800°C, is assumed to have reached a maximum level of graphitization at this temperature.

Although there is information available in the literature concerning the class of pyrolytic carbons to which ExCO belongs,[21] little specific information was available on the particular sample used in this research. X-ray diffraction showed that the sample was highly ordered, with a structure similar but not the same as graphite. The presence of an Ni (111) line indicated the presence of metallic Ni, and x-ray energy dispersive spectra also confirmed the presence of Ni (as well as Fe). These metals are present because the disproportion of CO takes place on bulk metal catalysts consisting of Fe, Co and/or Ni, which become pulverized and incorporated into the resulting carbon material.[21] The more structurally ordered materials are prepared at temperatures above 500°C.

It is evident that carbons are more resistant to electro-oxidation are available and that even better ones may be found. For example, it is not known whether the Ni and Fe present in the ExCO carbon were catalyzing the carbon oxidation process or perhaps were increasing the current with O_2 generation. It is possible that removing these metals beforehand could lower the residual anodic current even further. Specific attention to structural details of the carbons is also needed in the search for new, oxidation-resistant carbons.

IV. SUMMARY AND CONCLUSIONS

Oxygen reduction in alkaline solution in Teflon-bonded gas-fed electrodes made from carbons that have little peroxide-decomposing activity appears to be limited at the higher current densities by factors associated with the carbon itself and with the electrode fabrication. Three factors that are probably involved are: 1) electrocatalytic activity for O_2 reduction to peroxide and peroxide decomposition, 2) gas mass transport and 3) electronic conductivity.

It has been shown elsewhere and confirmed here that electro-oxidation of the carbon surface adversely affects the O_2 reduction activity. It is the three factors mentioned above that are specifically affected.

XPS and SEM analysis of long-cycled Westinghouse bifunctional air electrodes showed that carbon was removed from the surface and that the amount of bound oxygen increased. The surface area also appeared to decrease.

It was shown that the resistivity of Teflon-bonded Shawinigan black electrodes increased substantially after being held at +0.50 V vs. Hg/HgO, OH^- for several hours in N_2-saturated 4 M KOH at 25°C. This effect was lessened with an improved electrode fabrication method. The technique used to determine the resistivities could prove useful in the examination of practical oxygen electrodes.

Two carbons with a high degree of structural order were shown to yield both lower quantities of anodic charge and lower residual currents corresponding to carbon oxidation at 1000 min while the electrodes were held at +0.50 V. It is likely that other more oxidation-resistant carbons can be found. This would be a useful enterprise provided that such carbons could also perform the other functions required for carbon in both unifunctional and bifunctional electrodes, including electrocatalysis, mass transport, electronic conduction, catalyst support and physical structure. More than one type of carbon or graphite may be used simultaneously to best fill these functions; for example, one carbon as the catalyst support and a second carbon for structural and electronic conductivity functions.

ACKNOWLEDGEMENT

This work was supported by the U.S. Department of Energy. The authors would like to acknowledge the assistance of L.S. Staikoff, Department of Macromolecular Sciences, Case Western Reserve University, in obtaining the SEM photographs.

REFERENCES

1. W.M. Latimer, "The Oxidation States of the Elements and Their Potentials in Aqueous Solutions", Second Edition, Prentice-Hall, Englewood Cliffs, NJ, pp. 38-50.

2. J.P. Hoare, in "Encyclopedia of Electrochemistry of the Elements", Volume II, A.J. Bard, ed., Marcel Dekker, New York, 1970, Ch.II-5.

3. B. Demczyk and C. Liu, J. Electrochem. Soc., 129, 1159 (1982).

4. A. Proctor and P.M.A. Sherwood, Carbon, 21, 53 (1983).

5. T.A. Carlson, "Photoelectron and Auger Spectroscopy", Plenum Press, New York, 1975.

6. V.I. Gants, E.N. Smirnova, V.V. Sysoeva and N.N. Storchak, Zh. Prikl. Khim., 42, 2489 (1969); English translation: J. Appl. Chem. USSR, 42, 2345 (1969).

7. V.V. Sysoeva, V.I. Gants, E.N. Smirnova and N.N. Storchak, Zh. Prikl. Khim., 45, 550 (1972); English translation: J. Appl. Chem., USSR, 45, 555 (1972).

8. Z.W. Zhang, D. Tryk and E. Yeager, in this volume.

9. B.R. Puri, in "Chemistry and Physics of Carbon", Vol. 6, Marcel Dekker, New York, 1970, pp. 191-282.

10. J.van Muylder and M.Pourbaix in "Atlas of Electrochemical Equilibria", M. Pourbaix, ed., Pergamon Press, Oxford, 1966, p. 449-457.

11. P. Stonehart and J. MacDonald, in this volume.

12. Y. Oren and A. Soffer, J. Electrochem. Soc., 125, 869 (1978).

13. E.G. Gagnon, J. Electrochem. Soc., 122, 521 (1975).

14. L.G. Austin and E.G. Gagnon, J. Electrochem. Soc., 120, 251 (1973).

15. E.G. Gagnon, J. Electrochem. Soc., 120, 1052 (1973).

16. E.G. Gagnon, J. Electrochem. Soc., 121, 512 (1974).

17. P.N. Ross and H. Sokol, in this volume.

18. D.W. McKee, in "Chemistry and Physics of Carbon", Volume 16, P.L. Walker and P.A. Thrower, eds., Marcel Dekker, New York, 1981, pp. 1-118.

19. A.V. Yuzhanina, D.V. Kokoulina, L.A. Mashkovich, L.A. Dronseiko and A.F. Kuteinikov, Elecktrokhim., 15, 308 (1979); English translation: Sov. Electrochem., 15, 259 (1979).

20. K. Kinoshita and J.A.S. Bett, in "Corrosion Problems in Energy Conversion and Generation", C.S. Tedmon, ed., Electrochem. Soc., Princeton, NJ, 1974.

21. M. Audier, J. Guinot, M. Coulon and L. Bonnetain, Carbon, 19, 99 (1981).

TABLE I. FACTORS INVOLVED IN THE USE OF CARBON IN BIFUNCTIONAL O_2 ELECTRODES

MAJOR FUNCTIONS FOR CARBON IN BIFUNCTIONAL O_2 ELECTRODES	RELATED BASIC DATA
1. GAS MASS TRANSPORT	HYDROPHOBICITY, PORE STRUCTURE
2. SOLUTION SPECIES MASS TRANSPORT	ADSORPTION, PORE STRUCTURE
3. CURRENT COLLECTION	ELECTRONIC CONDUCTIVITY
*4. ELECTROCATALYSIS OF O_2 REDUCTION TO H_2O_2 (OR HO_2^-)	ELECTROCHEMICAL KINETICS
*5. PEROXIDE DECOMPOSITION	CHEMICAL KINETICS
6. CATALYST SUPPORT	ADSORPTION, SURFACE MORPHOLOGY
7. PHYSICAL STRUCTURE	PORE STRUCTURE, SURFACE AREA, MATERIAL STRENGTH
*8. RESISTANCE TO OXIDATION	OXIDATION THERMODYNAMICS AND KINETICS

* ASPECTS DISCUSSED IN THIS PAPER

TABLE II

XPS PEAK HEIGHT RATIOS[1] FOR CYCLED
WESTINGHOUSE BIFUNCTIONAL ELECTRODES[2]

CYCLES[3]	15[A.]	15[B.]	175[A.]	175[B.]	279[A.]	419[A.]
O(1s)/C(1s)	0.32	0.23	0.43	0.42	1.4	2.7
F(1s)/C(1s)	1.5	1.9	1.6	1.6	3.0	5.3

1. C(1s) AND O(1s) PEAK HEIGHTS WERE CORRECTED FOR INSTRUMENTAL BACKGROUND SIGNALS.

2. 4-LAYER ELECTRODES, OF WHICH A SAMPLE OF THE LAYER 2ND CLOSEST TO THE ELECTROLYTE WAS ANALYZED.

3. CYCLES CONSISTED OF 4 H AT -25 MA CM^{-2} AND 4 H AT +12.5 MA CM^{-2}.

A. REMOVED AFTER DISCHARGE

B. REMOVED AFTER CHARGE

TABLE III. DOUBLE-LAYER CAPACITANCES AND RESISTIVITIES OF SHAWINIGAN ACETYLENE BLACK-TEFLON ELECTRODES AT VARIOUS TIMES OF ANODIC POLARIZATION IN 4 M KOH AT 25°C. [OBTAINED FROM ANALYSIS OF CYCLIC VOLTAMMETRY ACCORDING TO THE METHOD OF AUSTIN AND GAGNON (11)]

FABRICATION*	TIME (H) AT +0.5 V vs. Hg/HgO, OH^-	SPECIFIC CAPACITANCE, F g^{-1}	RESISTIVITY, KΩ CM
1. HEAT TREATED AT 280°C, WORKED IN ISOPROPANOL, PRESSED AT 6000 PSI	0	2.4	0.75
	16	2.8	1.71
2. HEAT TREATED AT 280°C, CHOPPED, PRESSED AT 6000 PSI	0	2.3	1.04
	19	> 2.2≠	> 14.7≠
	48	3.2	22.5

* ELECTRODES WERE FABRICATED USING 100 MG CARBON PLUS 20 MG TEFLON T30B AND WERE DISK SHAPED, WITH A DIAMETER OF 17.5 MM, AREA OF 2.40 CM^2 AND THICKNESS OF 1 MM.

≠ DUE TO EXPERIMENTAL DIFFICULTIES, THESE VALUES CAN ONLY BE ESTIMATED.

TABLE IV. CARBONS USED IN ELECTROCHEMICAL OXIDATION TESTING

CARBON	SURFACE AREA, $M^2\ G^{-1}$	MEAN PARTICLE SIZE, NM	WT% OF IMPURITIES	MANUFACTURING PROCESS
SHAWINIGAN BLACK (GULF OIL)	64.5	42	< 0.1	ACETYLENE BLACK - THERMAL DECOMPOSITION OF ACETYLENE
KETJEN BLACK (ARMAK)	1000	30	0.5	FURNACE-TYPE BLACK WITH HIGH PORE VOLUME ($3.4\ CM^3\ G^{-1}$)
ExCO, $ExCH_4$ (CNRS)	35-50	-	7-36	CATALYTIC DISPROPORTIONATION OF CO OR CH_4 ON Fe, Ni, Co -- HIGHLY GRAPHITIC
V_3G (PENN STATE)	63	-	< 0.01	VULCAN 3 CARBON BLACK--GRAPHITIZED AT 3000°K

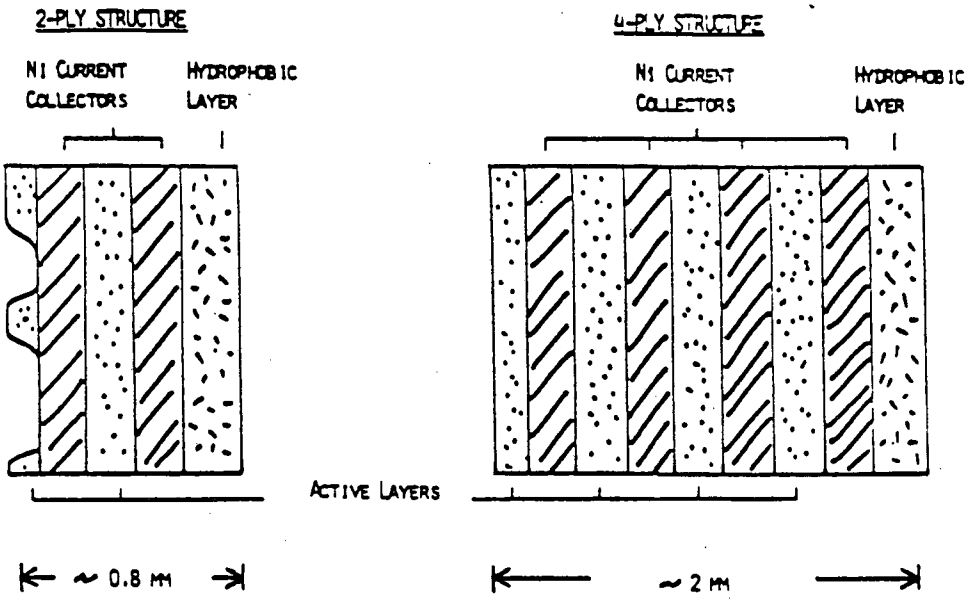

FIGURE 1. TWO TYPES OF BIFUNCTIONAL O_2 ELECTRODE STRUCTURES USED BY WESTINGHOUSE. PICTURED ARE SMALL LATERAL SECTIONS... ELECTRODES WERE TYPICALLY 40 CM^2 IN AREA (3).

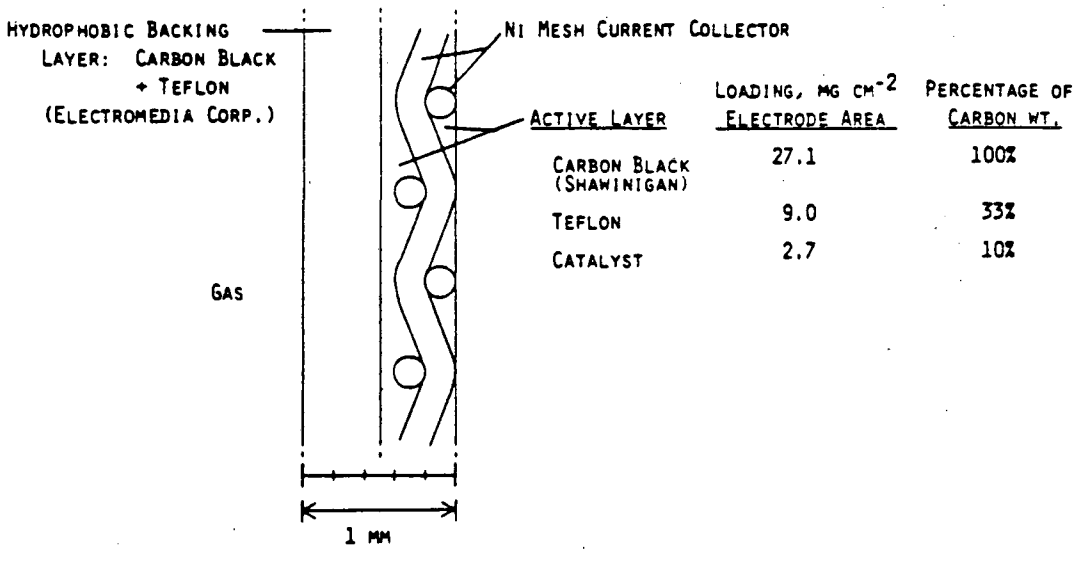

FIGURE 2. CWRU BIFUNCTIONAL O_2 ELECTRODE FOR CATALYST EVALUATION IN ALKALINE ELECTROLYTES.

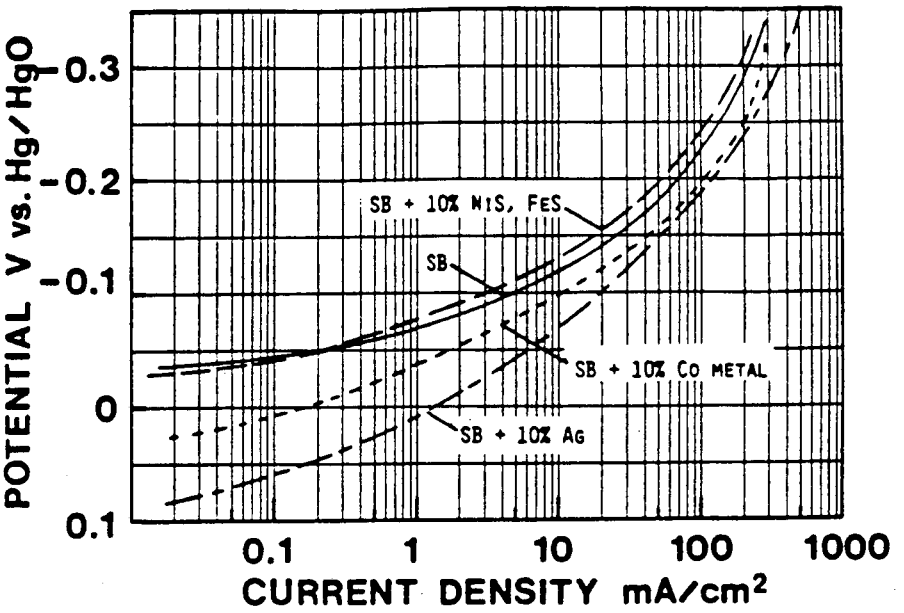

FIGURE 3. POLARIZATION CURVES FOR O_2 REDUCTION ON VARIOUS CWRU-FABRICATED O_2-FED ELECTRODES IN 5.5 M KOH AT 25°C ON PURE O_2 (1 ATM) AFTER 65 CYCLES (-26 mA cm^{-2} FOR 10 MIN; +13 mA cm^{-2} FOR 10 MIN). SB = SHAWINIGAN BLACK. COBALT WAS ADDED AS THE METAL POWDER BUT WAS PROBABLY CONVERTED COMPLETELY TO THE HYDROXIDE DURING CYCLING.

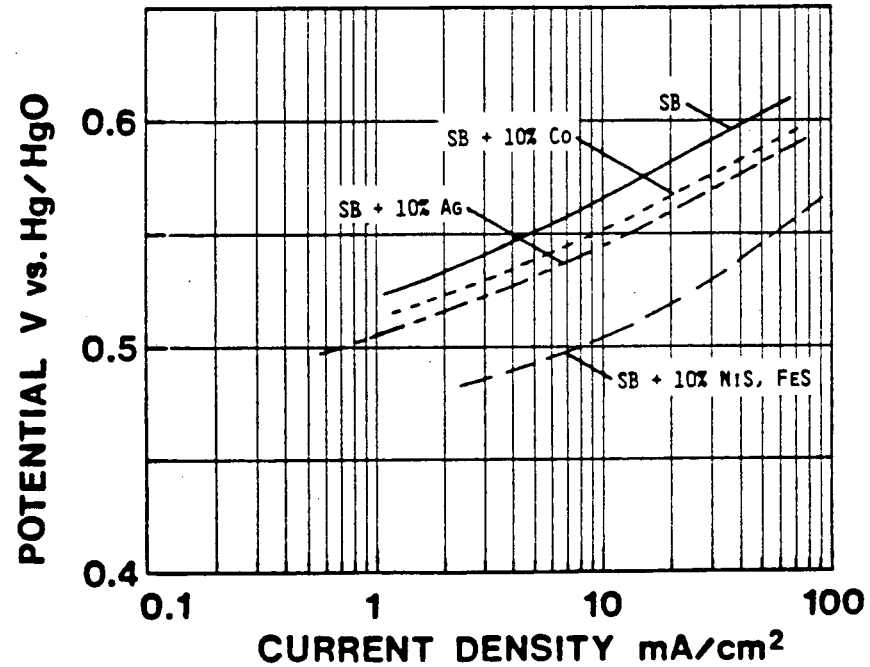

FIGURE 4. POLARIZATION CURVES FOR O_2 GENERATION ON VARIOUS CWRU-FABRICATED O_2-FED ELECTRODES IN 5.5 M KOH AT 25°C AFTER 65 CYCLES (-25 mA cm^{-2} FOR 10 MIN; +13 mA cm^{-2} FOR 10 MIN). CATHODIC CYCLE OPERATED IN PURE O_2 (1 ATM). SB = SHAWINIGAN ACETYLENE BLACK.

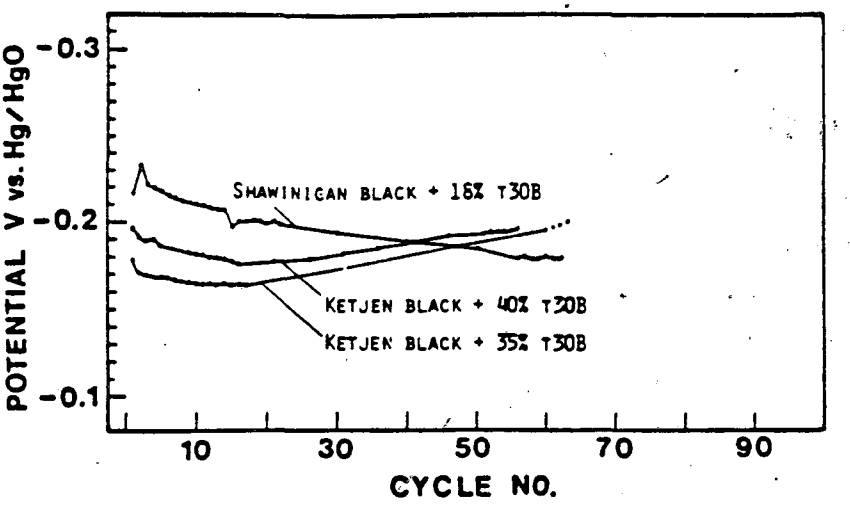

FIGURE 5. CATHODIC POTENTIALS REACHED AT THE END OF THE CATHODIC CYCLES DURING GALVANOSTATIC CYCLING (-26 MA CM^{-2} FOR 10 MIN; +13 MA CM^{-2} FOR 10 MIN) IN 5.5 M KOH AT 25°C FOR O_2-FED (1 ATM) ELECTRODES.

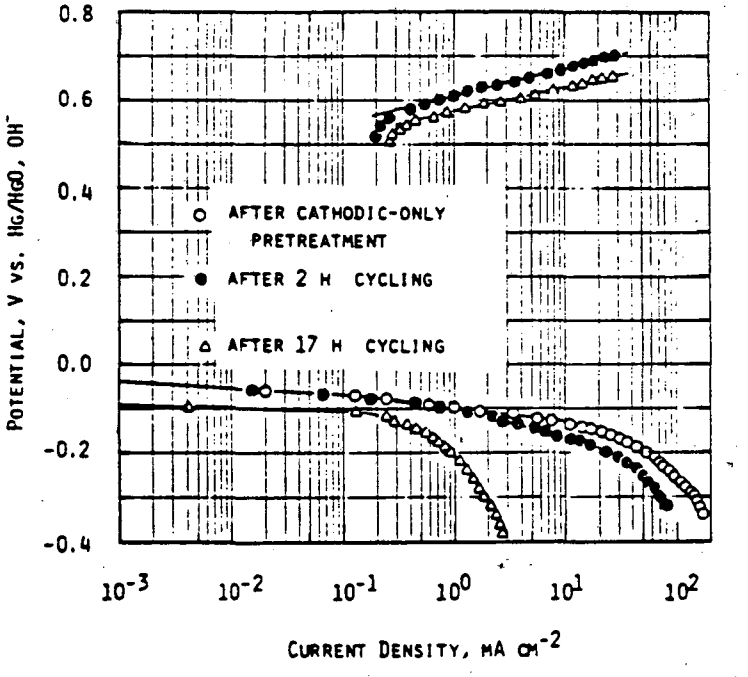

FIGURE 6. O_2 REDUCTION AND GENERATION POLARIZATION CURVES FOR A SHAWINIGAN BLACK FLOATING O_2-FED (1 ATM) ELECTRODE IN 4 M KOH AT 25°C AFTER CATHODIC-ONLY PRETREATMENT AND AFTER VARIOUS TIMES OF POTENTIAL SCANNING AT 5 MV S^{-1} BETWEEN -0.2 AND +0.67 V VS. $Hg/HgO,OH^-$.

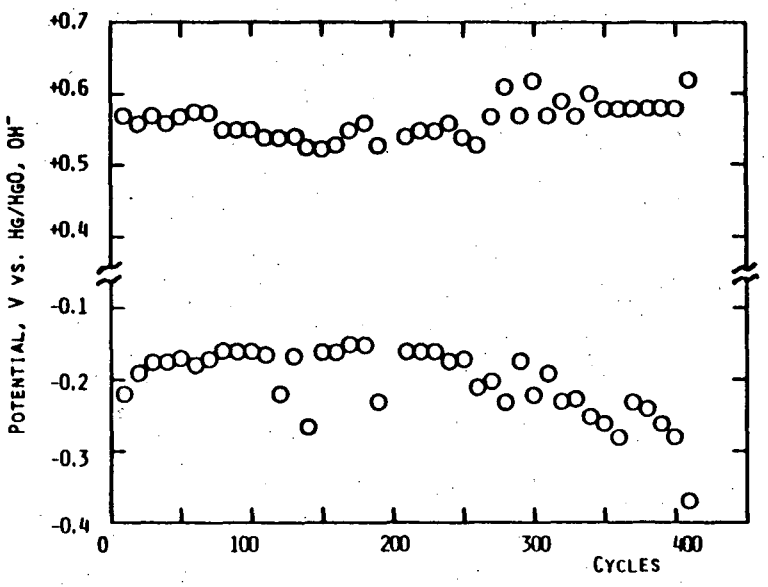

FIGURE 7. POLARIZATION POTENTIALS REACHED DURING CYCLING FOR A TYPICAL WESTINGHOUSE BIFUNCTIONAL AIR ELECTRODE (1 ATM): 4 DISCHARGE AT -25 MA CM^{-2} AND 4 H CHARGE AT +12.5 MA CM^{-2}. (TESTED AT WESTINGHOUSE)

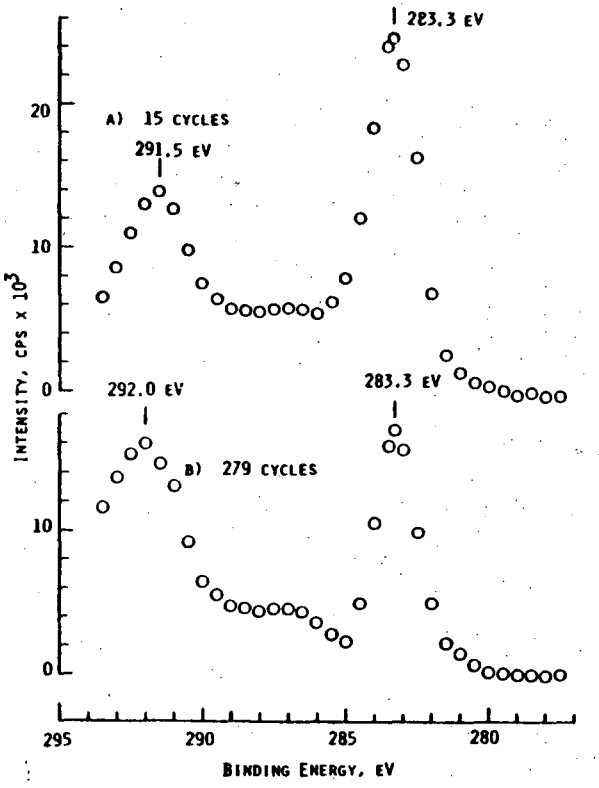

FIGURE 8. C(1S) XPS SPECTRA FOR ACTIVE LAYER MATERIAL FROM 4-LAYER WESTINGHOUSE BIFUNCTIONAL AIR ELECTRODES CYCLED ACCORDING TO THE CONDITIONS LISTED IN FIG. 7 FOR A) 15 CYCLES AND B) 279 CYCLES. THE PEAKS AT 283.3 EV ARE DUE TO GRAPHITE-LIKE CARBON, THE SMALL PEAKS AT 287 EV ARE DUE TO A PLASMON LOSS SATELLITE AND THE PEAKS AT 291.5 AND 292.0 EV ARE DUE TO FLUORINATED CARBON.

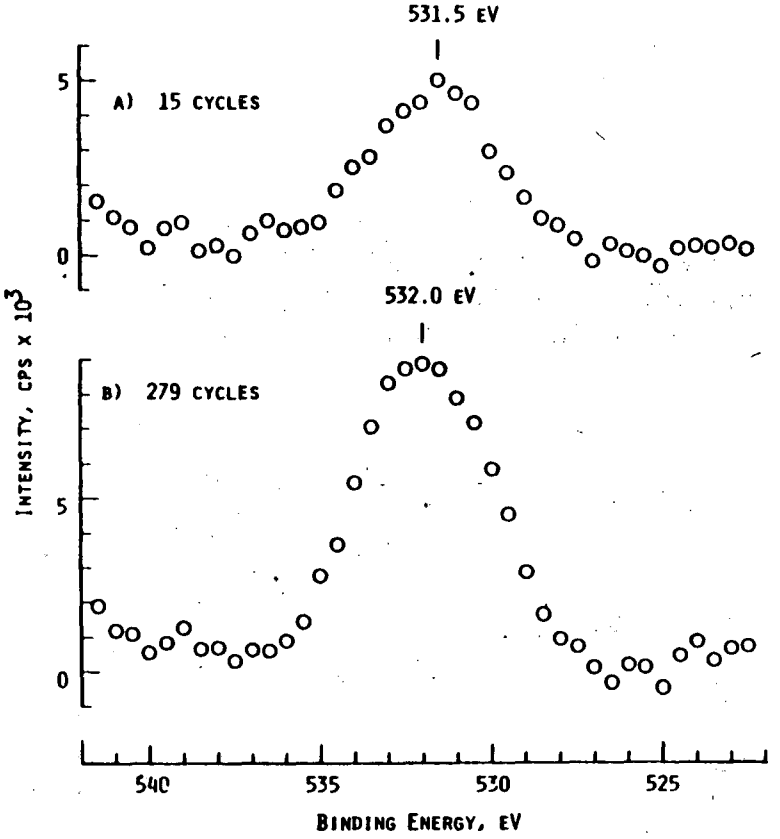

FIGURE 9. O(1s) XPS SPECTRA FOR ACTIVE LAYER MATERIAL FROM 4-LAYER WESTINGHOUSE BIFUNCTIONAL AIR ELECTRODES CYCLED ACCORDING TO THE CONDITIONS LISTED IN FIG. 7 FOR A) 15 CYCLES AND B) 279 CYCLES.

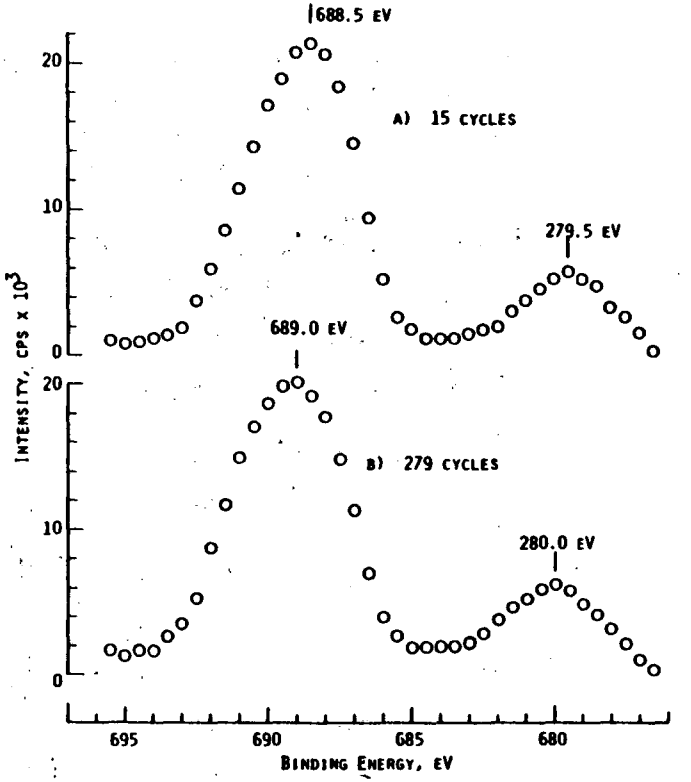

FIGURE 10. F(1s) XPS SPECTRA FOR ACTIVE LAYER MATERIAL FROM 4-LAYER WESTINGHOUSE BIFUNCTIONAL AIR ELECTRODES CYCLED ACCORDING TO THE CONDITIONS LISTED IN FIG. 7 FOR A) 15 CYCLES AND B) 279 CYCLES. THE PEAKS AT 288.5 AND 289.0 eV ARE DUE TO CARBON-BONDED FLUORINE AND THE PEAKS AT 279.5 AND 280.0 eV ARE DUE TO EXCITATION OF THE SAME TRANSITION WITH Mg $K_{\alpha_{3,4}}$ RADIATION.

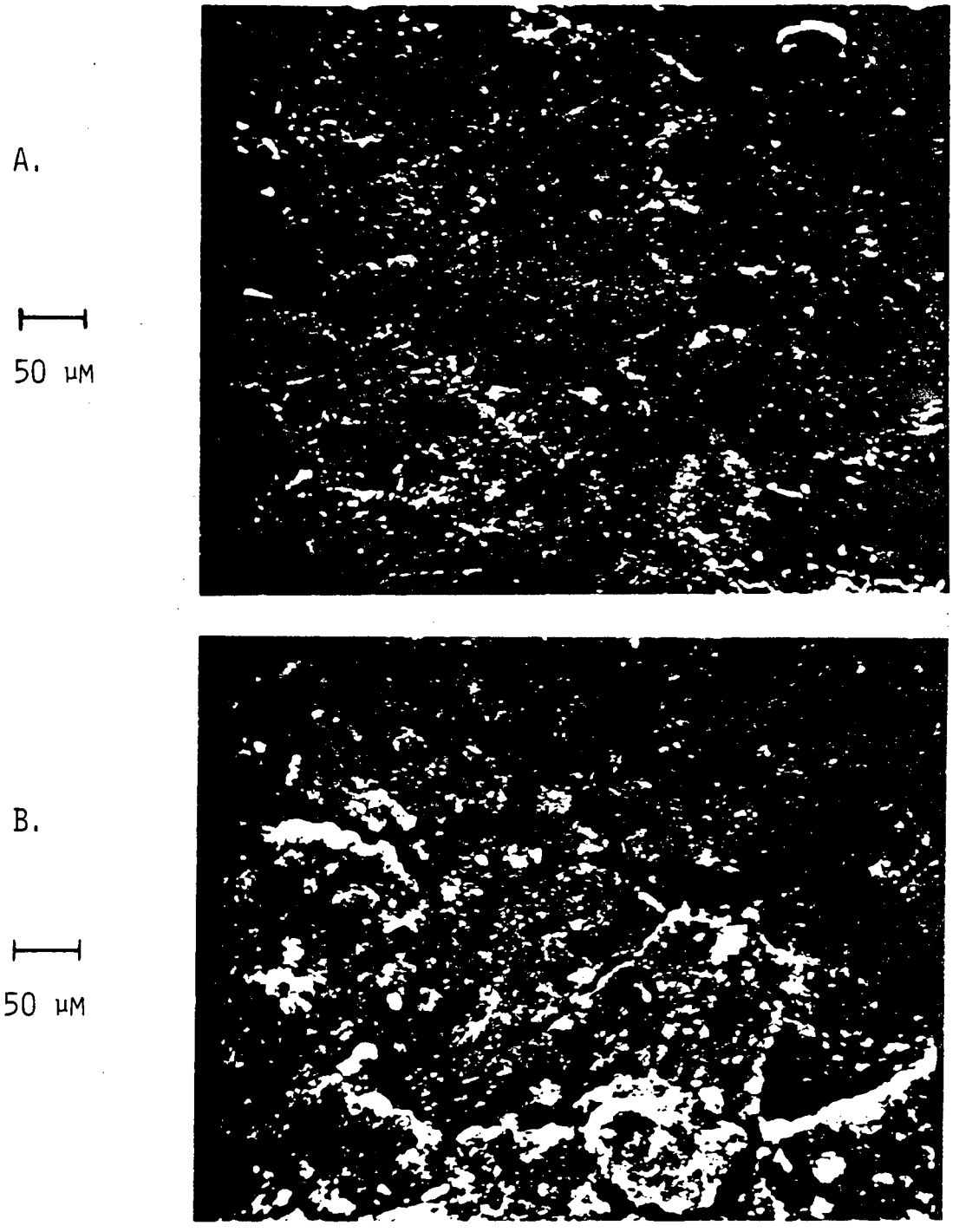

FIGURE 11. COMPARISON OF OUTER ACTIVE LAYERS OF UNUSED AND CYCLED WESTINGHOUSE ELECTRODES (FOUR ACTIVE LAYERS). (A) UNUSED; (B) FAILED AT 190 CYCLES. (SCANNING ELECTRON PHOTOMICROGRAPHS)

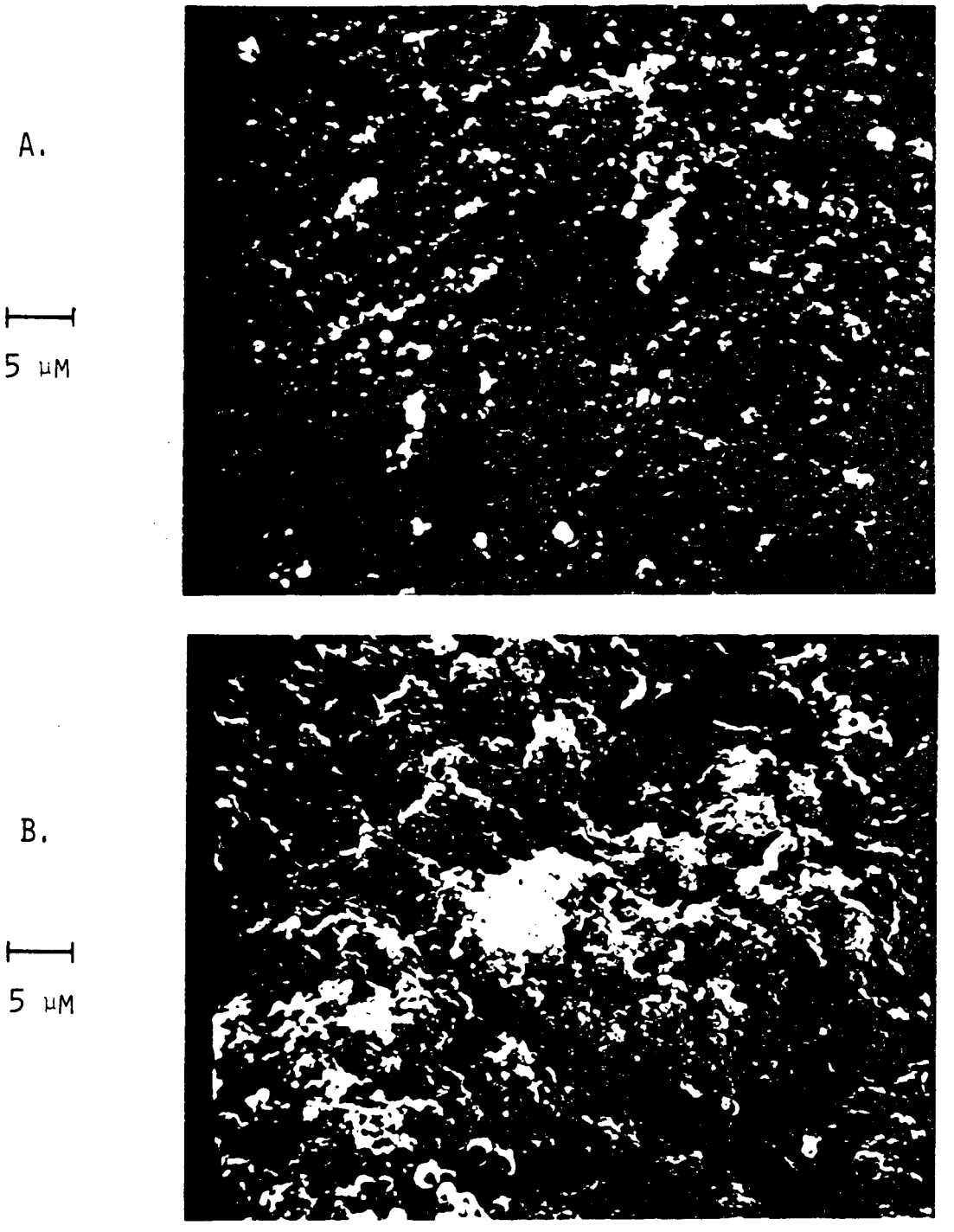

FIGURE 12. COMPARISON OF OUTER ACTIVE LAYERS OF UNUSED AND CYCLED WESTINGHOUSE ELECTRODES (FOUR ACTIVE LAYERS). (A) UNUSED; (B) FAILED AT 190 CYCLES. (SCANNING ELECTRON PHOTOMICROGRAPHS)

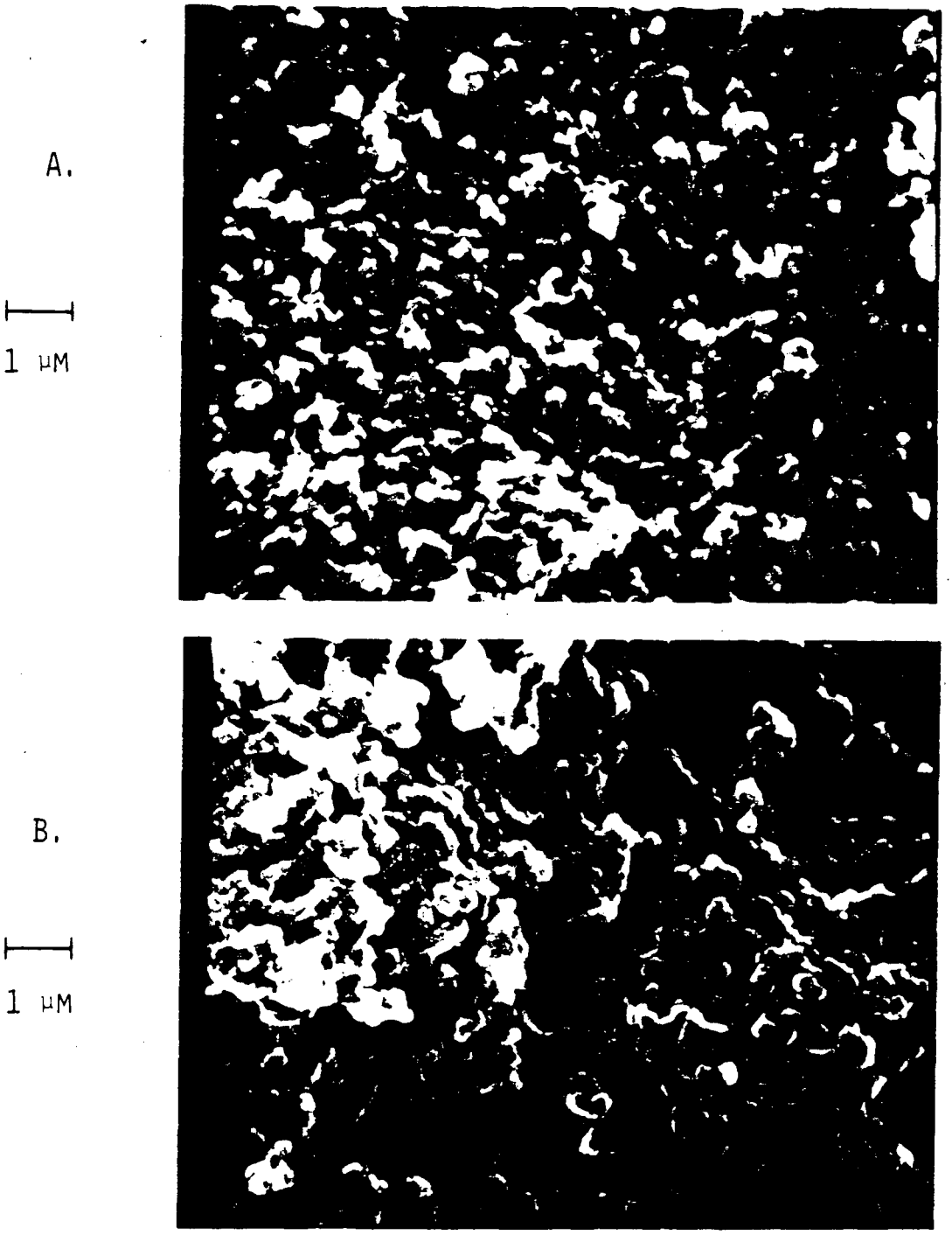

FIGURE 13. COMPARISON OF OUTER ACTIVE LAYERS OF UNUSED AND CYCLED WESTINGHOUSE ELECTRODES (FOUR ACTIVE LAYERS). (A) UNUSED; (B) FAILED AT 190 CYCLES. (SCANNING ELECTRON PHOTOMICROGRAPHS)

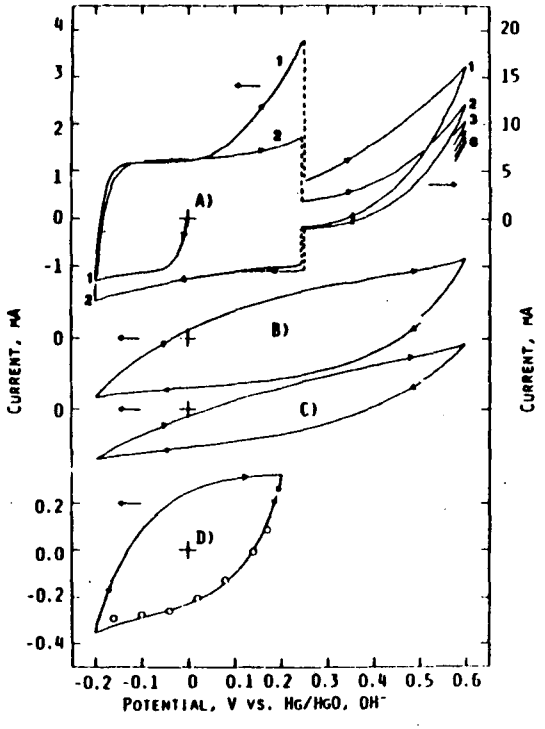

FIGURE 14. CYCLIC VOLTAMMETRY AT 5 MV S^{-1} FOR A FLOODED SHAWINIGAN BLACK ELECTRODE IN N_2-SATURATE 4.0 M KOH AT 25°C. A) FRESH ELECTRODE; B) AFTER 19 H AT +0.5 V; C) AFTER 48 H AT +0.5 V; AND D) AFTER 48 H AT +0.5 V BUT SCANNED AT 1 MV S^{-1}. OPEN CIRCLES: VALUES CALCULATED USING THE METHOD OF AUSTIN AND GAGNON (11), WITH C=0.32 F AND R=940 Ω. THE ELECTRODE CONTAINED 100 MG CARBON AND 20 MG TEFLON T30B AND HAD AN APPARENT AREA OF 2.4 CM^2.

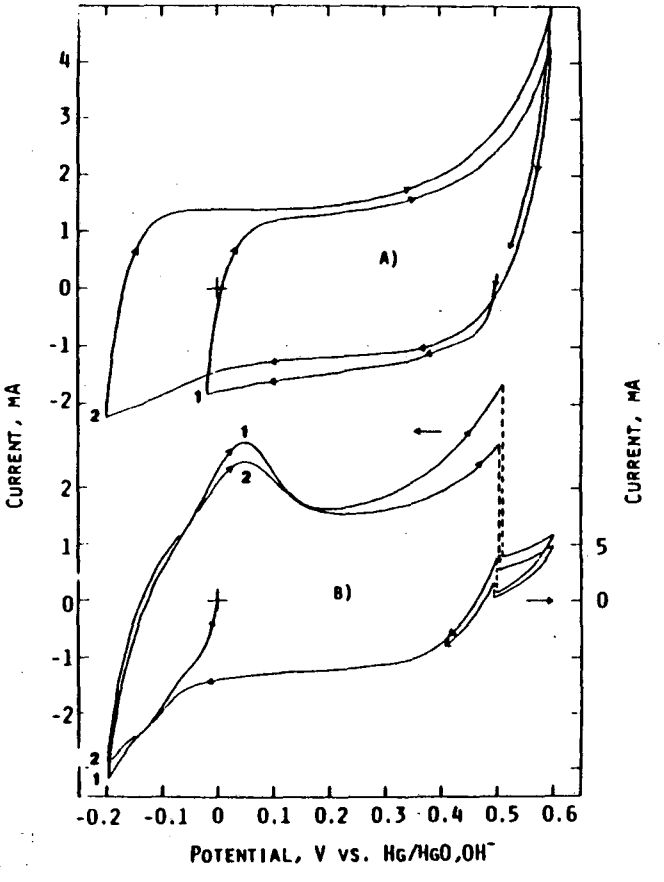

FIGURE 15. CYCLIC VOLTAMMETRY AT 5 MV S^{-1} FOR A FLOODED SHAWINIGAN BLACK ELECTRODE IN N_2-SATURATED 4.0 M KOH AT 25°C. A) AFTER 4.0 H AT +0.5 V; AND B) AFTER 3.5 H AT +0.5 V AND ANODIC POLARIZATION FOR SEVERAL MINUTES UP TO +0.65 V. ELECTRODES CONTAINED 100 MG OF SB CARBON AND 20 MG TEFLON T30B, AND HAD AN APPARENT AREA OF 2.4 CM^2.

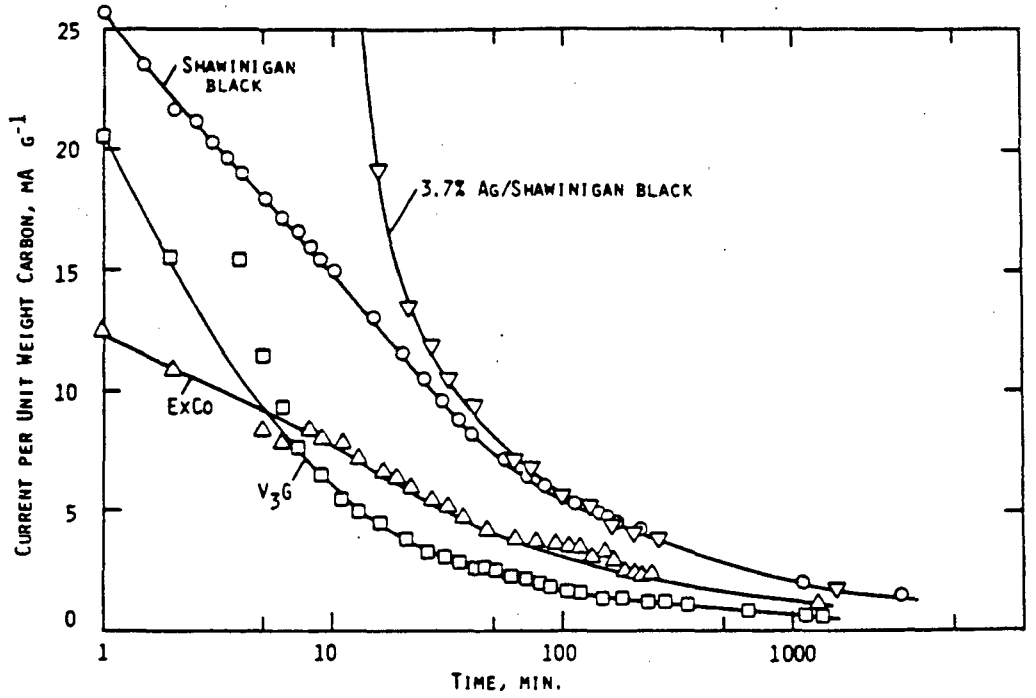

FIGURE 16. CURRENT PER UNIT WEIGHT CARBON AS A FUNCTION OF TIME, AT +0.50 V VS. Hg/HgO,OH^- IN N_2-SATURATED 4 M KOH AT 25°C. ELECTRODES WERE MADE USING 100 mg CARBON AND 20 mg TEFLON T30B.

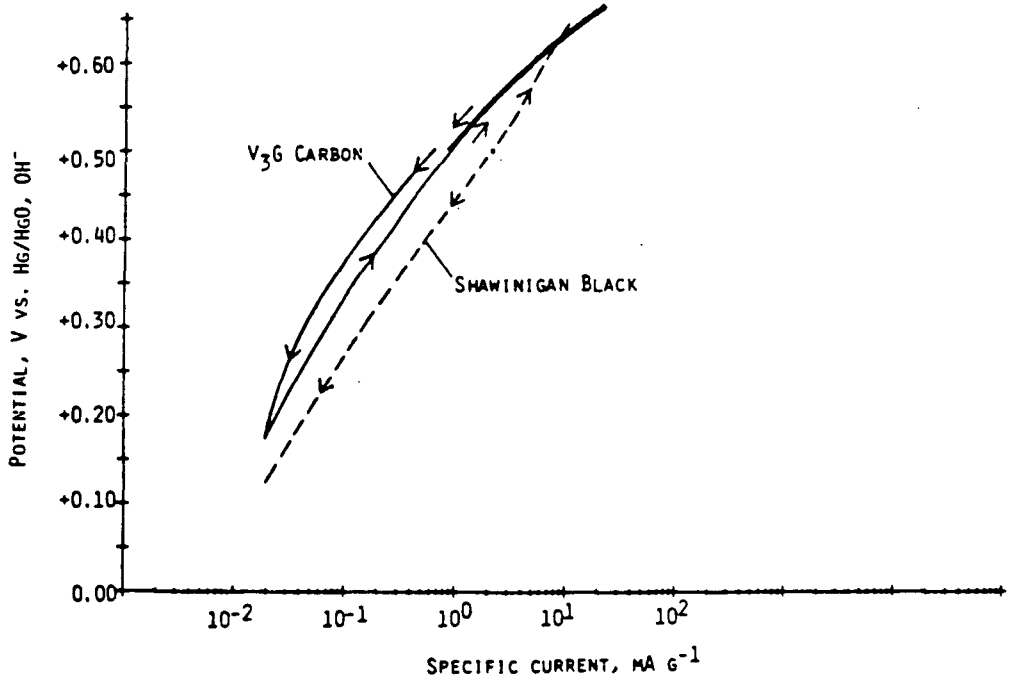

FIGURE 17. ANODIC POLARIZATION CURVES FOR CARBON ELECTRODES MADE FROM 100 mg CARBON PLUS 20 mg TEFLON T30B WITH APPARENT AREAS OF 2.4 cm^2 IN N_2-SATURATED 4 M KOH AT 25°C.

APPENDIX B

Z. W. Zhang, D. Tryk and E. Yeager, In "Proceedings of the Workshop on the Electrochemistry of Carbon," August, 1983, Cleveland, Ohio, The Electrochemical Society, Pennington, N.J., 1984, pp. 158-178.

EFFECT OF SURFACE TREATMENT OF GLASSY CARBON ON O_2 REDUCTION IN ALKALINE SOLUTION

Z. W. Zhang*, D. A. Tryk and E. B. Yeager
Case Center for Electrochemical Sciences
and The Department of Chemistry
Case Western Reserve University
Cleveland, Ohio 44106

ABSTRACT

Oxygen reduction kinetics and mechanisms have been examined on the electrochemically oxidized, the chemically oxidized and the fresh surfaces of glassy carbon in 1.0 M NaOH using cyclic voltammetry and rotating ring-disk electrode techniques. The activity for O_2 reduction varies markedly depending on the type of oxidation pretreatment. The mechanism for O_2 reduction on the electrochemically oxidized surface is somewhat different from that on the chemically oxidized and fresh surfaces. The activity of a glassy carbon surface first chemically oxidized and then reduced has also been examined to gain an understanding of the oxidized surface. The cyclic voltammetry for the chemically oxidized surface in Ar-saturated 1.0 M H_2SO_4 has been used to detect the formation of a quinone-like surface redox couple. The examination of O_2 reduction on the basal plane of highly ordered pyrolytic graphite preadsorbed with several types of quinones provides further evidence for the involvement of quinones in O_2 reduction.

INTRODUCTION

O_2 reduction on various carbon and graphite surfaces, including active carbons [1-5], graphite [6,7] and glassy carbon [8], has been extensively studied due in part to the technological importance of O_2 cathodes and the use of carbon in such electrodes. Considerable differences in the surface activity have been observed. The basal plane of highly ordered pyrolytic graphite (HOPG) does not show significant activity for O_2 reduction, while the edge plane exhibits much higher activity [6]. Differences in mechanisms for O_2 reduction appear to occur on different types of carbon electrodes. As a typical example, O_2 reduction on isotropic and anisotropic graphites yields Tafel slopes of -60 and -120 mV/decade, respectively, which implies different rate determining steps in the O_2 reduction kinetics [7]. From the standpoint of electrocatalysis, such differences in the activity and mechanism for O_2 reduction are the result of the different surface properties of various carbons, including different functional groups,

*Currently on leave from the Dalian Institute of Chemical Physics, Chinese Academy of Sciences, Dalian, People's Republic of China.

morphological factors and electronic effects. With some carbons the effects of ash and impurities must also be considered. Similarly, the surface properties can also be varied for a given carbon electrode by various treatments, resulting in changes of surface activity for O_2 reduction. Since surface oxygen-containing groups on carbon can play an important role for O_2 reduction [9,10], various oxidation pretreatments have been of particular interest. Several studies of the preoxidation of carbon black [5], graphite [11], and glassy carbon [8] have shown substantial effects on O_2 reduction activity but different and even completely contradictory results have been reported by individual groups. The reasons for these discrepancies have not yet been clearly explained.

The purpose of the present studies is twofold:

1) to examine the effects of electrochemical and chemical oxidation treatments, including subsequent chemical reduction, of glassy carbon on the kinetics of O_2 reduction in alkaline media;
2) to gain insight into the nature of the electrocatalytic active sites on glassy carbon.

Glassy carbon was chosen as the electrode material because of its high purity, low porosity and isotropic properties.

The results have shown that chemical and electrochemical oxidation pretreatment can lead to differing effects on O_2 reduction. The latter causes a decrease in surface activity and some change in the reduction mechanism. This study also provides evidence that the surface activity is related to the formation and further oxidation of surface quinone-type groups.

EXPERIMENTAL

The experiments were carried out in an all-Teflon cell which has separate compartments for the reference and counter electrodes. A Teflon Luggin capillary was used to minimize iR drop, with its tip ~3 mm below the center of the rotating disk electrode. A glassy carbon (GC) disk electrode (Fluorocarbon Co.) with an area of 0.46 cm^2 was mounted in a PTFE holder. The ring electrode was gold, with a collection efficiency N of 0.17 as determined from the disk and ring radii. The ring was typically set at +0.15 V vs. $Hg/HgO,OH^-$ to oxide peroxide at the mass-transport limited rate. The polishing procedure, yielding a mirror bright electrode surface, has been described previously [12]. A gold foil was used as the counter electrode and a $Hg/HgO,OH^-$ reference electrode was used. The electrolyte, 1.0 M NaOH, was prepared from 50% NaOH solution (Fisher, low in carbonate), and was preelectrolyzed as described previously [12].

The GC electrode was electrochemically oxidized *in situ* in Ar-saturated 1.0 M NaOH at potentials between 0.1 V and 0.5 V vs.

$Hg/HgO,OH^-$ for various times between 1 min and 3 h. The GC was chemically oxidized by dipping it in concentrated nitric acid (Fisher, reagent grade) at ambient temperature for either 0.5 or 1 min and then was rinsed with water which had been purified by reverse osmosis plus distillation. The $NaBH_4$ reduction treatment of the chemically oxidized electrode involved rotating the disk electrode in 0.1 M $NaBH_4$ aqueous solution for 0.5 h at room temperature. Then the electrode was thoroughly rinsed with water as mentioned above.

The 1.0 M H_2SO_4 used in the cyclic voltammetry measurements of chemically oxidized surfaces was prepared from Fisher reagent grade concentrated H_2SO_4. In such experiments, the saturated calomel electrode (SCE) was used as the reference electrode. The O_2 and Ar used to saturate the electrolyte were purified with gas trains to remove impurities: CO from O_2 and O_2 from Ar as well as organic impurities from both gases. All measurements were made at 22 ± 1°C.

Prior to each experiment, a fresh electrode surface was prepared by polishing with a water-paste of 0.05 μm γ-alumina. The electrode was then either rinsed with distilled water or placed in an ultrasonic distilled water bath for 10 min. Both treatments yielded similar results. The polarization curves for the kinetic measurements were made at different rotation rates following repeatedly scanning the electrode potential between 0 and -0.6 V vs. $Hg/HgO,OH^-$ at 20 mV/s at a rotation rate of 1000 rpm until a stable curve was obtained. The hysteresis obtained upon reversal of the sweep was usually negligible at a scan rate of 20 mV/s.

RESULTS AND DISCUSSION

Figure 1 shows cyclic voltammetry curves for O_2 reduction on chemically oxidized, electrochemically oxidized and fresh surfaces of a stationary glassy carbon electrode in O_2-saturated 1.0 M NaOH. Differing peak currents i_p and peak potentials E_p were observed on these surfaces. The i_p values were -370, -325 and -270 μA for an electrode of area 0.46 cm^2 and the corresponding E_p values were -0.19, -0.24 and -0.28 V vs. $Hg/HgO,OH^-$ for the chemically oxidized, the fresh, and the electrochemically oxidized surfaces, respectively. The chemically oxidized surface exhibits the largest i_p, -370 μA, and the most positive E_p, -0.19 V. In contrast, the electrochemically oxidized surface exhibits a smaller i_p, -270 μA, and a more negative E_p, -0.28 V, than that of the fresh surface.

The voltammetry curves in Fig. 1 are under combined kinetic and diffusion control. When only a sample charge transfer step is rate determining with negligible back reaction and no specific adsorption of reactants, intermediates or products, the peak current i_p and peak potential E_p are given by [13,14]:

$$i_p = (2.99 \times 10^5)\, n\, (\alpha n_a)^{1/2}\, A\, c_0^*\, D_0^{1/2}\, v^{1/2} \qquad (1)$$

$$E_p = E^{\circ\prime} - \frac{RT}{\alpha n_a F}\left[0.780 - \ln k^\circ + \ln \left(\frac{\alpha n_a F v D_0}{RT}\right)^{1/2}\right] \qquad (2)$$

where n = number of electrons passed in the overall electrochemical reaction

α = apparent transfer coefficient for the rate-determining charge transfer step

n_a = number of electrons involved in this step

A = cross-sectional area for diffusion subtended by the electrode in cm^2

c_0^* = bulk concentration of the oxidized species in mol/cm^3

D_0 = diffusion coefficient in cm^2/s

v = potential sweep rate in V/s

$E^{\circ\prime}$ = formal reversible potential in V

k° = standard heterogeneous rate constant for the charge transfer step in cm/s (based on first order kinetics).

The standard electrode potential for the O_2/HO_2^- couple is -0.065 V vs. NHE [16] or -0.163 V vs. $Hg/HgO,OH^-$ and corresponds to the formal potential $E^{\circ\prime}$ to a reasonably good approximation in eq. 2.

These equations are not applicable quantitatively to the voltammetry curves for O_2 reduction because the assumptions involved in their derivations are NOT fulfilled. Nonetheless, eq. 2 qualitatively indicates that the peak potential shifts in the cathodic direction with decreasing values of the rate constant. The expression given by eq. 1 for i_p depends on the kinetics only through αn_a for a simple charge transfer step rate controlling but will probably also involve the rate constants as well as the adsorption isotherms for a reaction such as O_2 reduction involving adsorbed intermediates. Since i_p does not necessarily depend on the rate constant, it is preferable to use the shift of the peak potential as some measure of the effects of electrode pretreatment on the rate constants. Changes in mechanism, however, may also occur with changes in the oxidation state of the carbon and cannot easily be recognized from the voltammetry curves alone.

This shift in the voltammetry curves with oxidative pretreatment in Fig. 1 can be explained on the basis of either an increase in surface or an increase in the rate constant per unit true area (i.e., an increase in surface activity). Later experiments indicate that the latter is the predominant contribution to the change in the voltammetry curves.

In order to gain further insight into the dependence of the kinetics on surface pretreatment, the O_2 reduction has also been examined on a glassy carbon surface reduced with 0.1 M $NaBH_4$ solution, following the oxidation treatment. Figure 2 gives the cyclic voltammetry curves of chemically oxidized and then reduced surfaces for O_2 reduction. The results show that the rate constant is decreased when the chemically oxidized surface is reduced with the $NaBH_4$ solution. The reduced surface has a slightly lower value for the rate constant than that of the fresh surface. When such a reduced surface was chemically oxidized again, the activity increased up to close to that of the original chemically oxidized surface, as is evident in Fig. 3. These results provide evidence that the activity increase produced by chemical oxidation is not caused by a change of the ratio of the true-to-apparent surface area but rather the formation of certain surface oxygen complexes as active sites for O_2 reduction. These complexes can be reduced by $NaBH_4$. However, the electrochemically oxidized surface does not show such behavior. As to the possible reason why electrochemical oxidation leads to a decrease of surface activity, it is likely that the inherent active sites on the glassy carbon surface can be oxidized to yield non-active sites for O_2 reduction.

Double layer capacitance measurements were done using cyclic voltammetry from -30 to +30 mV vs. $Hg/HgO,OH^-$ at a scan rate of 100 mV/s^{-1}. After graphically approximating the resulting current-potential wave form with a parallelogram, the capacitance was calculated. The differential capacitance of the electrochemically oxidized surface increases over that of the fresh surface (increasing from 60 $\mu F/cm^2$ to 95 $\mu F/cm^2$) because of either surface area increase or change of capacity per unit true area caused by strong polar surface group formation. The decrease in the rate constant following electrochemical oxidation treatment is also best explained by a change in the surface activity per unit true area rather than a change in surface area.

Differing effects of surface oxidation treatment have been reported by various laboratories as mentioned previously. Sysoeva *et al.* [5] concluded that for activated carbon electrodes in 1 M KOH, both electrochemical and chemical oxidation cause a decrease in activity for O_2 reduction. In contrast, Taylor and Humffray [8] concluded that on glassy carbon electrodes (non-porous) in NaOH solutions above pH 10, both electrochemical and chemical oxidation increase the activity for O_2 reduction. In our study, the chemical oxidation effect is consistent with the results of Taylor and Humffray, while the electrochemical oxidation effect is in accord with those of Sysoeva *et al.* This difference in the effect of oxidation is likely to be related to differences in the oxidation treatment conditions and differences in the initial surface properties of the carbons, which lead to different surface oxidation states. The activity of the surface for O_2 reduction is probably related to a specific type of surface functional group.

Figures 4-6 give the rotating ring-disk data at steady state for O_2 reduction on the fresh, the chemically oxidized and the electrochemically oxidized surfaces in O_2-saturated 1.0 M NaOH. Here the increase of the O_2 reduction disk currents on the chemically oxidized surface and the decrease on the electrochemically oxidized surface are consistent with the results obtained with cyclic voltammetry.

The Levich equation

$$\frac{1}{i} = \frac{1}{i_k} + \frac{1}{B\omega^{\frac{1}{2}}} \qquad (3)$$

has been used widely to analyze steady state reaction kinetics which are first order with respect to the diffusing reactant [17] where $B = 0.20\ D_0^{2/3}\ \nu^{-1/6}\ nFAc_0$. D_0 and c_0 are the diffusion coefficient and solubility of the oxidant (O_2) in the bulk electrolyte, ν is the kinematic viscosity, A is the electrode apparent area, F is the Faraday and n is the number of electrons transferred per molecule of O_2 diffusing through the Nernst diffusion layer, and ω is the rotation rate in radians per second. For convenience, r (rotations per minute) is usually used instead of ω. The equation then becomes:

$$\frac{1}{i} = \frac{1}{i_k} + \frac{1}{B'r^{\frac{1}{2}}} \qquad (4)$$

where $B' = (\frac{2\pi}{60})^{\frac{1}{2}}B$.

Figure 7 shows plots of 1/i vs. $r^{-1/2}$ at different potentials for electrochemically oxidized, chemically oxidized and fresh surfaces of glassy carbon. The experimental B' value of 1.90×10^{-2} mA $(rpm)^{-1/2}$ for the different surfaces is very close to the theoretical B' value, 2.0×10^{-2} mA $(rpm)^{-1/2}$ based on the quantitative 2-electron reduction of O_2 to HO_2^- [6].

For the analysis of the rotating ring-disk electrode data the following series reaction scheme for O_2 reduction can be considered, since the direct 4-electron reduction of O_2 to OH^- is negligible (only the series process is operative). In this diagram, i_2 is the current related to the electrochemical reduction of HO_2^- to OH^-, i is the disk current, i_r is the ring current, N is the collection efficiency, HO_2^- and $(HO_2^-)_e$ correspond to solution phase peroxide in the bulk and at the electrode surface, respectively, and i_4 and i_5 are the rates of desorption and adsorption of HO_2^- expressed as currents. The rate of the heterogeneous peroxide decomposition is indicated by i_6 (in units of current). The rate of diffusion of the HO_2^- from the surface $(HO_2^-)_e$ through the Nernst diffusion layer is expressed in terms of i_3 (current units). i_3 is related to the peroxide oxidation limiting current i_r on the ring by the equation $i_3 = i_r/N$.

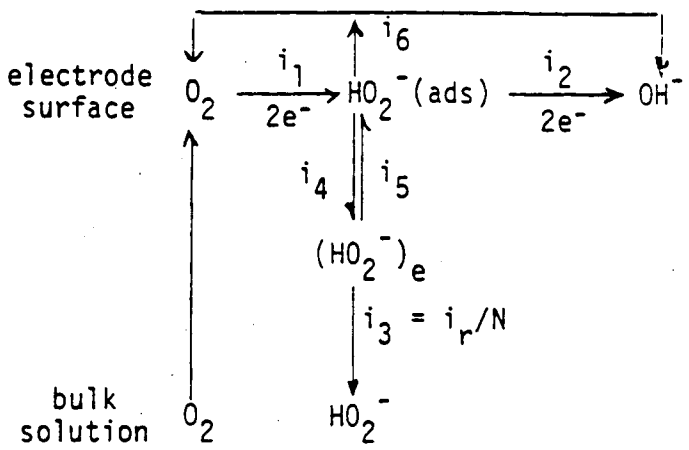

This reaction scheme predicts the relation [12]:

$$\frac{i}{i_r} = \frac{\frac{2k_2 + k_6}{k_4} + 1}{N} + \frac{(2k_2 + k_6)\, k_5\, (1.6\, \nu^{1/6})}{k_4 N D_p^{2/3}\, r^{1/2}} \qquad (5)$$

where i is the disk current for O_2 reduction

D_p is the diffusion coefficient for HO_2^-

ν is the kinematic viscosity of the electrolyte

r is the electrode rotation rate

and the k's represent the first order reaction rate constants for the respective steps.

If only the series mechanism is operative, the plots of $N(i/i_r)$ vs. $r^{-1/2}$ should be linear and the intercept should equal $1 + (2k_2 + k_6)/k_4$. If the kinetics of the desorption equilibrium corresponding to k_4 and k_5 are fast, then the intercept will be unity. Furthermore, if k_2 and k_6 are small, then the quantity $N(i/i_r)$ will be ~ 1 and independent of r.

Figure 8 gives evidence for the 2-electron reduction of O_2 to HO_2^- with negligible further reduction or decomposition of the peroxide on both the chemically oxidized and the fresh surfaces. The i/i_r values correspond to the quantitative reduction of O_2 to HO_2^- with no further reduction or decomposition.

In Fig. 9 are given plots of E vs. log $[i/(i_l - i)]$ with almost the same Tafel slope, $\sim$-60 mV/decade, on the chemically oxidized and fresh surfaces of glassy carbon and with the only difference being the exchange current density. This is in accord with the hypothesis that the electrocatalytic active sites for the O_2 reduction are the same on the chemically oxidized and fresh surfaces but differ in number on these

two surfaces. However, Fig. 9 shows a change of Tafel slopes for O_2 reduction on the electrochemically oxidized and the fresh surfaces. With an increase of anodic potential used to oxidize the surface, the Tafel slope changes from -60 mV/decade to -73 and -85 mV/decade. This implies that the rate-determining steps for O_2 reduction on the electrochemically oxidized and fresh surfaces of glassy carbon are somewhat different, or that a change in the potential distribution across the interface has occurred because of changes in the surface functional groups.

For the chemically oxidized surface the cyclic voltammetry indicates the presence of a surface functional group which undergoes oxidation-reduction. Figure 11 shows the cyclic voltammetry curves, which exhibit a cathodic peak at $\sim$+0.3 V and an anodic peak at $\sim$+0.4 V vs. SCE in Ar-saturated 1.0 M H_2SO_4. Kinoshita and Bett have obtained similar results with a chemically oxidized, moderately high surface area carbon black, Vulcan XC-72 (Cabot Corp.) in acid electrolytes [18]. These peaks do not show up, however, in alkaline media within the accessible voltage range, including the potentials where O_2 reduction occurs.

Various workers [18-21] have suggested that quinone-hydroquinone-like structures are responsible for the voltammetry peaks in Fig. 11. Even though the redox features of these groups do not show up in alkaline solutions, the structures may be involved as sites for the O_2 reduction reaction. Chemical oxidation of the glassy carbon surface may increase their concentration and thus increase the activity of its surface for O_2 reduction. The voltammetry peaks assigned to the quinone-hydroquinone couple for the chemically oxidized glassy carbon surface were <u>not</u> observed in either acid or alkaline electrolytes for the surface <u>electrochemically</u> oxidized in alkaline electrolytes. The electrocatalytic activity for O_2 reduction on this surface in alkaline solution was also lower, providing some evidence for the involvement of the quinone-hydroquinone structures in the O_2 reduction.

The effect of quinones pre-adsorbed on the basal plane of highly-ordered pyrolytic graphite (HOPG) has been examined for O_2 reduction in alkaline solution. The results provide evidence [22] that quinone-like structures can facilitate O_2 reduction. O_2 reduction is very inhibited on the basal plane of HOPG relative to that on the edge orientation of HOPG or the basal plane of ordinary pyrolytic graphite. Figure 12 gives the comparison of the activity for O_2 reduction on the bare basal plane of HOPG and also with pre-adsorbed 9,10-anthraquinone-2-SO_3^-. The quinone was pre-adsorbed by immersing the HOPG rotating disk electrode in a 0.1 M NaOH solution containing 10^{-3} M quinone for 30 min with r = 500 rpm. The surface with the adsorbed anthraquinone shows a considerable enhancement of the activity for O_2 reduction and gives polarization curves similar to those for glassy carbon. Similarly, Fig. 13 shows that the pre-adsorbed 1,4-naphthoquinone on the basal plane of HOPG also yields high activity for O_2 reduction. These results

demonstrate that various types of quinones can catalyze O_2 reduction to peroxide in alkaline solution.

Figure 14 gives the cyclic voltammetry for adsorbed 9,10-anthraquinone-2-SO_3^- on the basal plane of HOPG in Ar-saturated 1.0 M NaOH. The two cathodic and anodic peaks can be explained on the basis that the adsorbed anthraquinone was reduced in two steps, as follows:

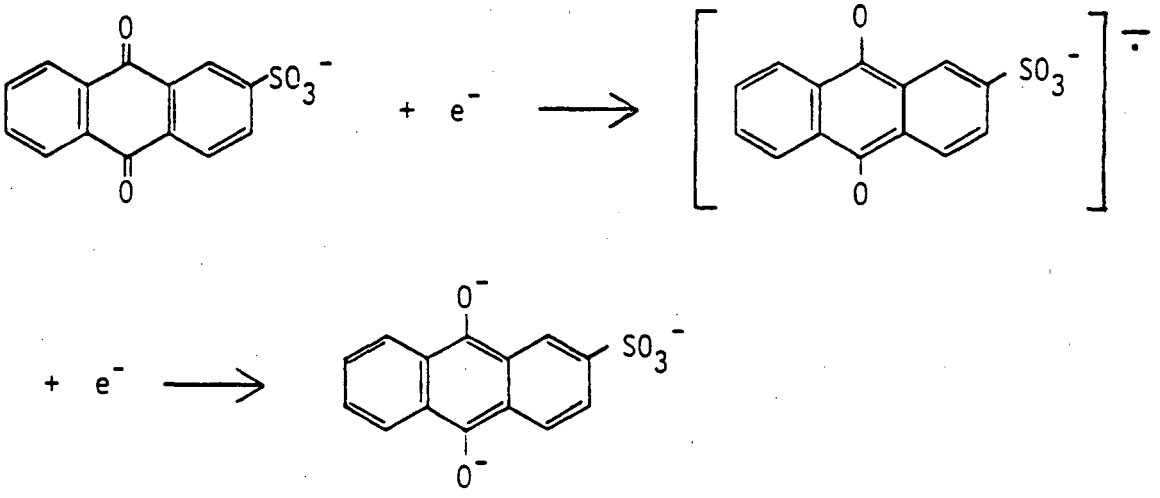

(6)

Degrand and Miller, however, have reported that the voltammetry in alkaline solutions for an anthraquinone derivative pre-adsorbed on Hg and carbon electrodes only exhibits a single pair of peaks [23]. In aprotic solvents quinones typically exhibit two separate reversible redox processes, corresponding to Eq. 6 [24-26]. This type of behavior would also be expected in highly alkaline solutions so that the protonation of the quinone radical anion $Q^{\cdot-}$ and subsequent rapid reduction (as discussed by Keita et al., ref. 27) would be disfavored:

$$Q^{\cdot-} + HD \longrightarrow QH\cdot + D^-$$

$$QH\cdot + e^- \longrightarrow QH^-$$

where HD is a proton donor.

The amount of $Q^{\cdot-}$ present is also determined by the equilibrium constant and kinetics for the disproportionation reaction:

$$2Q^{\cdot-} \rightleftharpoons Q + Q^{2-}$$

The equilibrium usually favors the radical anion at high pH but there can be widely diverging values for the equilibrium constant depending both on pH and on the nature of the compound [29,30]. If $Q^{\cdot-}$ is strongly favored, the reduction should proceed in two one-electron steps [28,30].

From a comparison of Figs. 12 and 14 it may be seen that the O_2 reduction polarization curve correlates in a general way with the voltammetry, although the detailed correspondence remains to be worked out. For example, the onset of O_2 reduction occurs almost 100 mV positive of the potential at which any current for anthraquinone reduction is evident. It seems reasonable, however, to suggest that the O_2 reduction catalysis by the adsorbed quinone involves a semiquinone-like species.

The semiquinone or more specifically the quinone radical anion $Q^{\cdot-}$ is known to react extremely rapidly with O_2 in homogeneous solution, with second order rate constants on the order of $10^8 - 10^9$ $M^{-1}s^{-1}$ to form superoxide $O_2^{\cdot-}$ in a one-electron reduction [31]. The semiquinone of 2-amylanthraquinone can be used as a chemical reductant of O_2 in the manufacture of hydrogen peroxide [32]. The hydroquinones, by contrast, although they are quite able to react with O_2, do so in general at somewhat lower rates [33].

Quinones have also been incorporated into porous carbon electrodes for industrial hydrogen peroxide manufacture in alkaline solution [34]. Electrocatalysis of O_2 reduction by 9,10-anthraquinone-2,6-disulfonate at pH 2 has been reported [35], but the effect is not as marked as that reported in the present work in alkaline solution. A possible reason for this difference is that the semiquinone species may have too short a lifetime at low pH either because of protonation and further reduction or because of disproportionation. Work is currently in progress to elucidate the mechanisms more fully.

The voltammetry curves in acid solution for the glassy carbon surface (Fig. 11) differ from those for the pre-adsorbed quinones on the basal plane of HOPG (not shown). Such differences, however, may reflect differences in the kinetics as well as the thermodynamics of the quinone-like structures when they are an integral part of the disordered glassy carbon surface vs. when they are part of an adsorbed molecule. The experiments with the pre-adsorbed quinones on the basal plane of HOPG have clearly demonstrated that these quinones can catalyze the O_2 heterogeneous reduction. The authors believe that quinone groups directly incorporated into the surface can do likewise.

Electrocatalysis of other reactions by electrodes containing quinone-like functionalities, either intrinsic or chemically attached, has been studied for a number of years. These include the electro-oxidation of ascorbic acid by plasma-treated glassy carbon [36] and catecholamine-attached glassy carbon [37,38] and the oxidation of NADH by electrochemically oxidized glassy carbon [39] and by catecholamine-attached glassy carbon (catechols become o-quinones when oxidized) [40]. Two-electron processes appear to be involved in these reactions.

SUMMARY

The oxidation treatment of glassy carbon can lead to the formation of surface oxygen complexes. The enhancement or decrease of O_2 reduction activity on the oxidized surface is explained by the formation of quinone-type surface oxide complexes. The chemical oxidation treatment in our work is proposed to cause the formation of quinone-like surface structure. As a result, the activity of O_2 reduction on such surfaces increases. On the other hand, if the oxidation pretreatment leads to the formation of surface oxides other than the quinone-type, the activity of O_2 reduction may be decreased.

ACKNOWLEDGEMENT

The authors acknowledge the support of this research by the U.S. Department of Energy.

REFERENCES

1. E. Yeager, P. Krouse and K. V. Rao, Electrochim. Acta, 9, 1057 (1964).
2. M. Appel and A.J. Appleby, Electrochim. Acta, 23, 1243 (1978).
3. A. J. Appleby and J. Mario, Electrochim. Acta, 24, 195 (1974).
4. G. V. Shteinberg, I. A. Kukushkina, V. S. Bagotskii and M. R. Tarasevich, Sov. Electrochem., 15, 443 (1979).
5. V. V. Sysoeva, V. I. Gants, E. N. Smirnova and N. N. Storchak, J. Appl. Chem. USSR, 45, 555 (1972).
6. I. Morcos and E. Yeager, Electrochim. Acta, 15, 953 (1970).
7. N. M. Zagudaeva, V. S. Vilinskaya and G. V. Shteinberg, Sov. Electrochem., 18, 478 (1982).
8. R. J. Taylor and A. A. Humffray, J. Electroanal. Chem., 64, 63 (1975).
9. V. A. Garten and D. E. Weiss, Austral. J. Chem., 8, 68 (1955).
10. E. Yeager, in "Electrocatalysis on Non-Metallic Surfaces," A. D. Franklin, Editor, Nat. Bur. Stand. (U.S.), Spec. Publ. 455, U.S. Government Printing Office, Washington, DC, 1970, pp. 203-219.
11. G. Mamantov, D. B. Freeman, F. J. Miller and H. E. Zittel, J. Electroanal. Chem., 9, 305 (1965).
12. R. W. Zurilla, R. K. Sen and E.Yeager, J. Electrochem. Soc., 125, 1143 (1978).
13. R. S. Nicholson and I. Shain, Anal. Chem., 36, 706 (1964).
14. A. J. Bard and L. R. Faulkner, "Electrochemical Methods," John Wiley, New York, 1980.
15. R. E. Davis, G. L. Horvath and C. W. Tobias, Electrochim. Acta, 12, 1287 (1967).
16. J. P. Hoare, in "Encyclopedia of Electrochemistry of the Elements," Vol. II, A. J. Bard, Editor, Marcel Dekker, New York, 1974, Chap. II-5.

17. V. G. Levich, "Physicochemical Hydrodynamics," Prentice-Hall, Englewood Cliffs, N.J., 1962.
18. K. Kinoshita and J.A.S. Bett, Carbon, 11, 403 (1973).
19. J. V. Hallum and H. V. Drushel, J. Phys. Chem., 62, 110 (1958).
20. H. V. Drushel and J. V. Hallum, J. Phys. Chem., 62, 1502 (1958).
21. J. F. Evans and T. Kuwana, Anal. Chem., 49, 1632 (1977).
22. Z. W. Zhang, D. Tryk and E. Yeager, manuscript in preparation.
23. C. Degrand and L. L. Miller, J. Electroanal. Chem., 117, 267 (1981).
24. S. Wawzonek, R. Berkey, E. W. Blaha and M. E. Runner, J. Electrochem. Soc., 103, 456 (1956).
25. M. E. Peover, J. Chem. Soc., 1962, 4540.
26. L. Jeftic and G. Manning, J. Electroanal. Chem., 26, 195 (1970).
27. B. Keita, I. Kawenoki, J. Kossanyi and L. Nadjo, J. Electroanal. Chem., 145, 311 (1983).
28. R. Gill and H. I. Stonehill, J. Chem. Soc., 1952, 1845.
29. C. A. Bishop and L.K.J. Tong, J. Am. Chem. Soc., 87, 501 (1965).
30. K. J. Vetter, "Electrochemical Kinetics," Academic Press, New York, 1967, pp. 40-45, 483-487.
31. K. B. Patel and R. L. Willson, J. Chem. Soc., Faraday Trans. I, 6[, 814 (1973).
32. L. H. Dawsey, U.S. Patent 3,041,143, June 1962, described in R. Powell, "Hydrogen Peroxide Manufacture, 1968,", Noyes Development Corp., Park Ridge, N.J., 1968.
33. J. E. Luvalle and A. Weissberger, J. Am. Chem. Soc., 69, 1576 (1947).
34. D. H. Grangaard, U.S. Patent 3,454,477, July 1969 (Chem. Abstr. 71:56109a, 1971).
35. B. Keita and B. Nadjo, J. Electroanal. Chem., 145, 431 (1983).
36. J. F. Evans, T. Kuwana, M. T. Henne and G. P. Royer, J. Electroanal. Chem., 80, 409 (1977).
37. D.C.S. Tse and T. Kuwana, Anal. Chem., 50, 1315 (1978).
38. K. J. Stutts and R. M. Wightman, Anal. Chem., 55, 1576 (1983).
39. W. J. Blaedel and R. A. Jenkins, Anal. Chem., 46, 1952 (1974); 47, 1337 (1975).
40. C. Degrand and L. L. Miller, J. Am. Chem. Soc., 102, 5728 (1980).

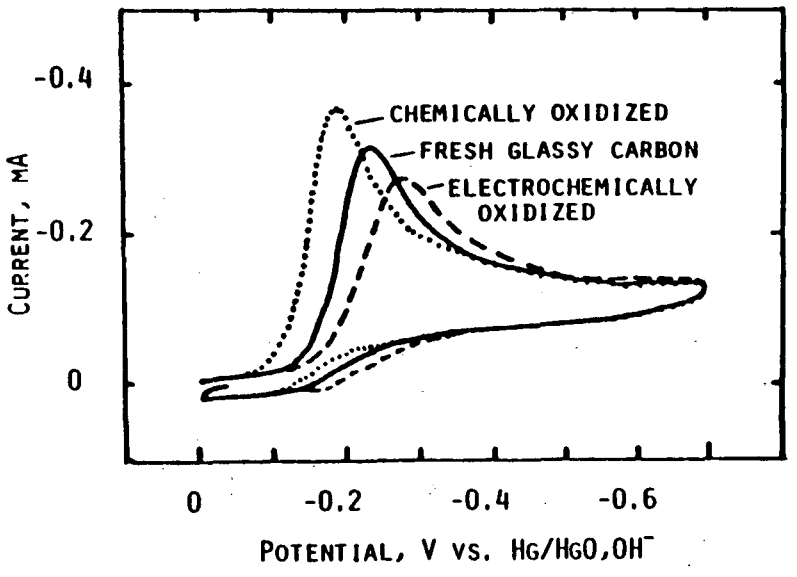

FIG. 1. CYCLIC VOLTAMMOGRAMS FOR O_2 REDUCTION ON THE CHEMICALLY OXIDIZED (····), ELECTROCHEMICALLY OXIDIZED (----) AND FRESH (——) SURFACES OF GLASSY CARBON IN O_2-SATURATED 1.0 M NAOH AT 22°C. SWEEP RATE: 150 MV S^{-1}. CHEMICAL OXIDATION FOR 0.5 MIN IN CONC. HNO_3; ELECTROCHEMICAL OXIDATION AT 0.5 V FOR 1 MIN IN AR-SATURATED 1.0 M NAOH.

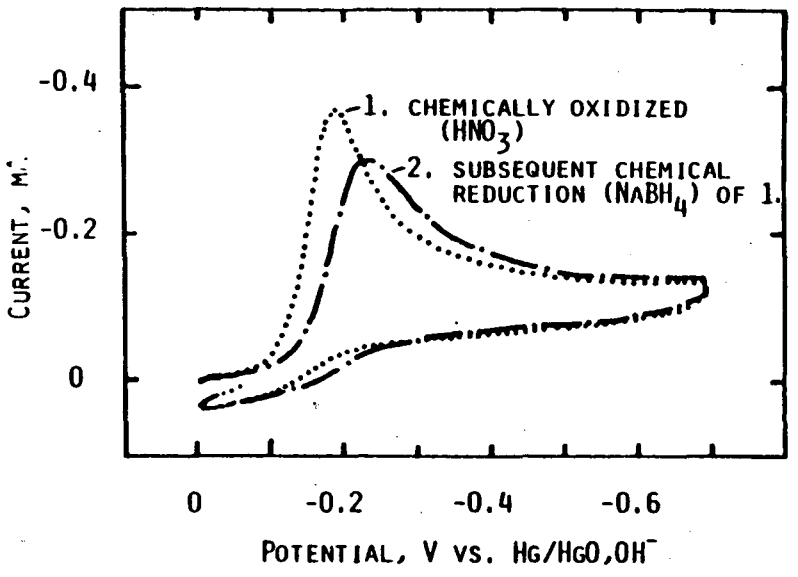

FIG. 2. CYCLIC VOLTAMMOGRAMS FOR O_2 REDUCTION ON THE CHEMICALLY OXIDIZED (····) AND THEN CHEMICALLY REDUCED SURFACES (-·-·) OF GLASSY CARBON IN O_2-SATURATED 1.0 M NAOH AT 22°C. SWEEP RATE: 150 MV S^{-1}.

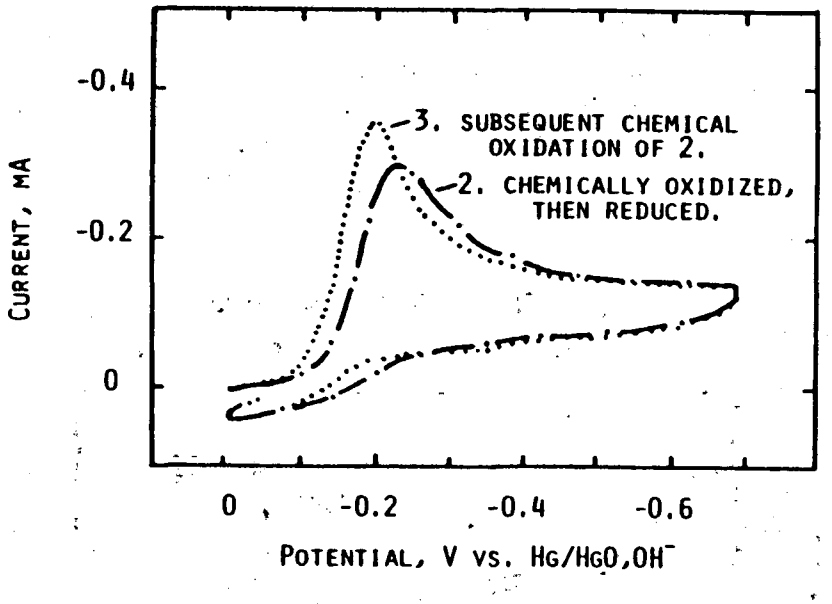

FIG. 3. CYCLIC VOLTAMMOGRAMS FOR O_2 REDUCTION ON THE CHEMICALLY REDUCED SURFACE (-·-·) FOLLOWING CHEMICAL OXIDATION, AND CHEMICAL REOXIDIZED SURFACE (····) IN O_2-SATURATED 1.0 M AT 22°C. SWEEP RATE: 150 MV S^{-1}.

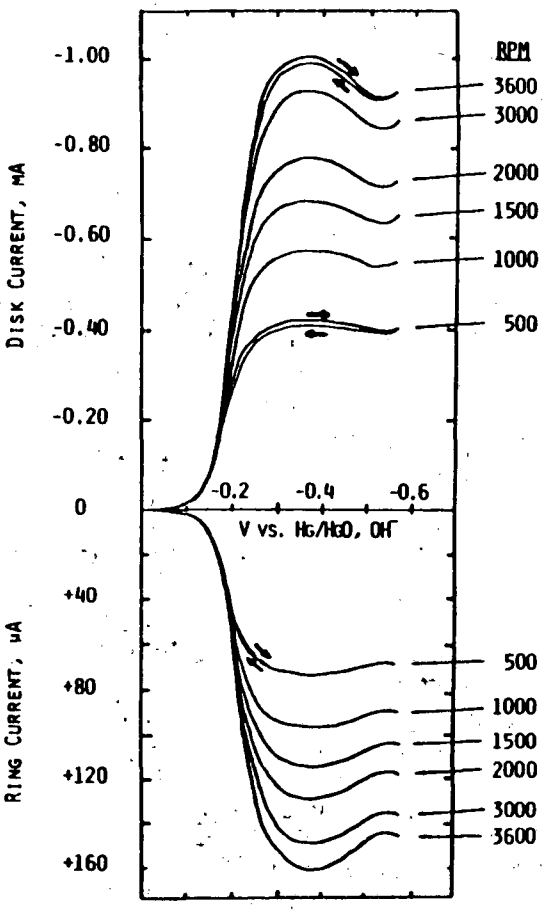

FIG. 4. DISK AND RING CURRENTS FOR O_2 REDUCTION ON THE FRESH SURFACE OF GLASSY CARBON IN O_2-SATURATED 1.0 M NAOH AT 22°C. DISK AREA: 0.46 CM^2; RING POTENTIAL: +0.15 V VS. HG/HGO; SWEEP RATE: 20 MV S^{-1}.

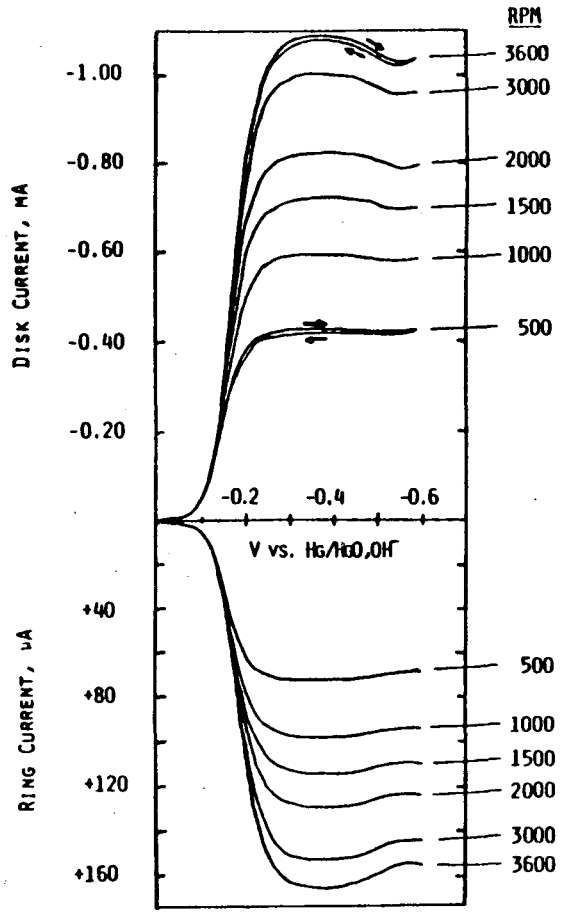

FIG. 5. DISK AND RING CURRENTS FOR OXYGEN REDUCTION ON THE CHEMICALLY OXIDIZED SURFACE OF GLASSY CARBON IN O_2-SATURATED 1.0 M NaOH AT 22°C. DISK AREA: 0.46 cm^2; RING POTENTIAL: +0.15 V vs. $Hg/HgO,OH^-$; SWEEP RATE: 20 mV s^{-1}.

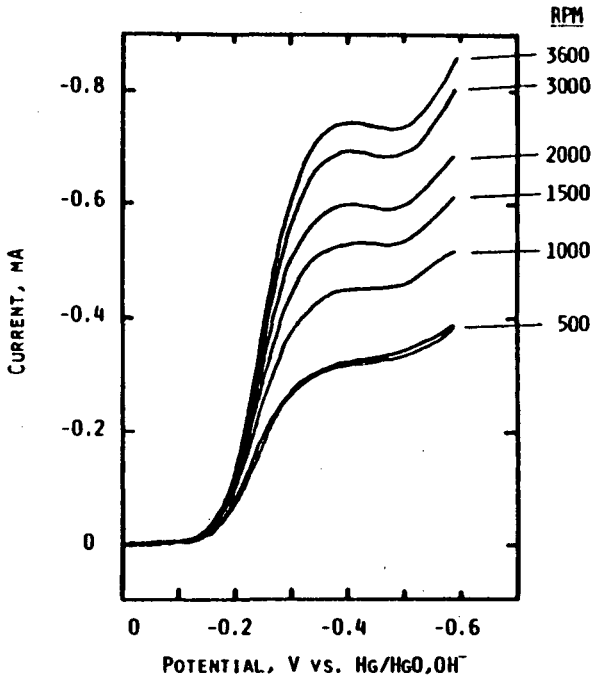

FIG. 6. DISK CURRENTS FOR O_2 REDUCTION ON THE ELECTROCHEMICALLY OXIDIZED SURFACE OF GLASSY CARBON IN O_2-SATURATED 1.0 M NaOH AT VARIOUS ROTATION RATES. DISK AREA: 0.46 cm^2; SWEEP RATE: 20 mV s^{-1}; TEMPERATURE: 22°C; ELECTROCHEMICAL OXIDATION: +0.5 V FOR 1 MIN.

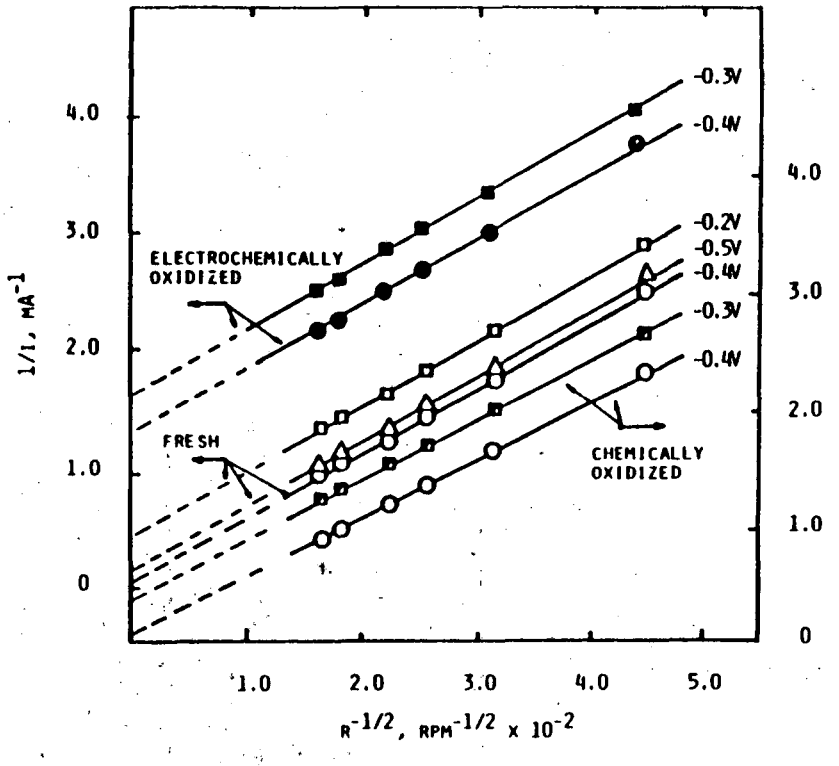

FIG. 7. PLOTS OF 1/I VS. $R^{-1/2}$ FOR O_2 REDUCTION ON THE FRESH (□Δ○), ELECTROCHEMICALLY OXIDIZED (■●) AND CHEMICALLY OXIDIZED (◪◐) SURFACES OF GLASSY CARBON AT VARIOUS POTENTIALS. B=0.029 MA RPM$^{-1/2}$ (EXPERIMENTAL); 0.020 MA RPM$^{-1/2}$ (THEORETICAL). ELECTROCHEMICAL OXIDATION AT +0.3 V FOR 45 MIN.

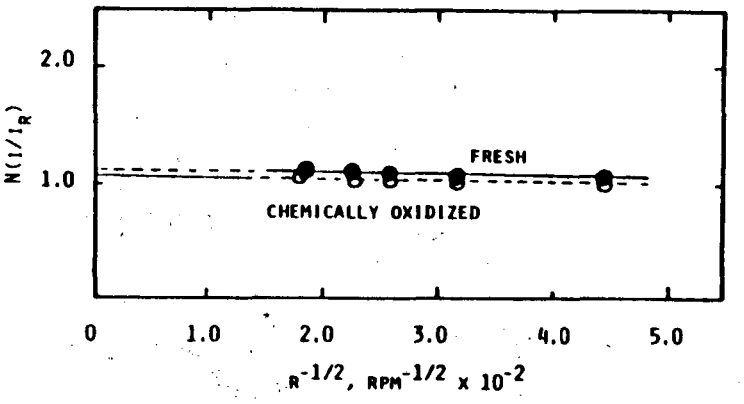

FIG. 8. PLOTS OF N(I/I_R) VS. $R^{-1/2}$ FOR O_2 REDUCTION ON THE FRESH (SOLID CIRCLES) AND CHEMICALLY OXIDIZED (OPEN CIRCLES) SURFACES OF GLASSY CARBON IN O_2-SATURATED 1.0 M NaOH AT 22°C. WITHIN EXPERIMENTAL ERROR, THE SAME POINTS WERE OBTAINED THROUGHOUT THE POTENTIAL RANGE -0.25 TO -0.60 V VS. Hg/HgO,OH^-.

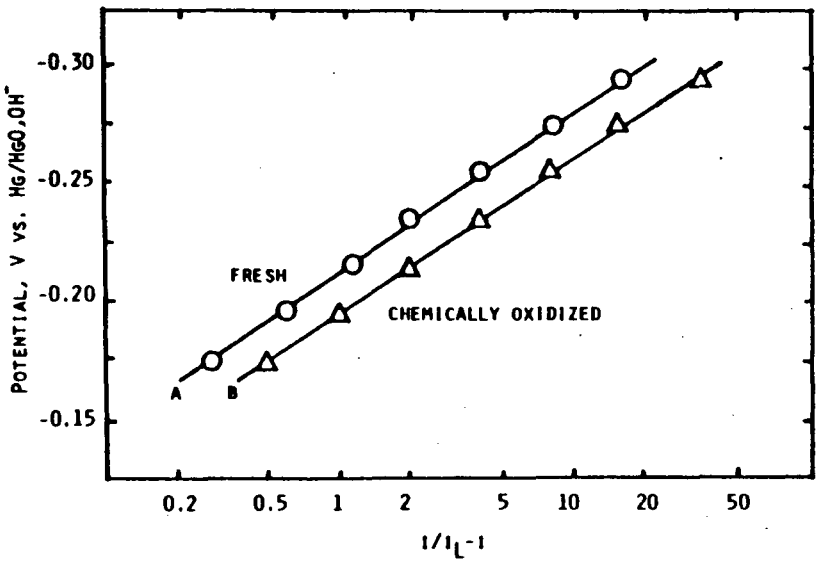

FIG. 9. POLARIZATION CURVES FOR O_2 REDUCTION ON THE FRESH (A) AND CHEMICALLY OXIDIZED (B) SURFACES OF GLASSY CARBON IN O_2-SATURATED 1.0 M NaOH AT 22°C; ROTATION RATE: 3600 RPM.

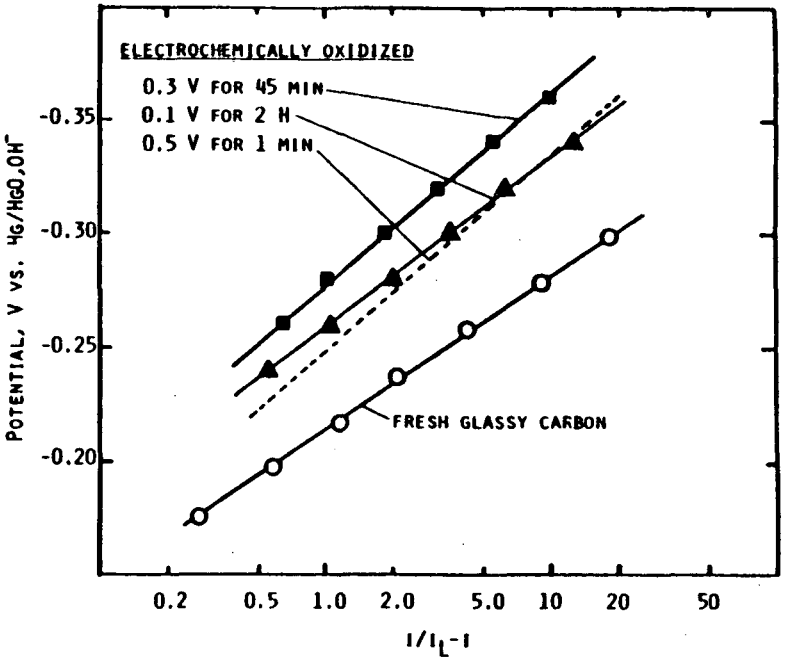

FIG. 10. POLARIZATION CURVES FOR O_2 REDUCTION ON THE FRESH (○) AND ELECTROCHEMICALLY OXIDIZED SURFACES (■▲) OF GLASSY CARBON IN O_2-SATURATED 1.0 M NaOH AT 22°C. ROTATION RATE: 3600 RPM; OXIDATION AT +0.1 V FOR 2 H (▲); AT +0.3 V FOR 45 MIN (■); DOTTED LINE: OXIDATION AT +0.5 V FOR 1 MIN.

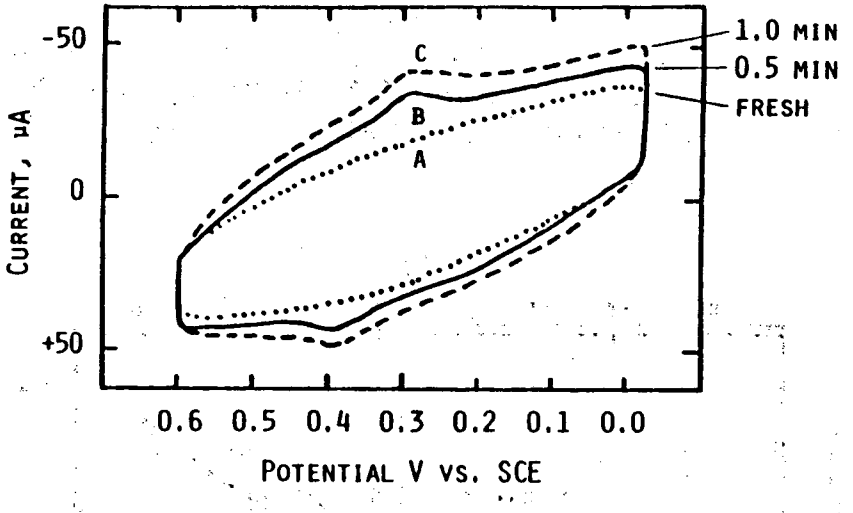

FIG. 11. CYCLIC VOLTAMMOGRAMS FOR THE CHEMICALLY OXIDIZED (IN CONC. HNO_3) AND FRESH SURFACES OF GLASSY CARBON IN AR-SATURATED 1.0 M H_2SO_4 AT 22°C. ELECTRODE AREA: 0.45 CM^2; (A) FRESH SURFACE; (B) OXIDIZED FOR 0.5 MIN; (C) OXIDIZED FOR 1.0 MIN. SWEEP RATE: 200 MV S^{-1}.

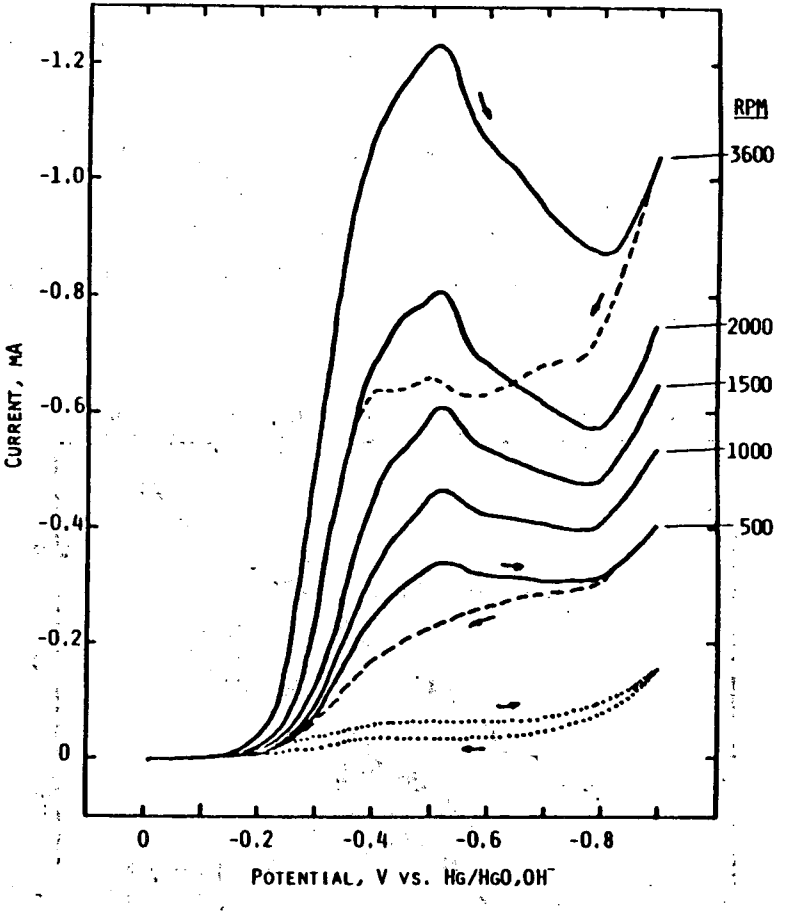

FIG. 12. DISK CURRENTS FOR O_2 REDUCTION ON THE BASAL PLANE OF HIGHLY-ORIENTED PYROLYTIC GRAPHITE (HOPG) PRE-ADSORBED WITH 9,10-ANTHRAQUINONE-2-SO_3^- IN O_2-SATURATED 1.0 M NAOH AT 22°C. ELECTRODE AREA: 0.48 CM^2; SWEEP RATE: 20 MV S^{-1}; CURVES WERE OBTAINED IN ORDER OF DECREASING ROTATION RATE. (····) FRESH BASAL PLANE HOPG AT 3600 RPM.

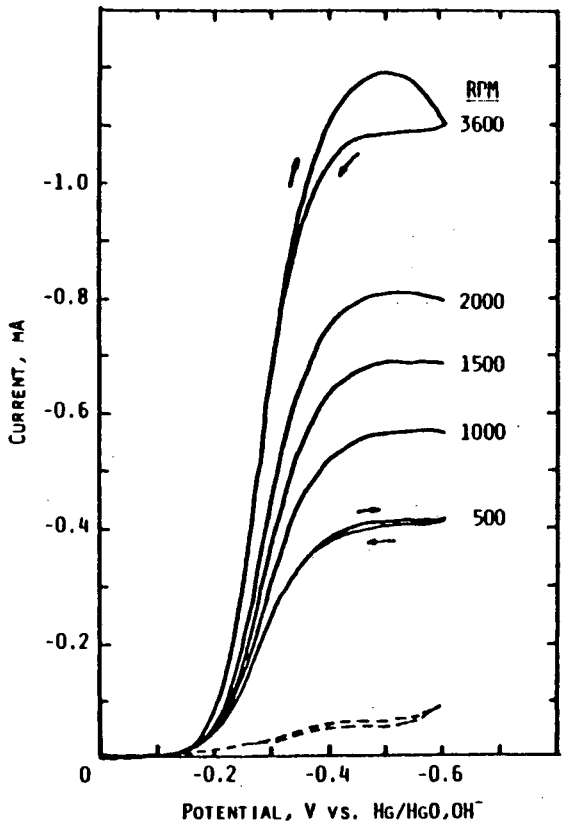

FIG. 13. DISK CURRENTS FOR O_2 REDUCTION ON BASAL PLANE HOPG PRE-ADSORBED WITH 1,4-NAPHTHOQUINONE IN O_2-SATURATED 1.0 M NaOH AT 22°C. ELECTRODE AREA: 0.48 cm^2; SWEEP RATE: 20 mV s^{-1}. THE CURVES WERE OBTAINED IN ORDER OF DECREASING ROTATION RATE.

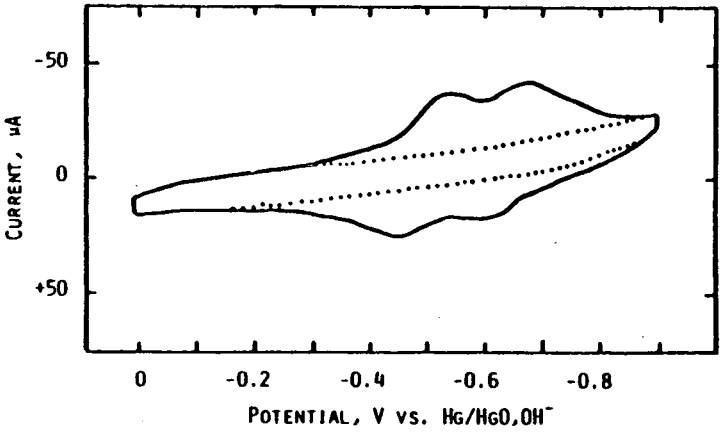

FIG. 14. CYCLIC VOLTAMMOGRAM FOR BASAL PLANE HOPG PRE-ADSORBED WITH 9,10-ANTHRAQUINONE-2-SO_3^- IN Ar-SATURATED 1.0 M NaOH SOLUTION AT 22°C. ELECTRODE AREA: 0.48 cm^2; SWEEP RATE: 200 mV s^{-1}; (····) FRESH BASAL PLANE HOPG.

DISCUSSION

Stephen G. Weber, University of Pittsburgh: Would you please describe the details of the polishing of the glassy carbon used in these experiments? Was the electrode embedded in any other material while being polished? What was the size and composition of polishing compounds, and what was the slurrying agent used? How was the electrode washed after polishing, but before being used as an electrode?

Authors: The Pine Co. glassy carbon rotating disk electrode (with gold ring) was put into a Teflon holder to keep it vertical during polishing. The electrode was polished manually in successive stages using the following materials:

i) silicon carbide paper, 600 grit (3M Co.)
ii) - iv) special emery grinding papers, grits 0, 000 and 0000 (Buehler, Ltd.)
v) and vi) γ-Al_2O_3, 0.3 μm and 0.05 μm particle sizes in water (Buehler, Ltd.)

Finally the electrode was either cleaned ultrasonically in water or merely rinsed with water, the results being similar in both cases. Between experiments the electrode was resurfaced by polishing with 0.05 μm γ-Al_2O_3.

S. D. James, U. S. Naval Surface Weapons Center: Dr. Yeager, in the previous talk, described how electrochemical oxidation of carbon can cause its severe mechanical disruption. Is it possible therefore that surface area changes caused by the erosion of electrochemically oxidized carbon surfaces could explain your observed activity changes?

Authors: The electrochemical oxidation treatment decreased the activity for O_2 reduction. On the other hand, this electrochemical oxidative treatment would be expected to cause an increase in surface area. Therefore the activity per unit time area decreased for the electrochemically oxidized carbon surface. With the chemical oxidation treatment, the voltammetry showed an increase in double layer capacitance of roughly 30% as compared to the fresh surface (Fig. 11). This change in double layer capacitance can be produced by both area and functional group changes, but implies that the area change was not by orders of magnitude. The change in the heterogeneous electron transfer rate constant, however, would have been by almost two orders of magnitude according to Eq. 2, using the peak potentials in Fig. 1. As mentioned, Eqs. 1 and 2 are not really quantitatively applicable but they illustrate the general trends.

Another piece of evidence also indicates that the enhancing effect of the chemical oxidation is not due entirely to an increase in surface area and that is the lowering of O_2 reduction activity by reducing the chemically oxidized surface with $NaBH_4$ (Fig. 2).

Norman L. Weinberg, Electrosynthesis Co., Inc.: Is it possible that HNO_3 oxidation causes nitration of the graphite, resulting in the cata-

lytic surface activity differences from the electrochemical method? Has nitrogen analysis been done? A nitrated quinone structure would be expected to show different properties than unnitrated.

Authors: This is certainly possible. We have not analyzed the surface for nitrogen but plan to in the future.

APPENDIX C

J. T. Lu, D. Tryk and E. Yeager, In "Extended Abstracts," International Society of Electrochemistry, 34th Meeting, September, 1983, Erlangen, West Germany, Abstr. No. 0519.

THE FORMATION OF THE O_2^- RADICAL ION DURING O_2 ELECTROREDUCTION IN ALKALINE SOLUTION

J.T. LU[+], D. TRYK AND E. YEAGER
Case Center for Electrochemical Sciences
and the Chemistry Department
Case Western Reserve University
Cleveland, Ohio 44106 USA

Sawyer and Seo[1] have proposed that the one-electron reduction of O_2 to O_2^- is reversible and independent of electrode surface. This implies that the O_2 reduction to hydrogen peroxide proceeds through a one-electron transfer of the outer sphere type to an O_2 molecule in the outer Helmholtz plane; i.e., in alkaline solution:

$$O_2 + e^- \longrightarrow O_2^-\cdot \qquad (1)$$

where $E^\circ = -0.286$V vs NHE[2] at 20°C. This reaction would then be followed by a dismutation reaction

$$2O_2^-\cdot + H_2O \rightleftharpoons O_2 + HO_2^- + OH^- \qquad (2)$$

[pK=7.51 at 20°C[2]]

or further reduction:

$$O_2^-\cdot + HOH + e^- \longrightarrow OH_2^- + OH^- \qquad (3)$$

Sen, Zagal and Yeager[3] have offered as evidence against such a mechanism the dependence of the overall first-order rate constant for O_2 reduction to peroxide on the particular electrode surface.

As a further argument they point out that the O_2 reduction to peroxide on such surfaces as ordinary graphite[4] and gold[5] yields two electrons per O_2 diffusing through the Nernst diffusion layer on the basis of rotating disk experiments. The kinetics of reaction 2, however, are far too slow for the dismutation reaction to proceed to completion in the Nernst layer as would be necessary to realize two electrons per O_2 diffusing through the Nernst layer. The second-order rate constant for reaction 2 has been recently evaluated in 2M NaOH and found to be 14.4 $M^{-1}s^{-1}$ at 20°C[6]. It also seems unlikely that $O_2^-\cdot$ produced in the outer Helmholtz plane would be quantitatively reduced (reaction 3) without substantial loss of $O_2^-\cdot$ into the bulk solution. Kinetic studies of the O_2-HO_2^- couple on gold[5] indicate a stoichiometric number $\nu=2$, which is compatible with reaction 1 followed by 2 but not 1 followed by 3.

Various workers have reported the reduction of O_2 to bulk phase $O_2^-\cdot$ in alkaline solutions[6-8]. When the electrode surface of mercury is covered with an organic layer, the generation of $O_2^-\cdot$ rather than reduction to peroxide appears to be favored.[8] This may reflect the stabilization of the $O_2^-\cdot$ by interaction with the adsorbed organic[8].

[+]On leave from the Wuhan University, China

An interesting surface on which to check for the outer Helmholtz plane reaction 1 is the basal plane of single-crystal graphite. Since all of the valency forces are satisfied in the plane of this surface, the reduction of O_2 to HO_2^- should be very inhibited on this surface if the reaction proceeds through a catalytic route involving adsorption sites. This has been confirmed[4] on the basal plane of stress-annealed pyrolytic graphite, a material which approximates the behavior of single-crystal graphite. The rate of O_2 reduction to peroxide on this surface in alkaline solution is suppressed by typically two orders of magnitude compared to that on ordinary pyrolytic graphite. The surface is far from perfect and it is likely that O_2 reduction via adsorbed states can still proceed on these surface defects but at a much reduced rate. The outer sphere electron transfer reaction, however, should proceed on the basal plane relatively unimpeded. With the catalytic reduction greatly suppressed the concentration of the HO_2^- produced by the catalytic reduction of O_2 becomes sufficiently low that very little O_2^- will be produced by the reverse of reaction 2 even if this reaction reaches equilibrium.

In recent work in our laboratory[6], a flow-type thin layer cell was used to reduce O_2 with the O_2 supplied to a stress-annealed pyrolytic graphite electrode in the electrolytic solution flowing through the cell (see Fig. 1). A Nafion cation exchange fluoropolymer membrane was located parallel to the graphite surface at a distance of 0.3 mm. The superoxide was monitored in the effluent from the cell by chilling the sample to liquid nitrogen temperatures and then examining the sample in a Varian E-3 electron spin resonance spectrometer. The lifetime of the O_2^-. in the 2M NaOH at 20°C is quite long ($\sim$1000 s) and a negligible amount decomposes in the 10s required for the transfer from the cell to the cooled esr tube.

Typical preliminary results are shown in Fig. 2. Curve 2 designated I_S corresponds to the rate of formation of O_2^-.(expressed in units of current) as evaluated from the esr measurements. The dashed line (curve 3) represents the difference between the observed total current I_T (curve 1) and the current I_S for O_2^-. formation and should then correspond to peroxide formation either by direct reduction of O_2 to HO_2^- or O_2^-. to HO_2^-. Probably both are involved with the former and perhaps also the latter occurring on imperfections on the graphite surface where edges with functional groups are exposed. The concentration of the O_2^-· ion in the effluent from the cell is far higher than would be expected if the O_2^-· is formed from the peroxide through the reverse of reaction 2. The calculated concentration of O_2^-· based on reaction 2 being at equilibrium is shown by the dashed line in Fig. 3 together with the experimental data (curve 1). Thus the O_2^-· must be produced directly and most likely by outer Helmholtz plane electron transfer. The overall interpretation of this and other results will be discussed in terms of the implications for O_2 electrocatalysis.

Acknowledgement

The authors acknowledge support of this research by the U.S. Department of Energy.

References

1. D. Sawyer and E. Seo, Inorg. Chem., 16, 499 (1977).
2. J.T. Lu, D. Tryk and E. Yeager, Determination of the Equilibrium Constant for Superoxide Dismutation, National Meeting, The Electrochem. Society, Montreal, May 1983. Extended Abstracts 82-1, abst. 674 (to be submitted for publication).

3. R.K. Sen, J. Zagal and E. Yeager, Inorg. Chem. 16, 3379-3380 (1977).
4. I. Morcos and E. Yeager, Electrochim. Acta, 15, 953 (1970).
5. R. Zurilla, R. Sen and E. Yeager, J. Electrochem. Soc., 124, 1103 (1978).
6. J.T. Lu, D. Tryk and E. Yeager, Electrochemical Formation of Superoxide on Graphite in Alkaline Solutions, National Meeting, The Electrochemical Society, Detroit, October 1982. Extended Abstracts 82-2, abst. 323 (to be submitted for publication).
7. B. Kastening and G. Kazemifard, Ber. Bunsenges. Physik. Chem., 74, 551 (1970).
8. M. Dubrovina and L. Nekrasov, Elektrokhim., 8, 1503 (1972).

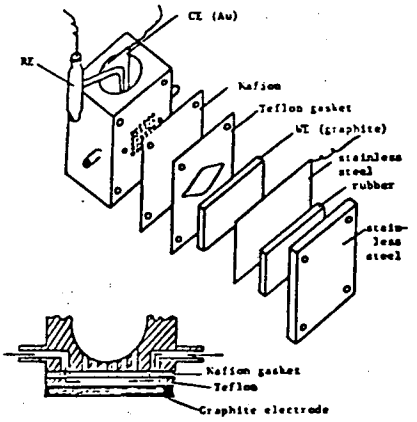

Fig. 1. Structure of the flow cell.

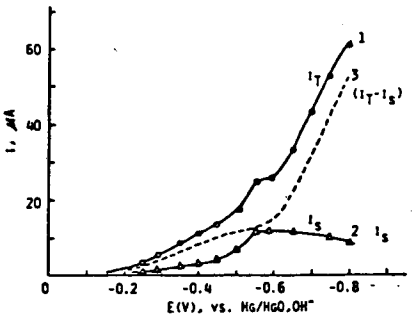

Fig. 2. Potential dependence of O_2 reduction currents on the basal plane of stress annealed graphite in 2 M NaOH at ∿ 20°C.
Electrode area: 3.0 cm^2 (apparent)
Flow rate: 5.0 x 10^{-3} cm^3/s.
1. Total current (I_T).
2. Current for $O_2^{\cdot-}$ generation I_S).
3. $I_T - I_S$

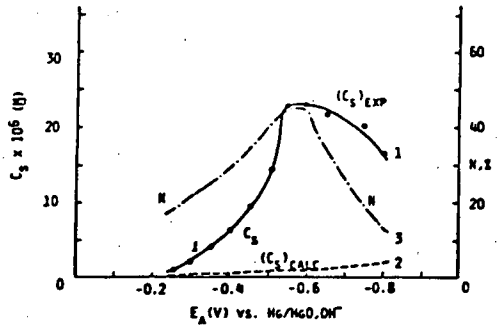

Fig. 3. Potential dependence of the concentration of the superoxide ion ($O_2^{\cdot-}$) electrogeneration on the basal plane of stress annealed pyrolytic graphite in 2 M NaOH at ∿ 20°C. Electrode area: 3.0 cm^2; flow rate: 5.0 x 10^{-3} cm^3/s.

1. $(C_S)_{exp}$, directly measured (ESR)
2. $(C_S)_{calc}$, calculated from the equilibrium $HO_2^- + O_2 + OH^- \rightleftharpoons 2O_2^{\cdot-} + H_2O$ (pK = -7.51), on the basis of measured peroxide concentration ($I_P = I_T - I_S$)
3. Percent of total current corresponding to $O_2^{\cdot-}$ formation (N)

APPENDIX D

Z. W. Zhang, D. Tryk and E. Yeager, In "Extended Abstracts, "Vol. 83-2, National Meeting of the Electrochemical Society, October, 1983, Washington, D.C., Abstr. No. 394, p.630.

ELECTRODE KINETICS OF THE O_2/HO_2^- COUPLE ON GLASSY CARBON IN ALKALINE SOLUTION

Z.W. Zhang, D. Tryk and E. Yeager
Case Center for Electrochemical Sciences and
The Department of Chemistry
Case Western Reserve University
Cleveland, Ohio 44106

The kinetics of O_2 reduction have been studied on various carbon and graphite surfaces in alkaline solution (1,2). Several such studies have been done on glassy carbon (3-5), but they have not considered the involvement of peroxide in detail. The present research has examined both the cathodic and anodic kinetics of the O_2/HO_2^- couple on glassy carbon in alkaline solution and an overall mechanism has been proposed.

The experiments were carried out in an all-Teflon cell with a rotating ring-disk electrode (Pine Instrument Co.) using a glassy carbon disk (Fluorocarbon Co.) and a gold ring. The collection efficiency N was 0.17. A gold foil was used as the counter electrode and a Hg/HgO, OH^- reference electrode was used. The electrolyte, 1.0 M NaOH, was prepared from 50% NaOH solution (low in carbonate, Fisher Chemical Co.) and was pre-electrolyzed as previously described (6,7). Solutions of various pH values were prepared by adding varying amounts of concentrated H_2SO_4 (reagent grade, Fisher) to 1.0 M NaOH. Various concentrations of hydrogen peroxide (without stabilizer, FMC Corp.) were used in the solutions thus prepared. O_2 and Ar used to saturate the electrolyte were purified using gas trains as described previously (6,7). Prior to each experiment a fresh electrode surface was prepared by polishing with a water paste of 0.05 μm γ-alumina. All measurements were made at 22 ± 1°C.

O_2 Reduction

The disk current i_d and ring current i_r are shown in Fig. 1 as a function of disk potential at different rotation rates ω. If the O_2 reduction process is first order with respect to dissolved O_2, the following equation should be satisfied:

$$1/i_d = (1/i_k) + (1/B\omega^{1/2})$$

The plots of $1/i_d$ vs. $\omega^{-1/2}$ are linear. The experimental B value, 0.0190 mA $rpm^{-1/2}$ from Fig. 2 is in accord with the calculated value, 0.0200 mA $rpm^{-1/2}$ based on a 2-electron reduction of O_2 to HO_2^- (2). Furthermore, the ratio i_d/i_r is equal to 1/N irrespective of disk potential and rotation rate over the potential range -0.25 to -0.60 V vs. Hg/HgO,OH^-, indicating that peroxide is produced quantitatively. A Tafel slope of ∿ -65 mV/decade has been obtained (Fig. 3) for this process on glassy carbon in contrast to the -120 mV/decade slope found for graphite electrodes. A stoichiometric number ν of ∿ 1.0 has been calculated from the data in Fig. 4 and the exchange current i_o evaluated from Fig. 3 using the equation

$$-\left(\frac{\partial \eta}{\partial i}\right)_{i=0} = \frac{\nu}{n} \cdot \frac{RT}{i_o F}$$

O_2 reduction currents as a function of HO_2^- concentrations from 0.001 to 0.107 M and of pH values from 11.6 to 14.0 have also been examined. The observed currents were essentially independent of peroxide concentration and pH over the ranges examined at potentials of -0.25 to -0.50 V vs. a pH insensitive reference, thus indicating zero reaction order with respect to both HO_2^- and OH^-.

HO_2^- Oxidation

Figure 5 shows the oxidation of HO_2^- on glassy carbon in Ar-saturated 1.0 M NaOH containing 0.001 M HO_2^-. Severe hysteresis and decrease of the anodic current are observed with cycling. The zero-current potential also shifts in the positive direction with cycling. The results suggest a change in the surface properties of the electrode at positive potentials, which complicates the examination of HO_2^- oxidation kinetics over a wide range of potentials. The study of electrochemical oxidation of glassy carbon in the authors' laboratory has provided evidence that the change of the electrode surface is related to the oxidation of surface functional groups, even at relatively negative potentials. If the potential scan is reversed negative of +0.25 V, however, the hysteresis becomes negligible, allowing kinetic data to be obtained. The dependence of HO_2^- oxidation on the HO_2^- concentration and pH at a given rotation rate and at a potential where the surface oxidation can be neglected is shown in Fig. 6. The reaction is first order in HO_2^- and zero order in OH^-.

Discussion of Mechanism

The following mechanism for the cathodic and anodic reactions is consistent with the experimental data:

$$O_2 \longrightarrow O_2(ads) \quad (1)$$

$$O_2(ads) + e^- \longrightarrow [O_2(ads)]^- \quad (2)$$

$$[O_2(ads)]^- \longrightarrow O_2^-(ads) \quad (3)$$

$$O_2^-(ads) + H_2O \longrightarrow HO_2(ads) + OH^- \quad (4)$$

$$HO_2(ads) + e^- \longrightarrow HO_2^-(ads) \quad (5)$$

$$HO_2^-(ads) \longrightarrow HO_2^- \quad (6)$$

The rate-determining step 3 involves an interconversion between two configurations of the adsorbed superoxide, only one of which can accept a proton from water, through the breakage of one of the adsorptive bonds under the influence of the polar water molecules, i.e.,

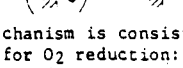

The above mechanism is consistent with the experimental findings for O_2 reduction: approximately -60 mV/decade Tafel slope, first order in O_2, zero order in HO_2^- and OH^-, and a stoichiometric number of one. If a rate-determining step 5 is assumed for HO_2^- oxidation, the mechanism is also consistent with the data for the anodic process: first order in HO_2^- and zero order in OH^-. The fact that the rds is different in the forward and reverse directions and thus that the OH^- reaction order is zero in both directions can be rationalized by noting that the nature of the surface at potentials positive of about +0.05 V is qualitatively different from that at more negative potentials.

Acknowledgements

Mr. Zhang is on leave from the Dalian Institute of Chemical Physics, People's Republic of China. The authors acknowledge partial support by the U.S. Department of Energy.

References

1. J.P. Randin, in "Encyclopedia of Electrochemistry of the Elements," Vol. VII, A.J. Bard., Ed., Marcel Dekker, New York, 1976, Chap. VII-1.
2. I. Morcos and E. Yeager, Electrochim. Acta 15, 953 (1970).
3. F.Z. Sabirov and M.R. Tarasevich, Sov. Electrochem. 5, 564 (1969).
4. M. Brezina and A. Hofmanova, Coll. Czech. Chem. Comm. 38, 985 (1973).
5. R.J. Taylor and A.A.Humffray, J. Electroanal. Chem. 64, 63 (1975).
6. J.A. Molla, Ph.D. Dissertation, Case Western Reserve University, 1983.
7. R.W. Zurilla, R.K. Sen and E. Yeager, J. Electrochem. Soc. 125, 1103 (1978).

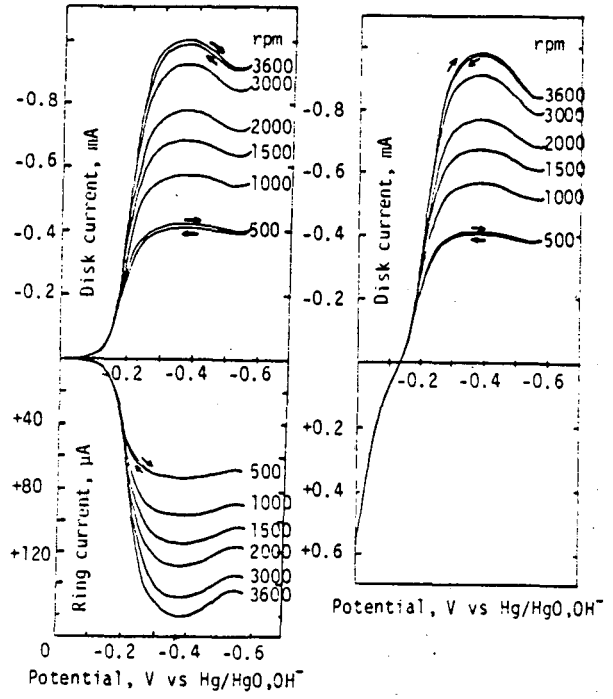

Fig. 1 (left). Disk and ring currents for O_2 reduction on glassy carbon in O_2-saturated 1.0 M NaOH at 22°C. Disk area: 0.46 cm^2. Ring potential: +0.15 V. Sweep rate: 20 mV s^{-1}.

Fig. 4 (right). Disk currents in O_2-saturated 0.107 M HO_2^- + 0.837 M NaOH. Sweep rate: 20 mV s^{-1}.

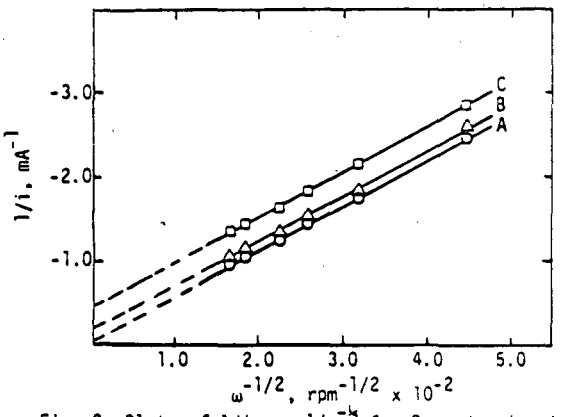

Fig. 2. Plots of 1/i vs. $1/\omega^{-\frac{1}{2}}$ for O_2 reduction in 1.0 M NaOH at given potentials: A) -0.40 V, B) -0.50 V, C) -0.24 V.

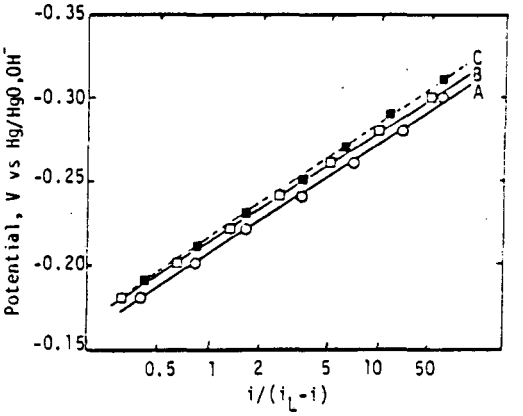

Fig. 3. Polarization curves for O_2 reduction in 1.0 M NaOH: A) 2000 rpm, B) 3600 rpm, C) 3600 rpm with 0.107 M HO_2^- + 0.837 M NaOH. i_L was taken to be the observed current maximum.

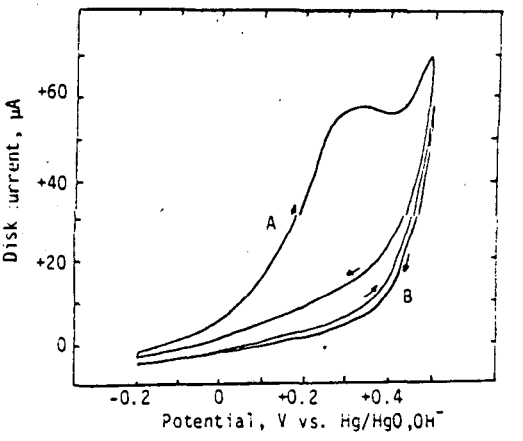

Fig. 5. Oxidation of HO_2^- in Ar-saturated 0.001 M HO_2^- + 1.0 M NaOH. Rotation rate: 2000 rpm. Sweep rate: 20 mV s^{-1}. A) 1st scan; B) 4th scan.

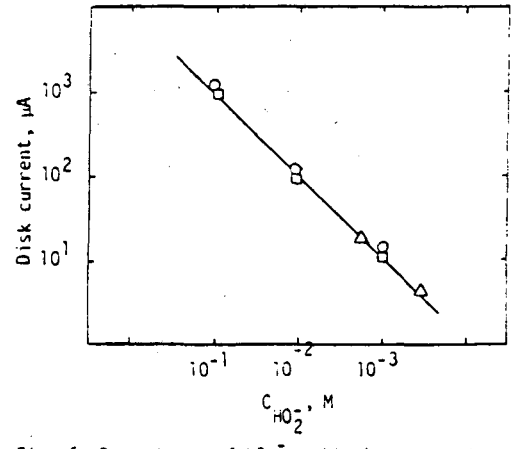

Fig. 6. Dependence of HO_2^- oxidation current on HO_2^- concentration at various pH values (Ar-saturated solutions). Rotation rate: 2000 rpm. Disk potential: +0.10 V. ○: pH 14; □: pH 13.1; △: pH 11.1.

APPENDIX E

Z. W. Zhang, D. Tryk and E. Yeager, In "Extended Abstracts, "Vol. 83-2, National Meeting of the Electrochemical Society, October, 1983, Washington, D.C., Abstr. No. 395, p. 632.

QUINONE-LIKE SURFACE STRUCTURES AND O_2 REDUCTION ACTIVITY ON GLASSY CARBON AND GRAPHITE SURFACES IN ALKALINE SOLUTION

Z.W. Zhang, D. Tryk and E. Yeager
Case Center for Electrochemical Sciences and
The Department of Chemistry
Case Western Reserve University
Cleveland, Ohio 44106

The nature of oxygen-containing surface groups on carbon and graphite has been studied in depth (1-6). Types of functional groups most often suggested are hydroxyl, carboxyl and quinone (1,2). The role such groups play in the electrochemical reduction of O_2 has not yet been fully elucidated, however. Garten and Weiss were the first to propose that surface quinones were important for O_2 reduction to hydrogen peroxide (6), and Yeager refined their model (7). So far there has been little direct experimental evidence. The aim of the present work is to find such evidence. The key features of this work are 1) chemical oxidation of glassy carbon, 2) the adsorptive attachment of quinones on the basal plane of stress annealed pyrolytic graphite (SAPG) and glassy carbon (GC) and 3) O_2 reduction studies on such surfaces. In the present work O_2 reduction was considered only in alkaline solution and the voltammetry was measured in acid as well as alkaline solutions for analytical purposes.

The electrochemical cell, glassy carbon disk-gold ring electrode, 1.0 M NaOH solution and gas purification train have already been described (8). In addition, a basal plane SAPG disk electrode (Union Carbide Carbon Products, Parma, Ohio) was compression-molded in Kel-F (Minnesota Mining and Manufacturing, St. Paul, MN). A mirror-like surface was prepared by peeling with adhesive tape. A Hg/HgO, OH^- reference electrode was used in the 1.0 M NaOH solution and a saturated calomel reference electrode was used in the 1.0 M H_2SO_4 solution (diluted from Fisher reagent grade concentrated acid). Benzoquinone, 1,2-naphthoquinone and 1,4-naphthoquinone (Eastman Kodak) and 9,10-anthraquinone-2-SO_3Na (97%, Fluka) were used as received. The quinones were preadsorbed on the glassy carbon and SAPG surfaces by rotating the electrode at 500 rpm for 0.5 hr. in the saturated aqueous quinone solutions. The electrode was then rinsed by rotating in water for 10 min. The GC electrode was polished as already described (8). It was chemically oxidized by dipping in concentrated nitric acid for either 0.5 or 1.0 min. and was gently rinsed with water. The $NaBH_4$ reduction treatment of the SAPG and glassy carbon electrodes involved rotating the electrode in a 0.1 M aqueous solution for 0.5 hr. at room temperature and then gently rinsing with water. All measurements were made at 22 ± 1°C.

The voltammetry curves with and without chemical oxidation of the GC are shown in Fig. 1. The peaks observed for the chemically oxidized surface occur at + 0.3 V (cathodic) and +0.4 V (anodic), potentials which are similar to those observed for carbon blacks (3) and for glassy carbon and edge-plane SAPG (4) in acid media. As has been observed with plasma-treated pyrolytic graphite, the charge associated with the surface redox couple increases with increasing degree of oxidation (5). It has already been suggested that these couples are of the quinone/hydroquinone type (3-5). If various quinones are preadsorbed on the polished GC surface without chemical oxidation, and on the basal plane of SAPG, the voltammograms are somewhat similar to that of the oxidized GC surface alone. As noted previously for graphite (3-5), the potential for the surface couple on GC most closely matches that for 1,2-naphthoquinone.

The disk current i_d and ring current i_r for O_2 reduction in alkaline solution as a function of disk potential at various rotation rates are shown in Fig. 3 for the polished GC surfaces without and with chemical oxidative treatment respectively. The latter shows greater activity. It is thought that this increase results from a higher surface coverage of quinone-like surface functional groups rather than from the increase in surface area (seen as an increase in capacitive current in Fig. 1). One reason is that the treatment of the oxidized GC surface with $NaBH_4$ solution results in activity very similar to that for the polished GC before oxidation. The $NaBH_4$ is known to reduce quinone to hydroquinone (9).

Based on Fig. 3 plots of $1/i_d$ vs. $\omega^{-\frac{1}{2}}$ (ω = rotation rate) are both linear, with slope corresponding to that for a 2-electron process for O_2 reduction. Plots of $(i_d/i_r)N$ [N = collection efficiency] vs. $\omega^{-\frac{1}{2}}$ show that there is quantitative production of hydrogen peroxide at potentials between -0.25 V and -0.60 V vs. Hg/HgO,OH^-. In addition, both surfaces yield approximately the same Tafel slope, -65 mV/decade but with different exchange current densities. The similarity of the O_2 reduction behavior on the two surfaces indicates that the mechanism is the same but that there is a higher coverage of active sites on the oxidized surface.

When the catalytically inactive basal plane of SAPG electrode is preadsorbed with 1,2-naphthoquinone there is a great increase in O_2 reduction activity (Fig. 4) but when 1,2- or 1,4-naphthoquinone is adsorbed on polished GC there is not a significant change in activity.

Figures 5 and 6 show the voltammetry and O_2 reduction curves, respectively, for the 9,10-anthroquinone-2-SO_3^- adsorbed on SAPG in 1.0 M NaOH. O_2 reduction commences at potentials which correlate with the first peak in the voltammogram, corresponding to the quinone-semiquinone reduction. This provides further evidence favoring the role of the quinone in O_2 reduction on ordinary pyrolytic graphite and glassy carbon. Unfortunately it was not readily possible to check this further with the naphthoquinones because of difficulty in obtaining the voltammetry curves for the adsorbed species at monolayer levels. The species apparently is not sufficiently strongly adsorbed on the electrode without having a substantial concentration in solution. This then interfered with the obtaining of the voltammetry peaks for the adsorbed species.

Acknowledgment

Mr. Zhang is on leave from the Dalian Institute of Chemical Physics, People's Republic of China. The authors acknowledge partial support by the U.S. Department of Energy.

References

1. B.R. Puri, in "Chemistry and Physics of Carbon," Vol. 6. P.L. Walker, Jr., Ed., Marcel Dekker, New York, 1970, pp. 191-282.
2. J.P. Randin, in "Encyclopedia of Electrochemistry of the Elements," Vol. VII. A. J. Bard, Ed., Marcel Dekker, New York, 1976, Chap. VII-1.
3. K. Kinoshita and J.A.S. Bett, Carbon, 11, 403 (1973).
4. J.P. Randin and E. Yeager, J. Electroanal. Chem. 58, 313 (1975).
5. J.F. Evans and T. Kuwana, Anal. Chem., 49, 1632 (1977).
6. V.A. Garten and P.E. Weiss, Austral. J. Chem. 8, 81 (1955).
7. E. Yeager, in "Electrocatalysis on Non-Metallic Surfaces," Natl. Bureau of Standards Publ. 455, A.D. Franklin, Ed., U.S. Government Printing Office, Washington, D.C., 1976, pp. 203-219.
8. Z.W. Zhang, D. Tryk and E. Yeager, Elec. Chem.Soc. Ext. Abstracts, Natl. Meeting, Washington, D.C., October 9-14, 1983
9. Y.Matsumura, H. Takahashi, Carbon, 17, 109 (1979).

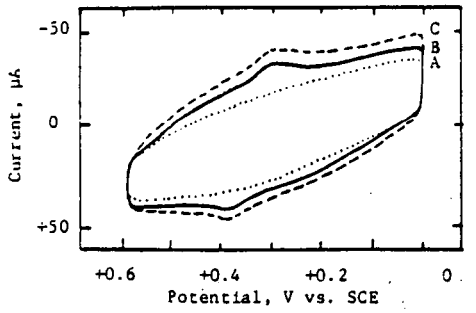

Fig. 1. Cyclic voltammograms for glassy carbon in Ar-saturated 1.0 M H_2SO_4 at 22°C, A) polished, B) oxidized for 0.5 min. and C) oxidized for 1.0 min. Sweep rate was 200 mV s^{-1}. Electrode area: 0.46 cm^2.

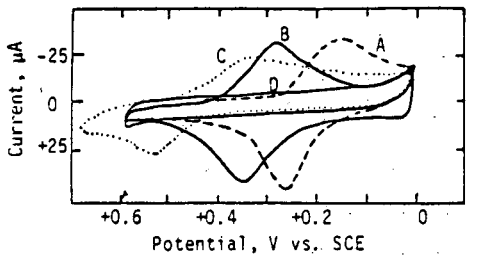

Fig. 2. Cyclic voltammograms in Ar-saturated 1.0 M H_2SO_4 on basal plane SAPG preadsorbed with A) 1,4-naphthoquinone, B) 1,2-naphthoquinone and C) 1,4-benzoquinone. D) was the virgin surface. Sweep rate: 200 mV s^{-1}. Electrode area: 0.48 cm^2.

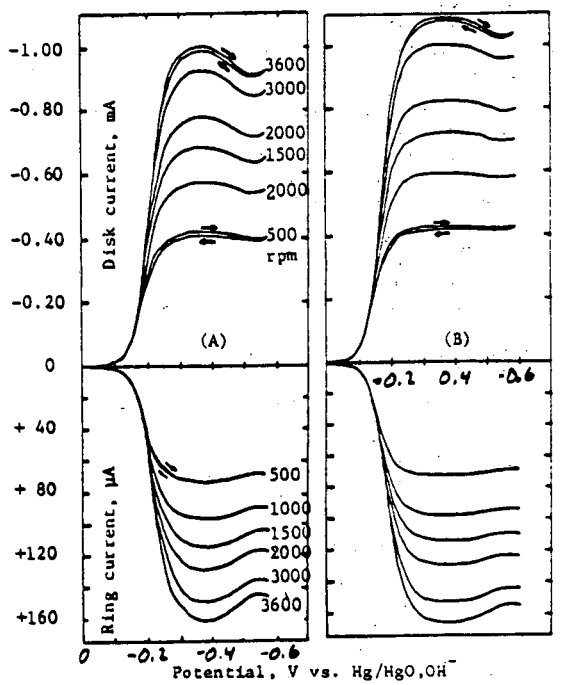

Fig. 3. Disk and ring currents for O_2 reduction in O_2-saturated 1.0 M NaOH on A) polished GC and B) chemi-

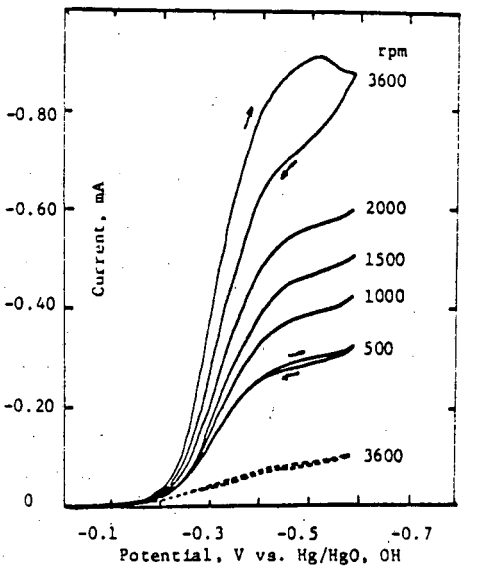

Fig. 4. Disk currents for O_2 reduction in O_2-saturated 1.0 M NaOH on basal plane SAPG pre-adsorbed with 1,2-naphthoquinone. Dashed line is for the virgin surface. Sweep rate: 20 mV s^{-1}. Electrode area: 0.48 cm^2. The curves were obtained in order of decreasing rotation rate.

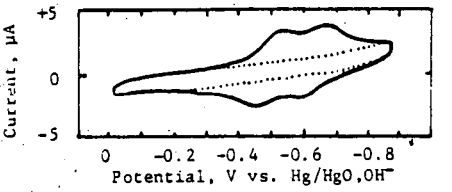

Fig. 5. Cyclic voltammograms of basal plane SAPG preadsorbed with 9,10-anthroquinone-2-SO_3^- in Ar-saturated 1.0 M NaOH. Other details as in Fig. 2.

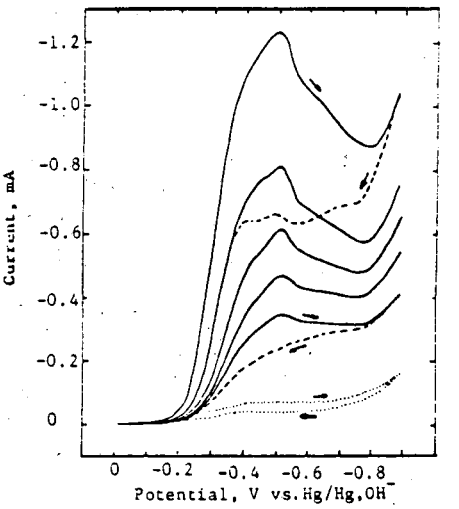

Fig. 6. Disk current for O_2 reduction on basal plane SAPG preadsorbed with 9,10-anthroquinone-2-SO_3^- in

TECHNICAL INFORMATION DEPARTMENT
LAWRENCE BERKELEY LABORATORY
UNIVERSITY OF CALIFORNIA
BERKELEY, CALIFORNIA 94720